

# **Regulation of mitochondrial gene copy number in plants and the influence of impaired chloroplast function on mitochondrial motility**

## **DISSERTATION**

zur Erlangung des akademischen Grades  
“doctor rerum naturalium”  
(Dr. rer. nat.)  
im Fach Biologie

eingereicht an der  
Mathematisch-Naturwissenschaftlichen Fakultät I  
Der Humboldt Universität zu Berlin

von  
Diplom-Ingenieurin Emilia Cincu

Präsident der Humboldt-Universität zu Berlin  
Prof. Dr. Jan-Hendrik Olbertz

Dekan der Mathematisch-Naturwissenschaftlichen Fakultät I  
Prof. Stefan Hecht PhD

Gutachter:   1. Prof. Dr. Thomas Börner  
                  2. Prof. Dr. Christian Schmitz-Linneweber  
                  3. Prof. Dr. Axel Brennicke

Tag der mündlichen Prüfung: 15.10.2014

**What I mostly like about research work is that it pushes the limits of human knowledge. It's all about being in the first row, looking straight into the unknown and daring to step forward. And, after a life of stepping, you realize that the journey was not only exterior: by discovering the world, you discover yourself. Personal life philosophy**

## Zusammenfassung

Mitochondrien sind die essentiellen Organellen der eukaryotischen Zelle. Sie sind der Ort der Zellatmung und besitzen ein eigenes Genom. Das mitochondriale Genom der Pflanze weist mit einer heterogenen Population linearer, häufig auch verzweigten und zusätzlichen kleineren, zirkulären Molekülen eine komplexe Struktur auf. Während im humanen System Veränderungen in der mitochondrialen Genkopienzahl mit Krankheiten wie Krebs, Neurodegeneration, Diabetes und Alterung assoziiert werden (Clay Montier *et al.*, 2009), gibt es nur sehr wenige Informationen über die generelle Abundanz mitochondrialer Gene in Pflanzen. Um Einblicke in die mitochondrialen Genkopienzahl und deren Regulation sowohl unter normalen als auch unter Stressbedingungen zu erhalten, wurde die Kopienzahl pro Zelle vier repräsentativer Gene (*atp1*, *nad6*, *rps4* und *cox1*) mittels qRT-PCR und Durchflusszytometrie ermittelt. Die Bestimmung der mitochondrialen Genkopienzahl in unterschiedlichen Spezies sowie in Organen der Modellpflanze *Arabidopsis thaliana* zeigte, dass die Kopienzahl mitochondrialer Gene sich nicht nur in den unterschiedlichen Spezies, sondern auch zwischen den unterschiedlichen Organen unterschied, wobei die höchsten Werte in der Wurzelspitze erreicht wurden. Darüber hinaus beeinflusst eine beeinträchtigte Funktion sowohl der Chloroplasten als auch der Mitochondrien die Abundanz mitochondrialer Gene. In *Arabidopsis* Keimlingen, welche zur Unterdrückung der plastidären Translation auf Spectinomycin-haltigem Medium angezogen wurden, wurde im Vergleich zu Kontrollpflanzen ein dreifacher Anstieg der Genkopienzahl festgestellt. Dieser Effekt erwies sich als spezifisch für Blatt- bzw. Kotyledonengewebe und war unabhängig vom Licht. Die Untersuchungen transplastomer Tabakmutanten mit Defekten in PSI, PSII, Elektronentransport oder ATP-Synthase (freundlicherweise von R. Bock und M.-A. Schöttler, Golm, zur Verfügung gestellt), zeigte unter Schwachlicht einen Anstieg der Genkopienzahl in den weißen Blättern von *atpB* und *atpH* Deletionsmutanten, aber keinen in den nicht völlig weißen Photosynthesemutanten. Diese Daten lassen auf einen möglichen Signalweg schließen, welcher in Beziehung zum Energiehaushalt der Zelle und/oder zum komplett weißen Phänotyp der Pflanzen steht.

Mutanten mit Defekten in der Respiration (*ndufs4*, Meyer *et al.* 2009; *mrpl11*, Pesaresi *et al.* 2006) zeigten ebenfalls erhöhte Genkopienzahlen, die durch Anzucht der Pflanzen auf Spectinomycin noch erhöht werden konnten. Dieses Ergebnis legt ein komplexes, regulatorisches Netzwerk nahe, in welchem sowohl Respiration als auch Photosynthese die Aufrechterhaltung einer stabilen Genkopienzahl innerhalb der Pflanzenzelle beeinflussen.

Es wurde kürzlich gezeigt, dass die Dynamik pflanzlicher Mitochondrien sich unter verschiedenen metabolischen Bedingungen verändert (Van Gestel und Verbelen, 2002; Yoshinaga *et al.*, 2005; Armstrong *et al.*, 2006; Zottini *et al.*, 2006; Scott und Logan, 2008). Darüber hinaus ändern Mitochondrien, zusammen mit den Chloroplasten, ihre Position in der Zelle unter unterschiedlichen Lichtverhältnissen (Islam *et al.*, 2009). Die Untersuchungen einer Spectinomycin-behandelter mt-GFP *Arabidopsis* Pflanzenlinie (Logan und Leaver, 2000) mittels CLSM zeigten einen Stillstand der Motilität der Mitochondrien in den epidermalen Zellen der weißen Kotyledonen, obwohl eine TEM Analyse eine normale, interne Morphologie ergab. Weitere Untersuchungen führten zu der Schlussfolgerung, dass es auch hier die Stärke der plastidären Beeinträchtigung, welche zu einem gelb-weißen Phänotyp führt, für den Arrest der Mobilität verantwortlich ist. Auf der anderen Seite zeigten die Mitochondrien in den Wurzeln weißer, Spectinomycin-behandelter und etiolierter Keimlinge durchaus Mobilität. Diese Ergebnisse weisen auf ein unbekannten regulatorischen Mechanismus der mitochondrialen Dynamik hin, der bei normalen Wachstumsbedingungen offenbar unter dem direkten Einfluss einer gestörten plastidären Entwicklung steht.

**Schlagworte:**

mitochondriale Genkopienzahlen

Signalwege

mitochondriale Dynamik

Spektinomycin

Chondriom



## Summary

Mitochondria are essential organelles of eukaryotic cells. They are the site of respiration and contain their own genomes. The plant mitochondrial genome has a complex structure. It exists in the form of a heterogeneous population of linear, often branched molecules with smaller than genome-size circular molecules being present in low abundance. Whereas in humans, changes in mitochondrial gene copy number were found to be related to cancer, neurodegeneration, diabetes and ageing (Clay Montier *et al.*, 2009), there is only little information on the abundance of mitochondrial genes in plants. In order to study the the mitochondrial genome abundance and its regulation in plants under both standard and stress conditions, we determined the gene copy number of four representative mitochondrial genes (*atp1*, *nad6*, *rps4*, and *cox1*) using qRT-PCR and flow-cytometry. Determination of mitochondrial gene copy number in different plant species and in organs of the model plant *Arabidopsis thaliana* showed that the copy number of the four investigated genes varied between species and also between different organs, having the highest values in the root tips. Moreover, impaired chloroplast and mitochondrial functions influence the abundance of mitochondrial genomes. The growth of *Arabidopsis* seedlings on MS medium containing spectinomycin (a plastid translation inhibitor) led to a three-fold increase in the copy number in white versus green seedlings, an effect that is leaf/cotyledon specific and light-independent. Investigations of transplastomic tobacco mutants with defects in PSI, PSII, electron transport or ATP synthase (obtained from R. Bock and M.A. Schöttler) showed that under low light conditions, knock-out of *atpB* and *atpH* but not of photosynthesis genes produced an increase in mitochondrial gene copy numbers. These results reveal a possible signaling pathway that is related to the energy status of the cell and/or the existence of a white leaf phenotype.

Respiration deficient mutants (*ndufs4*, Meyer *et al.*, 2009 and *mrpl11*, Pesaresi *et al.* 2006) also showed an increase in the gene copy number, this effect being further amplified when the mutants were grown on spectinomycin. The data suggest a complex regulatory network in which both photosynthesis and respiration influence the maintenance of a stable mitochondrial gene copy number within plant cells.

Plant mitochondrial dynamics was previously shown to vary under different metabolic conditions (Van Gestel and Verbelen, 2002; Yoshinaga *et al.*, 2005; Armstrong *et al.*, 2006; Zottini *et al.*, 2006; Scott and Logan, 2008). Moreover, mitochondria change their location within the cell together with the chloroplasts under varying light conditions (Islam *et al.*, 2009). CLSM investigations of a spectinomycin-treated mt-GFP line (Logan and Leaver, 2000) showed that in epidermal cells of white cotyledons most of the mitochondria are not motile with TEM analysis presenting normal internal morphology. Further investigations led to the conclusion that the threshold level of chloroplast impairment that leads to a motility arrest is represented by the appearance of a yellow-white cotyledon phenotype. However, motility was still present in the roots of white, spectinomycin treated seedlings and also in the cotyledons of etiolated seedlings. These results point to a new regulatory mechanism of mitochondrial dynamics that is directly influenced by impaired chloroplast development under standard growth conditions.

**Keywords:**

mitochondrial gene copy number

signaling

mitochondrial dynamics

spectinomycin

chondriome

## Contents

<b>Zusammenfassung.....</b>	<b>3</b>
<b>Summary.....</b>	<b>1</b>
<b>1 Introduction.....</b>	<b>1</b>
1.1 The origin of organelles and their roles in higher plants.....	1
1.1.1 Plastids .....	1
1.1.2 Mitochondria.....	4
1.2 Retrograde signaling .....	7
1.2.1 The retrograde signaling from plastids to the nucleus .....	8
1.2.2 The retrograde signaling from mitochondria to the nucleus.....	13
1.3 The plant chondriome.....	16
1.3.1 Chondriome organization in higher plants.....	16
1.3.2 Fusion and fission of plant mitochondria.....	18
1.3.3 Mitochondrial motility .....	19
1.3.4 Metabolic control of mitochondrial motility and morphology .....	20
1.4 Higher plant organellar genomes .....	22
1.4.1 The plastome .....	22
1.4.2 The chondrome .....	23
1.5 Organellar gene transcription .....	29
1.5.1 The transcription machinery of plastids.....	29
1.5.2 The transcription machinery of mitochondria.....	31
1.6 Aim of this work .....	33
1.6.1 Evaluation of mtDNA organization and abundance under standard and stress conditions.....	33
1.6.2 The influence of impaired chloroplast development on mitochondrial dynamics .....	34
<b>2 Materials and methods .....</b>	<b>35</b>
2.1 Materials.....	35
2.1.1 Providers .....	35
2.1.2 Plant material .....	36
2.1.3 Oligonucleotides .....	36
2.1.4 Software .....	40
2.2 Methods.....	40
2.2.1 Plant growth .....	40

2.2.2	Surface sterilization of <i>Arabidopsis thaliana</i> and <i>Nicotiana tabacum</i> seeds .....	43
2.2.3	Isolation of nucleic acids .....	43
2.2.4	Determination of nucleic acid concentrations.....	44
2.2.5	Gel electrophoresis of nucleic acids .....	44
2.2.6	Reverse transcription of total RNA.....	45
2.2.7	Quantitative real-time PCR using SYBR® Green.....	45
2.2.8	Amplification of DNA using PCR.....	48
2.2.9	Flow-cytometric analysis of nuclear endopolyploidy.....	49
2.2.10	Measurement of O <sub>2</sub> consumption.....	49
2.2.11	TCA-Ether extraction of metabolites.....	50
2.2.12	Determination of ATP, ADP and ATP/ADP ratio.....	50
2.2.13	Detection of proteins by Western blotting.....	51
2.2.14	Protoplast isolation.....	52
2.2.15	Confocal imaging.....	52
2.2.16	Determination of the mitochondria number per cell.....	53
2.2.17	Evaluation of mitochondrial motility.....	53
2.2.18	<i>Arabidopsis thaliana</i> crossings and selection of homozygous mutants .....	53
<b>3</b>	<b>Results .....</b>	<b>55</b>
3.1	Analysis of organellar gene copy number in <i>Arabidopsis thaliana</i> and <i>Hordeum vulgare</i> .....	55
3.1.1	Analysis of mitochondrial gene copy number in various <i>Arabidopsis</i> organs.....	55
3.1.2	Analysis of mitochondrial gene copy number in relation to mitochondria number during <i>Arabidopsis thaliana</i> leaf senescence .....	57
3.1.3	Comparison of organellar gene copy numbers in <i>Arabidopsis thaliana</i> and <i>Hordeum vulgare</i> diploid and tetraploid lines .....	61
3.2	The effects of impaired chloroplast translation on mitochondria .....	70
3.2.1	Reproduction of the barley <i>albostrians</i> mutant in <i>Arabidopsis</i> by treatment with the antibiotic spectinomycin.....	70
3.2.2	Determination of mitochondrial gene copy number in white, spectinomycin-treated seedlings .....	71
3.2.3	Steady-state transcript levels of mitochondrial genes in green and white, spectinomycin-treated <i>Arabidopsis</i> seedlings.....	72
3.2.4	Steady-state transcript level of nuclear genes involved in mtDNA replication, recombination and transcription .....	73

3.2.5	Confocal microscopic (CLSM) investigations of mitochondrial dynamics in green and white, spectinomycin-treated <i>Arabidopsis</i> seedlings .....	75
3.2.6	Transmission electron microscopic (TEM) evaluation of plastids/chloroplasts and mitochondria in green and white <i>Arabidopsis</i> cotyledons .....	79
3.2.7	Determination of oxygen consumption, ATP, ADP and ATP/ADP ratio in green and white <i>Arabidopsis</i> cotyledons .....	80
3.3	The effects of light and sucrose content on mitochondrial gene copy number..	82
3.4	Effects of chloroplast and mitochondrial dysfunction on mitochondrial gene copy number .....	84
3.4.1	Effects of chloroplast dysfunction on mitochondrial gene copy number ...	84
3.4.2	Effects of mitochondrial dysfunction on mitochondrial gene copy number .....	88
3.4.3	Interactions between chloroplast and mitochondrial dysfunction in determination of mitochondrial gene copy number.....	91
3.4.4	Differential regulation of mitochondrial gene copy number in cotyledons and roots .....	91
3.5	Investigation of the GUN and ABI4 signaling pathway .....	92
3.6	Investigation of mitochondrial motility in relation to impaired chloroplast development.....	94
3.6.1	Investigation of mitochondrial motility in <i>Arabidopsis</i> <i>RLD-Spc1xmtGFP</i> mutant grown in the presence of 500 mg/L spectinomycin	94
3.6.2	Determination of the threshold level of photosynthetic impairment leading to mitochondrial motility arrest .....	96
3.6.3	Investigation of mitochondrial motility in <i>Arabidopsis</i> etiolated seedlings....	100
<b>4</b>	<b>Discussion.....</b>	<b>103</b>
4.1	Organization and abundance of mitochondrial gene copy number in the model plants <i>Arabidopsis thaliana</i> , <i>Hordeum vulgare</i> and <i>Nicotiana tabacum</i> .....	103
4.1.1	The copy number of mitochondrial genes varies between species, ecotypes and organs .....	103
4.1.2	There exist generally low copy numbers of mitochondrial genes .....	106
4.2	Organellar gene copy number in relation to nuclear ploidy level and endocycles..	108
4.3	Possible reasons for elevated mitochondrial gene abundance in plants.....	110
4.3.1	Elevated number of mitochondrial gene copies as a result of increased number of mitochondria .....	111
4.3.2	Mitochondrial gene copy number may determine transcript abundance ..	115
4.3.3	Elevated gene copy number as compensatory mechanism for reduced mitochondrial motility in white tissue .....	116

4.4	Possible signaling pathways regulating mitochondrial gene copy number in plants.....	117
4.4.1	Origin of the signal .....	118
4.4.2	Transcriptional profile of nuclear genes involve in mitochondrial DNA replication, recombination and transcription .....	123
4.5	The influence of impaired chloroplast development on mitochondrial dynamics.....	125
4.5.1	Mitochondrial motility is arrested in white cotyledons of spectinomycin-treated seedlings, but not in roots .....	126
4.5.2	Possible reasons for motility arrest in white cotyledon .....	128
<b>References.....</b>		<b>132</b>
<b>Annexes .....</b>		<b>162</b>
<b>Abbreviations .....</b>		<b>175</b>
<b>Figure appendix .....</b>		<b>178</b>
<b>Acknowledgements .....</b>		<b>183</b>
<b>Eindesstattlich Erklärung .....</b>		<b>184</b>

## 1 Introduction

### 1.1 The origin of organelles and their roles in higher plants

#### 1.1.1 Plastids

The establishment of plastids as photosynthetic organelles in eukaryotes and the diversification of algae and plants were landmark evolutionary events. As it is currently accepted, plastids originated via a single, ancient endosymbiosis between a mitochondriate eukaryotic host and a photosynthetic prokaryote ancestral to present-day cyanobacteria (Douglas and Turner, 1991; Nelissen *et al.*, 1995; Reyes-Prieto *et al.*, 2007). This event took place approximately 1 billion years ago and is termed primary endosymbiosis (Gray, 1992; Martin *et al.*, 2001; Hedges *et al.*, 2004; Yoon *et al.*, 2004). Over time, the prokaryote was reduced to a double-membrane plastid and vertically transmitted to subsequent generations (Fig. 1). Once successfully established, this plastid spread into other lineages through eukaryote-eukaryote (secondary and tertiary) endosymbiosis (McFadden *et al.*, 1994; Delwiche, 1999; McFadden, 2001; Gould *et al.*, 2008).

Plastids are ubiquitous among lower and higher plants (Gould *et al.*, 2008), being also present in some unicellular parasites (Waller and McFadden, 2005; Obornik *et al.*, 2009) and marine mollusks (Rumpho *et al.*, 2001; Hoffmeister and Martin, 2003; Rumpho *et al.*, 2008).

In higher plants, all plastids develop from *proplastids*, small organelles ( $\sim 1 \mu\text{m}$ ) that are present in meristematic and embryonic cells and have the ability to generate a variety of different plastid forms in different types of plant cells (Fig. 2) (Lancer *et al.*, 1976). Proplastids derive from the few proplastids present in the zygote and in most Angiosperms are maternally inherited. However, paternal leakage does occur with low frequency (Zhang *et al.*, 2003; Azhagiri and Maliga, 2007). Various studies estimated that there exist approximately 10-20 proplastids in shoot meristematic cells with some differences existing in DNA content and morphology between cell layers (Cran and Possingham, 1972; Lyndon and Robertson, 1976; Pyke and Leech, 1992; Fujie *et al.*, 1994). DNA transcription, translation and metabolism shows low

This diagram illustrates the evolutionary relationships between various eukaryotic groups, focusing on the acquisition and loss of plastids. The tree is rooted at the bottom with a **Cyanobacterial ancestor** (1°).

**Primary endosymbiosis (1°):** The initial acquisition of plastids from cyanobacteria. This event led to the **Rhodophyta** (red algae) and **Chlorophyta** (green algae). The **Chlorophyta** lineage further includes **Embryophyta** (land plants) and **Chlorarachniophyta** (a group of green algae).

**Secondary endosymbiosis (2°):** The acquisition of plastids from a primary endosymbiont. This is shown in several lineages:
 

- Chlorarachniophyta** (2°): Acquired plastids from a green alga.
- Euglenophyta** (2°): Acquired plastids from a green alga.
- Rhodophyta** (2°): Acquired plastids from a red alga, leading to **Paulinella chromatophora** (1°) and **Glaucophyta** (2°).
- Chlorophyta** (2°): Acquired plastids from a green alga, leading to **Chlorarachniophyta** (2°).

**Tertiary endosymbiosis (3°):** The acquisition of plastids from a secondary endosymbiont. This is shown in the **Dinophyta** lineage, which acquired plastids from a secondary endosymbiont (likely a red alga) through tertiary endosymbiosis. The **Dinophyta** lineage includes **Perkinsidae**, **Apicomplexa**, **Heterokontophyta**, and **Cryptophyta**.

**Plastid loss:** Some lineages have lost their plastids, as indicated by the red text "plastid loss" near the **Oxyhiris** and **Ciliata** groups.

**Other groups:** The **Kryptoperidinium** and **Karlodinium** groups are also shown, along with **Rhopalodia gibba** and **Cyanothece** (1°).

The diagram uses various colors and shapes to represent different eukaryotic groups, and the lines indicate the flow of genetic information and the acquisition of plastids.

Chloroplasts, the most studied type of plastids, are typically ellipsoidal in shape with sizes between 5-10  $\mu\text{m}$  in diameter and 3-4  $\mu\text{m}$  in thickness (Staehelin, 2003; López-Juez and Pyke, 2005), a typical mesophyll cell containing 10-100 chloroplasts, in close correlation to cell size (Pyke and Leech, 1992; Pyke, 1999).

Chloroplasts, the most studied type of plastids, are typically ellipsoidal in shape with sizes between 5-10  $\mu\text{m}$  in diameter and 3-4  $\mu\text{m}$  in thickness (Staehelin, 2003; López-Juez and Pyke, 2005), a typical mesophyll cell containing 10-100 chloroplasts, in close correlation to cell size (Pyke and Leech, 1992; Pyke, 1999).



Their internal structure is represented by a double external membrane and an extensive thylakoid membrane system that is the site of photosynthetic electron transport and ATP synthesis. Thylakoids are composed of lamellae, which are arranged into a complex system of stacked lamellae called grana interconnected by single lamellae called stromal lamellae. The internal matrix, called stroma, is the site of carbon fixation reactions but it also contains the plastid genetic machinery. Chloroplasts differ in structure and function between C3 and C4 plants, and between shade- versus sun-grown leaves (Kirk, 1971; Wise, 2007). In addition to photosynthesis (Allen, 2005), chloroplasts are also the site of carbon oxidation via photorespiration and of multiple anabolic processes like fatty acid, lipid, amino acid and protein synthesis, N and S assimilation (Neuhaus and Emes, 2000). Moreover, even if they seem similar to mesophyll cell chloroplasts, the guard cell chloroplasts function in stomatal opening and closing and not primarily in photosynthesis (Zeiger *et al.*, 2002).

When plant development takes place in the dark or in very low light conditions, the proplastids transform into *etioplasts*. Upon illumination, etioplasts will soon develop thylakoids and photosynthetic complexes, transforming into a green, completely functional chloroplast (López-Juez and Pyke, 2005). *Leucoplasts* are colorless (i.e. non-pigmented) plastids, with three categories generally recognized: amyloplasts, elaioplasts, and proteinoplasts. Proplastids in root tissues typically develop into colorless starch-containing *amyloplasts*. Some amyloplasts, such as those in a potato tuber, function entirely in starch storage (Neuhaus and Emes, 2000). Other amyloplasts, found primarily in the root cap, are said to be “sedimentable” and are intimately involved in gravity perception (Inaba and Ito-Inaba, 2010). *Elaioplasts* play roles in oil storage and metabolism, and are centrally involved in pollen grain maturation (López-Juez and Pyke, 2005). *Proteinoplasts* are sites of protein storage (Wise, 2007). Brightly colored *chromoplasts* contain high levels of carotenoids and xanthophylls and provide the color to many flowers, fruits and vegetables (Weston and Pyke, 1999; Bramley, 2002; Egea *et al.*, 2010).

One particular characteristic of plastids is the ability to interconvert between their different forms under the influence of environmental and developmental signals (Fig. 2). The exception is the *gerontoplast* that represents a degrading stage in the plastid life cycle found in senescing tissues (Krupinska, 2006).

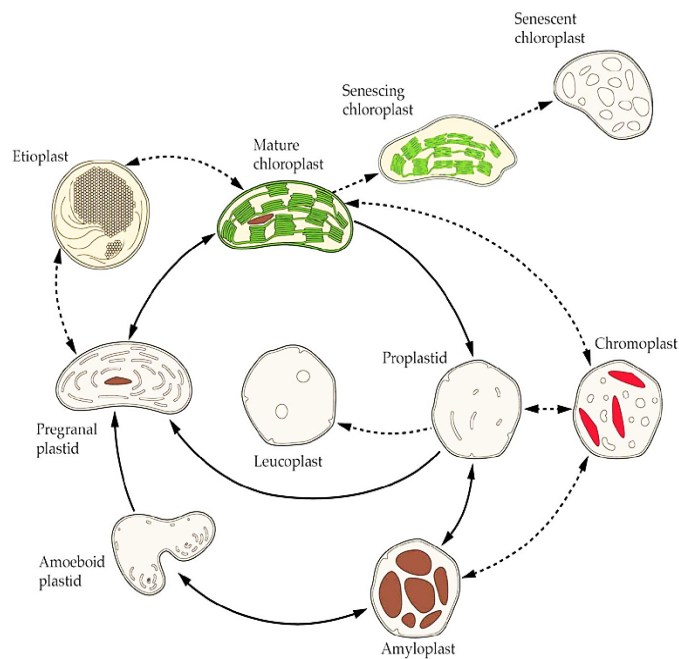


**Figure 2 Schematic representation of major types of plastids.** All plastid types originate from proplastids and can interconvert between different forms under the influence of environmental and developmental signals. The only exception is the gerontoplast that represents an irreversible degradation product of senescing chloroplast. Modified from Buchanan *et al.*, 2000.

### 1.1.2 Mitochondria

It is currently accepted that mitochondria evolved from free-living  $\alpha$ -proteobacteria following a single endosymbiotic event over 1.5 billion years ago (Martin and Muller, 1998; Gray *et al.*, 1999; Martin *et al.*, 2001). Since then, the reorganization of cell metabolism and gene transfer to the nucleus have helped the integration of the new organelle into the pre-existing cell making it semi-autonomous: although mitochondria contain their own genome and protein-synthesizing machinery (Leaver *et al.*, 1983; Unseld *et al.*, 1997; Gray *et al.*, 1999), the majority of mitochondrial polypeptides are encoded in the nuclear genome, synthesized in the cytosol and imported into mitochondria (Unseld *et al.*, 1997; Whelan and Glaser, 1997).

Initial investigations using light microscopy suggested that mitochondria are highly pleomorphic, an observation that was further supported by new *in vivo*

visualization techniques using mitochondrial targeted fluorescent proteins, especially GFP (Logan and Leaver, 2000). While yeast and animals contain tubular and reticular mitochondria that vary in size and shape depending on metabolic conditions (Bereiter-Hahn and Voth, 1994; Hermann and Shaw, 1998; Okamoto and Shaw, 2005; Otera and Mihara, 2011), plant mitochondria are discrete, small and oval with sizes varying between 1 – 2  $\mu\text{m}$  long and 0.1 – 0.5  $\mu\text{m}$  wide (Logan and Leaver, 2000; Logan, 2006). They display high motility, changing rapidly their location in the cell with speeds up to 10  $\mu\text{m s}^{-1}$  (Zheng *et al.*, 2009) and frequently perform fusion and fission (Sheahan *et al.*, 2005a). All together, the totality of mitochondria within a plant cell (the chondriome) is considered to act as a discontinuous whole, reflecting the connected nature of the mitochondrial population (Logan, 2006).

Mitochondria contain a smooth outer membrane and a highly convoluted inner membrane with finger-like projections called cristae that delimit six distinct compartments: the outer membrane, inner membrane, intermembrane space, cristal membranes, intercristal space and matrix (Logan, 2006) (Fig. 3A). The inner membrane and cristal membranes include the components of the mitochondrial electron transport chain (ETC) and the ATP synthase. Plant ETC has four protein complexes: Complex I (“NADH-ubiquinone oxidoreductase”) reduces ubiquinone by oxidizing NADH; Complex II (“succinate-ubiquinone oxidoreductase”) reduces ubiquinone by oxidizing succinate to fumarate; Complex III (“ubiquinone-cytochrome *c* oxidoreductase”), a cytochrome *bc1* complex, reduces cytochrome *c* by oxidizing ubiquinone; and Complex IV (cytochrome *c* oxidase), reduces  $\text{O}_2$  to  $\text{H}_2\text{O}$  by oxidizing cytochrome *c*. Proton pumping occurs at Complexes I, III and IV, establishing a pH and electrical gradient. The energy generated by this gradient produces ATP as protons flow back to the matrix via ATP synthase (Fig. 3B).

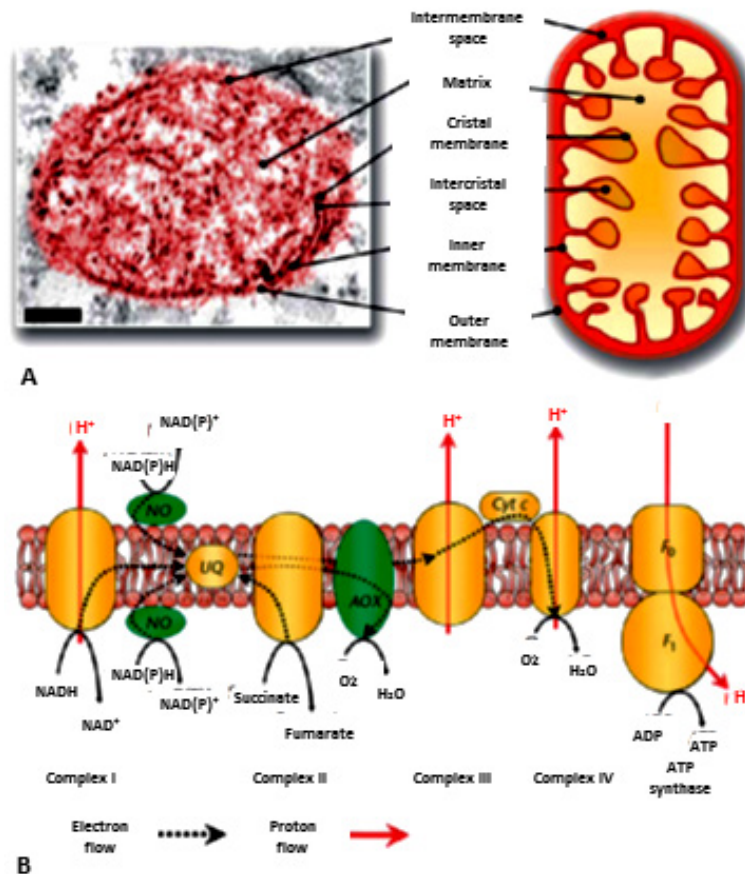


**Figure 3 Organization of mitochondrial membranes and the electron transport chain.** (A) False-colored transmission electron micrograph of a mitochondrion from *Vicia faba* and schematic diagram showing the subdivision of mitochondria into six distinct compartments. (B) The mitochondrial electron transport chain (ETC) in plants. The five complexes (Complexes I-IV and ATP synthase) are showed in yellow and the plant-specific complexes (AOX and NAD(P)H oxidoreductase) are shown in green. Bar: 0.1  $\mu\text{m}$ . Image modified after Rose *et al.* (2007).

In addition to the standard ETC, plants possess an alternate terminal oxidase (AOX) that stops electron flowing through Complexes III and IV, causing free energy to be lost as heat and in consequence reduces ATP production. Currently, the role of the AOX is still discussed, several hypothesis being present (Rasmusson *et al.*, 2009; van Dongen *et al.*, 2010). Except from Complex I, plants also possess type II NAD(P)H dehydrogenases that are not involved in proton translocation from the matrix into the intermembrane space. Therefore, they do not directly contribute to the formation of proton motive force and ATP synthesis. Their exact role and function is still under investigation (Moller, 2001; Rasmusson *et al.*, 2008; van Dongen *et al.*, 2010).

Apart from the ATP synthesis function, plant mitochondria are involved in several other biochemical pathways including the biosynthesis of amino acids

(Ishizaki *et al.*, 2005), fatty acids (Gueguen *et al.*, 2000; Baker *et al.*, 2006), vitamin co-factors: ascorbate (Bartoli *et al.*, 2000) , folate (Mouillon *et al.*, 2002) and Fe-S clusters (Kushnir *et al.*, 2001). Mitochondria are also one of the three compartments involved in photorespiration (Douce and Neuburger, 1999).

Current research also focuses on the involvement of mitochondria in cell signaling, especially on the aspect of retrograde signaling (Rhoads and Subbaiah, 2007) and programmed cell death (Jones, 2000; Youle and Karbowski, 2005; Scott and Logan, 2008a).

## 1.2 Retrograde signaling

Plastids and mitochondria originate by endosymbiosis from ancestral cyanobacteria and respectively from  $\alpha$ -proteobacteria (see 1.1). Following integration, massive gene transfer took place from the newly acquired endosymbiont to the cell nucleus, making it semiautonomous: the majority of proteins necessary for their functioning are now encoded in the nucleus, synthesized in the cytoplasm and then imported into the organelles (Gray *et al.*, 1999; Dyll *et al.*, 2004; Timmis *et al.*, 2004; Reyes-Prieto *et al.*, 2007; Bock and Timmis, 2008). The nuclear control over organellar functions is termed “anterograde control/anterograde signaling/anterograde regulation” and is complemented by a backward flow of information from the organelles to the nucleus, thus enabling nuclear gene expression to be modified in accordance to their status. This process is termed “retrograde control/retrograde signaling/retrograde regulation” and allows cellular adjustments in response to different kinds of stresses: abiotic, biotic and mutations (Rodermeil, 2001; Butow and Avadhani, 2004).

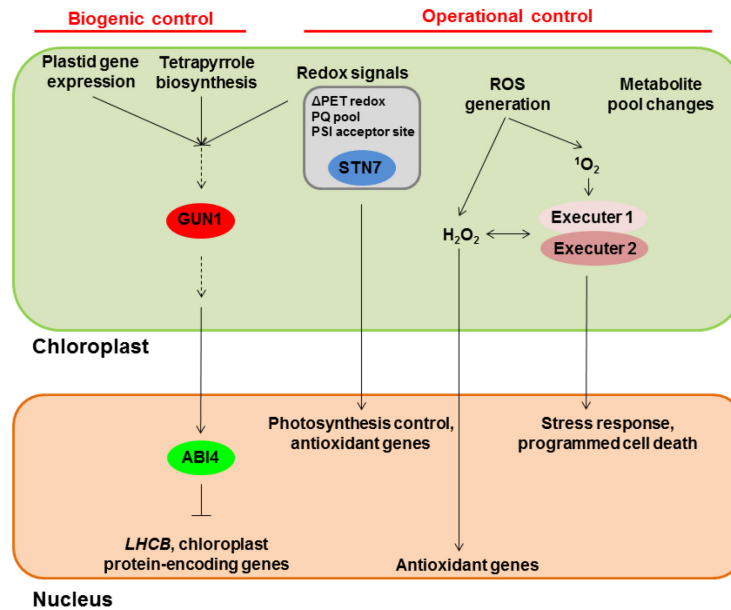


**Figure 4 Chloroplast-to-nucleus retrograde signaling.** The figure depicts chloroplast-to-nucleus retrograde signaling with two major control systems. The biogenic control takes place in early plastid development and includes all signals from plastid gene expression and tetrapyrrole biosynthesis. The operational control takes place in fully functional chloroplasts that perform photosynthesis and enables adjustment of nuclear gene expression in response to environmental changes. It includes the ROS production, the redox processes and metabolite pool changes. GUN1: genomes uncoupled 1; ABI4: abscisic acid insensitive 4;  $\Delta$ PET: impairment of photosynthetic electron transport chain; PQ: plastoquinone; PSI: photosystem I; STN: a thylakoid protein kinase; *LHCb*: gene encoding photosystem II chlorophyll a/b-binding protein. Image modified after Woodson and Chory, 2008.

### 1.2.1 The retrograde signaling from plastids to the nucleus

Plastid to nucleus retrograde signaling has been intensively studied in the last 30 years with five major groups being described depending on where the signals originate from: i) plastid gene expression (PGE) including transcription and translation; ii) pigment biosynthesis i.e. intermediates of tetrapyrrole and carotenoid biosyntheses; iii) reactive oxygen species (ROS) generation and ROS-related processes; iv) redox processes in photosynthesis and v) metabolite pool changes (Gray *et al.*, 2003; Nott *et al.*, 2006; Pesaresi *et al.*, 2007; Pogson *et al.*, 2008; Woodson and Chory, 2008; Kleine *et al.*, 2009; Pfannschmidt, 2010; Inaba *et al.*, 2011). Recently, the plastid signals have been alternatively classified based on the developmental stage of the plastid into “biogenic control” and “operational control” (Pogson *et al.*, 2008). The biogenic control takes place in early plastid development and includes all signals from PGE and pigment biosynthesis. They inform the nucleus

about the progress of the chloroplast developmental program. Secondly, the operational control takes place in fully functional chloroplasts that perform photosynthesis and enables rapid adjustments of nuclear gene expression in response to environmental changes. It includes the ROS production, the redox processes and metabolite pool changes (Fig. 4) (Pogson *et al.*, 2008). In addition, a third control was recently proposed and termed “degradational control”. It includes the signals generated by chloroplasts in old tissues or at the end of the vegetative stage (Pfannschmidt, 2010).

#### 1.2.1.1 The biogenic control

The first indication of a plastid-derived signal came from the analysis of Calvin cycle enzymes in the barley (*Hordeum vulgare* L.) *albostrians* and *Saskatoon* mutants. The white tissue of the *albostrians* leaves is deficient in plastid ribosomes and was shown to have decreased phosphoribulokinase and NADPH-glyceraldehyde-3-phosphate enzyme activities leading to the hypothesis of a plastid-derived signal since both enzymes are nuclear encoded (Bradbeer *et al.*, 1979). Moreover, further studies showed that a whole set of photosynthesis-related genes was down-regulated in the mutant while the mRNA levels of the stress-induced gene for chalcone synthase was up-regulated (Hess *et al.*, 1994).

Application of plastid translation inhibitors (chloramphenicol, erythromycin, lincomycin and streptomycin) and transcription inhibitors (tagetitoxin, rifampicin) also resulted in decreased expression of nuclear-encoded photosynthesis genes. However, the effect was present only in the first 2-3 days of seedling development (Rapp and Mullet, 1991; Adamska, 1995; Gray *et al.*, 2003). Furthermore, lincomycin and erythromycin negatively affected nuclear transcription also in the dark when applied to *lip1* (*light-independent photomorphogenesis 1*) or *cop1* (*constitutively photomorphogenic 1*) mutants that exhibit photomorphogenesis in the dark (Sullivan and Gray, 1999). This indicates that light is not an essential factor for this signaling pathway, but does not exclude the involvement of light-responsive developmental programs.

A recent study on *Arabidopsis* mutants with defects in organellar ribosomal L11 proteins demonstrate that a moderately impaired plastid translation (*prpl11*

mutant) does not lead to a strong down-regulation of nuclear photosynthetic genes, but an additional impairment in mitochondrial translation (*mrpl11* mutant) is necessary to obtain this effect (Pesaresi *et al.*, 2006). The same effect was observed when investigating the mutant with down-regulated PRORYL-tRNA SYNTHETASE 1 (PRORS1), an enzyme that is dual targeted to plastids and mitochondria. While complete absence of this gene is embryolethal, leaky mutants survive and exhibit strong down-regulation of nuclear photosynthesis gene transcription (Pesaresi *et al.*, 2006). This proves that plastid and mitochondrial translation can synergistically affect nuclear gene expression. However, in *prpl11*, *mrpl11*, and *prors1* mutants translation is just moderately impaired, while in *albostrians* and lincomycin-treated seedlings it is completely arrested. This demonstrates that complete absence of plastid translation or moderate reduction in both plastid and mitochondria is responsible for influencing photosynthesis gene expression.

The first genetic approach designed to identify components of plastid retrograde signaling was performed by growing *Arabidopsis* seedlings on medium containing norflurazon, a carotenoid biosynthesis inhibitor that induces the formation of white, photo-bleached seedlings under standard growth conditions. Five “genomes uncoupled” (*gun1*, *gun2*, *gun3*, *gun4* and *gun5*) mutants have been isolated that express *LHCB* under photobleaching conditions, proving that plastid-to-nucleus communication is disturbed (Susek *et al.*, 1993). GUN2, GUN3, GUN4 and GUN5 belong to the tetrapyrrole biosynthetic pathway (Fig. 5) whose major products are chlorophyll and heme (Nott *et al.*, 2006). Genome uncoupled mutants *gun2* (*hy1*) and *gun3* (*hy2*) have mutations in heme oxygenase and phytylchromobilin synthase, components of the heme branch of the tetrapyrrole biosynthetic pathway (Masuda and Fujita, 2008). GUN4 binds both protoporphyrin IX and Mg-protoporphyrin IX and stimulates the activity of Mg-chelatase (Davison *et al.*, 2005; Verdecia *et al.*, 2005). Disruption of *GUN4* reduces the cellular levels of heme, suggesting that GUN4 is also involved in heme biosynthesis and thus may control the flow of substrate into the heme or chlorophyll branch (Larkin *et al.*, 2003; Wilde *et al.*, 2004; Masuda and Fujita, 2008). *GUN5* encodes the H-subunit of Mg-chelatase (Mochizuki *et al.*, 2001) that catalyses the conversion of protoporphyrin IX (protoIX) to Mg-protoIX thereby implying Mg-protoIX could be the signaling molecule responsible for conducting the signal from plastid to the nucleus (Strand *et al.*, 2003; Ankele *et al.*, 2007). However,



recent investigations doubt the initial hypothesis that Mg-proto IX is the signaling molecule (Mochizuki *et al.*, 2008; Moulin *et al.*, 2008).

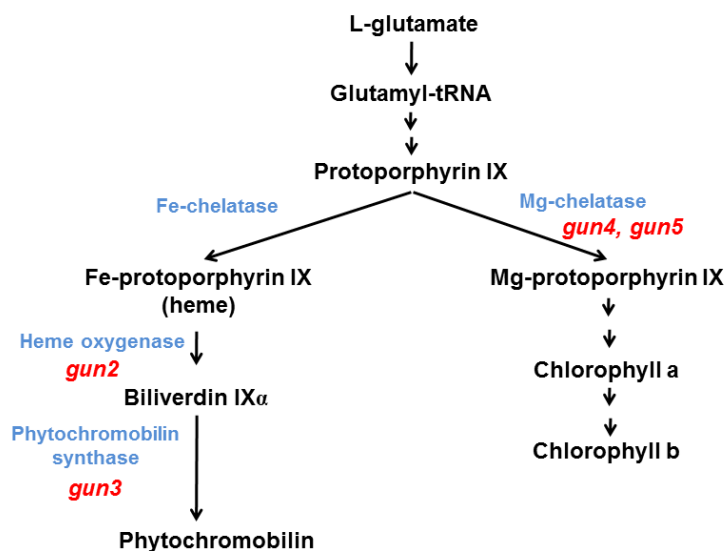


**Figure 5 Tetrapyrrole biosynthetic pathway.** The different steps in tetrapyrrole biosynthesis are indicated by arrows and the most important intermediates are provided. Protoporphyrin IX can be converted either to Fe-protoporphyrin IX (haem), leading to phytychromobilin, or to Mg- protoporphyrin IX leading to chlorophyll. Mutants for enzymes involved in tetrapyrrole biosynthesis are indicated by italic letters. *gun*: genome uncoupled. Image modified after Kleine *et al.*, 2009.

While GUN2-GUN5 are involved in tetrapyrrole biosynthesis, GUN1 is a chloroplast localized pentatricopeptide repeat (PPR) protein that has high similarity to PLASTID TRANSCRIPTIONALLY ACTIVE CHROMOSOME PROTEIN 2 (PTAC2) (Koussevitzky *et al.*, 2007). PTAC2 is a component of a large multi-protein complex associated with plastid transcription (Pfalz *et al.*, 2006) and was shown to colocalize with GUN1 (Koussevitzky *et al.*, 2007). While other PPR proteins are known to bind RNA and modulate organellar RNA metabolism (Schmitz-Linneweber and Small, 2008), the function of GUN1 might be different, a possible role in plastid gene expression being implied. Further investigations have shown that GUN1 and GUN5 are components of the same pathway, with GUN1 acting downstream of GUN5. Moreover, *gun1*, but not other *gun* mutants, was shown to derepress the expression of nuclear photosynthesis genes also in the presence of lincomycin, making it also a component of the PGE pathway (Koussevitzky *et al.*, 2007).

Another important component of the plastid retrograde signaling was discovered by analyzing the promoter regions of the genes derepressed in both *gun1* and *gun5*. An ACGT motif, the core of both the light-responsive G box (CACGTG) (Terzaghi and Cashmore, 1995) and the abscisic acid (ABA) response element (ABRE) (Himmelbach *et al.*, 2003) appeared frequently leading to the hypothesis of ABA involvement in signaling. ABI4, an AP2-like transcription factor involved in response to abscisic acid was identified as a component of the retrograde pathway acting downstream of GUN1 (Koussevitzky *et al.*, 2007). However, other ABA-deficient mutants did not show a *gun* phenotype indicating that ABA is unlikely to be the actual retrograde signal (Koussevitzky *et al.*, 2007). Nevertheless, other experiments proved that GUN5 specifically binds ABA (Shen *et al.*, 2006; Wu *et al.*, 2009c).

#### 1.2.1.2 The operational control

Photosynthetic light energy fixation is a highly sensitive process that requires rapid adjustments in response to environmental and developmental constraints (Pfannschmidt, 2005). Several compensation mechanisms have evolved in order to maintain high efficiency under such variable conditions (Walters, 2005): regulation of enzyme activities (Buchanan *et al.*, 1994), adaptation of plastid gene expression (Pfannschmidt and Liere, 2005) and changes in nuclear gene expression (Fey *et al.*, 2005). Plastid to nucleus signaling is an important mechanism for regulating nuclear gene expression and several components have already been identified. Reactive oxygen species (ROS) generation (Wagner *et al.*, 2004) and redox processes in photosynthesis (Pfannschmidt *et al.*, 2003; Fey *et al.*, 2005) are plastid-localized processes that were shown to induce a nuclear responses.

Reactive oxygen species (ROS) are permanently produced as byproducts of numerous metabolic pathways in several cell compartments with a major site for ROS production being represented by the energy-transducing organelles, chloroplasts and mitochondria. The chloroplastic electron transport chain produces singlet oxygen ( $^1\text{O}_2$ ) at PSII (Rinalducci *et al.*, 2004; Krieger-Liszkay, 2005) and on the acceptor site of PSI, electron transfer to  $\text{O}_2$  can result in the production of superoxide ( $\text{O}_2^-$ ), hydrogen peroxide ( $\text{H}_2\text{O}_2$ ) and hydroxyl radicals ( $\text{OH}^\bullet$ ) (Ivanov and Khorobrykh, 2003). Singlet oxygen ( $^1\text{O}_2$ ) and hydrogen peroxide ( $\text{H}_2\text{O}_2$ ) function as signals in chloroplast to nucleus retrograde signaling (Nott *et al.*, 2006; Pogson *et al.*, 2008).

Hydrogen peroxide has induced the expression of the high-light (HL)-inducible cytosolic ascorbate peroxidase *APX1* and *APX2*, the zinc finger transcription factors *ZAT10* and *ZAT12* and the chlorophyll-binding protein *ELIP2* (Davletova et al., 2005; Rossel et al., 2007). Due to its longer half-life and lower toxicity when compared to other ROS,  $H_2O_2$  is believed to act as an intra- and intercellular signaling molecule (Vranova et al., 2002; Mullineaux et al., 2006). Chloroplast-derived singlet oxygen ( $^1O_2$ ) might also play an important role in retrograde signaling. However, it has short half-life and limited diffusion, making it a probable short-distance signal (Krieger-Liszkay, 2005). The *Arabidopsis fluorescent (flu)* mutant enabled the study of  $^1O_2$  – generated effects by a controlled dark-light cycle. Two thylakoid-localized proteins, EXECUTER1 (EX1) and its homologue EXECUTER2 (EX2) were identified as putative  $^1O_2$  –signaling components (Wagner et al., 2004; Lee et al., 2007).

The redox state of the components of photosynthetic ETC is also a source of signal in chloroplast to nucleus retrograde signaling (Pfannschmidt and Liere, 2005). The signal is triggered by the redox state of the plastoquinone pool (PQ) and the thioredoxin system. Recently, a thylakoid-localized protein kinase STN7 (Bonardi et al., 2005) has been identified that senses PQ redox signals and transduces them via putative phosphorylation cascades to the gene expression machinery (Pfannschmidt et al., 2009).

GUN1 and ABI4 were also shown to be involved in PET-derived signaling. While *Zat10* and *Zat12* are highly expressed in response to high light, their expression was delayed in *gun1* and *abi4* mutants. Altogether, ABI4 and GUN1 play a role in three retrograde signaling pathways: plastid gene expression, tetrapyrrole biosynthesis and PET-derived signaling, in agreement with a previously proposed “master switch”, which controls the expression of a large number of nuclear genes in response to plastid-derived signals (Richly et al., 2003; Koussevitzky et al., 2007).

### 1.2.2 The retrograde signaling from mitochondria to the nucleus

The retrograde signaling from mitochondria to the nucleus is currently named mitochondrial retrograde regulation (MRR) (Rhoads and Subbaiah, 2007) and, in comparison to chloroplast retrograde regulation, it is a young field with mechanisms and components that are just beginning to be discovered (Fig. 6) (Rhoads, 2011).

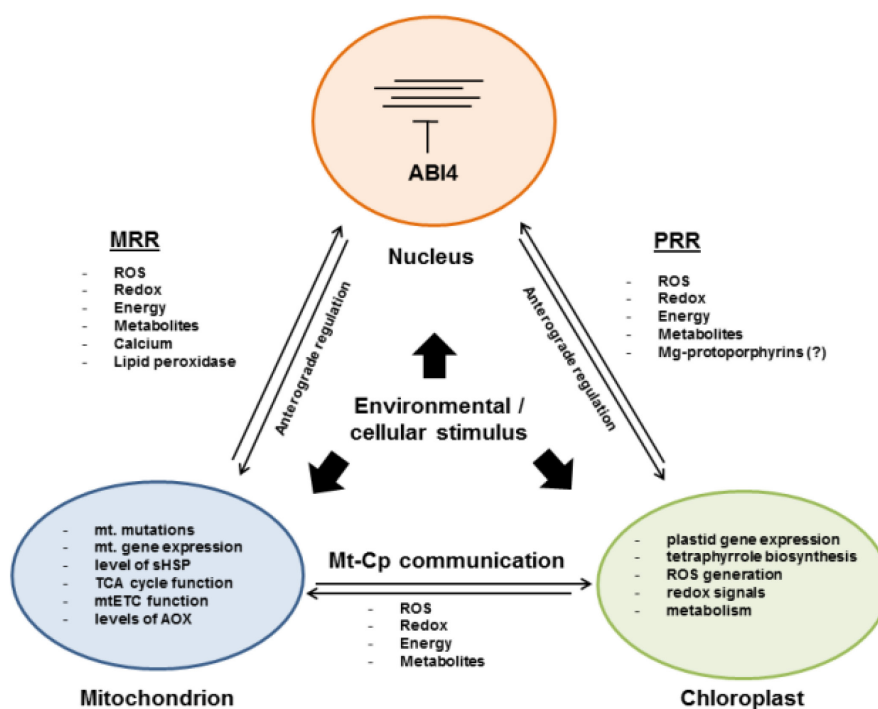


**Figure 6 Schematic representation of inter-organellar communication in plants.** Environmental and / or cellular changes cause altered functions in all organelles. Changes in nuclear gene expression can result in alteration of organelle functioning, a process termed anterograde regulation. The backward flow of information, from plastid / chloroplast or mitochondrion to the nucleus is termed mitochondrial retrograde regulation (MRR) or plastid retrograde regulation (PRR). A permanent communication between mitochondria (Mt) and chloroplasts (Cp) takes place within the cell. ROS: reactive oxygen species; ABI4: abscisic acid insensitive 4; mt.: mitochondria; sHSP: small heat shock proteins; TCA: tricarboxylic acid; mtETC: mitochondrial electron transport chain; AOX: alternative oxidase. Image modified after Rhoads, 2011.

Until now, several factors determining mitochondrial dysfunctions were shown to be initiators of MRR: mutations, chemical inhibitors, biotic and abiotic stress (Rhoads, 2011). One of the well-studied mutations that induce mitochondrial dysfunction is the family of maize nonchromosomal stripe (NCS) mutants (Newton *et al.*, 2004). NCS mutants are impaired in mitochondrial function due to mtDNA rearrangement (NCS2) or gene deletion (NCS3, NCS4, NCS5, NCS6) and show a variegated leaf phenotype. As a consequence of impaired mitochondrial function, there exists a unique pattern of AOX genes induction (Karpova *et al.*, 2002), as well as expression of nucleus-encoded heat shock proteins (HSPs) (Kuzmin *et al.*, 2004). The CMSII mutant of tobacco, which lacks functional Complex I exhibits an adjustment of the cellular redox state as well as increased expression of AOX and alternative NAD(P)H dehydrogenase activity (Gutierrez *et al.*, 1997; Dutilleul *et al.*,

2003). The induction of alternative oxidase genes following mtETC inhibition with chemical inhibitors (rotenone, antimycin A etc.) has been extensively studied (Mackenzie and McIntosh, 1999; Rhoads and Subbaiah, 2007) and the results further confirm the retrograde pathways obtained by affecting the same components of mtETC as in NCS mutants.

Apart from the previously presented examples, plant mitochondria are also believed to be stress sensors, perceiving environmental signals and adjusting the plant metabolism accordingly by MRR. Oxygen deprivation, heat stress, oxidative stress and aluminium stress were shown to be connected to altered mitochondrial functions and specifically induced nuclear responses (Basu *et al.*, 2001; Yamamoto *et al.*, 2002; Geigenberger, 2003; Rhoads *et al.*, 2005; Licausi *et al.*, 2011).

Although the precise roles have not yet been elucidated, there is increasing evidence that mitochondria play important roles during pathogen attack and MRR might be involved (Curtis and Wolpert, 2002; Ordog *et al.*, 2002; Samuel *et al.*, 2005; Zaninotto *et al.*, 2006). One example is represented by the hypersensitive response, a form of programmed cell death that occurs at the site of infection to limit pathogen spread (Zaninotto *et al.*, 2006). The current hypothesis connects the hypersensitive response to the alternative respiratory pathway, especially with increased AOX functioning. This assumption is supported by the observation that over-expression of AOX in tobacco plants results in smaller lesions after the infection with tobacco mosaic virus (Ordog *et al.*, 2002).

One key problem in understanding MRR is the lack of information about the signaling components from mitochondria to the nucleus. There are data suggesting that reactive oxygen species (ROS) can be involved in MRR, producing a unique ROS profile or “signature” for various treatments (Mahalingam and Fedoroff, 2003; Gadjev *et al.*, 2006). However, ROS signaling is complex and difficult considering the imprecise methods for quantifying individual ROS, the existence of ROS metabolizing enzymes, short-life and the general high-ROS response of various biotic and abiotic stresses (Apel and Hirt, 2004). Apart from ROS, calcium level changes, redox changes and modifications in metabolite levels are leading candidates for nonprotein signaling components (Butow and Avadhani, 2004; Foyer and Noctor, 2005). Potential protein components of MRR are represented by several signal transduction proteins (protein kinases) and transcription factors (Pitzschke and Hirt, 2006; Ho *et al.*, 2008). Until now, the only specific protein that was shown to be

involved in plant MRR is represented by the Absciscic Acid Insensitive 4 (ABI4) transcription factor. Recent investigations have shown that ABI4 acts as promoter-binding, negative regulator of gene expression that allows derepression during MRR (Giraud *et al.*, 2009).

Growing evidence indicates that MRR overlaps with other signaling pathways, including those from chloroplast (see 1.2.1). This situation is a result of the two organelles being intimately connected through energy status, metabolism, ROS and redox status (Raghavendra and Padmasree, 2003; van Lis and Atteia, 2004). Pesaresi *et al.* (2006) demonstrated the existence of such a mechanism by using mutants of prolyl-tRNA synthetase: a chloroplast form, a mitochondrial form and the double mutant. While single mutants did not result in down-regulation of nuclear genes encoding photosynthetic proteins, the double mutant was the only one that presented this molecular phenotype (Pesaresi *et al.*, 2006). A common component of plastid and mitochondrial retrograde regulation is represented by ABI4 (see 1.2.1 and Giraud *et al.*, 2009).

### **1.3 The plant chondriome**

#### **1.3.1 Chondriome organization in higher plants**

The plant chondriome, that represents all the mitochondria within a cell, is typically organized as a population of several hundred physically discrete organelles that have circular, vermiform or sausage-like shape (Logan, 2006). A number of 600-700 mitochondria could be observed in tobacco and *Medicago truncatula* mesophyll protoplasts (Sheahan *et al.*, 2004; Sheahan *et al.*, 2005a), approximately 400 mitochondria in *Arabidopsis thaliana* roots (Kato *et al.*, 2008) and up to 10000 mitochondria in onion bulb epidermal cells (Arimura *et al.*, 2004b). This structure is in contrast with the more tubular and reticular organization in yeast and animals. While in the yeast *Saccharomyces cerevisiae* the chondriome is organized as a network of interconnected tubules (Hermann and Shaw, 1998; Okamoto and Shaw, 2005), in animal cells the structure is variable depending on animal and cell type, but

generally being tubular and ramified (Fig. 7A, B, C) (Bereiter-Hahn and Voth, 1994; Otera and Mihara, 2011).

Together with the pleomorphic structure, plant mitochondria are also highly dynamic, moving through the cytoplasm with speeds up to  $10 \mu\text{m s}^{-1}$  (Watanabe *et al.*, 2007; Zheng *et al.*, 2009) and being involved in frequent fusion and fission events (Arimura *et al.*, 2004b). This observation led to the “discontinuous whole” hypothesis that proposes the existence of a ‘need to meet’ phenomenon: frequent mitochondria fusion and fission events are thought to be necessary for mixing and exchanging of mtDNA, membranes and metabolites that altogether determine a proper functioning of plant mitochondria (Logan, 2006).

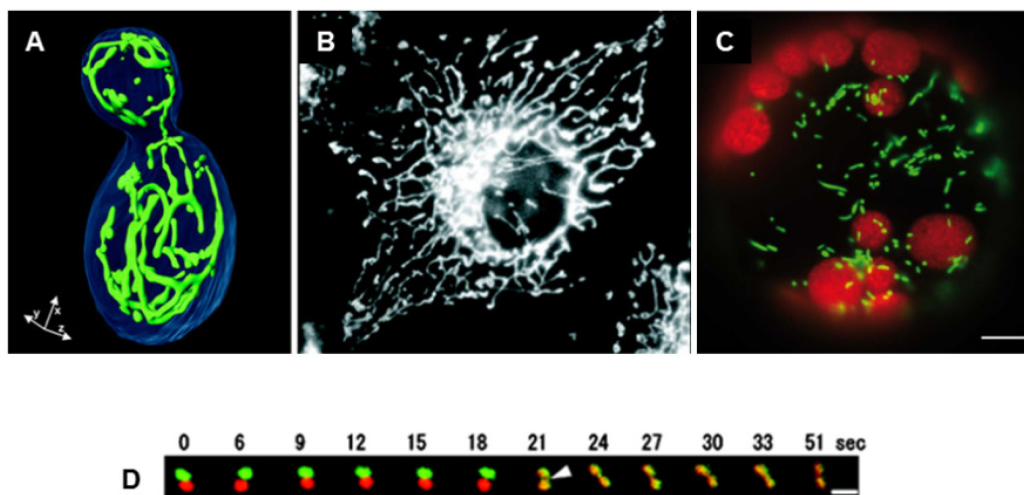


**Figure 7 Chondriome organization in yeast, animals and plants.** A) Branched mitochondrial network from a *S. cerevisiae* cell. A cell expressing mitochondria-targeted GFP was grown on the non-fermentable carbon source glycerol to logarithmic growth phase. The cell was stained with calcofluor white and the 3D image was obtained with a confocal microscope. Reproduced from Egner *et al.*, 2002; B) Extended and interconnected mitochondrial filaments in a COS-7 cell (African green monkey fibroblast). Mitochondria were stained by indirect immunofluorescence against cytochrome c. Reproduced from Westermann, 2002 after Ansgar Santel, Stanford University, CA.; C) Plant chondriome in an *Arabidopsis* leaf protoplast from a stable transgenic line expressing GFP in mitochondria. Reproduced after Scott and Logan, 2008a; D) Time-course observations of green (Kaede) and red (photoconverted Kaede) mitochondria fusion in onion bulb epidermal cell. The appearance of yellow mitochondria demonstrates the fusion process between two distinct mitochondria. Reproduced after Arimura *et al.*, 2004b.

### 1.3.2 Fusion and fission of plant mitochondria

Fusion and fission are two processes that control mitochondrial shape, size and number, and up to now, several investigations have been performed in order to identify the proteins involved in their control.

While several components of the yeast and animal fusion apparatus have already been identified and studied (Hermann and Shaw, 1998; Wong *et al.*, 2000; Santel and Fuller, 2001; Olichon *et al.*, 2002), homology searches did not identify any component involved in plant mitochondrial fusion. Even if genetic evidence is missing, there is no doubt that plant mitochondria fuse. In order to clearly prove and quantify mitochondrial fusion, Arimura *et al.* (Arimura *et al.*, 2004b) transiently expressed in onion epidermal cells, a matrix-targeted fluorescent protein called Kaede that can change its emission spectrum by illumination with UV light. After converting half of the organelles in a single cell from green to red, the appearance of yellow mitochondria undoubtedly proved the fusion of the organelles. After only 1-2 hours the mitochondria showed a uniformly yellow color, indicating that fusion is a relatively rapid and constitutive event (Fig. 7D).

Extensive fusion of mitochondria, termed massive mitochondria fusion (MMF) could be observed before the first division of freshly-isolated protoplasts, a process that was shown to appear only during dedifferentiation (Sheahan *et al.*, 2005a). Moreover, mitochondrial reticulation is a permanent process that appears in shoot apical meristem and leaf primordium (Segui-Simarro *et al.*, 2008), an event that is believed to be necessary for homogenization of mtDNA and proteins prior to gamete formation (Segui-Simarro and Staehelin, 2009).

The mitochondrial division apparatus has been intensively studied in the last years with several components being discovered. Most studies have been performed in *S. cerevisiae* where at least four proteins were shown to be involved in the division process: Dnm1p, Mdv1p, Caf4p and Fis1p (Otsuga *et al.*, 1998; Mozdy *et al.*, 2000; Tieu and Nunnari, 2000; Okamoto and Shaw, 2005). The proteins involved in plant mitochondrial division were identified by homology searches to known yeast and mammalian proteins but also by investigating mitochondrial morphology mutants obtained by chemical mutagenesis. Two dynamin-like proteins, DRP3A and DRP3B were shown to be implicated in mitochondrial division by localization to constriction



sites of dividing mitochondria. Genetic knockout of these genes leads to an increased number of large, elongated mitochondria (Arimura and Tsutsumi, 2002; Arimura *et al.*, 2004a; Logan *et al.*, 2004). In *Arabidopsis* also exist two orthologues of Fis1p, termed BIGYN 1 and BIGYN2 located in the outer mitochondrial membrane. Disruption of either gene leads to a decrease in mitochondrial division as evidenced by a decrease in organelle number per cell and increased size (Scott *et al.*, 2006). Recently, another component of the fission apparatus has been identified in a screen for novel plant mitochondrial morphology proteins (Logan *et al.*, 2003). The NETWORK mutant exhibits an elongated mitochondria phenotype and the respective protein was shown to interact with DRP3A and DRP3B, supporting the supposition that NETWORK might function as an adapter protein, similar to Mdv1p / Caf4 in yeast (Arimura *et al.*, 2008).

### 1.3.3 Mitochondrial motility

Plant mitochondria are highly motile organelles that can change their position in the cytoplasm with high speed. For example, in growing root hairs mitochondria moved with a gradient of velocities between 0.6 and 10  $\mu\text{m s}^{-1}$  depending on the position in the hair (Zheng *et al.*, 2009), single organelle tracking in tobacco BY2 cells revealed average speeds of 0.1 - 0.5  $\mu\text{m s}^{-1}$  (Watanabe *et al.*, 2007) and values of 0.16 to 10.35 were measured in *Picea wilsonii* pollen tubes (Zheng *et al.*, 2010). While movement of mitochondria in mammals and most yeast is microtubule based (Boldogh and Pon, 2007), mitochondria in *S. cerevisiae*, *Aspergillus* and plants move predominantly on the actin cytoskeleton (Simon *et al.*, 1995; Olyslaegers and Verbelen, 1998; Van Gestel *et al.*, 2002; Sheahan *et al.*, 2004) with microtubules playing just a role in maintaining the geometry of the actin cytoskeleton (Zheng *et al.*, 2009).

Myosins, the motor proteins that propel cargo along the actin fibers, have been shown to be involved in movement of plant mitochondria and other organelles. The *Arabidopsis* myosin gene family contains 17 members, four of them being involved directly or indirectly in the movement of mitochondria in *N. benthamia*: XI-C, IX-E, IX-I and IX-K (Avisar *et al.*, 2008; Sparkes *et al.*, 2008; Avisar *et al.*, 2009). Except from the myosin-motor dependent mechanism, mitochondria were shown to move

also on a myosin-motor independent mechanism in which the rate of actin turnover plays an important role (Zheng *et al.*, 2009).

A novel group of proteins belonging to the family of MIRO-GTPases has been recently proposed to be involved in mitochondrial dynamics in *Arabidopsis*. From the three Miro orthologues, two are transcribed ubiquitously. Knockout of *MIRO2* had no effect on plant development but mutation of *MIRO1* led to arrest of embryogenesis and impaired pollen germination and tube growth (Yamaoka and Leaver, 2008). These effects are due to an abnormal morphology of pollen mitochondria, being larger and more tubular than wild type. Moreover, a disruption in their normal streaming movement within the pollen tube could also be observed (Yamaoka and Leaver, 2008). Recent investigations proved that in *miro1* mutant egg cells mitochondria are abnormally enlarged and the two-celled embryo contained a significantly reduced number of mitochondria in its apical cell compared with the wild type, suggesting that the *miro1* mutation inhibits proper intracellular distribution of mitochondria. The findings prove that proper mitochondrial morphology and intracellular distribution are maintained by MIRO1 and are vital for embryonic cell division (Yamaoka *et al.*, 2011).

#### **1.3.4 Metabolic control of mitochondrial motility and morphology**

The metabolic status of the cell is an important factor influencing mitochondrial dynamics. In plants, changes in mitochondrial size and motility have been observed in several conditions as senescence, cell death, anoxia, cold and oxidative stress (Van Gestel and Verbelen, 2002; Yoshinaga *et al.*, 2005; Armstrong *et al.*, 2006; Zottini *et al.*, 2006; Scott and Logan, 2008a; b).

Cell death represents one of the best described metabolic conditions that influence mitochondrial dynamics. Treatment of *Arabidopsis* protoplasts with strong oxidants or heat shock determines changes in the inner membrane permeability and probably in the mitochondria-cytoskeleton interactions that finally lead to an increase in size and arrest of motility (Yoshinaga *et al.*, 2005; Scott and Logan, 2008b). In other observations, senescent *Medicago truncatula* cell suspensions contained giant mitochondria that were associated with dying cells (Zottini *et al.*, 2006). Moreover, low oxygen pressure induces fast and reversible formation of giant mitochondria that

have unusual shapes, length of  $\sim 80 \mu\text{m}$  and even form a reticulum (Van Gestel and Verbelen, 2002).

Another important aspect in mitochondrial dynamics is represented by the association with energy-consuming structures and organelles (Bereiter-Hahn and Voth, 1994). While in non-plant organisms such interactions have already been described, in plants this aspect is still discussed. As it was previously shown, in plant tissues containing chloroplasts, there exists a frequent association of these two organelles (Fig. 8) (Stickens and Verbelen, 1996; Logan and Leaver, 2000; Sheahan *et al.*, 2004). It is supposed that proximity is needed in order to facilitate exchange of respiratory gases and metabolites between the two metabolically-connected organelles. A recent paper shows that chloroplast moving under different light regimes was associated with changes in the location of mitochondria (Islam *et al.*, 2009; Islam and Takagi, 2010). These observations open the door to new investigations regarding the influence of chloroplasts on mitochondrial dynamics.

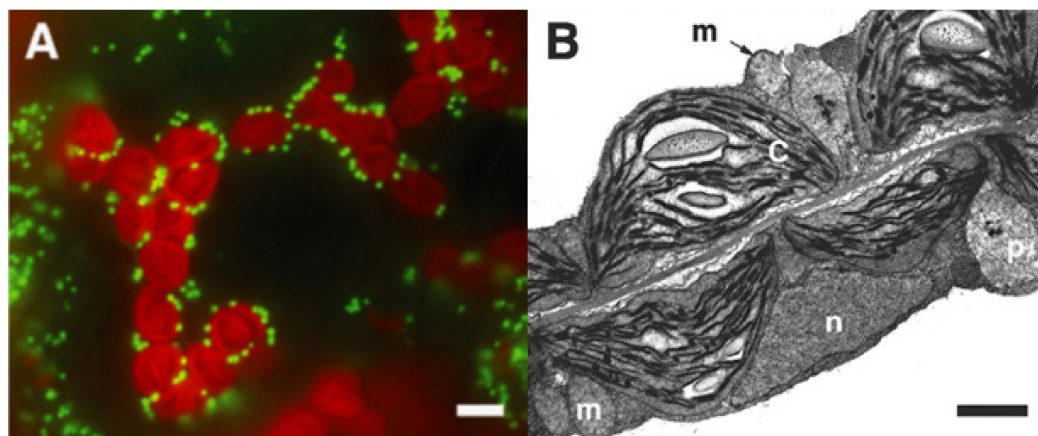


**Figure 8 Association between mitochondria and chloroplasts.** Close association between mitochondria and chloroplasts can be observed in *Arabidopsis* mesophyll tissue of a 14 day-old seedling. A) Association between mitochondria (mitochondrial targeted GFP, green) and chloroplasts (autofluorescing, red). Scale bar:  $1 \mu\text{m}$ . B) Transmission electron micrograph of the same material presenting the organelles in the cortical cytoplasm of mesophyll cells (m: mitochondria; n: nucleus; c: chloroplast; p: peroxisome). Scale bar:  $5 \mu\text{m}$ . Image reproduced after Logan, 2010.

## 1.4 Higher plant organellar genomes

### 1.4.1 The plastome

Following the putative single endosymbiotic event that resulted in the present-day plastids, massive gene transfer took place from the newly acquired organelle to the nucleus, resulting in dramatic size reduction of its genome: whereas the genome of the cyanobacteria *Synechocystis* contains more than 3000 genes (Kaneko *et al.*, 1996), the plastid genome of land plants (termed “plastome”) harbors only approximately 115 genes (Fig. 9). Gene transfer from the plastid to the nucleus is considered “frequent and in big chunks”, being an on-going process (Martin, 2003; Stegemann *et al.*, 2003; Stegemann and Bock, 2006).

Generally, the plastid genome (plastome) is maternally inherited in most plant species and thus excluded from sexual recombination, paternal transmission being excluded by several mechanisms: organelle exclusion by unequal cell division, plastid destruction or selective degradation of plastid DNA from the paternal parent. However, paternal plastid transmission exists in conifers and biparental inheritance in some eudicot angiosperms (Hagemann, 2004; Hagemann, 2010).

In contrast to the reduced nuclear ploidy, plant cells are highly polyploid for their plastid genomes, 1000-1700 copies being present in a single leaf cell without significant differences during leaf development and senescence (Li *et al.*, 2006; Zoschke *et al.*, 2007). In contrast, non-green plastids often possess fewer plastomes: the copy number in root plastids being about one fifth of that in chloroplasts (Aguettaz *et al.*, 1987; Isono *et al.*, 1997). Multiple copies are densely packed into nucleoprotein structures called nucleoids, several nucleoids being present in a single plastid depending on species and developmental stage: proplastids often contain only a single nucleoid, while mature chloroplasts can easily contain several or even dozens of nucleoids (Kuroiwa, 1991).

The plastid genome of higher plants maps as a single circular molecule of double-stranded DNA (ptDNA) with sizes varying between 120-160 kb (Sugiura, 1989; 1992; Wakasugi *et al.*, 2001; Wicke *et al.*, 2011). However, electron microscopic investigations and pulse-field gel electrophoresis revealed a great structural plasticity: in addition to genome-sized circles, various linear and branched

conformations have been identified (Bendich and Smith, 1990; Lilly *et al.*, 2001; Bendich, 2004; Oldenburg and Bendich, 2004).

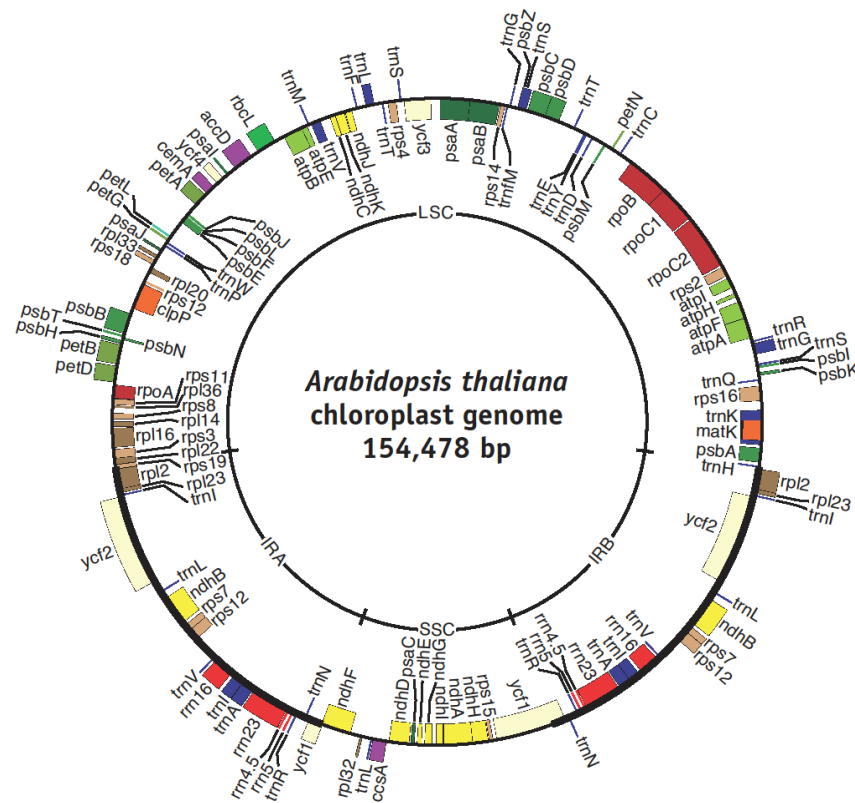


**Figure 9** **Plastid genome of *Arabidopsis thaliana*.** The plastid genome of *Arabidopsis thaliana* has a tetrapartite structure with two inverted repeats (IR<sub>A</sub> and IR<sub>B</sub>) separated by a small single copy region (SSC) and a large single copy region (LSC). The plastome comprises ~ 120 genes encoding 87 proteins, 4 rRNAs and 30 tRNAs. Hypothetical chloroplast reading frames (*yef*) are colored in white. Made with OGDRAW v1.2 (Lohse *et al.*, 2007).

### 1.4.2 The chondrome

#### 1.4.2.1 The structure of plant mitochondrial genome

Land plants possess particularly complex mitochondrial genomes that are characterized by a multitude of peculiarities. While the mitochondrial genome of animals (metazoan) is small and compact, rarely exceeding 16-17 kbp (Anderson *et al.*, 1981; Lavrov, 2007; Gissi *et al.*, 2008), higher plant mitochondrial genome is

large and complex with sizes varying between 208 kbp in white mustard (*Brassica hirta*) and over 2900 kbp in muskmelon (*Cucumis melo*) (Ward *et al.*, 1981; Palmer and Herbon, 1987; Kubo and Newton, 2008; Alverson *et al.*, 2010). However, plant chondromes do not encode a proportionally higher number of genes: while human mitochondria possess 37 genes in 16 kbp, the model plant *Arabidopsis thaliana* has just 57 genes in 366 kbp (Fig. 10) (Unseld *et al.*, 1997), resulting in a reduced gene density within the genome. The existing genes encode proteins that are subunits of the mitochondrial electron transport chain (ETC) and ATP synthase, ribosomal proteins and also transfer and ribosomal RNAs (Unseld *et al.*, 1997; Kubo *et al.*, 2000; Notsu *et al.*, 2002; Handa, 2003; Clifton *et al.*, 2004; Sugiyama *et al.*, 2005). Several genes contain group II introns that are spliced during RNA maturation (Bonen, 2011). Except from splicing, RNA editing and generation of 5' and 3' ends are also present (Binder *et al.*, 2011; Bruhs and Kempken, 2011).

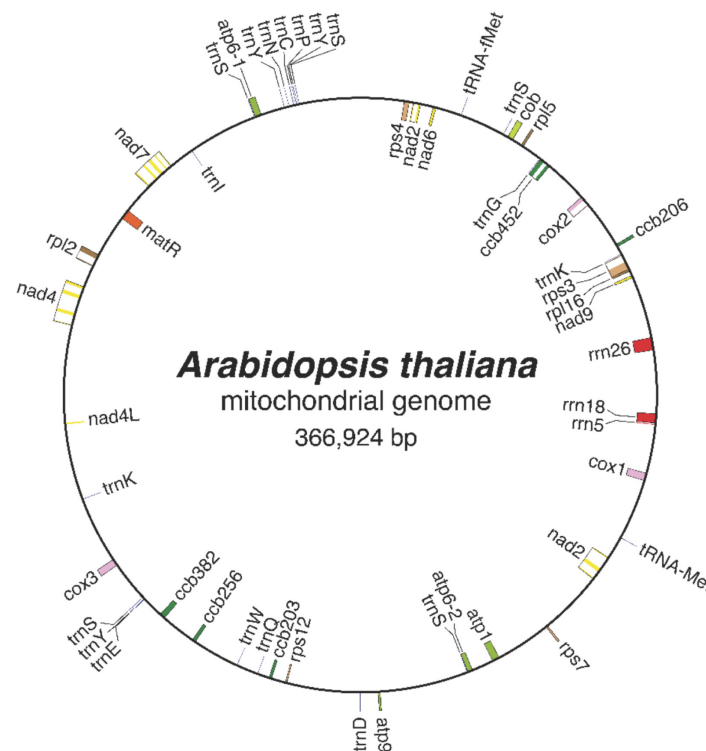


**Figure 10 Mitochondrial genome of *Arabidopsis thaliana*.** The chondrome has a size of 366 kbp and comprises 57 genes that encode components of the mitochondrial electron transport chain, ribosomal proteins and also rRNAs and tRNAs. The existing introns are colored in white (Unseld *et al.*, 1997). Made with OGDRAW v1.2 (Lohse *et al.*, 2007).

An interesting particularity of the plant mitochondrial genome is represented by an ongoing process of endosymbiotic gene transfer (EGT) in recent times of evolution (Timmis *et al.*, 2004). The functional transfer of genes from the mitochondrion to the nucleus has reached an apparent stasis in the animal lineage where the same gene complement is conserved across phylogenetic distances dating back to 500 million years. However, plant mitochondrial gene complement varies widely among angiosperms in particular for *rps*, *rpl* and *sdh* genes (Knoop, 2004; Liu *et al.*, 2009; Knoop *et al.*, 2011). Apart from the variable gene content, fragments of mitochondrial DNA (termed NUMTs, nuclear mitochondrial DNA) have been reported to be present in the nuclear genomes of many eukaryotes (Richly and Leister, 2004; Timmis *et al.*, 2004; Noutsos *et al.*, 2005; Hazkani-Covo *et al.*, 2010).

Besides EGT, plant mitochondrial genomes were showed not only to loose DNA but also to have a surprising ability to integrate and perpetuate foreign DNA (termed “promiscuous DNA”) especially from the nucleus or plastids, a process that does not have a clear physiologic significance (Knoop *et al.*, 2011). An extreme situation is represented by acquisition of foreign DNA *via* horizontal gene transfer (HGT) with host-parasite interactions playing an important role (Archibald and Richards, 2010). Current opinion connects the ability to integrate foreign DNA with two representative features of plant mitochondria: the frequent fusion and fission events and the high recombination activity of mtDNA, which altogether increase the probability of foreign DNA integration (Archibald and Richards, 2010; Knoop, 2011).

The plant mitochondrial genome is usually presented as a circular “master chromosome” comprising all genes and non-coding sequences, which is in balance with sub-genomic circles originating from the master circle by recombination between large direct repeats (Lonsdale *et al.*, 1988). However, the real structure seems to be more complex, as deduced from *in vivo* studies. Until now, circular structures of the size of the master chromosome have not been detected in preparations of plant mtDNA. Instead, mostly linear molecules of different sizes, small circular molecules and more complex molecules were found that altogether have been interpreted as products of recombination and recombination-mediated replication (Bendich, 1996; Oldenburg and Bendich, 1996; Backert *et al.*, 1997; Backert and Börner, 2000). Although the process of mitochondrial genome replication is not well understood, observations of *in vivo* structure points to a recombination-dependent strand invasion

and rolling circle mechanisms (Backert *et al.*, 1997; Backert and Börner, 2000; Oldenburg and Bendich, 2001).

#### 1.4.2.2 Nuclear control of mitochondrial DNA maintenance

A general characteristic of plant chondromes is represented by the existence of multiple repeated sequences of different sizes that are active in homologous recombination. This process occurs with high frequency between large repeated sequences (>1,000 bp) that produce a subdivision of the genome into a complex, inter-recombining population of heterogenous molecules (Fauron *et al.*, 1995). This type of recombination generally results in equimolar amounts of the parental and recombinant forms (Woloszynska, 2010; Arrieta-Montiel and Mackenzie, 2011). Secondly, intermediate repeated sequences (ca. 50 to 500 bp) mediate low-frequency, asymmetric DNA exchange that is associated with the emergence of novel DNA polymorphism, intraspecific genomic variation and substoichiometric shifting (SSS). The process of SSS represents the rapid amplification or suppression of distinct mtDNA configurations that are present in the cell in substoichiometric amounts (approximately one copy per 100-200 cells) (Arrieta-Montiel *et al.*, 2001; Arrieta-Montiel *et al.*, 2009). Usually SSS occurs rarely under natural conditions and may give rise to cytoplasmic male sterility (CMS) and also to spontaneous reversion to fertility (Janska *et al.*, 1998; Sandhu *et al.*, 2007). Small repeated sequences (4-25 bp) are also present in the genomes of higher plants. However, they do not participate in intra- and intermolecular homologous recombination but are believed to participate in nonhomologous end joining (NHEJ), a process involved in double strand breaks repair but also in integrating foreign DNA into mtDNA (Huertas, 2010; Arrieta-Montiel and Mackenzie, 2011).

In the last years, mtDNA recombination has gained a lot of attention and several genes that influence this process have been described (Abdelnoor *et al.*, 2003; Zaegel *et al.*, 2006; Shedje *et al.*, 2007; Maréchal *et al.*, 2008; Shedje *et al.*, 2010). A common characteristic of these proteins is their involvement in the suppression of recombination between repeated DNA sequences. Mutation or elimination of these proteins induces large-scale rearrangements of organellar genomes that perturb their



normal functioning resulting in strong phenotypes like leaf variegation or cytoplasmic male sterility (Maréchal and Brisson, 2010).

The first identified protein is MutS homologue 1 (MSH1, previously *chloroplast mutator* - CHM), a protein with high similarity to bacterial MutS with roles in DNA recombination and mismatch repair (Abdelnoor *et al.*, 2003). Mutation in *MSH1* gene determines a variegated leaf phenotype and extensive mitochondrial genome rearrangements as a result of recombination events at intermediate repeated sequences (108-560 bp) (Arrieta-Montiel *et al.*, 2009). RecA-like recombinases have also been found in the genome of higher plants with functions in plant organelles (Shedge *et al.*, 2007). From the four *RecA* genes present in the nucleus of *Arabidopsis*, *RecA3* was shown to be involved in large-scale mtDNA rearrangements caused by homologous recombination between repeated sequences larger than 150 bp. However, the effect of *RecA3* mutation is different from that observed in *msh1* plants, the affected repeats being a subset of the ones perturbed in *msh1* (Shedge *et al.*, 2007; Arrieta-Montiel *et al.*, 2009). Surprisingly, the mutant plants do not show a phenotype indicating that a certain level of rearrangements can be accepted (Shedge *et al.*, 2007).

The organellar single-stranded DNA-binding proteins (OSB) form a recently discovered family of plant-specific proteins that share an affinity for ssDNA (Vermel *et al.*, 2002; Zaegel *et al.*, 2006). From the four different OSBs present in *Arabidopsis*, OSB1 participates in mtDNA rearrangements that result in variegated and distorted leaf phenotypes in T4 and T5 generations. In some *osb1* plants the accumulation of aberrant mtDNA is reversible by reintroducing a WT *OSB1* allele, but just in the first generations (Arrieta-Montiel *et al.*, 2009). This includes OSB1 in the mitochondrial recombination surveillance machinery in *Arabidopsis*.

The Whirly proteins form another small family of ssDNA-binding proteins that is mainly present in the plant kingdom (Desveaux *et al.*, 2005). While AtWhy1 and AtWhy3 are plastid-localized, AtWhy2 is mitochondria-localized but disruption of the gene does not determine changes in mtDNA. However, when *AtWhy2* is overexpressed, a reduced mtDNA content can be observed together with altered plant morphology (Maréchal *et al.*, 2008). These results were interpreted as indication that the *AtWhy2* gene has a redundant function.

Apart from the proteins involved in the control of mtDNA recombination, plant genomes also encode organellar DNA polymerases (Heinhorst *et al.*, 1990; Kimura *et al.*, 2002; Mori *et al.*, 2005; Ono *et al.*, 2007; Parent *et al.*, 2011). In

*Arabidopsis* and tobacco, two *Poll*-like genes encode proteins that localize to both organelles (Elo *et al.*, 2003; Christensen *et al.*, 2005; Ono *et al.*, 2007; Wamboldt *et al.*, 2009). In addition, the recombinant proteins have a high processivity, which allows them to replicate complete organellar genomes (Kimura *et al.*, 2002; Mori *et al.*, 2005; Ono *et al.*, 2007). The *Arabidopsis* *PollA* and *PollB* (previously named *Poly2* and *Poly1*) were shown to be involved in organellar DNA replication. While the single mutants showed low amounts of plastid and mitochondrial DNA, double mutants could not be recovered, indicating that they play an essential, partly redundant role (Parent *et al.*, 2011). In addition, the *pollb* mutants are impaired in their capacity to repair DNA double-strand breaks, suggesting that *PollB* is also specialized in DNA repair (Parent *et al.*, 2011). Until now, mutants that overexpress the organellar DNA polymerases have not been produced.

#### 1.4.2.3 Organization and abundance of mtDNA in plants

Mitochondrial DNA is usually organized in membrane-associated nucleoprotein structures called “nucleoids”, which are located in the matrix (Fey *et al.*, 1999; Dai *et al.*, 2005). Until now, the proteins associated with these chromatin-like structures have not been identified (Sakai *et al.*, 2004). As a result of frequent fusion and fission events, nucleoids are mixed and then unequally shared between the newly formed mitochondria (Arimura *et al.*, 2004b), with some of them even completely lacking a detectable nucleoid (Takanashi *et al.*, 2006).

Investigations into the mtDNA amount in higher plants suggested that the DNA content of individual mitochondria is lower than the size of mitochondrial genomes (Ward *et al.*, 1981; Kuroiwa, 1982; Bendich and Gauriloff, 1984; Kuroiwa *et al.*, 1992; Takanashi *et al.*, 2006). Therefore, only few or even none of the mitochondria may contain a complete genome. Taking into consideration also the multipartite structure of the genome and frequent recombination events, the maintenance of a functional genome structure is probably under strict control. However, not much is known about the existence and regulation of mitochondrial DNA amounts both under normal and stress conditions. Until now, most of the attention has been focused on mtDNA evolution, structure, recombination and

transmission. Additionally, some reports have connected the abundance of mitochondrial genomes with the photosynthetic activity (Hedtke *et al.*, 1999; Ballesteros *et al.*, 2009). In the white leaves of the barley (*Hordeum vulgare*) *albostrians* mutant and in albino plants of rye (*Secale cereale*) there exist higher amounts of mtDNA compared to green leaves (Hedtke *et al.*, 1999), pointing to an inter-organellar cross-talk that has never been studied in detail.

## 1.5 Organellar gene transcription

### 1.5.1 The transcription machinery of plastids

Transcription is the first step to decode the genetic information encoded on the DNA into gene products. The plastid genome of higher plants is transcribed by two different types of RNA polymerases (RNAPs) (Liere and Börner, 2007a; Liere *et al.*, 2011). The plastid-encoded plastid RNA polymerase (PEP) inherited from the eubacterial ancestor is a multimeric enzyme consisting of five core subunits (two  $\alpha$ , one  $\beta$ , one  $\beta'$  and one  $\beta''$ ) (Suzuki *et al.*, 2004). PEP can be isolated from plastids together with DNA in an insoluble form called “transcriptionally active chromosome” (TAC) that contains up to 50 proteins that are associated with or are part of the PEP complex (Suzuki *et al.*, 2004; Pfalz *et al.*, 2006; Schröter *et al.*, 2010). In addition to the plastid-encoded subunits, PEP activity is complemented by nuclear-encoded regulatory transcription factors termed sigma factors ( $\sigma$ -factors) that play important roles in differential regulation of gene expression (Shiina *et al.*, 2009; Lerbs-Mache, 2010; Schweer *et al.*, 2010). As a result of the cyanobacterial origin of chloroplasts, plastid genes contain typical eubacterial-type promoter sequences: -35 (TTGaca) and -10 (TATAaT).

A second RNA polymerase activity in plastids is represented by the existence of nuclear-encoded plastid RNA polymerase (NEP). NEP is represented by a small family of monomeric phage-type enzymes that have been named RpoT (RNA polymerase of the T3/ T7 phage-type). While monocotyledonous plants have one RpoT targeted into the plastids (RpoTp), dicotyledonous species have two: RpoTp

targeted to plastids and RpoTmp that is dual targeted to both plastids and mitochondria (Fig. 11) (Shiina *et al.*, 2005; Liere and Börner, 2007a; b; Liere *et al.*, 2011). Experimental evidence proved that both RpoTp and RpoTmp are present in chloroplasts (Chang *et al.*, 1999; Kusumi *et al.*, 2004; Azevedo *et al.*, 2006) where they function in plastid gene transcription and recognize specific promoters that altogether are termed “NEP promoters”. NEP promoters have been classified into three types based on their sequence properties: type I, type II and *rrn16* Pc promoter (Weihe and Börner, 1999; Liere and Maliga, 2001).

NEP and PEP have been shown to be active in all investigated types of plastids: chloroplasts, etioplasts, amyloplasts and chromoplasts (Marano and Carrillo, 1992; Tiller and Link, 1993; Wurbs *et al.*, 2007; Barsan *et al.*, 2010) with NEP promoters being active in young, non-green tissue in the beginning of leaf development, while PEP increases its activity during maturation of chloroplasts (Swiatecka-Hagenbruch *et al.*, 2007; Zoschke *et al.*, 2007; Swiatecka-Hagenbruch *et al.*, 2008). While most genes have both NEP and PEP promoters, a few house-keeping genes have only NEP promoters and some photosynthesis genes just PEP promoters (Liere and Maliga, 2001; Swiatecka-Hagenbruch *et al.*, 2007; Zhelyazkova *et al.*, 2012). As example, the *rpoB* operon encoding three of the four PEP subunits is solely transcribed by NEP (Hajdukiewicz *et al.*, 1997; Hübschmann and Börner, 1998; Silhavy and Maliga, 1998; Swiatecka-Hagenbruch *et al.*, 2007). As a result, the nucleus plays a central role in regulating plastid gene expression.

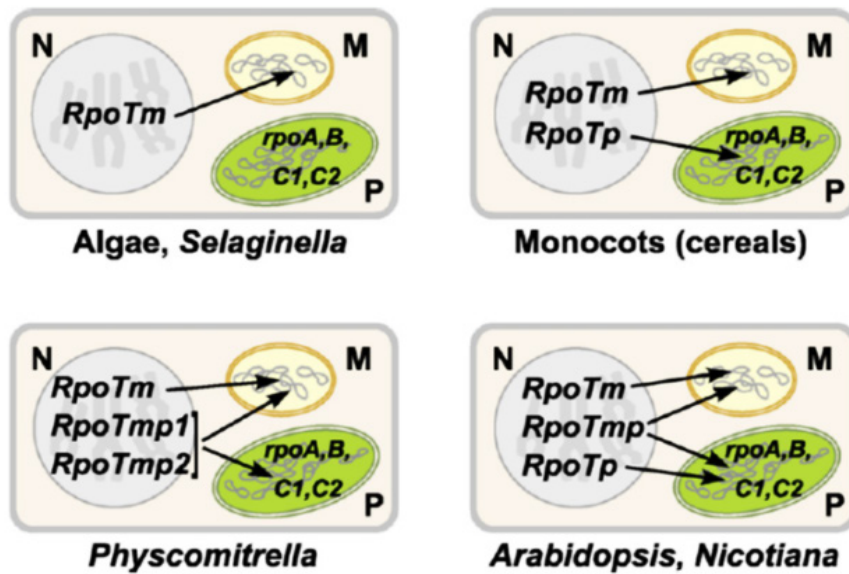


**Figure 11** Localization of organellar phage-type RNA polymerases in different organisms. The RpoT gene family is encoded in the nucleus (N) and imported into plastids (P) or mitochondria (M). Green algae such as *Chlamydomonas* and the lycophyte *Selaginella* possess only one *RpoT* gene encoding a mitochondria-targeted polymerase. Nuclear genomes of cereals encode two *RpoT* genes: one that is plastid-targeted (RpoTp) and one mitochondria-targeted (RpoTm). Arabidopsis and other eudicots additionally contain a dual-targeted polymerase: RpoTmp. The moss *Physcomitrella* possesses two dual-targeted RpoT proteins (RpoTmp1 and RpoTmp2) and one exclusively consigned to mitochondria (RpoTm). Image reproduced after Liere *et al.*, 2011.

### 1.5.2 The transcription machinery of mitochondria

Mitochondrial transcription relies on nuclear-encoded phage-type RNA polymerases with the protist *Reclinomonas americana* and other jakobids being the only known organisms which have retained the ancestral bacterial RNAP genes in their chondrome (Lang *et al.*, 1997; Burger *et al.*, 2013). While *Chlamydomonas*, algae, the lycophyte *Selaginella moellendorffii* and monocots contain a single mitochondria-targeted RNA polymerase (RpoTm), the transcription machinery in *Physcomitrella*, *Nuphar* and eudicots is more complex, based on a small family of RpoTs: *Physcomitrella* encodes one RpoTm and two dual-targeted RpoTs, named RpoTmp1 and RpoTmp2, *Nuphar* has two RpoTm (RpoTm1 and RpoTm2) while eudicots encode one RpoTm and one RpoTmp (Fig. 11) (Tracy and Stern, 1995; Hess and Börner, 1999; Weihe, 2004; Liere and Börner, 2011; Richter *et al.*, 2013). This complex structure of mitochondrial transcriptional apparatus is the result of several

independent duplications and losses of RpoT genes during evolution (reviewed by Liere *et al.*, 2011).

A common feature of both monocot and dicot mitochondrial genes is represented by the existence of multiple promoters and multiple transcription initiation sites (Kühn *et al.*, 2005). In dicotyledoneous plants a consensus sequence motif (CRTA) is part of a nonanucleotide sequence that includes the initiation site (CRTAaGaGA, transcription initiation site underlined) (Binder *et al.*, 1996) and that is highly similar between different genes and also conserved between different species. Apart from the CRTA-type motif, other loose or unusual motifs were identified (ATTA and RGTA) with some putative promoters even lacking consensus sequences (Kühn *et al.*, 2005). In contrast to dicots, monocot promoters are less conserved (Fey and Maréchal-Drouard, 1999; Weihe, 2004). The CRTA tetranucleotide motif is complemented by an AT-rich region of six nucleotides located upstream (Rapp *et al.*, 1993; Tracy and Stern, 1995). Apart from them, degenerated YRTA, AATA and CTTA could also be observed in *Sorghum* (Yan and Pring, 1997).

Several investigations targeted the specific role of RpoTm and RpoTmp in *Arabidopsis thaliana* mitochondrial gene transcription. While *RpoTm* and *RpoTmp* genes displayed overlapping expression pattern (Emanuel *et al.*, 2006), analysis of a RpoTmp null mutant revealed decreased amounts of *nad6*, *nad2* and *coxI* transcripts with low abundance of the respiratory chain complexes I and IV, revealing the specific role of RpoTm as the main RNAP in mitochondria of eudicots required for the transcription of most, if not all, mitochondrial genes. The gene-specific transcription of RpoTmp might be a mechanism that is used to independently control the abundance of complexes I and IV, allowing a fine-tuning of the electron flow through this complexes (Kühn *et al.*, 2009).

## 1.6 Aim of this work

### 1.6.1 Evaluation of mtDNA organization and abundance under standard and stress conditions

Until now, little is known about replication, recombination, distribution and function of plant mitochondrial genomes. Moreover, even less is known about DNA abundance under both standard and stress conditions, possible regulatory pathways not being yet described.

The present work aims to extensively evaluate mitochondrial DNA organization and abundance in both standard and stress conditions and to propose possible regulatory pathways that control these features. Moreover, by comparing three different model plants (*Arabidopsis*, barley and tobacco), differences and similarities will be revealed. To this end, quantitative real-time PCR will be used as a standard method to establish the copy numbers of representative mitochondrial genes. At first, the copy number will be determined in different organs of the model plant *Arabidopsis thaliana* and then, DNA abundance will be investigated in relation to the existing number of mitochondria as well as to the diploid/tetraploid/endopolyploid status of the nuclei. Secondly, the previously described condition of absence of plastid ribosomes in the barley *albostrians* mutant will be reproduced in *Arabidopsis* by treatment of the seedlings with the antibiotic spectinomycin. This experimental system aims to evaluate the changes in mitochondrial genetic apparatus in relation to impaired chloroplast development as well as the effects of complete absence of photosynthesis on mitochondrial dynamics, internal structure and respiratory activities. Next, the changes in copy number will be evaluated in relation to photosynthesis and respiration impairment.

### **1.6.2 The influence of impaired chloroplast development on mitochondrial dynamics**

The totality of mitochondria within a plant cell, termed “chondriome”, is represented by a population of several hundred individual organelles that are characterized by frequent fusion – fission events and high motility (Logan, 2010). This highly dynamic nature can vary under different metabolic conditions like senescence, anoxia, cell death cold and oxidative stress (Van Gestel and Verbelen, 2002; Yoshinaga *et al.*, 2005; Armstrong *et al.*, 2006; Zottini *et al.*, 2006; Scott and Logan, 2008a; b). A particular condition is represented by the relation between photosynthesis and mitochondrial motility since chloroplasts and mitochondria have been frequently found in close association (Stickens and Verbelen, 1996; Logan and Leaver, 2000; Sheahan *et al.*, 2004). To investigate chondriome dynamics in the absence of photosynthesis, mitochondrial size, shape, density and motility will be evaluated in cotyledons with impaired photosynthesis ranging from pale-green, over yellow, to white cotyledon phenotypes. In addition, etiolated cotyledons will be analyzed in order to evaluate chondriome dynamics in the absence light.



## 2 Materials and methods

### 2.1 Materials

#### 2.1.1 Providers

The chemicals, biochemicals, laboratory instruments and consumables used in this study were provided by the following companies:

Applied Biosystems	Applied Biosystems, Weiterstadt, Germany
Ambion	Ambion, Inc., Austin, TX, USA
Amersham Biosciences	Amersham Biosciences Europe GmbH, Freiburg, Germany
Bender & Hobein	Bender & Hobein GMBH Labortechnik Chemikalien Baden-Württemberg, Germany
Biometra	Biometra GmbH, Göttingen, Germany
Bio-Rad	Bio-Rad Laboratories, Richmond, VA, USA
Biozym	Biozym Diagnostik GmbH, Hameln, Germany
Braun	Braun GmbH, Kronberg, Germany
Calbiochem	Calbiochem Merck Biosciences GmbH, Schwalbach, Germany
DuPont	DuPont de Nemours GmbH, Bad Homburg, Germany
Duschefa Biochemie	Duschefa Biochemie, Haarlem, The Netherlands
Epicentre	Epicentre Biotechnologies, Madison, WI, USA
Eppendorf	Eppendorf, Hamburg, Germany
Eurogentec	Eurogentec, Seraing, Belgium
Fermentas	Fermentas GmbH, St. Leon-Rot, Germany
GE Healthcare	GE Healthcare Europe GmbH, Freiburg, Germany
Heraeus	Heraeus, Hanau, Germany
Hettich	Hettich Zentrifugen, Tuttlingen, Germany
Invitrogen	Invitrogen GmbH, Karlsruhe, Germany
Jenoptik	Jenoptik L.O.S. GmbH, Jena, Germany
Kendro Laboratory Products	Kendro Laboratory Products GmbH, Langenselbold, Germany
Macherey-Nagel	Macherey-Nagel, Düren, Germany
Metabion	metabion international AG, Martinsried, Germany
Millipore	Millipore Corp., Bedford, USA
Nalgene	Nalgene®Labware, Rochester, NY, USA
neoLab	neoLab, Heidelberg, Germany
Operon	Operon Biotechnologies GmbH, Köln, Germany
peqLab	peqLab Biotechnologie GmbH, Erlangen, Germany
Perkin Elmer	Perkin Elmer LAS (Germany) GmbH, Rodgau, Germany
Pierce	Pierce, Rockford, IL, USA
Promega	Promega Corp., Madison, WI, USA

Qiagen	Qiagen, Hilden, Germany
Roche	Roche Diagnostics GmbH, Mannheim, Germany
Roth	Carl Roth GmbH & Co. KG, Karlsruhe, Germany
Serva	Serva Feinbiochemika, Heidelberg, Germany
Sigma	Sigma Chemical Company, St. Luis, MO, USA
Sorvall	Kendro Laboratory Products GmbH, Langenselbold, Germany
Starlab	STARLAB GmbH, Hamburg, Germany
Stratagene	Stratagene, La Jolla, CA, USA
Thermo Scientific	Thermo Scientific LED GmbH, Langenselbold, Germany
USF	USF, Seral Reinstwassersysteme GmbH, Germany
Whatman	Whatman Paper, Maidstone, UK
Zeiss	Carl Zeiss MicroImaging GmbH, Jena, Germany

### 2.1.2 Plant material

The plant material used in this study was provided by different research groups, as described in **Table 1**.

### 2.1.3 Oligonucleotides

The oligonucleotides used in this study were provided by Sigma-Genosys or Operon. Sequences of nucleotides are provided in respective chapters (2.2.7 and 2.2.8).

**Table 1 Plant lines used in this work**

<i>ndufs4</i>	mutant of <i>FRO1</i> (At5g67590) gene encoding NADH dehydrogenase (ubiquinone) Fe-S protein 4	Col-0	Yuri Konstantinov, SIFIBR, Irkutsk, Russia	Tarasenko <i>et al.</i> , 2010
<i>gun1-1</i>	mutant of <i>GUN1</i> gene (At2g31400) encoding a chloroplast-localized pentatricopeptide-repeat protein involved in regulation of nuclear gene expression	Col-0	Bernhardt Grimm, HU Berlin, Germany	Susek <i>et al.</i> , 1993
<i>gun2-1</i>	mutant of <i>GUN2</i> gene (At2g26670) encoding heme oxygenase, involved in plastid to nucleus retrograde signaling	Col-0	Bernhardt Grimm, HU Berlin, Germany	Susek <i>et al.</i> , 1993
<i>gun4-1</i>	mutant of <i>GUN4</i> gene (At3g59400) encoding a porphyrin-binding protein that enhances the activity of Mg-chelatase and is involved in plastid to nucleus retrograde signaling	Col-0	Bernhardt Grimm, HU Berlin, Germany	Susek <i>et al.</i> , 1993
<i>gun5-1</i>	mutant of <i>GUN5</i> gene (At5g13630) encoding the H subunit of magnesium chelatase, involved in plastid to nucleus retrograde signaling	Col-0	Thomas Börner, HU Berlin, Germany	Susek <i>et al.</i> , 1993
<i>abi4-1</i>	mutant of <i>ABI4</i> gene (At2g40220) encoding a transcription factor involved in abscisic acid (ABA) signal transduction and retrograde signaling from plastids and mitochondria	Col-0	Takehito Inaba, Iwate University, Japan	Kakizaki <i>et al.</i> , 2009
<i>RLD-Spc1</i>	spectinomycin-resistant mutant carrying a point mutation in the plastid 16S rRNA gene ( <i>rrn16</i> )	RLD	Pal Maliga, The State Univ. of New Jersey, USA	Azhagiri and Maliga, 2007
<i>Hordeum vulgare</i>				
WT (2x)	<i>Hordeum vulgare</i> cv. Golden Promise		J. Kumlehn, IPK Gatersleben, Germany	

<b>L150 (4x)</b>	<b>spontaneously-derived tetraploid line</b>			<b>unpublished</b>
<b>MBE (4x)</b>	spontaneously-derived tetraploid line	<i>H. vulgare</i> cv. Golden Promise (2x)	J. Kumlehn, IPK Gatersleben, Germany	unpublished
<i>Nicotiana tabacum</i>				
<b>WT (PH)</b>	<i>Nicotiana tabacum</i> cv. Petit Havana		Ralph Bock, MPI-MP, Potsdam, Germany	
<i>aadA</i>	transplastomic tobacco mutant containing the <i>aadA</i> gene conferring spectinomycin / streptomycin resistance	<i>N. tabacum</i> cv. Petit Havana	Ralph Bock, MPI-MP, Potsdam, Germany	Bock <i>et al.</i> , 1994
<i>atpB 4</i>	transplastomic tobacco mutant with KO of <i>atpB</i> gene encoding ATPase beta chain	<i>N. tabacum</i> cv. Petit Havana	Ralph Bock, MPI-MP, Potsdam, Germany	unpublished
<i>atpH 31</i>	transplastomic tobacco mutant with KO of <i>atpH</i> gene encoding ATPase III subunit	<i>N. tabacum</i> cv. Petit Havana	Ralph Bock, MPI-MP, Potsdam, Germany	unpublished
<i>atpH 13</i>	transplastomic tobacco mutant with KO of <i>atpH</i> gene encoding ATPase III subunit	<i>N. tabacum</i> cv. Petit Havana	Ralph Bock, MPI-MP, Potsdam, Germany	unpublished
<i>ndhC 13</i>	transplastomic tobacco mutant with KO of <i>ndhC</i> gene encoding NADH dehydrogenase subunit 3	<i>N. tabacum</i> cv. Petit Havana	Ralph Bock, MPI-MP, Potsdam, Germany	unpublished
<i>petN 12</i>	transplastomic tobacco mutant with KO of <i>petN</i> gene encoding cytochrome b6/f complex subunit N	<i>N. tabacum</i> cv. Petit Havana	Ralph Bock, MPI-MP, Potsdam, Germany	Hager <i>et al.</i> , 1999
<i>psaI 1A</i>	transplastomic tobacco mutant with KO of <i>psaI</i> gene encoding photosystem I protein I	<i>N. tabacum</i> cv. Petit Havana	Ralph Bock, MPI-MP, Potsdam, Germany	unpublished
<i>psaI 9</i>	transplastomic tobacco mutant with KO of <i>psaI</i> gene encoding photosystem I protein I	<i>N. tabacum</i> cv. Petit Havana	Ralph Bock, MPI-MP, Potsdam, Germany	unpublished

<b><i>psaJ 20</i></b>	<b>transplastomic tobacco mutant with KO of <i>psaJ</i> gene encoding photosystem I protein J</b>			<b>Schöttler, 2007</b>
<b><i>psaJ 9</i></b>	transplastomic tobacco mutant with KO of <i>psaJ</i> gene encoding photosystem I protein J	<i>N. tabacum</i> cv. Petit Havana	Ralph Bock, MPI-MP, Potsdam, Germany	Schöttler, 2007
<b><i>psbB 3</i></b>	transplastomic tobacco mutant with KO of <i>psbB</i> gene encoding photosystem II P680 chlorophyll A apoprotein	<i>N. tabacum</i> cv. Petit Havana	Ralph Bock, MPI-MP, Potsdam, Germany	unpublished
<b><i>psbB 5</i></b>	transplastomic tobacco mutant with KO of <i>psbB</i> gene encoding photosystem II P680 chlorophyll A apoprotein	<i>N. tabacum</i> cv. Petit Havana	Ralph Bock, MPI-MP, Potsdam, Germany	unpublished
<b><i>psbD 11</i></b>	transplastomic tobacco mutant with KO of <i>psbD</i> gene encoding photosystem II protein D2	<i>N. tabacum</i> cv. Petit Havana	Ralph Bock, MPI-MP, Potsdam, Germany	unpublished
<b><i>psbJ 4</i></b>	transplastomic tobacco mutant with KO of <i>psbJ</i> gene encoding photosystem II protein J	<i>N. tabacum</i> cv. Petit Havana	Ralph Bock, MPI-MP, Potsdam, Germany	Hager <i>et al.</i> , 2002
<b><i>psbJ 5</i></b>	transplastomic tobacco mutant with KO of <i>psbJ</i> gene encoding photosystem II protein J	<i>N. tabacum</i> cv. Petit Havana	Ralph Bock, MPI-MP, Potsdam, Germany	Hager <i>et al.</i> , 2002
<b><i>psbJ 9</i></b>	transplastomic tobacco mutant with KO of <i>psbJ</i> gene encoding photosystem II protein J	<i>N. tabacum</i> cv. Petit Havana	Ralph Bock, MPI-MP, Potsdam, Germany	Hager <i>et al.</i> , 2002
<b><i>ycf3</i></b>	transplastomic tobacco mutant with KO of <i>ycf3</i> gene encoding photosystem I assembly protein YCF3	<i>N. tabacum</i> cv. Petit Havana	Ralph Bock, MPI-MP, Potsdam, Germany	Ruf <i>et al.</i> , 1997
<b><i>rbcL 66-8</i></b>	transplastomic tobacco mutant with KO of <i>rbcL</i> gene encoding RuBisCO large subunit	<i>N. tabacum</i> cv. Petit Havana	Ralph Bock, MPI-MP, Potsdam, Germany	Kanevski <i>et al.</i> , 1994
<b><i>rpoA</i></b>	transplastomic tobacco mutant with KO of <i>rpoA</i> gene encoding RNA polymerase $\alpha$ chain	<i>N. tabacum</i> cv. Petit Havana	Pal Maliga, The State Univ. of New Jersey, USA	Serino and Maliga, 1998

#### 2.1.4 Software

Primers used for quantitative real-time PCR were designed using the ProbeFinder Software of the Universal ProbeLibrary Assay Design Center (Roche Applied Science, <https://www.roche-applied-science.com/sis/rtpcr/upl>) or the Primer3 v.0.4.0 software (<http://frodo.wi.mit.edu/>). Database and homology searches in public sequence databases at the National Center for Biotechnology Information (NCBI; <http://www.ncbi.nlm.nih.gov>) were conducted using the BLAST algorithm, version 2.2.16 (Altschul *et al.*, 1990; Altschul *et al.*, 1997).

Images from the Confocal Laser Scanning Microscope were processed using the FV10-ASW 2.0 Viewer software: ([https://support.olympus.co.jp/cf\\_secure/en/lisg/bio/download/ga/fv10\\_asw/](https://support.olympus.co.jp/cf_secure/en/lisg/bio/download/ga/fv10_asw/)) and ImageJ (<http://rsbweb.nih.gov/ij/>).

Text writing, calculations and image processing were carried out using Microsoft® Office Word 2010, Microsoft® Office Excel 2010, Microsoft® Office Power Point 2010 and Microsoft® Office Picture Manager.

## 2.2 Methods

### 2.2.1 Plant growth

#### 2.2.1.1 Growth conditions for *Arabidopsis thaliana*

*Plants used for harvesting of different organs and for protoplast isolation (Chapter 3.1.1 and 3.1.2)*

*Arabidopsis thaliana* (ecotype Columbia and *mtGFP* line) seeds were sown on vermiculite/soil mix (1:4) and grown under long-day conditions (16 h light/8 h darkness), at 23 °C and 150  $\mu\text{mol photons m}^{-2}\text{s}^{-1}$ . Stems, fully developed green siliques and fully expanded flowers were harvested from 40 days-old plants. Root tips (first 3-4 mm from the root tip) or roots (remainder of the root after removal of the tip) were harvested from plants grown for 40 days in hydroculture, under short-day conditions (8 h light / 16 h darkness) at 23 °C and 150  $\mu\text{mol photons m}^{-2}\text{s}^{-1}$ . Roots

were continuously aerated. Age determination and harvesting of leaves used for protoplast isolation were carried out as described by Zoschke *et al.*, (Zoschke *et al.*, 2007).

Medium <i>Arabidopsis</i> hydroculture	for 3 mM KNO <sub>3</sub> , 0.5 mM MgSO <sub>4</sub> x 7 H <sub>2</sub> O, 1.5 mM CaCl <sub>2</sub> x 6H <sub>2</sub> O, 1.5 mM K <sub>2</sub> SO <sub>4</sub> , 1.5 mM NaH <sub>2</sub> PO <sub>4</sub> x 2H <sub>2</sub> O, 25 µM H <sub>3</sub> BO <sub>3</sub> , 1 µM MnCl x 4H <sub>2</sub> O, 0.5 µM ZnSO <sub>4</sub> x 7H <sub>2</sub> O, 0.05 µM (NH <sub>4</sub> ) <sub>6</sub> Mo <sub>7</sub> O <sub>24</sub> , 0.3 CuSO <sub>4</sub> x 5H <sub>2</sub> O, 40 µM FeEDTA, pH 6
----------------------------------------------	-------------------------------------------------------------------------------------------------------------------------------------------------------------------------------------------------------------------------------------------------------------------------------------------------------------------------------------------------------------------------------------------------------------------------------------------------------------------------------------------

*Growth of Arabidopsis diploid and tetraploid lines (Chapter 3.1.3.1)*

Seeds of *Arabidopsis thaliana* ecotypes Col-0, Ws, Wa-1 and Wilna were sown on vermiculite/soil mix (1:4) and grown under long-day conditions (16 h light/8 h darkness), at 23 °C and 150 µmol photons m<sup>-2</sup>s<sup>-1</sup>. Complete rosettes of individual plants were harvested at 20 days and further used for molecular investigations.

*Plants used for determining the influence of spectinomycin, light and sucrose content (Chapter 3.2.1 – 3.2.4, 3.3)*

Surface sterilized *Arabidopsis thaliana* seeds (ecotype Col-0) were sown on SEA medium containing 1% (w/v) sucrose and grown for 10 days under long-day conditions (16 h light/8 h darkness) at 23 °C and 120 µmol photons m<sup>-2</sup>s<sup>-1</sup>. For determining the effects of darkness, spectinomycin and sucrose addition, the seedlings were kept for 10 days in complete darkness, the culture medium was supplemented with 500 mg/L spectinomycin dihydrochlorid pentahydrate (Sigma-Aldrich) and sucrose was subtracted where stated. Whole seedlings were harvested and used for DNA/RNA isolation.

*Growth of Arabidopsis plants for separate investigations of cotyledons and roots (Chapter 3.4.4)*

For differential investigation of cotyledons and roots, the seedlings were grown in leaning position on SEA medium containing 1% (w/v) sucrose and grown for 10 days under long-day conditions (16 h light/8 h darkness) at 23 °C and 120

$\mu\text{mol photons m}^{-2}\text{s}^{-1}$ . Where stated, 500 mg/L spectinomycin was added to the medium.

*Growth of Arabidopsis respiration and signaling mutants (Chapter 3.4.1 – 3.4.3 and 3.5)*

Surface sterilized *Arabidopsis thaliana* seeds (Col-0, *prpl11-1*, *mrpl11-1*, *prpl11 mrpl11*, *ndufs4*, *gun1*, *gun2*, *gun4*, *gun5*, *abi4*) were sown on SEA medium containing 1% (w/v) sucrose and grown for 10 days under long-day conditions (16 h light/8 h darkness) at 23 °C and 120  $\mu\text{mol photons m}^{-2}\text{s}^{-1}$ . Where stated, 500 mg/L spectinomycin was added in the medium.

*Growth of Arabidopsis seedlings for CLSM, TEM investigations and determination of O<sub>2</sub> consumption, ATP / ADP ratio (Chapter 3.2.5 -3.2.7 and 3.6)*

For CLSM investigations on mitochondria motility, the seedlings were grown in a sloping position on SEA medium containing 1% (w/v) sucrose and kept for 10 days under long-day conditions (16 h light/8 h darkness) at 23 °C and 120  $\mu\text{mol photons m}^{-2}\text{s}^{-1}$ . Where stated, 0.5, 5, 50 or 500 mg/L spectinomycin was added in the medium. Etiolated seedlings were obtained by growing the seedlings in the dark on SEA medium containing 1% (w/v) sucrose.

#### **2.2.1.2 Growth conditions for *Nicotiana tabacum***

*Growth conditions for transplastomic tobacco mutants (Chapter 3.4.1)*

Tobacco (*Nicotiana tabacum* cv. Petit Havana) WT and transplastomic plants were grown on RM medium under long-day conditions (16 h light/8 h darkness) at 25 °C and light intensity of  $\sim 5 \mu\text{mol photons m}^{-2}\text{s}^{-1}$ . One month after transferring the cuttings into new medium, leaves of similar sizes were harvested.

RM medium                      0.44 % (w/v) MS elements and vitamins, 0.45 % (w/v) agar, 3 % (w/v) sucrose, pH 5.7



For determining the effect of spectinomycin on mitochondrial gene copy numbers in mature tobacco leaves, fresh cuttings from WT plants were transferred to RM medium containing 500 mg/L spectinomycin and after one month, completely white leaf fragments were cut and used for DNA isolation.

### **2.2.1.3 Growth conditions for *Hordeum vulgare***

#### *Growth of *Hordeum vulgare* diploid and tetraploid lines (Chapter 3.1.3.2)*

Seeds of *Hordeum vulgare* cv. Golden Promise diploid and tetraploid lines were sown on vermiculite / soil mix (1:4) and grown under long-day conditions (16 h light/8 h darkness), at 23 °C and 150  $\mu\text{mol photons m}^{-2}\text{s}^{-1}$ . Individual leaves were harvested after 10 days and assessed for the ploidy level. Only the plants that showed specific diploid and tetraploid profiles were further used for molecular investigations.

### **2.2.2 Surface sterilization of *Arabidopsis thaliana* and *Nicotiana tabacum* seeds**

*Arabidopsis thaliana* and *Nicotiana tabacum* seeds were immersed in sterilization solution and gently shaken for 7 minutes. The seeds were then spun down, the supernatant was aspirated and the seeds were washed 5 times with ultrapure sterile water.

Sterilization solution	20 ml DanKlorix (Colgate-Palmolive GMBH), 40ml ultrapure water, 2.5 ml N-lauryl-sarcosine sol. (20%)
------------------------	------------------------------------------------------------------------------------------------------

### **2.2.3 Isolation of nucleic acids**

#### **2.2.3.1 Isolation of genomic DNA**

The isolation of genomic DNA was performed following the CTAB protocol (Murray and Thompson, 1980) containing an RNA digestion step (RNaseA / T1 mix, Fermentas) or by using the DNeasy® Plant Mini Kit from Qiagen, according to the

manufacturer's protocol. DNA quality was controlled by agarose gel electrophoresis (see 2.2.5.1).

#### **2.2.3.2 Isolation of total RNA**

Total RNA from *Arabidopsis* samples was isolated using the RNeasy® Plant Mini Kit (Qiagen) following the manufacturer's protocol (with buffer RLT). RNA quality was controlled by denaturing agarose gel electrophoresis (see 2.2.5.2).

#### **2.2.4 Determination of nucleic acid concentrations**

Nucleic acid concentration was determined spectrophotometrically using the Nanodrop® ND-1000 system (peqLab).

#### **2.2.5 Gel electrophoresis of nucleic acids**

##### **2.2.5.1 Agarose gel electrophoresis of DNA**

Analysis of gDNA quality and PCR products was performed by agarose gel electrophoresis. DNA samples were mixed with 6x DNA loading dye (Fermentas) and loaded on agarose gels of 0.8 – 2% concentration containing 0.2 µg / ml EtBr in 1x TAE. Electrophoresis was carried out at 5-10 V / cm in a horizontal electrophoresis chamber (PerfectBlue Gelsystem Mini S or Mini L, peqLab Biotechnologie GmbH) and GeneRuler™ 1 kb DNA Ladder, 100 bp Plus DNA Ladder or 50 bp DNA Ladder (Fermentas) were used as molecular weight markers. DNA bands were subsequently visualized under UV-light excitation in the Gel Doc XR System (Bio-Rad).

1x TAE

40 mM Tris; 20 mM acetic acid; 1 mM EDTA

### 2.2.5.2 Agarose gel electrophoresis of RNA

Total RNA were mixed with RNA loading dye, heated at 95 °C for 10 min, incubated on ice for 5 min and loaded on 1% agarose gel containing 1/40 vol formaldehyde in 1x MEN running buffer. Electrophoresis was carried out at 5 V/cm in horizontal electrophoresis chamber (PerfectBlue Gelsystem Mini S, peqLab Biotechnologie GmbH). Separated RNA was visualized under UV-light excitation in the Gel Doc XR System (Bio-Rad).

1x MEN	200 mM MOPS; 50 mM NaAc; 10 mM EDTA; pH 7.0 with NaOH
RNA loading buffer	1 ml formamide; 350 µl formaldehyde, 200 µl 10x MEN; 400 µl glycerol; 5 µl 0.5 M EDTA, pH 8.0; 10 µl 10 mg/ml EtBr; 2 mg bromophenol blue; 2 mg xylene cyanol; ad 2ml ultrapure water 2

### 2.2.6 Reverse trascription of total RNA

Elimination of remaining gDNA and reverse transcription of RNA samples were performed using the QuantiTect® Reverse Transcription Kit (Qiagen) following manufacturer's protocol.

### 2.2.7 Quantitative real-time PCR using SYBR® Green

Quantitative real-time PCR was performed in a 7500 Real-Time PCR system (Applied Biosystems, <http://www.appliedbiosystems.com>) using Power SYBR® Green PCR Master Mix (Applied Biosystems). Each reaction contained 1 ng of total DNA or 50 ng of cDNA and 1 µM of each primer. Primer sequences are listed in Table 2 and 3. The cycle protocol consisted of an initial step at 95 °C for 10, followed by 40 cycles of 15 sec at 95 °C and 1 min at 60 °C. To verify the specificity of DNA amplification products, a dissociation curve was determined for each reaction by subjecting the samples to a heat denaturation over a temperature gradient from 60 °C to 95 °C at 0.03 °C/s. In order to verify the complete removal of genomic DNA from

cDNA samples, a negative control (without addition of reverse transcriptase) was included for each sample. Two independent technical repetitions were performed and each sample was tested in triplicate on plate. A no template control (NTC) was included for each primer pair. Data were analyzed using the SEQUENCE DETECTION Software v1.4 (Applied Biosystems). All mtDNA quantitations were normalized to the amount of the nuclear encoded single-copy gene *RpoTm* (for *Arabidopsis* and barley) and *RpoTp* (for tobacco) as internal standards (Liere and Börner, 2011). The steady-state transcript level was quantified using the *UBQ11* as reference gene (Sun and Callis, 1997). For both mtDNA and cDNA determinations the  $\Delta C_T$  method was used ( $2^{(-\Delta C_T)}$  = relative amount of gene copies;  $\Delta C_T = C_T^{\text{target}} - C_T^{\text{internal standard}}$ ).

**Table 2 Primers used in quantitative real-time PCR analysis for determination of mitochondrial gene copy number per cell**

Primer denotation	Nucleotide sequence (5'-3')
q-At-atp1-fw	CTTAGAAAGAGCGGCTAAACGA
q-At-atp1-rev	GGGAATATAGGCCGATACGTCT
q-At-cox1-fw	GCCATGATCAGTATTGGTGTCTT
q-At-cox1-rev	CTACGTCTAAGCCCACAGTAAACA
q-At-rps4-fw	CCCATCACAGAGATGCACAGA
q-At-rps4-rev	GGAGACGAAGCGGAATAACGT
q-At-nad6-fw	AGGATGTATTCCGACGAAATGC
q-At-nad6-rev	CGTGAGTGGGTCAGTCGTCC
q-At-psbA-fw	CATCCGTTGATGAATGGCTAT
q-At-psbA-rev	AACTAAGTTCCCACTCACGACC
q-At-clpP-fw	TATGCAATTTGTGCGACCC
q-At-clpP-rev	TTGGTAATTGCTCCTCCGACT
q-At-RpoTm-fw	AGCCTGTGCGTAATGCTATTCA
q-At-RpoTm-rev	GCCATCTTATCAGCCGGTAACT
q-Nt-atp1-fw	CAGAAGCGAATGCTTTGGA
q-Nt-atp1-rev	GCCAAAAATTGTAGAGGAGCA
q-Nt-cox1-fw	AGTGCCGCTACCCACTTCTA
q-Nt-cox1-rev	TTGCCTCCAAGTCTCTTGCT
q-Nt-rps4-fw	AGAAAAGGGATATATGAAGTTCGTTC
q-Nt-rps4-rev	TGGAGATTTACCCATCACAGAG
q-Nt-nad6-fw	AACGGAATGTACCGGATTTTT
q-Nt-nad6-rev	TTTTGTGCGAGCCCTGCTTT
q-Nt-RpoTp-fw	CTAAATGGAAATCGATGGTGGT
q-Nt-RpoTp-rev	GCAAGCTGCTAAGCACTGAA
q-Hv-atp9-fw	TTTGATTCATTCCGTGGCG
q-Hv-atp9-rev	TGCAATAGCTTCGGTGAGAGC
q-Hv-rps2-fw	GGCGTTTTTGACCAATTCTT
q-Hv-rps2-rev	CACAATCAGGTTGTTGGTTCA
q-Hv-psbA-fw	GGAACCATGCATAGCACTGA
q-Hv-psbA-rev	TGTATTCCAGGCAGAGCACA
q-Hv-clpP-fw	GGCTTGCCTGTTCTTAGTGC
q-Hv-clpP-rev	TATTATCGGGCAAGGACACC
q-Hv-RpoTm-fw	AGATCATCGCAGAGCAGGAG
q-Hv-RpoTm-rev	GCTTGTGCATGGTGATAACG

**Table 3** Primers used in quantitative real-time RT-PCR analysis for determination of relative transcript level

Primer denotation	Nucleotide sequence (5' - 3')	Locus tag
q-At-atp1-fw	CTTAGAAAGAGCGGCTAAACGA	<i>atp1</i>
q-At-atp1-rev	GGAATATAGGCCGATACGTCT	
q-At-cox1-fw	GCCATGATCAGTATTGGTGTCTT	<i>cox1</i>
q-At-cox1-rev	CTACGTCTAAGCCACAGTAAACA	
q-At-rps4-fw	CCCATCACAGAGATGCACAGA	<i>rps4</i>
q-At-rps4-rev	GGAGACGAAGCGGAATAACGT	
q-At-nad6-fw	AGGATGTATTCCGACGAAATGC	<i>nad6</i>
q-At-nad6-rev	CGTGAGTGGGTCAGTCGTCC	
q-At-msh1-fw	AGCATTATTTCCCATGCTTGT	At3g24320
q-At-msh1-rev	TTTGCGCCCTCATCTAAACT	
q-At-osb1-fw	CAAGAGCTCCAGCGATGTATATAGT	At1g47720
q-At-osb1-rev	GTGGAGCCGCCACATAAT	
q-At-why2-fw	CGTGGATTCCCTGGTAAAGA	At1g71260
q-At-why2-rev	TGGGAAGAACAGGTTCAACA	
q-At-poly1-fw	ACGTGCCCAAAGAACCATA	At3g20540
q-At-poly1-rev	TAGCAACATCAGCCGCACT	
q-At-poly2-fw	GAAGGCCAAATTTGCAGAAC	At1g50840
q-At-poly2-rev	GGCCTTACGAATCTTGTACCG	
q-At-recA3-fw	GATGCACATATGGCTATGCAA	At2g19490
q-At-recA3-rev	CCTCCAAACGTAGATAGTTTTGATCT	
q-At-RpoTm-fw	ACAGAAATTGCGGCTAGGG	At1g68990
q-At-RpoTm-rev	GGCATATGTGGCATTGGA	
q-At-RpoTmp-fw	CGATGCCATTGAACAAGAGAT	At5g15700
q-At-RpoTmp-rev	TGTTCTTCATAGAAGTTTCATTTTC	
q-At-UBQ11-fw	CTTATCTTCGCCGAAAGC	At4g05050
q-At-UBQ11-rev	GAGGGTGGATTCTTCTGG	

### 2.2.8 Amplification of DNA using PCR

In order to select homozygous mutants after crossings, approximately 100 ng gDNA was amplified using the primers listed in Table 4. A 20 µl reaction contained 1x Taq reaction buffer, 250 µM of each dNTP, 1 µM of each primer and 0.5 µl of laboratory-produced Taq polymerase. Starting with an initial denaturation step at 95 °C for 3 min, the standard PCR program was consisting of 40 cycles: 95 °C for 30s, primer specific annealing temperature for 1 min and 72 °C for 1 min. The final

elongation step was performed at 72 °C for 5 min. PCR products were analysed by electrophoretic separation in agarose gels.

10x Taq buffer                      100 mM KCl, 100 mM Amonium sulfate, 200 mM Tris-HCl  
pH 8.8, 20 mM MgSO<sub>4</sub>, 1% Triton X-100

**Table 4 Primers used for identification of homozygous plants after crossings**

Primer denotation	Nucleotide sequence (5' - 3')
At-prpl11-fw	GCGGGGTCTTGAGAATAAAC
At-prpl11-rev	CTTCTCTACATCCCAACTCC
At-prpl11-T-DNA	ATAATAACGCTGCGGACATCTACATTTT

### 2.2.9 Flow-cytometric analysis of nuclear endopolyploidy

Flow cytometric measurements of nuclear ploidy level were performed with the help of Dr. Jörg Fuchs (IPK Gatersleben, Germany) as described by Barow and Meister (Barow and Meister, 2003) using a FACS Aria flow cytometer (BD Biosciences, <http://www.bdbiosciences.com>). Data were analyzed using CELL QUEST version 3.3 software (BD Biosciences) and the mean C-level (where 1C equals the DNA content of the monoploid genome), representing the mean degree of endopolyploidization, was determined by using the formula:  $[(2 \cdot n2C) + (4 \cdot n4C) + (8 \cdot n8C) \dots] / [n2C + n4C + n8C \dots]$ , where n is the number of nuclei with DNA content corresponding to 2C, 4C, 8C etc. At least three independent samples were measured for each experimental condition. The mean C-levels of all experiments are listed in Annex 1.

### 2.2.10 Measurement of O<sub>2</sub> consumption

Oxygen consumption was measured using an OXI-4 mini (4-channel minisensor oxygen meter) from PreSens. The respiration rates of 40-60 mg of plant material were determined in 1.5 mL 100 mM HEPES buffer pH 7.4 in the dark, at 25 °C.

### 2.2.11 TCA-Ether extraction of metabolites

50 mg of frozen plant powder was mixed with 500  $\mu$ l 16% (w/v) TCA (trichloroacetic acid) / ether (diethyl ether) and incubated on ice for 15-20 minutes. 800  $\mu$ l 16% TCA / water containing 5mM EGTA were added followed by mixing and incubating for 1-3 hours at 4 °C on shaker. After 10 min centrifugation at full speed (4°C), the upper phase was discarded and the water phase (on the bottom) was transferred in a new tube and mixed with 800  $\mu$ l water saturated cold diethylether. This step was repeated 4 times in order to remove the TCA from the water phase. The pH was adjusted to pH 5-6 with 5M KOH / 1M TEA and the remaining diethyl ether was evaporated by leaving the Eppendorf tubes open for 3 h. After 10 min centrifugation at full speed (4 °C), the supernatant was divided into aliquots and stored at -80 °C.

### 2.2.12 Determination of ATP, ADP and ATP/ADP ratio

ATP and ADP concentrations were determined using the ATP Bioluminescence Assay Kit CLS II (Roche) following the manufacturer's instructions. For ATP determination a reaction contained 200 mM triethanolamine pH 7.6, 2 mM  $MgCl_2$ , 240 mM KCl, 4.6 mM phosphoenolpyruvate, 10  $\mu$ l of TCA-Ether extracted sample and 100  $\mu$ l luciferase reagent. After 15 min incubation on ice the luminescence was read in a GLOMAX 20/20 Luminometer (Promega). For ADP determinations a reaction contained 200 mM triethanolamine pH 7.6, 2 mM  $MgCl_2$ , 240 mM KCl, 4.6 mM phosphoenolpyruvate, 3U pyruvate kinase and 10  $\mu$ l of TCA-Ether extracted sample. After 10 min incubation at 37 °C, 100  $\mu$ l luciferase reagent was added and after 15 min on ice the luminescence was measured. ATP and ADP standard curves were performed before each set of measurements and an ATP / ADP recovery test was also included.



### 2.2.13 Detection of proteins by Western blotting

#### 2.2.13.1 Extraction of total proteins

For the isolation of total protein 100 mg of plant material was ground in liquid nitrogen and resuspended in 100  $\mu$ l extraction buffer. The suspension was centrifuged for 5 min at 14,000 rpm at 4 °C and the supernatant was used for determination of protein concentration by comparison to BSA standards as described by Bradford (Bradford, 1976), using the Bio-Rad Protein Assay.

extraction buffer	100 mM Tris pH 7, 10% sucrose, 5 mM EDTA, 40 mM $\beta$ -mercaptoethanol, 1% Triton X-100 and 2 mM Complete Protease Inhibitor (Roche)
-------------------	----------------------------------------------------------------------------------------------------------------------------------------

#### 2.2.13.2 SDS polyacrylamide gel electrophoresis (SDS-PAGE)

10  $\mu$ g of total protein extract were mixed with 5x sample buffer, heated at 70 °C for 10 min and shortly spun down. Samples were loaded on a 10% SDS-PAGE gel in BioRad Mini Protean vertical gel system. Fermentas PageRuler™ Prestained Protein Ladder #SM0671 and PageRuler Unstained Protein Ladder #SM0661 were used as molecular weight markers. Electrophoresis was performed at 150V.

5x sample buffer	62.5 mM Tris pH 6.8; 10% glycerol; 2% SDS; 0.1% bromophenol blue; 5% $\beta$ -mercaptoethanol
separating gel	10% AA/BIS, 375 mM Tris/HCl pH 8.8, 0.1% (w/v) SDS, 0.1% APS, 0.05% TEMED
stacking gel	2.5% AA/BIS, 125 mM Tris/HCl pH 6.8, 0.05% (w/v) SDS, 0.05% APS, 0.025% TEMED
10X electrophoresis	0.25 M Tris, 1.91 M glycine, 1% (w/v) SDS

#### 2.2.13.3 Transfer of proteins and immunodetection

Following PAGE, the separated proteins were transferred onto nitrocellulose membranes (Hybond-C extra, Amersham Biosciences) by electrotransfer in a Semi Dry Blot chamber (Bio-Rad). Electrotransfer was performed at 25V for 1 h. After transfer, the membrane was briefly stained with Ponceau red, blocked in TBS-T with 5% skim milk powder for 1 h and incubated with polyclonal RbcL antibody (Agrisera) in 1:200000 dilution in TBS-T with 1% skim milk powder for 1.5 h. The

membrane was then washed 2 x 5 min and 2 x 15 min in TBS-T. Goat anti-rabbit IgG peroxidase (Sigma) was used as secondary antibody in a 1: 250.000 dilution for 45 min, followed by repeated washing (2x 5 min and 2x 15 min in TBS-T). Visualization of signals was performed using the Amersham ECL Advanced Western Blotting Detection Kit (Amersham Biosciences) according to manufacturer's instructions. X-ray films were developed and fixated according to standard photographic conditions.

transfer buffer	39 mM glycine; 48 mM Tris; 0.0375 % SDS; 20 % methanol
TBS-T	100 mM Tris pH 7.5, 150 mM NaCl, 0.1% Tween 20

#### 2.2.14 Protoplast isolation

Mesophyll protoplasts were isolated from leaves of an *Arabidopsis thaliana* transgenic line expressing mitochondrial-targeted GFP (Logan and Leaver, 2000) using the Tape-Arabidopsis sandwich method, as described by Wu (*Wu et al.*, 2009b). The peeled leaves were transferred to 10 ml of enzyme solution and gently shaken (40 rpm) in the light for 1 h. Protoplasts were briefly washed twice in W5 solution, incubated on ice for 30 min and resuspended in MMg solution. After isolation, protoplasts were kept constantly on ice and visualized immediately by CLSM.

enzyme solution	1% cellulase R10 (Yakult Pharmaceutical); 0.25% macerozyme R10 (Yakult Pharmaceutical); 0.4 M mannitol; 20 mM KCl; 10 mM CaCl <sub>2</sub> ; 0.1% BSA and 20 mM MES, pH 5.7
W5 solution	154 mM NaCl; 125 mM CaCl <sub>2</sub> ; 5 mM KCl and 2 mM MES, pH 5.7
MMg solution	0.4 M mannitol; 15 mM MgCl <sub>2</sub> and 4 mM MES, pH 5.7

#### 2.2.15 Confocal imaging

Green fluorescent protein targeted to mitochondria (Logan and Leaver, 2000) from isolated protoplasts or crossed transgenic plants was visualized using an Olympus FV 1000 confocal laser scanning microscope (<http://www.olympus-global.com>) equipped with a 60x water-immersion objective and an 488 argon laser.

### 2.2.16 Determination of the mitochondria number per cell

Determination of mitochondria number in protoplasts was performed by acquiring half cells as 1  $\mu\text{m}$  z-series (see Video 1). The images were overlapped using the ImageJ software (<http://rsbweb.nih.gov/ij/index.html>) and the number of mitochondria per cell was determined using the “analyze particle” function. Twenty randomly chosen protoplasts were investigated for each developmental stage (40/6, 50/3 and 50/6) and their size (diameter) and mitochondria content were determined. At least three protoplast preparations (derived from independently grown plants) were used to obtain quantitative data. To investigate the correlation between protoplast size and mitochondria content, protoplasts from all three age stages were considered (180 protoplasts).

### 2.2.17 Evaluation of mitochondrial motility

Evaluation of mitochondrial motility was performed by acquiring 60 frames of the same focal plane taken at 1.1 seconds interval. The 60 images were then overlapped using the FV10-ASW 2.0 Viewer software and a single final image was exported. The supplementary videos represent the 60 frames taken at 1.1 seconds interval and rolled 3 times faster.

### 2.2.18 *Arabidopsis thaliana* crossings and selection of homozygous mutants

In order to evaluate the influence of plastid/chloroplast dysfunction on mitochondrial motility, two crossings have been performed that introduced mitochondrial GFP fluorescence in *RLD-Spc1* and *prp111-1* mutant plants (see Table 1). For this, a line with mitochondrial-targeted GFP (termed “*mtGFP*”) was used (Logan and Leaver, 2000). The line 43C5 contains a  $\beta$ -ATPase mitochondrial presequence downstream of a CaMV 35S promoter. The construct produces uniformly distributed mitochondrial GFP fluorescence that allows an easy visualization of the organelles with epifluorescent or confocal microscopy. Crossings were performed as described by NASC

([http://arabidopsis.info/InfoPages?template=crossing;web\\_section=arabidopsis](http://arabidopsis.info/InfoPages?template=crossing;web_section=arabidopsis)) and the double mutants were selected as following:

***RLD-Spc1xmtGFP*** At first, the crossing was performed between the two parent lines using the *RLD-Spc1* line as maternal parent. *RLD-Spc1* contains a point mutation in the plastid 16S rRNA gene (*rrn16*) that confers resistance to spectinomycin. The inheritance of the plastid genome in *Arabidopsis thaliana* is maternal with a very low frequency of paternal transmission (Azhagiri and Maliga, 2007). The plants that resulted after crossing (F1 generation) were grown under standard growth conditions and left to self-pollinate. The selection of the double mutants was performed in F2 generation as following: F2 seeds were sterilized and grown for 10 days on Petri dishes with MS medium supplemented with 1% sucrose and 500 mg/L spectinomycin dihydrochlorid pentahydrate (Sigma-Aldrich). The spectinomycin-resistant seedlings were transferred to soil and left to further develop. After approximately 10 days, the cotyledons were harvested for mtGFP fluorescence using an epifluorescent microscope. Only plants that showed intense and uniformly-distributed mtGFP fluorescence were left to self-pollinate and the resulting seeds (F3) were used for CLSM investigations.

***prp111-1xmtGFP*** The crossing was performed between the two parent lines using either *mtGFP* or *prp111-1* line as maternal parent. The plants from the F1 generation were grown under standard growth conditions and left to self-pollinate. The selection of the double mutants was performed in F2 generation. F2 plants were grown under standard growth conditions and the plants that showed specific mutant phenotype (delayed growth and development, pale green leaves) were selected for microscopic evaluation of mtGFP fluorescence. The plants that showed intense and uniformly-distributed mtGFP fluorescence were further genotyped by PCR. *prp111-1xmtGFP* plants homozygous for *prp111-1* were selected using the primers listed in Table 4 and representative PCR results are presented in Annex 2. Seeds from F3 generation were used for CLSM investigations.

### 3 Results

#### 3.1 Analysis of organellar gene copy number in *Arabidopsis thaliana* and *Hordeum vulgare*

The plant mitochondrial genome has a large and complex structure when compared to other eukaryotes (see 1.4.2). Moreover, it has to function properly in the context of a highly dynamic chondriome and pass the genetic information unaltered to subsequent generations. This requests a fine tuning of mitochondrial DNA abundance by replication and recombination, partition between individual mitochondria and transmission through gametes. Until now, there exists little information on mitochondrial DNA (mtDNA) abundance in both normal and stress conditions, possible regulatory mechanisms not yet being described. A first step in the analysis of possible regulatory networks is represented by the determination of mtDNA abundance in model plants grown under standard growth conditions. For this, three aspects are being investigated. At first, the existence of mtDNA content in various organs of the model plant *Arabidopsis thaliana*. Secondly, the correlation between DNA content and the number of mitochondria is made by counting the mitochondria in protoplasts isolated from leaves of different ages. Lastly, the mtDNA content is evaluated in relation to the basic ploidy and endopolyploidy level of the plants. Diploid and tetraploid *Arabidopsis* and barley plants are compared. Moreover, the plastid DNA (ptDNA) content is investigated in this context.

##### 3.1.1 Analysis of mitochondrial gene copy number in various *Arabidopsis* organs

In order to observe variations in the mitochondrial genome abundance we determined the copy numbers of four representative mitochondrial genes *atp1*, *nad6*, *rps4* and *cox1* using quantitative real-time PCR. The selected genes represent the chondrome-dependent mitochondrial functions of ATP synthesis, electron transport and gene expression. They are distributed over the physical map of the *Arabidopsis* mitochondrial genome (Unseld *et al.*, 1997) but also include two genes (*nad6* and *rps4*) that are located adjacent to each other. Data is normalized to the nuclear-

encoded single-copy gene *RpoTm* (mitochondrial targeted RNA polymerase of the phage type, Liere and Börner, 2011) on the basis of  $2^{(-\Delta C_T)}$  values ( $\Delta C_T = C_T^{\text{target}} - C_T^{\text{internal standard}}$ ) leading to a relative amount of gene copies. A final value termed “mitochondrial gene copies per cell” is calculated as the product of the relative amount of gene copies and the mean nuclear endopolyploidization level (“mean C-level”) determined by flow cytometry, taking into consideration the nuclear copies of mitochondrial genes NUMTs). In *Arabidopsis*, the mean C-level (where 1C equals the DNA content of unreplicated nuclei in haploplastic tissue) (Barow and Jovtchev, 2007) is highly variable depending on the analyzed tissue / organ due to extensive endoreduplication (Galbraith *et al.*, 1991; Barow and Meister, 2003; Zoschke *et al.*, 2007). Therefore, exact quantification of nuclear ploidy by flow cytometry is necessary in order to precisely calculate the final mitochondrial gene copy number.

Moreover, nuclear copies of mitochondrial genes (NUMTs) were also taken into consideration. When total DNA is subjected to real-time PCR, NUMTs can influence the final quantification of mitochondrial gene copies since they are co-amplified with their mitochondrial siblings. In *Arabidopsis*, the nuclear genome contains only one copy of each of the DNA sequences used in quantitative real-time PCR analysis for *atp1*, *nad6*, and *rps4*. Therefore, the mean C-level equivalent of one nuclear gene copy was subtracted to calculate exactly the mitochondrial copy numbers of these genes.

First, we determined the copy number of the four representative mitochondrial genes *atp1*, *nad6*, *rps4*, and *cox1* in flowers, stems, green siliques, roots (plant roots without root tips) and root tips originating from 50 days-old *Arabidopsis* plants. The root tips (the first 3-4 mm of the root tip) were investigated separately as they contain meristematic cells that are actively dividing and transmitting their mitochondrial DNA to the daughter cells. At first, we measured the endopolyploidization status of the nuclear genome by flow cytometry. While the mean C-level of fully developed flowers was 2.7C, stems and green siliques had similar values (4C). The highest values were present in roots and root tips, approximately 6C (Fig.12A and Annex 1).

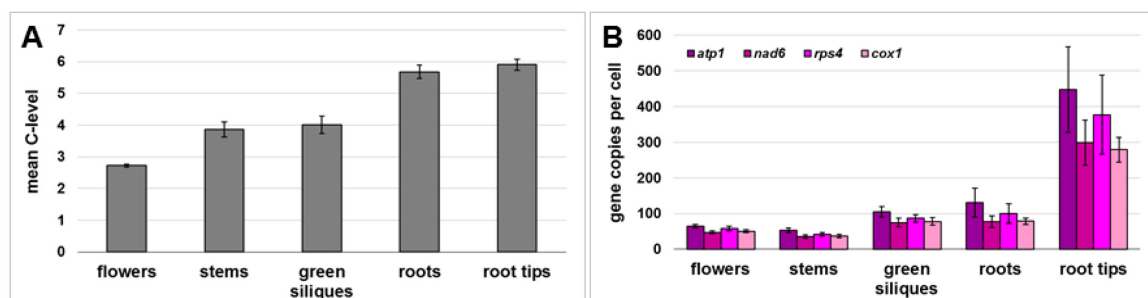


**Figure 12 Mean C-level and mitochondrial gene copy number in different *Arabidopsis* organs.** A) Mean C-level of different organs as determined by flow cytometry; B) Relative gene copy numbers of four mitochondrial genes *atp1*, *nad6*, *rps4* and *cox1*, were measured using quantitative real-time PCR. The nuclear-encoded single-copy gene *RpoTm* was used as internal standard. Total number of gene copies per cell was then calculated as described above using the relative gene copy number, the mean C-level and the number of NUMTs.

Determination of the mitochondrial gene copy number revealed significant differences between individual genes with *atp1* being the most abundant in flowers, stems and siliques, whereas in roots and root tips a high variability in gene amount was observed (Fig. 12B). The existence of distinctive number of individual genes within the same sample represents a real condition and not an artifact of the quantitative real-time PCR. Equal amplification efficiencies of the four gene fragments were found in previous determinations, as discussed in Preuten *et al.* (Preuten *et al.*, 2010).

Generally, all genes investigated showed low levels of copy numbers with values ranging between 50-70 in flowers and stems until 100-140 (*atp1* in siliques and roots). The highest values were observed in root tips (300-450) that contain actively dividing meristematic cells, representing the region with the highest mtDNA synthesis (Fujie *et al.*, 1993).

### 3.1.2 Analysis of mitochondrial gene copy number in relation to mitochondria number during *Arabidopsis thaliana* leaf senescence

#### 3.1.2.1 Determination of mitochondria number in protoplasts from representative leaf senescence stages

Recently, mitochondrial gene copy numbers during *Arabidopsis* leaf development have been investigated in our group (Preuten *et al.*, 2010). For this, rosette leaves (Ros) from 20-, 30-, 40- and 50-days old plants were used, as well cotyledons (Cot) and cauline (Cau) leaves (Fig. 13). The samples represent the whole

range of leaf developmental stages starting from 5-days old cotyledons until yellow, senescent leaves (Ros50/8). Determination of mitochondrial gene copy number showed a variable gene amount, starting from a minimum of 40 in cauline leaves (*rps4*, *cox1*, *Cau50/1*) to a maximum of around 280 (*atp1*, Ros50/6). Copy numbers of all analyzed genes had a pronounced increase in older rosette leaves, at the onset of leaf senescence, peaking in 31-days-old leaves of 50-days-old plant (Ros50/6; Preuten *et al.*, 2010). With further aging, the number of gene copies rapidly decreased again (Ros50/8; Preuten *et al.*, 2010).

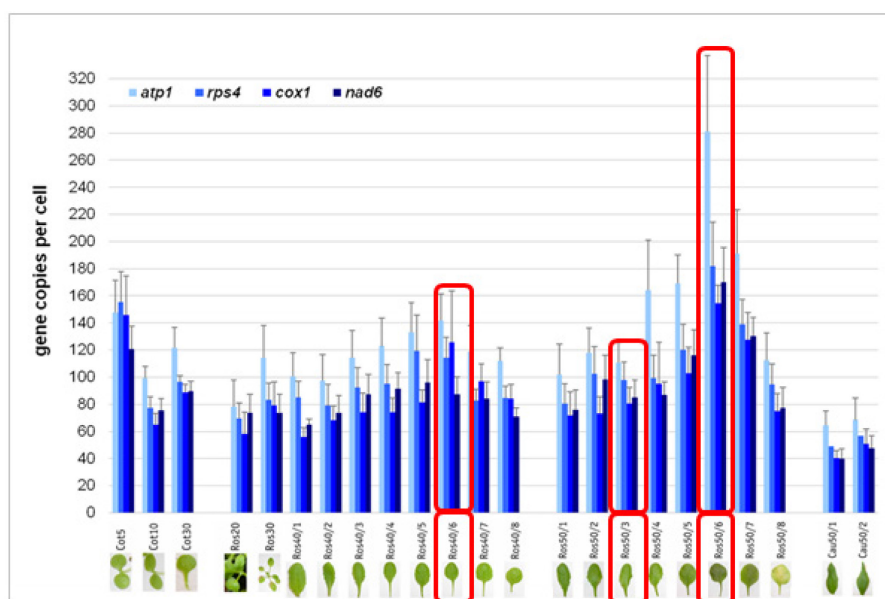


**Figure 13 Copy numbers of mitochondrial genes during cotyledon and leaf development in *Arabidopsis*.** Relative gene copy numbers of four mitochondrial genes *atp1*, *rps4*, *cox1* and *nad6* were measured using quantitative real-time PCR. The nuclear-encoded single-copy gene *RpoTp* was used as internal standard. Total number of gene copies per cell was then calculated as described at 3.1.1 using the relative gene copy number, the mean C-level and the number of NUMTs. A representative image of each leaf developmental stage is presented and the three stages investigated for mitochondria number are depicted in red. Modified after Preuten, 2009 (dissertation).

In this context, an evaluation of mitochondria number per cell could bring important information on a possible relation between the number of organelles and their DNA content. To this end, the mitochondria number was investigated in protoplasts isolated from rosette leaves corresponding to samples Ros40/6, Ros50/3 and Ros50/6 (Fig. 13). These stages were chosen since they represent the same leaves (leaves number 5 and 6) at younger (Ros40/6) and 10-days older (Ros50/6) developmental stages, but also younger (number 11-12) and older leaves (number 5 and 6) from the same age stage (50 days), represented by Ros50/3 and Ros50/6,



respectively (Fig.13 and 14A). The previously observed peak in gene abundance is included in this evaluation (50/6).

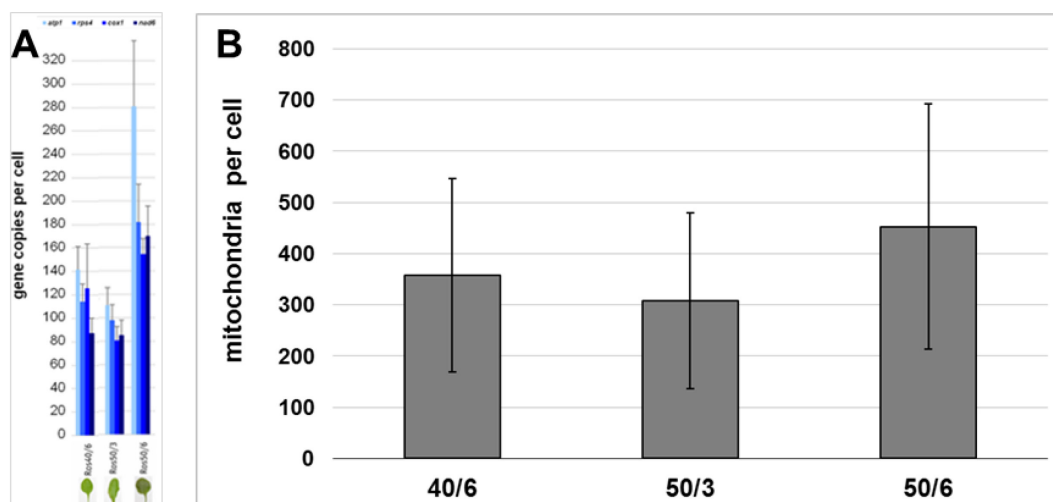


**Figure 14 Mitochondrial gene copy number and mitochondria number in three representative leaf developmental stages.** A) Mitochondrial gene copy number of Ros40/6, Ros50/3 and Ros50/6 leaves. Relative gene copy numbers of four mitochondrial genes *atp1*, *nad6*, *rps4* and *cox1*, were measured using quantitative real-time PCR. The nuclear-encoded single-copy gene *RpoTp* was used as internal standard. Total number of gene copies per cell was then calculated as described at 3.1.1 using the relative gene copy number, the mean C-level and the number of NUMTs. Modified after Preuten, 2009. . B) The number of mitochondria in protoplasts originating from Ros40/6, Ros50/3 and Ros50/6 leaves was determined using confocal laser scanning microscopy (see 2.2.16 and Annex 3). The mean values were obtained from three independent isolations that encompass 60 protoplasts for each stage.

Transgenic *Arabidopsis* expressing GFP in mitochondria (Logan and Leaver, 2000) was used to generate protoplasts. Counting of mitochondria within each protoplast was performed by confocal laser scanning microscopy (see 2.2.16 and Annex 3), with 20 randomly chosen protoplasts being investigated in each developmental stage. Three independent isolates resulted in evaluation of a total number of 60 protoplasts for each age stage. All analyzed protoplasts contained chloroplasts, i.e. were derived from photosynthetically active leaf cells. The calculated mean number of mitochondria was 358 in Ros40/6, 308 in Ros50/3 and 452 in Ros50/6 (Fig. 14B). However, a high variability existed in the number of mitochondria in protoplasts from the same age stage, leading to an insignificant difference between the three investigated age stages (Fig. 14B and Annex 3). When comparing these results to the mitochondrial gene copy number in the same leaves (Fig. 14A), no correlation could be observed between increased copy numbers at the

onset of leaf senescence and the determined mitochondria number in the same age stage (Ros50/6; Fig. 14A and B). This led to the conclusion that the observed increased mitochondrial gene copy number is not determined by multiplication of mitochondria within the cells, but that existing mitochondria probably contain more DNA.

Moreover, the existing mitochondria had the same size and morphology, without obvious differences between leaf age stages (Fig. 15).

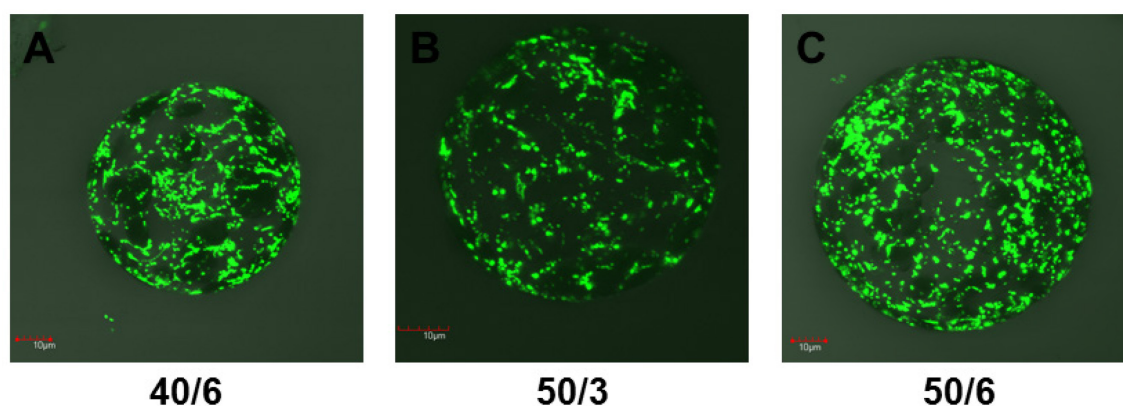


**Figure 15** Representative images of mitochondria in protoplasts originating from Ros40/6, Ros50/3 and Ros50/6 leaves. Protoplasts were isolated from Ros40/6 (A), Ros50/3 (B) and Ros50/6 (C) leaves originating from a line with mitochondria-targeted GFP (Logan and Leaver, 2000). Half cells were scanned as 1  $\mu$ m z-series and the resulting images were overlapped using the FV1000-ASW 2.0 Viewer software.

### 3.1.2.2 Analysis of mitochondria number in relation to protoplast size

It is already well known that *chloroplast* number is dependent on cell size, a direct relation existing between these two parameters. However, even if mitochondria number per cell has been previously determined in protoplasts, root cells, cell suspension cultures and callus of different species (Sheahan *et al.*, 2004; Sheahan *et al.*, 2005a; Kato *et al.*, 2008), until now, nothing is known about the relation between mitochondria number and cell size. Because of that, we have determined the size (diameter) of the same protoplasts used for mitochondria quantification (see 3.1.2.1 and Annex 3). A mean cell size of 40 - 50  $\mu$ m was observed for all three leaf developmental stages, with high variations between individual protoplasts (Fig. 16A and Annex 3). While no significant differences being observed between particular leaf

stages (Fig. 16A), the protoplasts of all three stages (in total 180 protoplasts) were used for evaluating the relation between cell size and mitochondria number. The protoplasts were separated on 7 size categories and the mean number of mitochondria was determined for each category. Interestingly, with increasing cell size, a linear increase in the number of mitochondria was observed (Fig. 16B). While small protoplasts (10 - 20  $\mu\text{m}$ ) contain approximately 80 mitochondria, medium size (40 – 50  $\mu\text{m}$ ) have 350 and the largest ones (70 – 80  $\mu\text{m}$ ) up to 700 mitochondria. These results suggest that the number of both chloroplasts and mitochondria are adjusted to cell size, maintaining a constant ratio throughout leaf development.

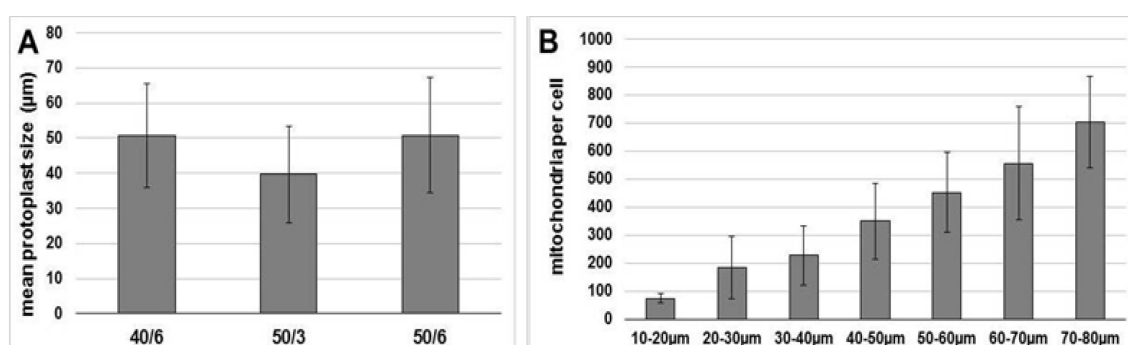


**Figure 16 Mean protoplast size and the relation with mitochondria number.** A) Mean protoplast size in Ros40/6, Ros50/3 and Ros50/6 leaves. 60 protoplasts were measured for each stage. B) The protoplasts from all three age stages (180) were separated into size categories and the mean number of mitochondria was determined for each category.

### 3.1.3 Comparison of organellar gene copy numbers in *Arabidopsis thaliana* and *Hordeum vulgare* diploid and tetraploid lines

Chloroplasts and chloroplast DNA amounts have been intensively studied in the context of leaf development and senescence (Rowan *et al.*, 2004; Li *et al.*, 2006; Oldenburg *et al.*, 2006; Shaver *et al.*, 2006; Zoschke *et al.*, 2007; Rowan *et al.*, 2009; Rauwolf *et al.*, 2010). Moreover, it has been observed that in mesophyll cells of mature leaves of *Beta vulgaris* differing in ploidy (di-, tri- and tetraploid), there exists a relative constant plastome/nuclear genome ratio (Rauwolf *et al.*, 2010). This seems not to be the case during *A. thaliana* leaf development where elevated nuclear ploidy levels are present as a result of endopolyploidization (Zoschke *et al.*, 2007). The 3.5-fold difference in mean ploidy level (mean C-level) between the stages Ros40/1 and

Ros50/7 is not observed in plastome copy numbers of the same leaves. Instead, a constant plastome amount is found throughout leaf development until first stages of senescence (Zoschke *et al.*, 2007). The situation is different with mtDNA amounts where significant elevation of mitochondrial gene copy number could be observed during aging of leaves, the highest values being present at the onset of leaf senescence in stage Ros50/6 (Fig. 13).

Until now, the relation between nuclear ploidy levels and organellar DNA amounts is not clear. To further investigate this process, both mitochondrial and plastid gene copy number were determined in diploid and tetraploid lines of *A. thaliana* and barley. Two different species were chosen because they differ in the natural occurrence of endopolyploidization. Endopolyploidy represents the existence of nuclei with different ploidy levels (named 2C, 4C, 8C...) in adjacent cells of the same tissue (Barow and Meister, 2003). It varies between plant families, species, organs and even between different tissues of the same organ (Barow and Meister, 2003; Barow, 2006; Barow and Jovtchev, 2007). While *A. thaliana* is a diploid species ( $2n = 2x = 10$ ) with high endopolyploidy (Galbraith *et al.*, 1991; Barow and Meister, 2003), barley is a diploid plant ( $2n = 2x = 14$ ) with low endopolyploidy (Barow and Meister, 2003).

### **3.1.3.1 Analysis of organellar gene copy number in *Arabidopsis thaliana* diploid and tetraploid lines**

#### **3.1.3.1.1 Confirmation of ploidy status**

To investigate if a direct relation exists between nuclear ploidy level and organellar DNA amounts, two diploid and two tetraploid *Arabidopsis* lines were used. While Col-0 and Ws are natural diploid ecotypes, Wa-1 is a natural tetraploid ecotype and Wilna represents a tetraploid line obtained by colchicine treatment (Karcz *et al.*, 2000) (Table 1). The plants were grown in soil for 20 days and total rosettes of individual plants were harvested and used for ploidy and gene copy number determinations (Fig. 17A-D). This age stage was chosen because there exist differences in plant development between individual lines and this is the oldest stage that allows for individual harvesting of plants while having 4 rosette leaves in all

lines. Three individual plants were harvested from each line in three biological repetitions, altogether 9 individual plants from each line.

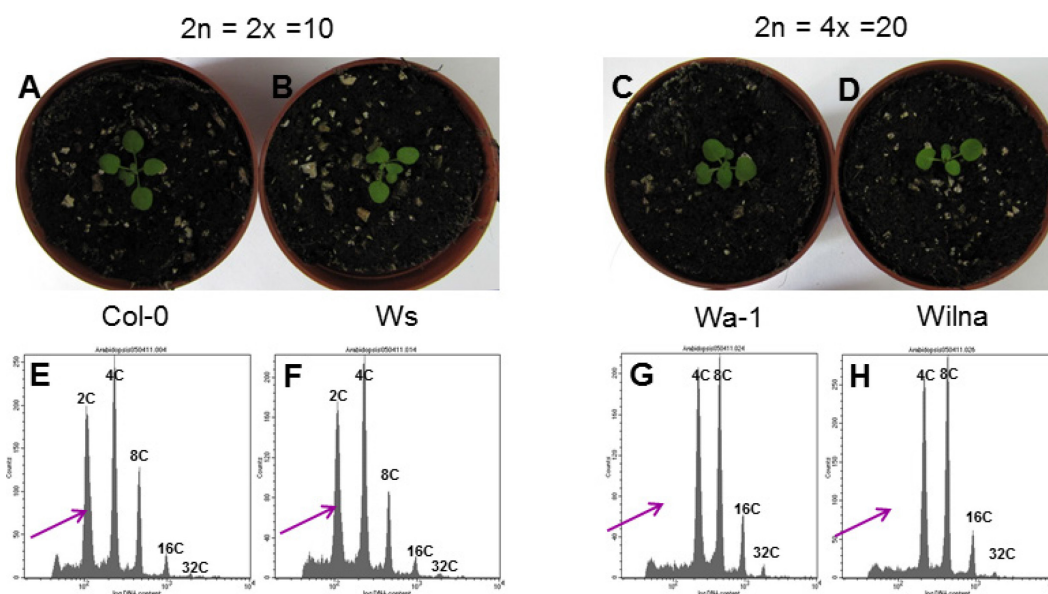


**Figure 17 Determination of ploidy status.** The basal ploidy level and the degree of endopolyploidization were determined by flow cytometry. A-D) Representative images of 20-days old diploid (Col-0, Ws) and tetraploid (Wa-1, Wilna) lines; E-H) Representative histograms of diploid and tetraploid lines. The grey peaks represent 2C, 4C, 8C etc. nuclei and the height of the peak represents the abundance of nuclei. The violet arrow points to the 2C peak, demonstrating its absence in tetraploid lines.

At first, the ploidy status of the 4 lines was determined by flow cytometry. Representative histograms are shown with each peak representing the ploidy level of the nuclei and the height of the peak representing the abundance of respective nuclei in the total nuclei preparation (Fig. 17E-H). Col-0 and Ws were confirmed to be diploid by the existence of a 2C peak (Fig. 17E-F). As expected, higher nuclear ploidy levels are also present by the appearance of 4C, 8C, 16C and 32C peaks. Additionally, Wa-1 and Wilna were confirmed to be tetraploid by the absence of the 2C peak, proving that the basal ploidy level of the lines is tetraploid (Fig. 17G-H). The mean ploidy levels of the investigated lines were 5.2C for the diploid Col-0 and Ws and 8.8C for Wa-1 and 7.4C for Wilna (Fig. 18 and Annex 1). Surprisingly, these results do not show a complete doubling of the mean ploidy level in the tetraploid ecotypes. This situation is a result of lower degree of endopolyploidization in tetraploid ecotypes in comparison to the diploid ones, an observation previously made by Jovtchev *et al.* (2006).

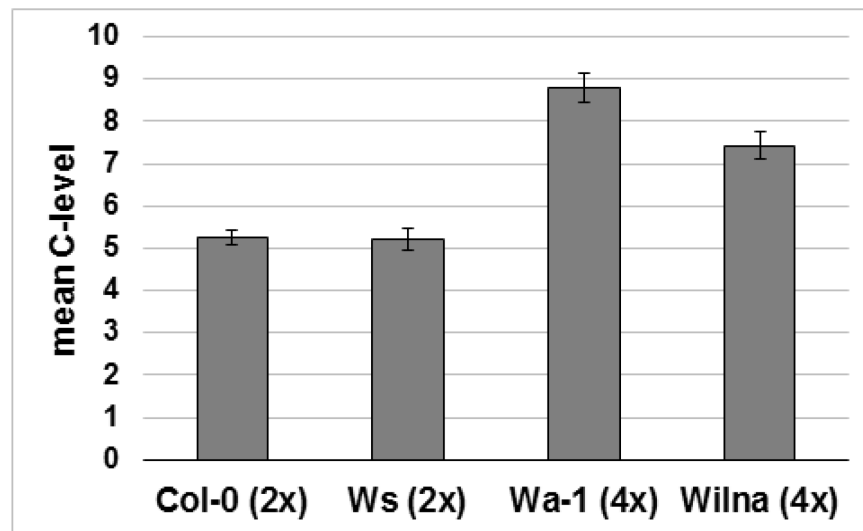


**Figure 18 Mean C-level of *Arabidopsis* diploid and tetraploid lines.** The mean C-level of diploid and tetraploid lines was determined by flow cytometry as described by Barow and Meister (2003).

### 3.1.3.1.2 Determination of mitochondrial gene copy number

Determination of mitochondrial gene copy number showed no significant difference between diploid and tetraploid lines (Fig. 19A). However, a high variability was present between individual plants, where the representative value of *atp1* is shown (Fig. 19B). The diploid line Col-0 represents the line with the most stable copy number values (approx. 65-90 *atp1*) between individual plants and biologic repetitions (Fig. 19B). The second diploid line, Ws, presented higher variability between individual plants with some plants having 3.4-fold more copies than others belonging to the same line (between 25 and 85 *atp1*). The same situation could be observed in the tetraploid line Wilna, having between 30 and 110 copies of *atp1*. The tetraploid ecotype Wa-1 had the highest variability with values starting from 40 until 240. This represents a 6-fold difference between individual plants. The results indicate that mitochondrial gene copy number is highly variable between individual plants even under standard growth conditions. While one of the investigated ecotypes seems to be more stable (Col-0), the other three present high variability with some of the plants having between 2-fold until 6-fold more mitochondrial gene copies than other plants belonging to the same line.

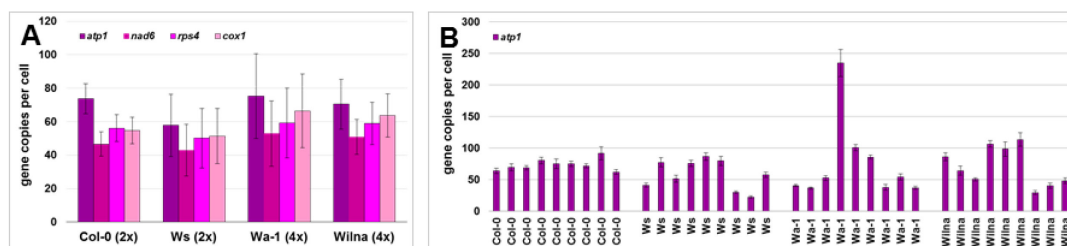


**Figure 19 Mitochondrial gene copy number in *Arabidopsis* diploid and tetraploid lines.** Relative gene copy numbers of four mitochondrial genes *atp1*, *nad6*, *rps4* and *cox1*, were measured using quantitative real-time PCR. The nuclear-encoded single-copy gene *RpoTm* was used as internal standard. Total number of gene copies per cell was then calculated as described in 3.1.1 using the relative gene copy number, the mean C-level and the number of NUMTs. A) Mitochondrial gene copy number in different lines. B) Representative copy number of *atp1* in individual plants representing three independent biological repetitions, in total 9 plants per line.

### 3.1.3.1.3 Determination of plastid gene copy number

The copy number of two representative plastid genes, *psbA* and *clpP* was determined by quantitative real-time PCR in diploid and tetraploid *Arabidopsis* lines. The same total DNA samples were used as for 3.1.3.1.2. *psbA* and *clpP* are single copy genes present in the large single copy region (LSC) of the plastome and, as expected, *psbA* and *clpP* showed identical copy numbers in all investigated samples (Fig. 20A). Both diploid and tetraploid lines presented high variability in copy numbers, with values varying between 500 and 3600 copies (Fig. 20B). Even if a high variability exists, the mean plastid copy number significantly relates to the ploidy level (Fig. 20A).

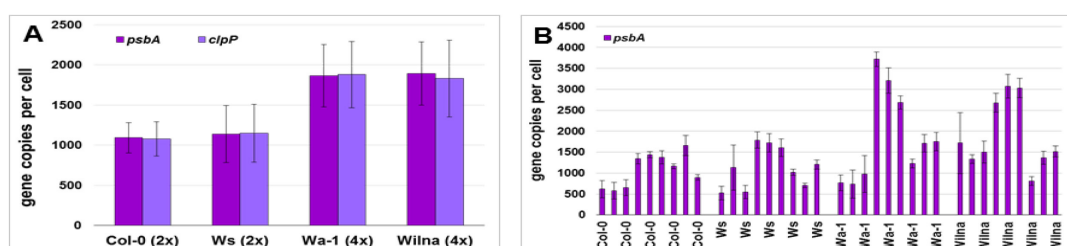


**Figure 20 Plastid gene copy number in *Arabidopsis* diploid and tetraploid lines.** Relative gene copy numbers of two plastid genes, *psbA* and *clpP*, were measured using quantitative real-time PCR. The nuclear-encoded single-copy gene *RpoTm* was used as internal standard. Total number of gene copies per cell was then calculated as described at 3.1.1 using the relative gene copy number and the mean C-level. A) Plastid gene copy number in different lines. B) Representative copy number of *psbA* in individual plants representing three independent biological repetitions, in total 9 plants per line.

### **3.1.3.2 Determination of organellar gene copy number in *Hordeum vulgare* diploid and tetraploid lines**

#### **3.1.3.2.1 Confirmation of ploidy status**

The second investigated species was barley (*Hordeum vulgare* cv. “Golden Promise”). Barley is a diploid plant ( $2n = 2x = 14$ ) that has a low degree of endopolyploidy (Barow and Meister, 2003). For the present experiments we used one diploid (WT) and two tetraploid lines L150 and MBE (unpublished, see Table 1). The plants were grown for 10 days under long-day conditions and the primary leaf was cut and used for determination of ploidy level and gene copy number. Three individual plants were harvested from each line, and three biologic repetitions were made, in total 9 individual plants from each line (Fig. 21A-C).





**Figure 21 Determination of the ploidy status of barley diploid and tetraploid lines.** The basal ploidy level and the degree of endopolyploidisation were determined by flow cytometry. A-C) Representative images of 10-days old diploid (WT) and tetraploid (L150, MBE) barley lines; D-F) Representative histograms of diploid and tetraploid lines. The grey peaks represent 2C, 4C, 8C and 16C nuclei and the height of the peak represents the abundance of nuclei. The violet arrow points to the 2C peak, demonstrating its absence in tetraploid lines.

At first, we determined the ploidy status of these lines and their degree of endopolyploidization by flow cytometry. Representative histograms are shown with each peak representing a ploidy status of the nuclei and the height of the peak representing the abundance of respective nuclei in the total nuclei preparation from leaf blade. The original WT line was confirmed to be diploid by the existence of a major 2C peak. A minor 4C and hardly visible 8C and 16C peaks (Fig. 21D) were also observed, demonstrating the low endopolyploidy level of barley. L150 and MBE were confirmed to be tetraploid by the absence of the 2C peak, proving that the basal ploidy level of these lines is tetraploid (Fig. 21E, F). The mean ploidy level was 2.4C

for the diploid line and 4.7C and 4.8C for L150 and MBE respectively (Fig. 22 and Annex 1). In this case, the tetraploid lines show a complete doubling of the mean ploidy level in respect to the diploid line. This result might be a consequence of a better cell cycle control in plants without extensive endopolyploidization.

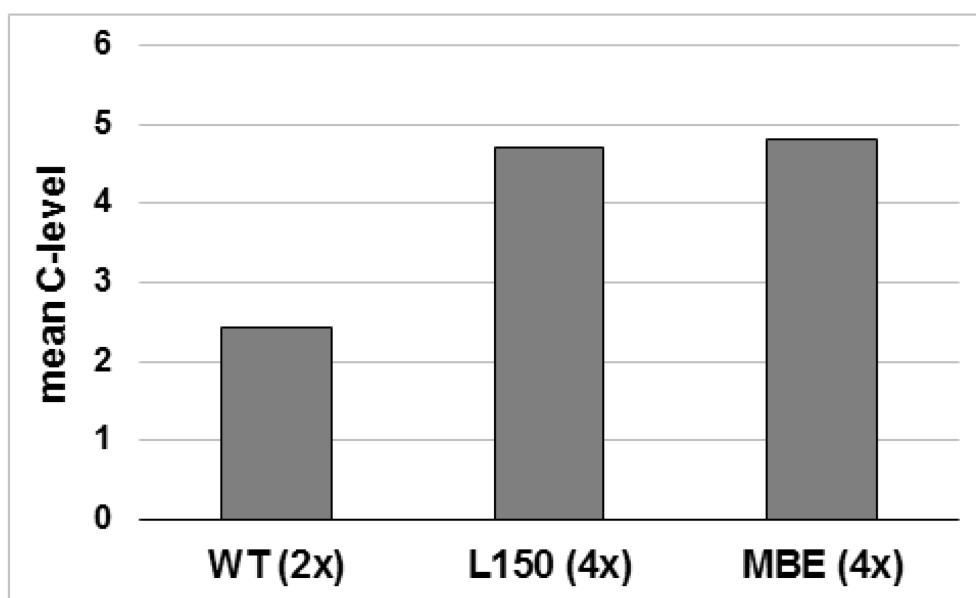


**Figure 22 Mean C-level of barley diploid and tetraploid lines.** The mean C-level of diploid and tetraploid lines was determined by flow cytometry as described by Barow and Meister (2003). Error bars are not visible as a result very low difference between repetitions.

### 3.1.3.2.2 Determination of mitochondrial gene copy number

Determination of copy numbers of the mitochondrial genes *atp9* and *rps2* was performed in both diploid and tetraploid lines. The observed difference between *atp9* and *rps2* in the same sample is not an error of the PCR, but a result of the complex mtDNA structure that exists *in vivo*, as discussed in Chapter 3.1.1. As observed in figure 23A, significant difference exists in relation to the nuclear ploidy level. While the investigated genes were present at an average of 40 - 90 copies in the diploid wild-type, both tetraploid lines doubled these values, having between 80 - 210 copies (Fig. 23A). The variability between individual plants and biological repetitions was low in all three lines, with copy numbers varying between 30 and 110 (Fig. 23B). These results reveal that mitochondrial gene copy number is more stable in barley leaves when compared to *Arabidopsis*. This points to a connection between cell cycle and

mtDNA abundance/replication. Moreover, when low endopolyploidy is present, a stable chondrome/nuclear genome ratio also exists and is maintained in higher ploidy levels. This ratio is about 17 copies per 1C for *atp9* and 37 copies per 1C for *rps2*, respectively.

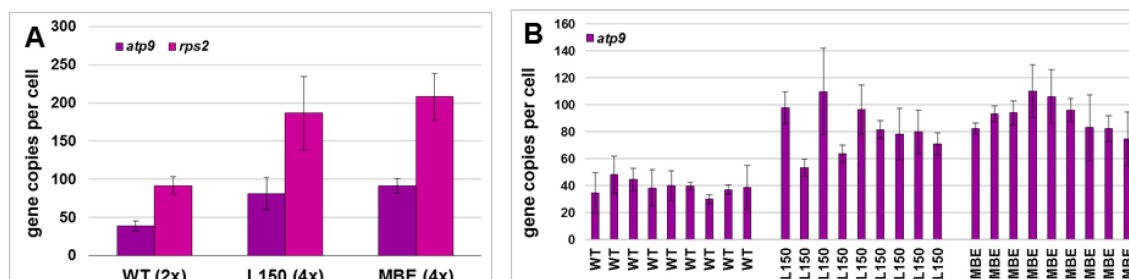


**Figure 23 Mitochondrial gene copy number in barley diploid and tetraploid lines.** Relative gene copy numbers of two mitochondrial genes *atp9* and *rps2*, were measured using quantitative real-time PCR. The nuclear-encoded single-copy gene *RpoTm* was used as internal standard. Total number of gene copies per cell was then calculated as the product of the relative gene copy number and the mean C-level. No corresponding NUMTs are present in barley genome. A) Mitochondrial gene copy number in different lines. B) Representative copy number of *atp9* in individual plants representing three independent biological repetitions, in total 9 plants per line.

### 3.1.3.2.3 Determination of plastid gene copy number

While a clear influence of nuclear ploidy could be observed on mitochondrial gene abundance, the plastome copy numbers were also investigated. The copy numbers of *psbA* and *clpP* were determined by quantitative real-time PCR in diploid and tetraploid lines. The same total DNA samples were used as for 3.1.3.2.2. *psbA* and *clpP* are single copy genes present in the large single copy region (LSC) of the barley plastome and, as expected, *psbA* and *clpP* showed identical copy numbers in investigated samples (Fig. 24A). Evaluation of mean plastome copies resulted in the observation that, together with the doubling of the nuclear ploidy, there exists also a doubling of the plastome copies, from 1100 in WT to 2200 (MBE) or almost 3000 in L150 (Fig. 24A). When individual plants were compared, a low variability was observed in all three lines. Plastome copy numbers varied between 1000 and 4200 copies per cell, with highest values being present in tetraploid lines (Fig. 24B). These results prove that in barley there exists a relative constant plastome/nuclear genome ratio of approximately 400 plastome copies per 1C.

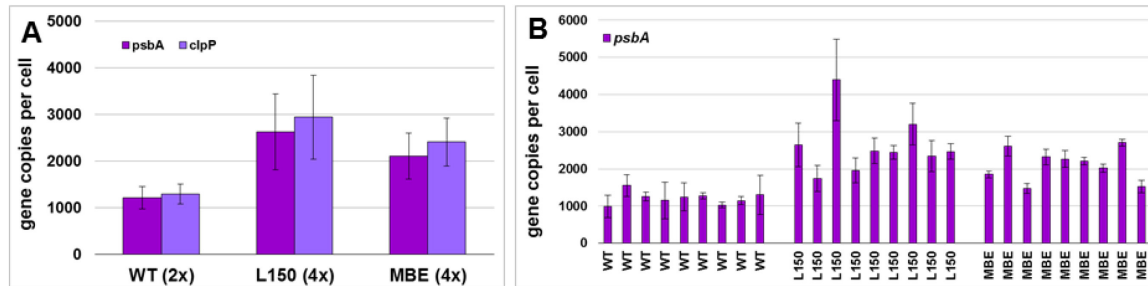


**Figure 24 Plastid gene copy number in barley diploid and tetraploid lines.** Relative gene copy numbers of two plastid genes, *psbA* and *clpP*, were measured using quantitative real-time PCR. The nuclear-encoded single-copy gene *RpoTm* was used as internal standard. Total number of gene copies per cell was then calculated as the product of the relative gene copy number and the mean C-level. No corresponding NUPTs are present in the barley genome. A) Plastid gene copy number in different lines. B) Representative copy number of *psbA* in individual plants representing three independent biological repetitions, in total 9 plants per line.

### 3.2 The effects of impaired chloroplast translation on mitochondria

#### 3.2.1 Reproduction of the barley *albostrians* mutant in *Arabidopsis* by treatment with the antibiotic spectinomycin

Chloroplasts/plastids and mitochondria have to collaborate in order to maintain the energetic status of plant cells and they contribute to common metabolic pathways. For this reason, extensive signaling takes place between these organelles that regulate each other's function.

A specific form of interaction between plastids and mitochondria was observed for the first time in the barley *albostrians* mutant (Hedtke *et al.*, 1999). *Albostrians* is a nuclear mutant that lacks plastid ribosomes in cells of the white tissue (Hagemann and Scholz, 1962). Previous investigations have shown that in white leaves of the mutant there exists a 2.5-3 fold elevation in mitochondrial gene abundance, an increase that was correlated with a similar elevation in transcript abundance of the investigated genes (Hedtke *et al.*, 1999). This work provides evidence for the existence of inter-organellar communication and makes the *albostrians* mutant a valuable tool in studying the mechanisms involved in this complex signaling network. Until now, an equivalent mutant has not been described in *A. thaliana*, requesting an alternative approach in order to recreate this condition.

The antibiotic spectinomycin is an inhibitor of plastid translation (Wallace *et al.*, 1974; Moazed and Noller, 1987) and growth of *Arabidopsis* seedlings in presence of the antibiotic results in white, photosynthetically inactive seedlings (Fig. 25A; Svab *et al.*, 1990; Hess *et al.*, 1994a; Zubko and Day, 1998; Swiatecka-Hagenbruch *et al.*, 2008). Inhibition of plastid protein synthesis was proved by protein immunoblot analysis using the RbcL antibody. RbcL is a highly abundant plastid-encoded protein that could not be detected in white seedlings (Fig. 25B).

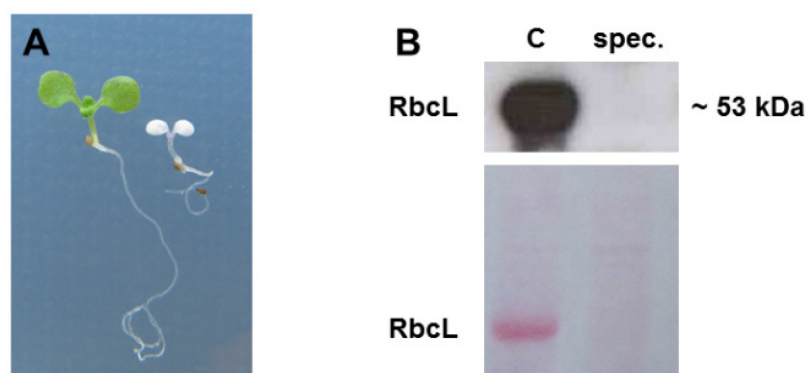


**Figure 25** The phenotype of spectinomycin-treated *Arabidopsis* seedlings and protein immunoblot. *Arabidopsis* seeds (ecotype Col-0) were grown for 10 days on SEA medium containing 1% sucrose and 500 mg/L spectinomycin. (A) Representative phenotype of green and white seedlings; (B) Protein immunoblot with RbcL antibody.

### 3.2.2 Determination of mitochondrial gene copy number in white, spectinomycin-treated seedlings

In order to investigate the mtDNA abundance in green and in white, spectinomycin-treated seedlings, we have determined the mitochondrial gene copy number of *atp1*, *nad6*, *rps4* and *cox1* by quantitative real-time PCR. At first, the mean ploidy level was determined by flow cytometry. While the mean C-level of green seedlings was found to be 5.1C, white seedlings contained a slightly increased endopolyploidization level, 6.3C (Fig. 26A).

Comparison of four mitochondrial genes *atp1*, *nad6*, *rps4*, and *cox1* showed 3-fold elevated copy numbers per cell for all of them in white seedlings: *atp1* increased from 100 gene copies per cell to 300, while *nad6*, *rps4*, and *cox1* from 50-70 to 150-200 (Fig. 26B). A differential amplification of any gene could not be observed, a correct ratio between the genes being maintained also in white seedlings. This

suggests that white cells contain elevated levels of the whole mitochondrial genome and not of a particular subgenomic molecule. However, since we did not determine the abundance of all genes, a separate amplification of a subgenomic molecule cannot be completely excluded.

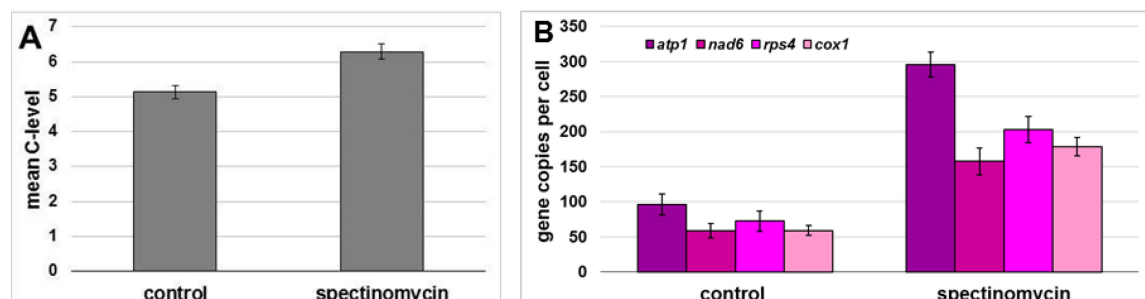


**Figure 26 Mean C-levels and mitochondrial gene copy numbers in green and white, spectinomycin-treated *Arabidopsis* seedlings.** Wildtype (Col-0) *Arabidopsis* seedlings were grown for 10 days on SEA medium containing 1% sucrose and 500 mg/L spectinomycin. (A) Mean C-levels were determined flow-cytometrically as described by Barow and Meister (2003); (B) Mitochondrial gene copy numbers in green and white seedlings were determined by quantitative real-time PCR using the single-copy nuclear gene *RpoTm* as internal standard. The final value was calculated as described in chapter 3.1.1 by using the relative gene copy number, the mean C-level and the number of NUMTs.

### 3.2.3 Steady-state transcript levels of mitochondrial genes in green and white, spectinomycin-treated *Arabidopsis* seedlings

The previously observed elevation of mtDNA abundance in white seedlings could play an important role in determining the amount of mitochondrial gene transcripts within the cell. To test this, the steady-state transcript level of the four investigated genes was determined using quantitative real-time RT-PCR and the nuclear-encoded housekeeping gene *UBQ11* as an internal standard. As the mitochondrial genes investigated in this study do not contain introns (Unseld *et al.*, 1997), the primers designed for the analysis of gene copy numbers were also used for this purpose. Determination of transcript levels of the four genes of interest showed a general elevation of the analyzed transcripts. While *atp1* and *cox1* showed just a slight increase in their transcript abundance, *rps4* and *nad6* RNA levels followed the increase observed in mtDNA levels, showing an approximately 3-fold elevation in comparison to untreated, green seedlings (Fig. 27). As shown in *albostrians* (Hedtke

*et al.*, 1999), impaired chloroplast development in *Arabidopsis* also seems to induce an increase in mitochondrial transcript abundance.

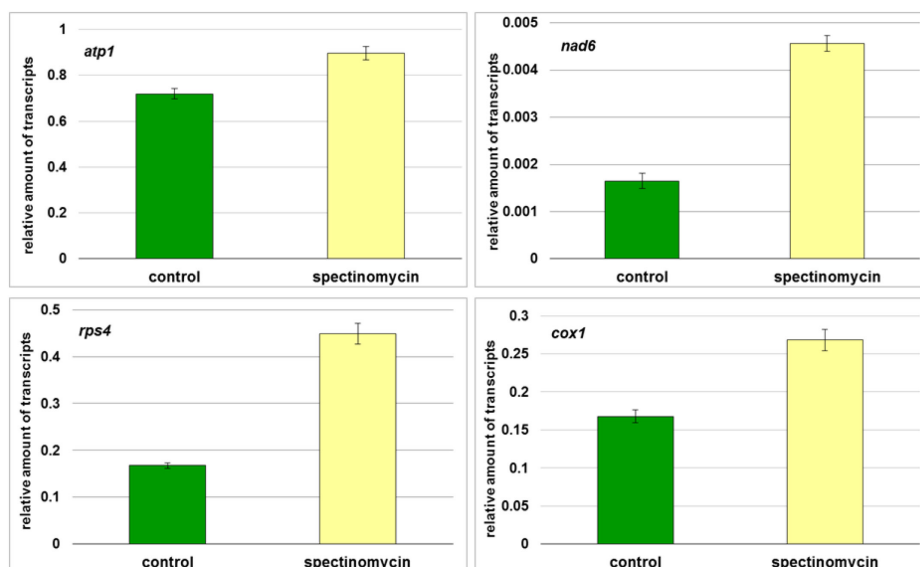


**Figure 27** Steady-state transcript level of selected mitochondrial genes in green and white, spectinomycin-treated *Arabidopsis* seedlings. Wildtype (Col-0) *Arabidopsis* seedlings were grown for 10 days on SEA medium containing 1% sucrose and, where specified, 500 mg/L spectinomycin. Relative transcript levels of the four investigated genes were determined by quantitative real-time RT-PCR using the *UBQ11* housekeeping gene as internal standard.

### 3.2.4 Steady-state transcript level of nuclear genes involved in mtDNA replication, recombination and transcription

Mitochondrial DNA replication, recombination, maintenance and transcription are under strict nuclear control (see 1.4.2.2 and 1.5.2). Until now, several genes have been identified that encode proteins involved in these processes. Mutation or elimination of these proteins induces large-scale rearrangements of the mitochondrial genome, reduced genome abundance or transcription that lead to perturbed functioning of mitochondria and severe plant phenotypes. (Maréchal and Brisson, 2010; Woloszynska, 2010; Arrieta-Montiel and Mackenzie, 2011; Liere and Börner, 2011; Parent *et al.*, 2011).

Based on their importance, we investigated the transcript levels of nuclear genes involved in mtDNA replication *Poly1*, *Poly2* (termed *PolIB* and *PolIA* by Parent *et al.*, 2011), in maintenance *Why2* (Maréchal *et al.*, 2008), in recombination



*Msh1*, *RecA3*, *Osbl* (Abdelnoor *et al.*, 2003, Arrieta-Montiel *et al.*, 2009, Shedje *et al.*, 2007, Zaegel *et al.*, 2006), and in transcription *RpoTm*, *RpoTnp* (Kühn *et al.*, 2009, Liere *et al.*, 2011). Evaluation of steady-state transcript levels of the investigated genes showed a three-fold upregulation for *recA3* and *why2*, two-fold for *RpoTm* and *RpoTnp*, while *Poly1*, *msh1* and *osbl* presented a small, yet significant, increase (Fig. 28). *Poly2* was the only gene with constant expression. These results indicate that an upregulation of nuclear genes involved in mtDNA replication and recombination is probably necessary for increased abundance of mitochondrial gene copies in white seedlings and the maintenance of a correct ratio between the genes (Fig. 26). Moreover, an increased expression of *RpoTm* and *RpoTnp* could be a reason for increased transcript levels of some mitochondrial genes (Fig. 27). However, the regulation of mitochondrial gene transcription seems to be complex (Liere and Börner, 2011) and the present results are not sufficient to draw a conclusion on the transcriptional process.

The nuclear genes involved in mtDNA replication and recombination could be a target for signaling pathways resulting in increased mtDNA abundance under different stress conditions. Until now, the signaling pathway still needs to be discovered.

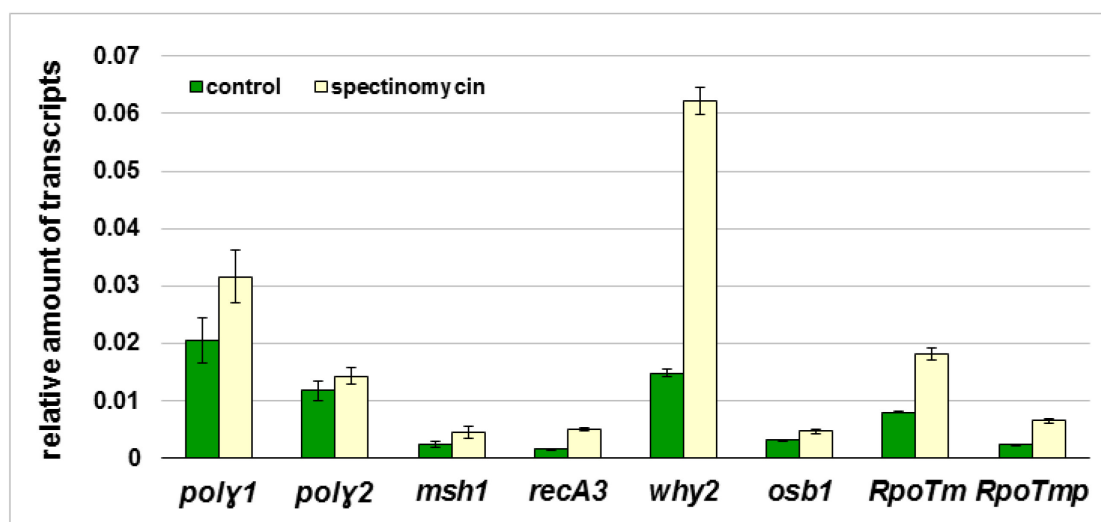


**Figure 28** Steady-state transcript levels of nuclear genes involved in mtDNA replication, recombination and transcription in green and white, spectinomycin-treated seedlings. Wildtype (Col-0) *Arabidopsis* seedlings were grown for 10 days on SEA medium containing 1% sucrose and, where specified, 500 mg/L spectinomycin. Relative transcript levels of the investigated genes were determined by quantitative real-time RT-PCR using the *UBQ11* housekeeping gene as internal standard.



### 3.2.5 Confocal microscopic (CLSM) investigations of mitochondrial dynamics in green and white, spectinomycin-treated *Arabidopsis* seedlings

The plant chondriome (see 1.3) is represented by a highly dynamic population of mitochondria that can be influenced by the metabolic status of the cell (Robertson *et al.*, 1995; Griffin *et al.*, 2001; Van Gestel and Verbelen, 2002; Yoshinaga *et al.*, 2005; Armstrong *et al.*, 2006; Zottini *et al.*, 2006; Scott and Logan, 2008b). A special situation is represented by the complex interaction between chloroplasts and mitochondria. Apart from the metabolic interactions (Noguchi and Yoshida, 2008), the two organelles were frequently found in close association in mesophyll cells of green leaves (Stickens and Verbelen, 1996; Logan and Leaver, 2000; Sheahan *et al.*, 2004) and even together changed their location in the cell under variable light conditions (Islam *et al.*, 2009; Islam and Takagi, 2010). Moreover, a white leaf phenotype is sometimes associated with a higher abundance of mitochondria, as observed in albino leaves of a transgenic bean (*Phaseolus vulgaris* L.; Soares *et al.*, 2005) and in albino rye plants (*Secale cereale* L.; Ballesteros *et al.*, 2009), but not in albino leaves of the barley *albostrians* mutant (Hedtke *et al.*, 1999).

Based on their impaired photosynthesis, white *Arabidopsis* cotyledons/leaves may represent a metabolic condition that could influence mitochondrial dynamics. Furthermore, evaluation of the number of mitochondria may give a possible explanation for the enhanced mitochondrial gene abundance found in white seedlings (Fig. 26). The observed 3-fold increase of gene copy numbers could have been the result of an increased number of mitochondria within the cell or of an increased DNA amount per mitochondrion. Therefore, mitochondrial dynamics (number, size, shape and motility) was investigated in both green and spectinomycin-treated, white seedlings.

To this end, confocal microscopic investigations were performed on a line with mitochondrial-targeted GFP, termed “*mtGFP*” (Logan and Leaver, 2000). The *mtGFP* seedlings were grown in leaning position for 10 days on SEA medium containing 1% sucrose and supplemented, where stated, with 500 mg/L spectinomycin. Mitochondria size, shape, density and motility were assessed in adaxial epidermal cells of both green and white cotyledons.

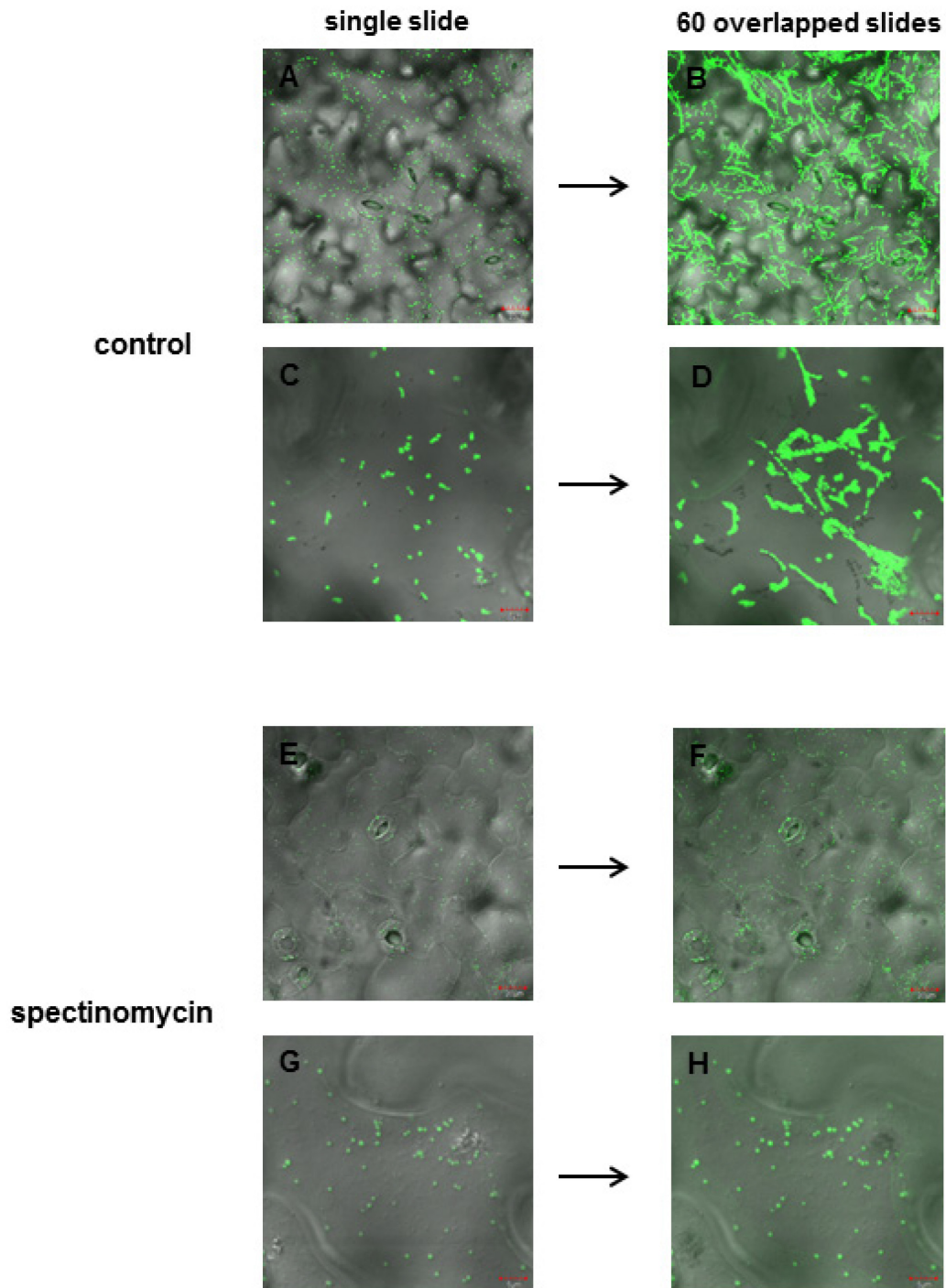


**Figure 29 Confocal microscopic images of mitochondria in epidermal cells of green and white cotyledons.** Seeds from a line with mitochondrial-targeted GFP (Logan and Leaver, 2000) were grown for 10 days on SEA medium containing 1% sucrose supplemented (where stated) with 500 mg/L spectinomycin. Mitochondria size, shape, density and motility were assessed using confocal microscopy. Single slides (A, C, E, G) and 60 overlapped slides (B, D, F, H) taken at 1.1 s interval are presented, representing mitochondria in adaxial epidermal cells of green (A, B, C, D) and white (E, F, G, H) cotyledons. Scale bar: 20  $\mu\text{m}$  (A, B, E, F) and 5  $\mu\text{m}$  (C, D, G, H).

Investigation of mitochondria in adaxial epidermal cells of green cotyledons showed characteristic spherical or sausage-like shape (Fig. 29A, C). Mitochondrial motility was assessed by overlapping 60 frames of the same focal plane taken at 1.1 s intervals. Motility pathways can be easily seen, revealing highly motile mitochondria with frequent fusion and fission events (Fig. 29B, D and Video 2). Visual comparison of mitochondrial density in epidermal cells of white cotyledons showed no difference when compared to green cotyledons (Fig. 29E). However, a more round shape of the existing mitochondria could be observed (Fig. 29G). When evaluating mitochondrial motility, a surprising observation was made: most of the mitochondria were found to be immotile, having just an oscillatory movement around their position (Fig. 29F, H and Video 3). The overlapped image representing a 60 second time span indeed showed only separate GFP dots that represent single, non-motile mitochondria. Nevertheless, a high variability between individual cotyledons existed. While in some cotyledons 100% of the mitochondria were immotile, other cotyledons presented approximately 30% motility (evaluated by visual observation). Altogether, over 15 cotyledons originating from individual seedlings were evaluated.

However, these observations were made on a single type of cells, adaxial epidermal cells of cotyledons and a more detailed analysis was necessary to draw firm conclusions. For this reason, other cell types were also studied: guard cells, mesophyll cells, vascular tissue and root cells. Visual evaluation of mitochondrial size, shape in different cell types in both green and white seedlings revealed a characteristic morphology with a tendency of more round mitochondria in spectinomycin-treated tissue (Fig. 30E, G, I, K, Q, and S). The vascular tissue presented also elongated and worm-like structures (Fig. 30M and O). As previously observed (Logan and Leaver, 2000), the existence of sausage-like and worm-like mitochondria in the vascular tissue represents a normal condition. Evaluation of the motility trails resulted in the observation that while in green seedlings, all investigated cell types had highly motile mitochondria with frequent fusion and fission events (Fig. 30B, F, J, N, R and Video 4, 6, 8, 10), in guard cells of the stomata, mesophyll cells and vascular tissue of white cotyledons motility was arrested in almost all mitochondria (Fig. 30H, L, P and Video 5, 7, 9). Surprisingly, a particular situation could be observed in root cells, where high motility was present also in the roots originating from white seedlings (Fig. 30T and Video 11).

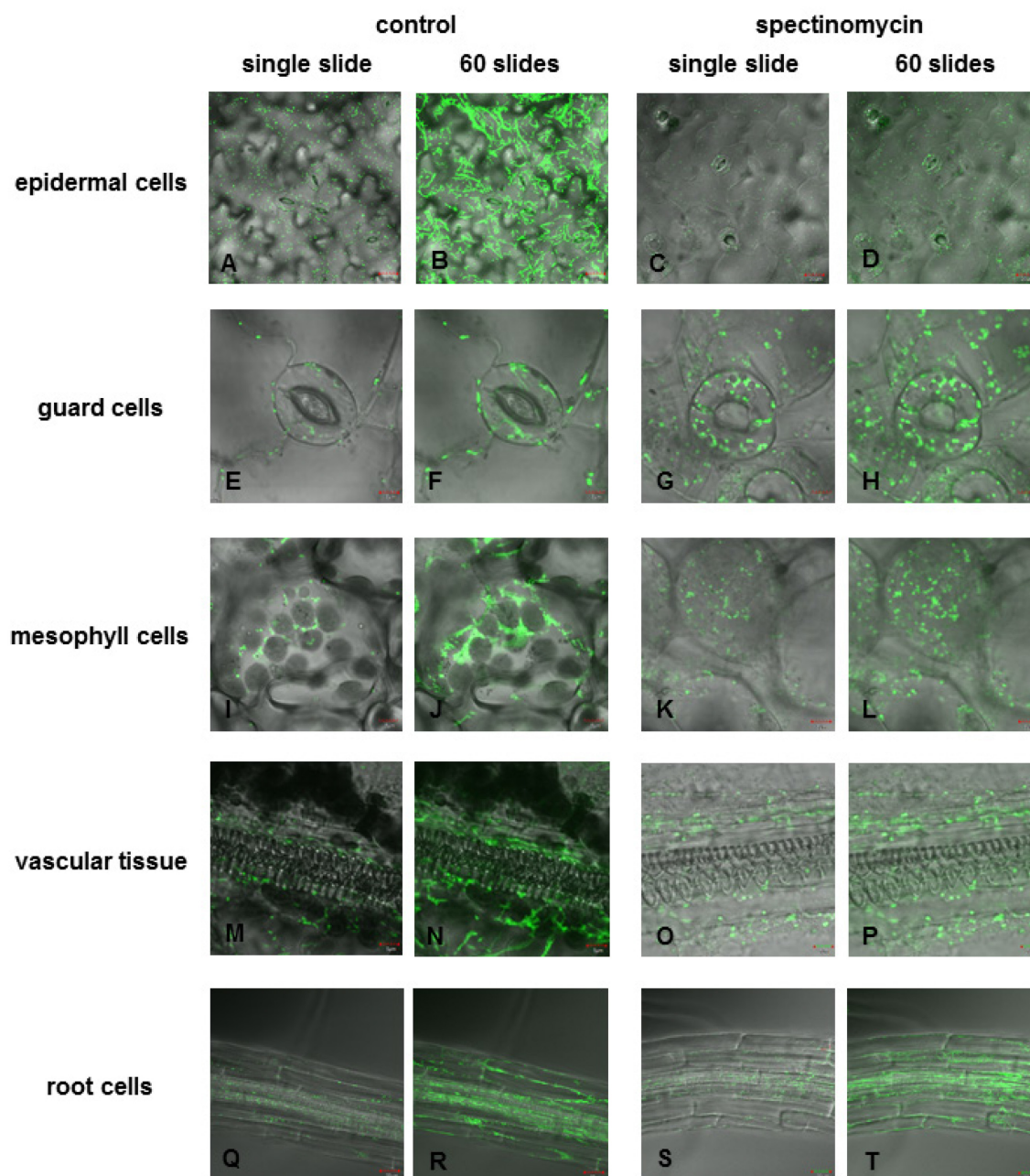


**Figure 30 Confocal microscopic evaluation of mitochondrial morphology, density and motility in different cell types of *Arabidopsis* seedling.** Seeds from a line with mitochondrial-targeted GFP (Logan and Leaver, 2000) were grown for 10 days on SEA medium containing 1% sucrose supplemented (where stated) with 500 mg/L spectinomycin. Mitochondrial morphology, density and motility were assessed using confocal microscopy. While determination of mitochondria morphology and density is presented by a single scanning of the tissue, mitochondria motility is presented as motility pathways obtained by overlapping 60 slides taken at 1.1 s interval. A, E, I, M, Q) Mitochondria morphology and density in epidermal cells, guard cells, mesophyll cells, vascular tissue and root cells of green seedlings; B, F, J, N, R) Mitochondria motility in epidermal cells, guard cells, mesophyll cells, vascular tissue and root cells of green seedlings; C, G, K, O, S) Mitochondria morphology and density in epidermal cells, guard cells, mesophyll cells, vascular tissue and root cells of white seedlings; D, H, L, P, T) Mitochondria motility in epidermal cells, guard

cells, mesophyll cells, vascular tissue and root cells of white seedlings; Scale bar: 20  $\mu\text{m}$  (A-D, Q-T) and 5  $\mu\text{m}$  (E-P).

These results indicate a yet unknown connection between plastids/chloroplasts and mitochondria. While previous investigations proved that under various light conditions mitochondria change their location within the cells together with the chloroplasts (Islam *et al.*, 2009; Islam and Takagi, 2010), the present study further demonstrates that impaired chloroplast development in white cotyledons of spectinomycin-treated seedlings leads to a motility arrest of most mitochondria in both photosynthetic (guard cells, mesophyll cells) and non-photosynthetic cells (epidermal cells, vascular tissue). However, blocked plastid protein synthesis in roots did not have an effect on motility, suggesting that the observed effect is organ-specific.

Moreover, visual evaluation of mitochondrial density in plant cells resulted in an equal number of mitochondria in both green and white seedlings. This result leads to the conclusion that mitochondria of white cotyledons contain more DNA than the ones in green cotyledons.

### **3.2.6 Transmission electron microscopic (TEM) evaluation of plastids/chloroplasts and mitochondria in green and white *Arabidopsis* cotyledons**

The motility arrest observed in white cotyledons raises questions as to the internal morphology and respiratory function of static mitochondria. In order to evaluate cotyledon cross-sections, transmission electron microscopic investigations were performed with the help of Dr. Melzer (IPK Gatersleben). Comparative ultrastructural analysis of green and white cotyledons showed that green cotyledons contained chloroplasts with typical grana stacks and thylakoid membranes (Fig. 31A and C), while the proplastid-like structures of plants grown on medium containing spectinomycin appeared undifferentiated. They are characterized by a high amount of plastoglobulin-type structures with only few thylakoids (Fig. 31B and D). However, the mitochondria had normal internal structures and evaluation of size and abundance showed no difference between green and white cotyledons (Fig. 31E and 31F).

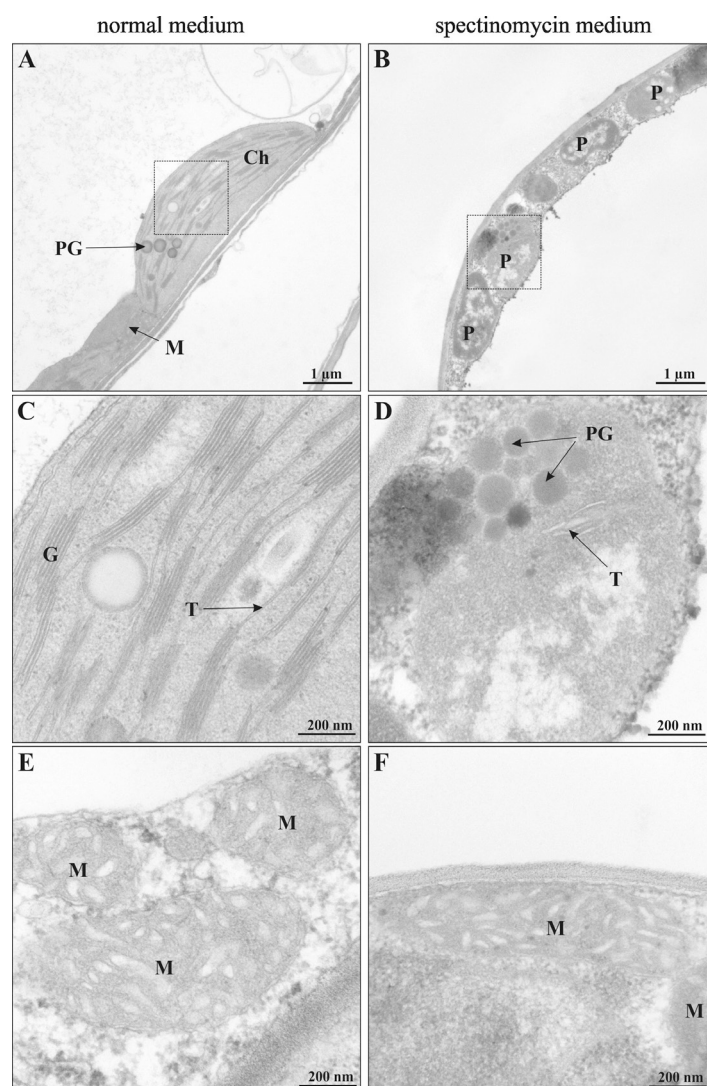


**Figure 31 Transmission electron microscopy of *Arabidopsis thaliana* cotyledon cross sections.** Comparative ultrastructural analysis of *Arabidopsis thaliana* Col-0 cotyledons grown in normal medium (A, C, E) and spectinomycin medium (B, D, F). Overview (A, B) and close up (C, D) of chloroplast and plastids respectively; (E, F) mitochondria. Ch, chloroplast; G, grana; M, mitochondrion; P, plastid; PG, plastoglobuli; T, thylakoid. Investigation performed by Dr. Melzer (IPK Gatersleben).

### 3.2.7 Determination of oxygen consumption, ATP, ADP and ATP/ADP ratio in green and white *Arabidopsis* cotyledons

Mitochondria are the central organelles involved in plant respiration. They contain enzymes of the citric acid cycle as well as the electron transport chain necessary for the final step of ATP synthesis (see 1.1.2). Evaluation of plant respiration includes oxygen consumption measurements and determination of

ATP/ADP ratios. An increased respiration would lead to increased oxygen consumption and an elevated ATP/ADP ratio.

As previously shown, white seedlings grown on medium containing spectinomycin exhibited elevated mitochondrial gene copy numbers (Fig. 26), but a normal number of mitochondria, which however have impaired motility (Fig. 29, 30). This condition might be an effect of impaired respiratory condition of the existing mitochondria. Until now, a direct correlation between increased respirational activity, elevated number of mitochondria and mtDNA content was observed in germinating peanut cotyledons (Breidenbach *et al.*, 1967). Moreover, the arrest of motility in white cotyledons not only raises questions on mitochondrial performance but also on ATP availability, since in plant cells mitochondrial motility and fusion are ATP dependent (Van Gestel *et al.*, 2002; Wakamatsu *et al.*, 2010).

In order to evaluate the respiration activity of mitochondria in green and white *Arabidopsis* cotyledons, oxygen consumption was determined by using a 4-channel minisensor oxygen meter (OXI-4 mini from PreSens). A significant difference in O<sub>2</sub> consumption was not observed between investigated cotyledons (Fig. 32A). Next, ATP and ADP levels were determined and the ATP/ADP ratio was calculated. Similar ATP and ADP amounts were obtained, with a constant ATP/ADP ratio (Fig. 32B - D).

These results should be interpreted taking into consideration that both green and white seedlings were grown on culture medium containing 1% sucrose. For this reason, respiration in white seedlings is not deprived of substrate. Further, the results show that in both green and white seedlings, respiration is probably at its maximum capacity, without an influence of photosynthesis. Moreover, the existence of a normal ATP content in white cotyledons proves that the arrest of motility is not a result of ATP depletion.



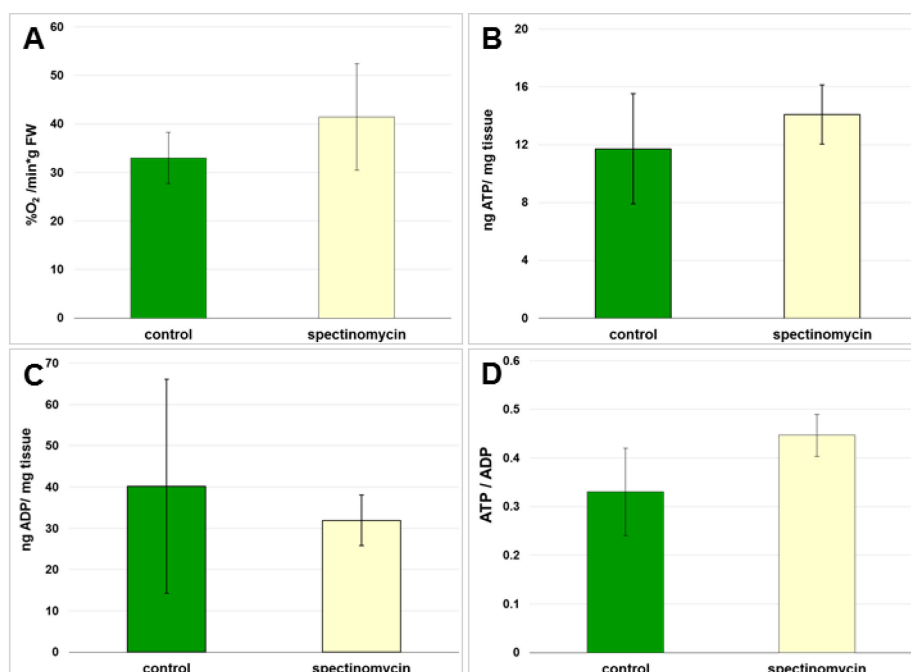


**Figure 32 O<sub>2</sub> consumption, ATP, ADP levels and ATP/ADP ratio in green and white seedlings.** Wildtype (Col-0) Arabidopsis seedlings were grown for 10 days on SEA medium containing 1% sucrose and, where specified, 500 mg/L spectinomycin. Total cotyledons were used for A) O<sub>2</sub> consumption measurements; B) ATP level; C) ADP level; D) ATP/ADP ratio.

### 3.3 The effects of light and sucrose content on mitochondrial gene copy number

In plants, the regulation of mtDNA abundance is a process with components and factors that are just beginning to be discovered. To elucidate the involvement of light and sucrose content on the abundance of mtDNA, the previously described experimental system was utilized (Chapter 3.2). The mitochondrial gene copy number was compared in 10-day-old seedlings grown in light or darkness on medium supplemented with 1% sucrose and, where stated, with 500 mg/L spectinomycin. Representative images of seedlings grown in these conditions are present in Figure 33A. Surprisingly, non-treated etiolated seedlings had the same level of gene abundance as green seedlings, showing that conversion of proplastids into either functional chloroplasts or etioplasts determines the existence of the same mitochondrial genome abundance (Fig. 34A). Moreover, it proved that in certain conditions, the absence of photosynthesis does not automatically lead to elevated gene copy number levels in mitochondria.



However, comparing light-grown with etiolated, dark-grown seedlings, both spectinomycin-treated, a similar increase in mitochondrial gene copy number was observed indicating that inhibition of plastid translation elevates the amount of mtDNA in a light-independent manner (Fig. 34A).

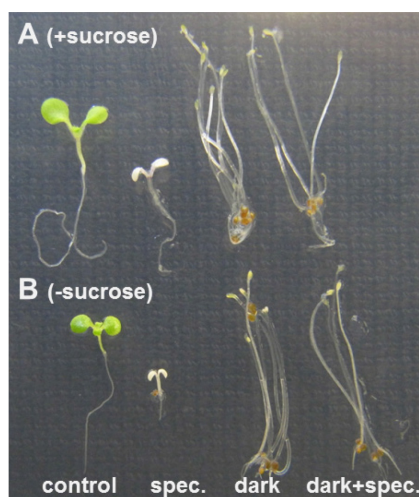


**Figure 33** Representative images of seedlings grown for 10 days in the light or dark on SEA medium containing (where stated) 500 mg/L spectinomycin. A) Seedlings grown on medium supplemented with 1% sucrose; B) Seedlings grown in the absence of sucrose.

The influence of sucrose on the regulatory network between plastids/chloroplasts and mitochondria was studied by growing the seedlings in the same experimental conditions on culture medium without sucrose. Ten-day-old green seedlings grown on medium without sucrose had a slower developmental rate than the control seedlings grown on medium with sucrose. Spectinomycin treated seedlings not only exhibited a reduced size on medium without sucrose, but died soon after the development of the two cotyledons (Fig. 33B). Investigation of mitochondrial gene copy number in green and etiolated seedlings revealed general lower gene abundance (~30%) when compared to the heterotrophically-grown seedlings (Fig. 34B). This effect is even more distinct in seedlings grown on spectinomycin where the gene copies reached only a two-fold increase, when compared to the three-fold increase observed on medium containing sucrose (Fig. 34B). These results point to the involvement of sucrose availability in determining the amount of mitochondrial genes under spectinomycin conditions.

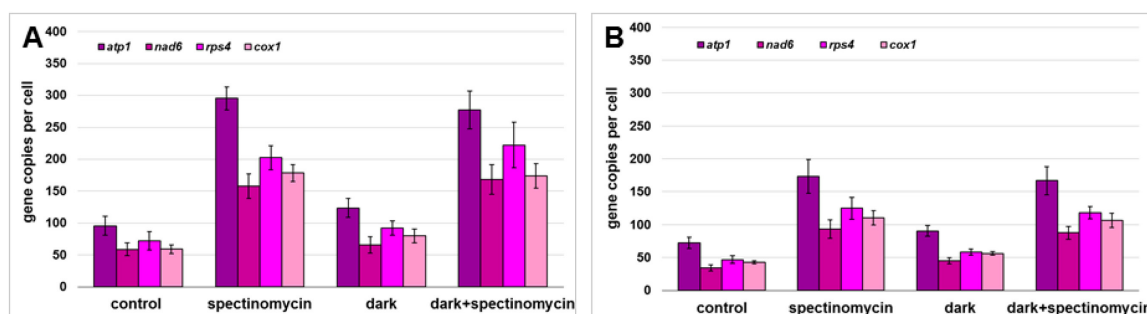


**Figure 34 Mitochondrial gene copy numbers in *Arabidopsis* seedlings grown in the presence (A) or absence (B) of 1% sucrose.** Mitochondrial gene copy number per cell was determined by quantitative real-time PCR using the single-copy nuclear gene *RpoTm* as internal standard. The final value was calculated as described in chapter 3.1.1 by using the relative gene copy number, the mean C-level (see Annex 1) and the number of NUMTs.

### 3.4 Effects of chloroplast and mitochondrial dysfunction on mitochondrial gene copy number

#### 3.4.1 Effects of chloroplast dysfunction on mitochondrial gene copy number

An increase in mtDNA abundance could be observed in white leaves of a barley mutant, which completely lack plastid ribosomes (Hedtke *et al.*, 1999) and in seedlings grown on medium containing spectinomycin, an inhibitor of plastid translation (Fig. 26B). Moreover, elevated mtDNA levels were also observed in albino plants of rye (Ballesteros *et al.*, 2009) and recently, in white sectors of variegated leaves from different ornamental plants (Toshoji *et al.*, 2011). However, in the last two examples the cause that induces this effect is unknown, since the rye mutant and the variegated plants were not genetically characterized (Ballesteros *et al.*, 2009; Toshoji *et al.*, 2011). The increase of mtDNA abundance in white leaves implies a possible crosstalk of mitochondria with plastids depending on their metabolic and/or developmental state. However, as shown in chapter 3.3, it is not generally the impairment of photosynthesis which is responsible for increased mtDNA levels, but rather impairment of plastid translation, since etiolated seedlings did not show an increase in mitochondrial gene copies.

To get a deeper insight into the mechanism of the observed plastid-mitochondria interaction, tobacco was used as a further subject in our investigations.

To investigate first if the absence of plastid translation also induces elevation of mtDNA abundance in *Nicotiana tabacum*, heterotrophically grown tobacco shoots (*Nicotiana tabacum* var. Petit Havana) were transferred onto RM medium containing 500 mg/L spectinomycin. After one month, the completely white parts from the newly developed leaves were cut and used for the determination of mitochondrial gene copy numbers (Fig. 35A). The same four genes were investigated as in *Arabidopsis*: *atp1*, *nad6*, *rps4*, and *cox1*. Determination of the gene copy number in tobacco wild type plants showed a different ratio between the individual investigated genes. While in *Arabidopsis* *atp1* was usually the most abundant, it was the least abundant in tobacco (approximately 50 copies). However, the genes *nad6*, *rps4*, and *cox1* showed similar amounts in their copy per cell (100-150; Fig. 35B). In white leaf tissue from spectinomycin-treated tobacco shoots, a three-fold higher amount of gene copies was observed. While the copy number of *atp1* increased from 50 to approx. 180, *nad6*, *rps4*, and *cox1* increased from 100-140 to 330-400 (Fig. 35B). This result further confirmed that inhibition of plastid translation induces elevation mtDNA levels in all three investigated species: barley, *Arabidopsis* and tobacco.

In order to further test the possibility of a plastid signal generated by a white plastid phenotype, i.e., by suppressed chloroplast development and impaired chloroplast function, mtDNA levels were investigated in tobacco *rpoA* knock-out mutants (Fig. 36A). The *rpoA* gene encodes the  $\alpha$ -subunit of the plastid-encoded plastid RNA polymerase (PEP) and deletion of this gene yields photosynthetically inactive plants that lack PEP (plastid-encoded plastid RNA polymerase), while maintaining transcription from NEP (nucleus-encoded plastid RNA polymerase); (Fig. 36A and Serino and Maliga, 1998). Although still containing functional ribosomes (De Santis-Maciossek *et al.*, 1999), these plastids lack most of their plastome-encoded proteins. Evaluation of the mitochondrial gene copy number showed a two-fold increase in white leaves: *atp1* increased from 46 to 126 copies, *nad6* from 103 to 250, and both *rps4* and *cox1* from 150 to 320 (Fig. 36B). This result suggested that the loss of certain plastid proteins resulting in a white phenotype might be connected to an increase of mitochondrial gene copy numbers.

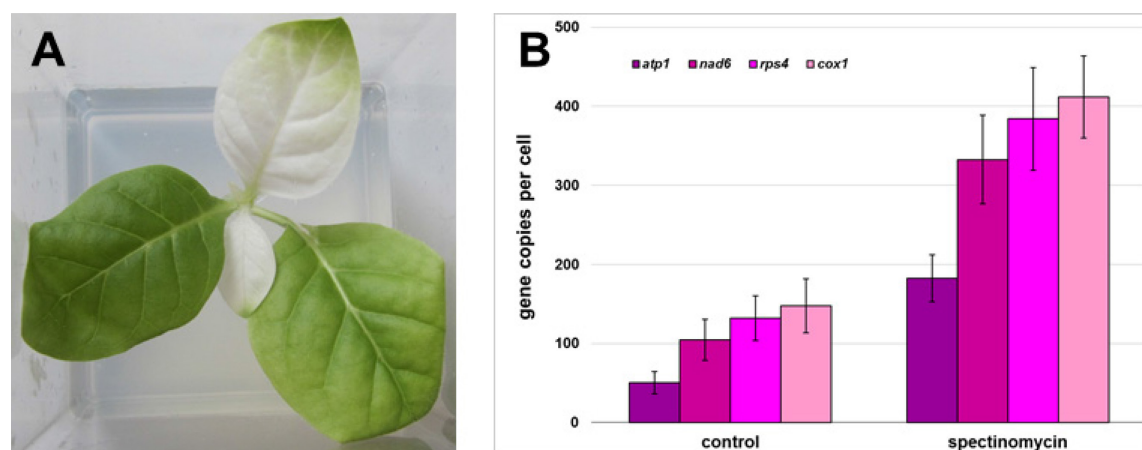


**Figure 35 Wild-type tobacco shoot grown for one month on spectinomycin.**

A) Representative image of WT (Petit Havana) tobacco shoot grown for one month on RM medium containing 500 mg/L spectinomycin; B) Mitochondrial gene copy number in control and white leaf tissue obtained from spectinomycin-treated tobacco shoots. The copy number per cell was determined by quantitative real-time PCR using the single-copy nuclear gene *RpoTp* as internal standard. The final value was calculated as described in chapter 3.1.1 by using the relative gene copy number and the mean C-level (see Annex 1). Since the tobacco genome is currently not sequenced, the number of NUMTs is unknown and could not be used in final calculations.

Both, high doses of spectinomycin and the loss of PEP lead to a loss of plastid-encoded proteins. The plastome contains genes for protein subunits of photosystem I, II, cytochrome b6f, ATP synthase, as well as NADH dehydrogenase, and RuBisCo. In order to identify plastid-encoded genes that are possibly involved in the mitochondrial-plastid crosstalk regulating mtDNA levels, mitochondrial gene copy numbers were examined in transplastomic knock-out mutants of tobacco with defects in PSII (*psbD*, *psbB*, *psbJ*), cytochrome b6/f complex (*petN*), PSI (*psaI*, *psaJ*, *ycf3*), ATP synthase (*atpB*, *atpH*), NAD(P)H dehydrogenase (*ndhC*) and RuBisCO (*rbcL*) (Bock *et al.*, 1994; Kanevski and Maliga, 1994; Ruf *et al.*, 1997; Hager *et al.*, 1999; Hager *et al.*, 2002; Schottler *et al.*, 2007). The plants were grown for one month on RM medium containing 3% sucrose, under low-light conditions ( $\sim 5 \mu\text{E}$ ). When grown under low light, the mutants presented green (*petN*, *psaI*, *psaJ*, *ndhC*), pale green (*psbB*, *psbD*, *psbJ*, *ycf3*, *rbcL*) or completely white phenotypes (*atpB*, *atpH*; Annex 4). Leaves of similar size were harvested and used for the evaluation of mtDNA abundance. However, determination of the mitochondrial gene copy number showed an elevation (about two-fold) only in *atpB* and *atpH* mutants that have a completely white leaf phenotype (Fig. 37, Annex4, unpublished). This result suggests a possible connection between mitochondrial gene abundance and the plastid ATP

synthase complex and/or another plastid signal originating from the completely white leaf phenotype.

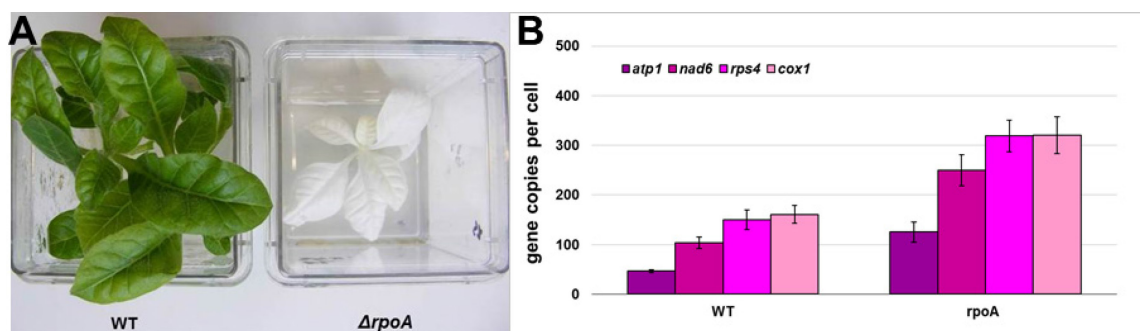


**Figure 36 Representative image of the *rpoA* mutant and mitochondrial gene copy number.** A) Representative image of WT (Petit Havana) and *rpoA* mutant grown under low-light conditions ( $\sim 5 \mu\text{E}$ ) on RM medium supplemented with 3% sucrose; B) Mitochondrial gene copy number in WT and *rpoA* mutant. The copy number per cell of *atp1*, *nad6*, *rps4* and *cox1* was determined by quantitative real-time PCR using the single-copy nuclear gene *RpoTp* as internal standard. The final value was calculated as described in chapter 3.1.1 by using the relative gene copy number and the mean C-level (see Annex 1). Since the tobacco genome is currently not sequenced, the number of NUMTs is unknown and could not be used in final calculations.

Interestingly, the increase of mitochondrial gene abundance in white tobacco mutants (*atpB*, *atpH*, *rpoA*) was less pronounced when compared to mitochondrial gene copy numbers in plants with complete absence of plastid protein synthesis. This observation raised the question if reduced translation efficiency of plastid ribosomes, thereby lowering the amount of plastid-encoded proteins, is able to induce an increase of mitochondrial gene copies. To answer this question, the Arabidopsis *prpl1-1* mutant was used (Pesaresi *et al.*, 2001). The *Prpl1* gene encodes the plastid ribosomal protein 11 (PRPL11), a component of the 50S subunit of the ribosome. The mutant plants have pale green leaves and are reduced in size in comparison to the wild type (Fig. 38). The photosynthetic efficiency is severely reduced as a result of a drastic reduction (up to 67%) in the level of plastid-encoded thylakoid proteins as a consequence of the impaired plastid translation (Pesaresi *et al.*, 2001). The mitochondrial activity is unaffected (Pesaresi *et al.*, 2006). However, similar to the formerly tested pale-green, transplastomic mutants (*psbB*, *psbD*, *psbJ*, *ycf3*, *rbcL*), investigation of the *prpl1-1* mutant showed no increase in the mitochondrial gene copy number (Fig. 39).

Altogether, these results indicate the existence of a threshold level of chloroplast impairment that leads to an increased abundance of mitochondrial genes. The threshold level is represented by the appearance of a white cotyledon/leaf phenotype, with the possible involvement of the chloroplast ATP synthase complex.

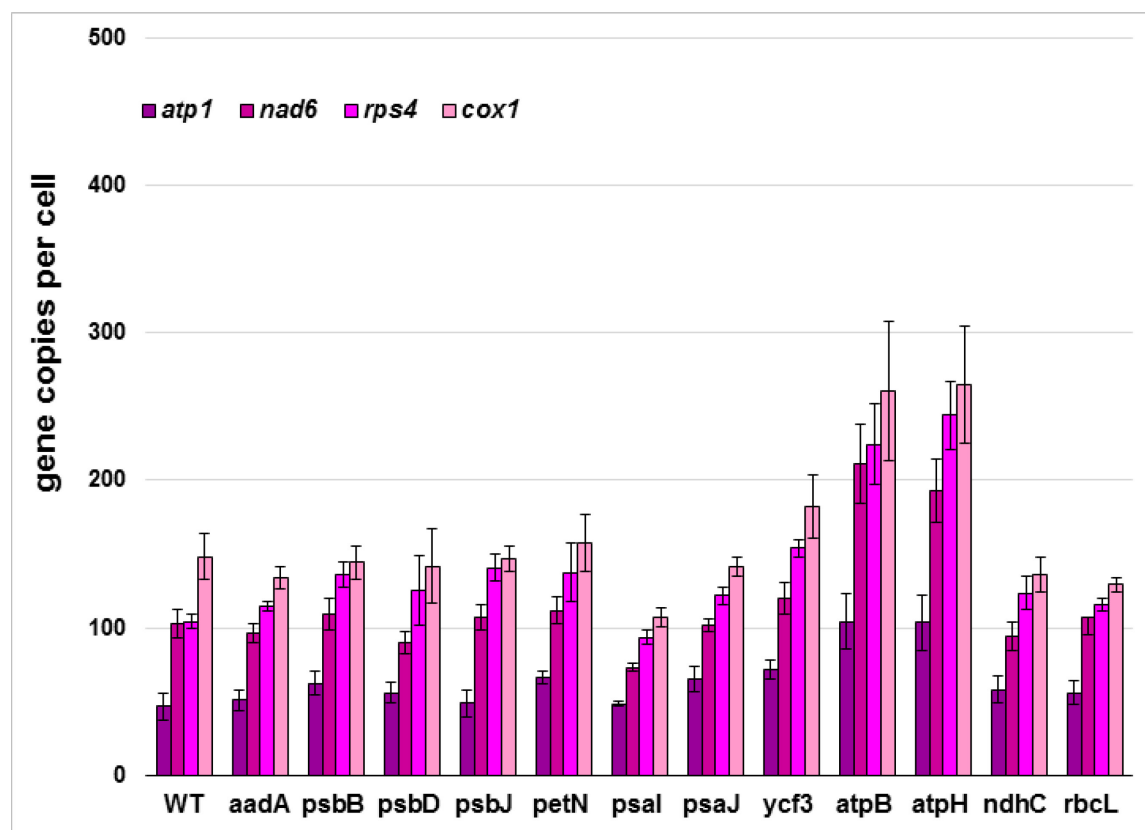


**Figure 37 Mitochondrial gene copy number in transplastomic tobacco mutants.** The copy number per cell of *atp1*, *nad6*, *rps4* and *cox1* was determined by quantitative real-time PCR using the single-copy nuclear gene *RpoTp* as internal standard. The final value was calculated as described in chapter 3.1.1 by using the relative gene copy number and the mean C-level (see Annex 1). Since the tobacco genome is currently not sequenced, the number of NUMTs is unknown and could not be used in final calculations.

### 3.4.2 Effects of mitochondrial dysfunction on mitochondrial gene copy number

A two- to three fold increase in mitochondrial gene copy number could be observed in an *Arabidopsis rpoTnp* mutant (Kühn *et al.*, 2009) that showed reduced abundance of the respiratory chain complexes I and IV. A higher number of mitochondria were observed in dexamethasone-treated anti-*atp3* and anti-*atp5* plants that affect the  $\delta$  (ATP5) and the  $\gamma$  (ATP3) subunits of the mitochondrial ATP synthase

(Robison *et al.*, 2009). These results point to another possible regulatory mechanism, in which mitochondrial gene abundance/number is determined by the functioning of the mitochondrial electron transport chain. To get an insight into this process, mitochondrial gene abundance was determined in seedlings of two previously-described respiration mutants: *mrpl11-1* (Pesaresi *et al.*, 2006) and *ndufs4* (Meyer *et al.*, 2009). The *mrpl11-1* mutant represents the counterpart of the *prpl11-1* in mitochondria. The MRPL11 protein is a component of the 50S subunit of the mitochondrial ribosome. Mutant plants are reduced in size, show darker leaf coloration than the wild type and have reduced mitochondrial translation (Fig. 38). This defect leads to a reduction in the abundance of all ETC complexes that limits but does not arrest at any point the electron flow. The photosynthetic performance is normal (Pesaresi *et al.*, 2006). The *ndufs4* mutant of *Arabidopsis* (Meyer *et al.*, 2009; Tarasenko *et al.*, 2010) lacks the NDUFS4 subunit from the complex I of the respiratory chain and prevents its assembly without effects on other respiratory components (Meyer *et al.*, 2009). Mutant seeds were grown for 10 days on culture medium and whole seedlings were harvested for DNA isolation and gene copy number determination (Fig. 38). Evaluation of mtDNA abundance in the *mrpl11-1* and *ndufs4* mutant seedlings shows a two-fold and three-fold increase, respectively, when compared to the Col-0 wild type (Fig. 39). When compared to the situation in plastid mutants, where a strong white phenotype is necessary in order to induce an effect in mtDNA abundance, plants seem to be more sensitive to disturbances in mitochondrial respiration. In this case, impaired mitochondrial translation that leads to a minor impairment of respiration is enough to trigger the increase in the gene copy number (Fig. 39). The situation is even more dramatic in the *ndufs4* mutant that completely lacks complex I (Fig. 39).

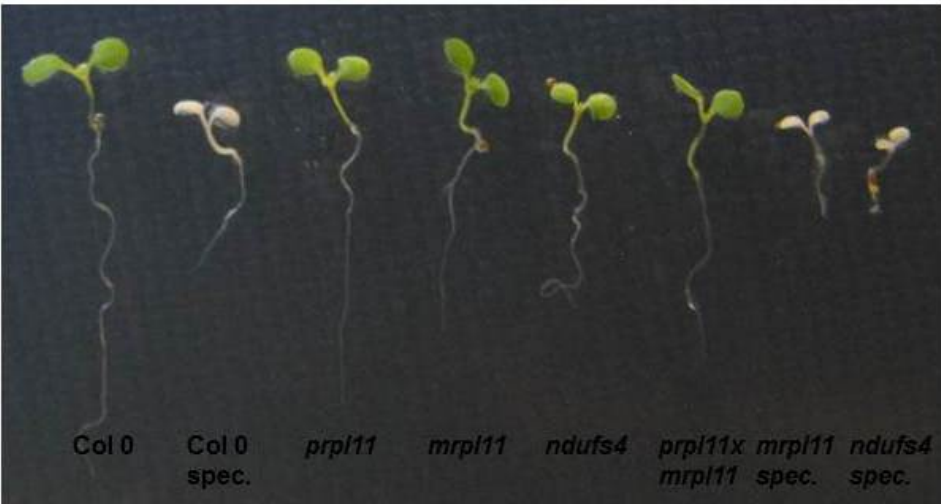


**Figure 38** The phenotype of *Arabidopsis* wild-type and *prpl11*, *mrpl11*, *prpl11mrpl11* and *ndufs4* mutant plants. Seeds of wild-type (Col-0) and mutant plants (*prpl11*, *mrpl11*, *ndufs4*, *prpl11 mrpl11*) were grown for 10 days on SEA medium containing 1% sucrose and, where stated, 500 mg/L spectinomycin.

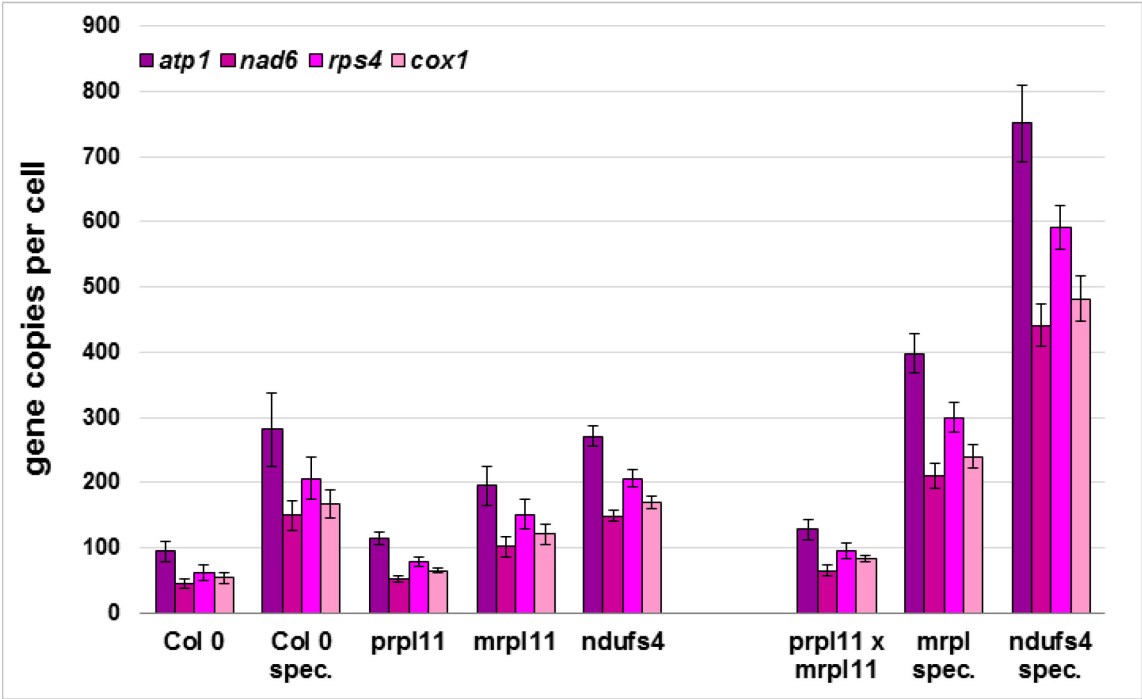


**Figure 39** Mitochondrial gene copy number per cell in wild-type and mutant seedlings. Mitochondrial gene copy number per cell was determined by quantitative real-time PCR using the single-copy nuclear gene *RpoTm* as internal standard. The final value was calculated as described in chapter 3.1.1 by using the relative gene copy number, the mean C-level (see Annex 1) and the number of NUMTs.



### 3.4.3 Interactions between chloroplast and mitochondrial dysfunction in determination of mitochondrial gene copy number

Thus far, we demonstrated a separate influence of photosynthesis and respiration impairment on the abundance of mitochondrial gene copies. However, permanent and complex cross-talk takes place between these organelles in order to adjust the energetical status of the cells. Therefore, the interaction between plastids/chloroplasts and mitochondria was investigated in the context of mitochondrial DNA abundance. Two experiments were performed: at first, the *prp111 mrp111* double mutant was used since it has impaired translation in both chloroplasts and mitochondria (Pesaresi *et al.*, 2006). Secondly, a more severe condition was created by growing the respiration mutants on culture medium containing spectinomycin.

The *prp111-1 mrp111-1* double mutant exhibits pale-green leaves, a drastic reduction in size and photosynthetic performance similar to *prp111-1* (Fig. 38). This implies that the mitochondrial defect does not have an additive effect on plastid function (Pesaresi *et al.*, 2006). When evaluating mitochondrial gene copy numbers in 10-day-old seedlings, just a small elevation could be observed, which does not even resemble the one seen in the *mrp111-1* mutant. This suggests that there might be a compensatory mechanism when the function of both organelles is impaired. In the case of severe stress conditions, when respiration mutants are grown on medium containing spectinomycin, a dramatic effect in gene copy number could be observed, starting from 4-fold elevation for *mrp111-1* up to even 8-9-fold for the *ndufs4* growing on spectinomycin (Fig. 39). This result further implies that both plastids/chloroplasts and mitochondria contribute to the final amount of mitochondrial DNA levels in cells.

### 3.4.4 Differential regulation of mitochondrial gene copy number in cotyledons and roots

As a result of specific interactions between photosynthesis and respiration in green tissue, we wanted to investigate if the effect of increased genome abundance observed in white seedlings and in respiration mutants is leaf /cotyledon specific or if

it is present also in roots. For this reason, we separated cotyledons and roots from 10 days-old control, spectinomycin-treated seedlings and also from the respiration mutants *mrpl11-1* and *ndufs4*. When comparing control (green) and white (spectinomycin-treated) seedlings we could observe an increase in genome abundance only in cotyledons but not in roots, suggesting an organ-specific effect (Fig. 40A). However, the situation is different in case of respiration mutants, where a clear effect could be observed also in roots (Fig. 40B).

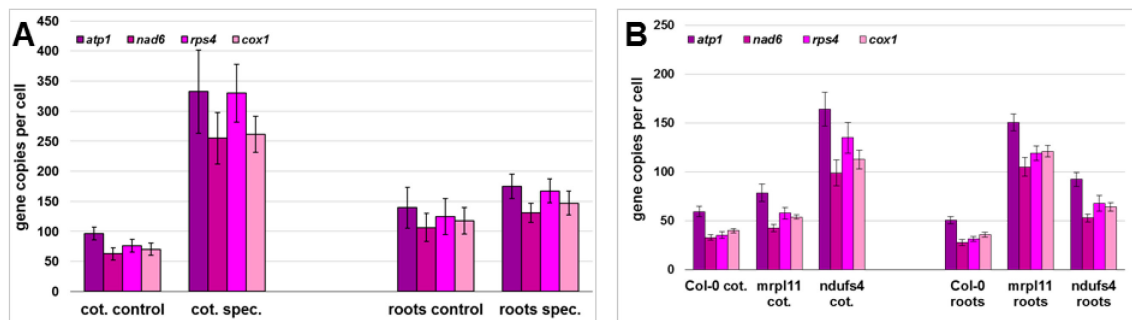


**Figure 40 Mitochondrial gene copy number in cotyledons and roots.** Wild-type (Col-0) and mutant (*mrpl11*, *ndufs4*) plants were grown in leaning position for 10 days on SEA medium SEA medium containing 1% sucrose and, where stated, 500 mg/L spectinomycin. Mitochondrial gene copy number per cell was determined by quantitative real-time PCR using the single-copy nuclear gene *RpoTm* as internal standard. The final value was calculated as described in chapter 3.1.1 by using the relative gene copy number, the mean C-level (see Annex 1) and the number of NUMTs. Mitochondria gene copies per cell in A) Col-0 cotyledons and roots grown on control and spectinomycin-containing medium; B) Col-0, *mrpl11* and *ndufs4* cotyledons and roots.

### 3.5 Investigation of the GUN and ABI4 signaling pathway

This work revealed new aspects in mtDNA organization and abundance, under both normal and stress conditions. The importance of both plastids/chloroplasts and mitochondria in determining the final mtDNA abundance in plants has been demonstrated, which probably involves complex signaling networks. Until now, nothing is known about the components of this signaling networks, a first step was taken by evaluating mtDNA abundance in some mutants that are currently known to be involved in chloroplast to nucleus retrograde communication (*gun*), as well as in the *abi4* mutant that represents a common component of both chloroplast to nucleus and mitochondria to nucleus retrograde pathways (see Chapter 1.2). Arabidopsis *gun*

(genome uncoupled) mutants (Susek *et al.*, 1993) have been intensively studied in the last years in the effort to describe the regulation of the plastid / chloroplast to nucleus retrograde signaling pathway (see 1.2). To test if the GUN mutants are also involved in the signaling pathway that we investigate (from undeveloped chloroplasts to the nucleus with final effects on mitochondrial DNA), *gun1-1*, *gun2-1*, *gun4-1* and *gun5-1* seedlings were grown for 10 days culture medium containing spectinomycin (Fig. 41A). Determination of mitochondrial gene copy number in green seedlings showed a small significant elevation in the *gun2-1* mutant, a condition that is probably the result of the pale-green cotyledon phenotype (Fig. 42). Evaluation of gene abundance in white, spectinomycin-treated seedlings showed no significant difference in the mutants when compared to the wild-type, proving that the GUN mutants are not involved in the signaling pathway that we investigate (Fig. 42). An uncoupling effect would be expected in case any of these mutants would be involved in signaling. An interesting result appeared from the *abi4-1* mutant: while the green mutant has the same amount of gene copies as the wild-type, the treated mutant has an uncoupling effect, with just two-fold elevation in white seedlings (Fig. 42). This result brings ABA into attention as a possible signaling component.

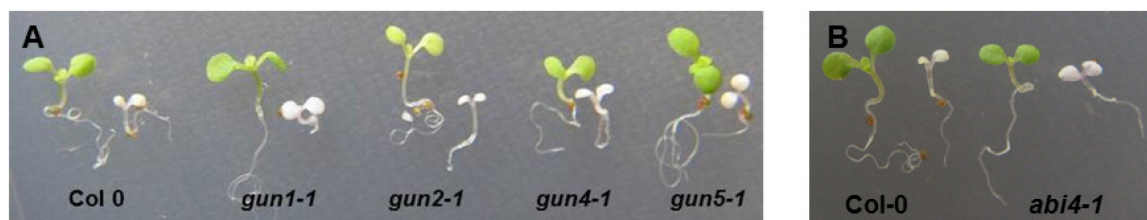


**Figure 41 Phenotype of wild-type, *gun* and *abi4-1* mutant seedlings.** Seeds of wild-type (Col-0) and mutant plants (*gun1-1*, *gun2-1*, *gun4-1*, *gun5-1* and *abi4-1*) were grown for 10 days on SEA medium containing 1% sucrose and, where stated, 500 mg/ L spectinomycin.

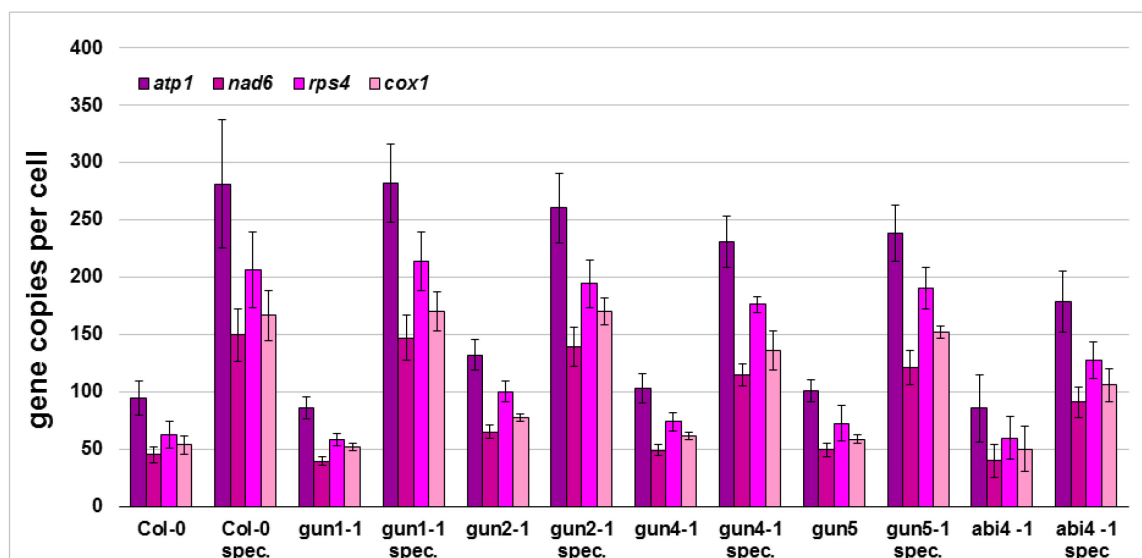


**Figure 42 Mitochondrial gene copy number per cell in wild-type, *gun* and *abi4-1* mutant seedlings.** Mitochondrial gene copy number per cell was determined by quantitative real-time PCR using the single-copy nuclear gene *RpoTm* as internal standard. The final value was calculated as described in chapter 3.1.1 by using the relative gene copy number, the mean C-level (see Annex 1) and the number of NUMTs.

### 3.6 Investigation of mitochondrial motility in relation to impaired chloroplast development

#### 3.6.1 Investigation of mitochondrial motility in *Arabidopsis RLD-Spc1xmtGFP* mutant grown in the presence of 500 mg/L spectinomycin

Previous investigations of mitochondrial dynamics in green and white, spectinomycin-treated seedlings revealed a new relation between chloroplasts and mitochondria: an arrest of mitochondrial motility is seen in the cotyledons of white seedlings but not in roots (see 3.2.5). The question arises as to an possible effect of spectinomycin on mitochondrial motility via a side-effect on mitochondrial function. Even though spectinomycin is considered to be a specific inhibitor of plastid translation (Wallace *et al.*, 1974; Moazed and Noller, 1987) and is generally used as selection marker in chloroplast transformation (Svab *et al.*, 1990), we wanted to be sure that the influence of spectinomycin on mitochondrial motility was indeed via its effect on plastid translation. Therefore, we crossed the mitochondrial-targeted GFP line (*mtGFP*, Logan and Leaver, 2000) with the *RLD-Spc1* spectinomycin-resistant

mutant carrying a point mutation in the plastid 16S rRNA gene (*rrn16*) (Azhagiri and Maliga, 2007), the resulting plants being named *RLD-Spc1xmtGFP* (for crossing protocol and selection of mutants see 2.2.18). The double mutant developed normally under standard growth conditions (see Annex 5). When grown in the presence of 500 mg/L spectinomycin it showed a green phenotype (Fig. 43) together with mitochondrial GFP fluorescence.

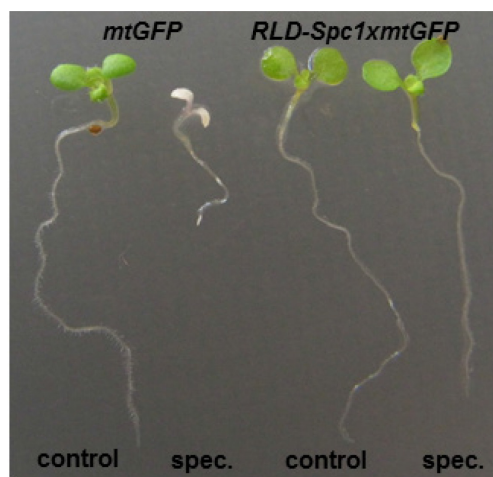


**Figure 43** Phenotype of 10-day-old *mtGFP* and *RLD-Spc1xmtGFP* seedlings grown on control and spectinomycin-containing medium. Seeds of the mitochondrial-targeted GFP line - *mtGFP* (Logan and Leaver, 2000) and of the crossed *RLD-Spc1xmtGFP* spectinomycin-resistant mutant were grown for 10 days on SEA medium containing 1% sucrose supplemented (where stated) with 500 mg/L spectinomycin.

Investigation of mitochondrial size, shape, density and motility by confocal microscopy showed no difference between the *RLD-Spc1xmtGFP* control and spectinomycin-treated plants which remained green due to their plastid-based resistance against spectinomycin. Normal motility could be observed under both conditions (Fig. 44, Video 12 and 13) indicating that the mitochondrial motility arrest in cotyledons of white seedlings was indeed due the spectinomycin effect on plastid translation.

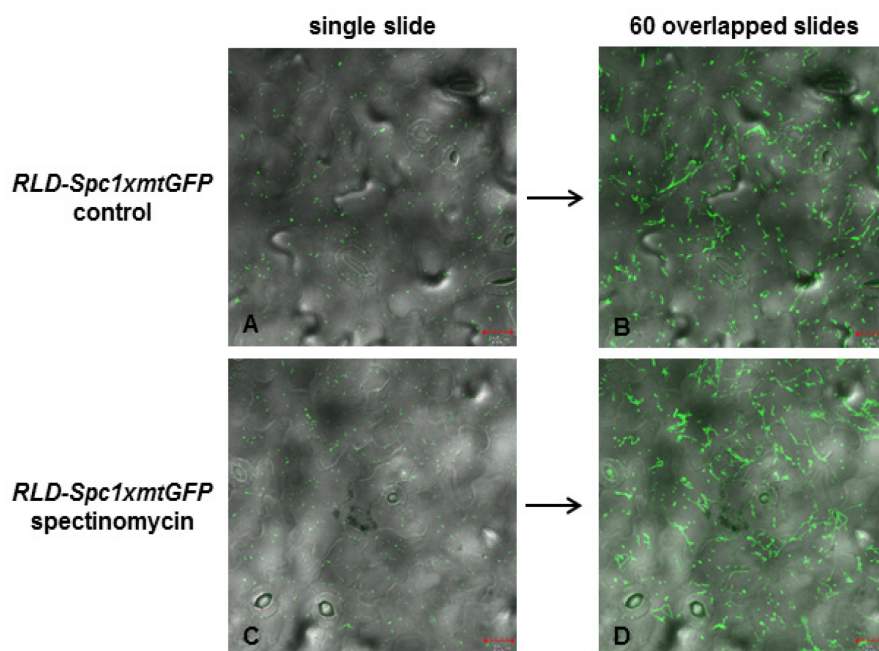


**Figure 44 Confocal microscopic images of mitochondria in epidermal cells of the *RLD-Spc1xmtGFP* mutant.** Seeds of the *RLD-Spc1xmtGFP* spectinomycin-resistant mutant were grown for 10 days on SEA medium containing 1% sucrose supplemented (where stated) with 500 mg/L spectinomycin. Mitochondrial size, shape, density and motility were assessed in epidermal cells of the cotyledons using confocal microscopy. Single slides (A, C) and 60 overlapped slides (B, D) taken at 1.1 s interval are presented. A, B) Mitochondria in epidermal cells of the *RLD-Spc1xmtGFP* mutant grown on control medium; C, D) Mitochondria in epidermal cells of the *RLD-Spc1xmtGFP* mutant grown on spectinomycin-containing medium. Scale bar: 20  $\mu$ m.

### 3.6.2 Determination of the threshold level of photosynthetic impairment leading to mitochondrial motility arrest

Arrest of mitochondrial motility was related to the complete absence of photosynthesis and the presence of a white cotyledon phenotype (see 3.2.5). To further investigate the effect of photosynthesis on mitochondrial motility, we determined the threshold level of photosynthetic impairment that leads to motility arrest. To this end, a two-step approach was performed. At first, mitochondrial motility was studied in the *Arabidopsis prp111-1* mutant that has reduced photosynthetic performance and a pale-green leaf phenotype (Pesaresi *et al.*, 2001). Secondly, wild-type *Arabidopsis* seedlings were grown on various spectinomycin concentrations in order to determine the optimal treatment that would result in a yellow cotyledon phenotype which represents an intermediate step between the pale-green *prp111-1* mutant and the completely white phenotype obtained after the

treatment with high concentrations (500 mg/L) of spectinomycin. Then, *mtGFP* seeds were grown on the selected optimal antibiotic concentration (5 mg/L) and mitochondrial motility was evaluated in yellow cotyledons.

### 3.6.2.1 Investigation of mitochondrial motility in *Arabidopsis prpl11-1xmtGFP*

The first step in determining the threshold level of photosynthetic impairment leading to mitochondrial motility arrest was the evaluation of mitochondrial motility in the *Arabidopsis prpl11-1* mutant (Pesaresi *et al.*, 2001). The *prpl11-1* mutant was crossed with the previously described mitochondrial-targeted GFP line (*mtGFP*), resulting in the *prpl11-1xmtGFP* double mutant (for crossing protocol and selection of mutants see 2.2.18). The double mutant resembles the phenotype of the *prpl11-1* mutant (see Annex 6) and presents also in addition mitochondrial GFP fluorescence. Mutant seedlings were grown for 10 days on SEA medium containing 1% sucrose (Fig. 45). The mitochondrial dynamics was evaluated by CLSM.



**Figure 45 Phenotype of 10-day-old *mtGFP*, *prpl11-1* and *prpl11-1xmtGFP* seedlings.** Seeds of the mitochondrial-targeted GFP line - *mtGFP* (Logan and Leaver, 2000), of *prpl11-1* mutant (Pesaresi *et al.*, 2001) and of the crossed *prpl11-1xmtGFP* double mutant were grown for 10 days on SEA medium containing 1% sucrose.

The visual determination of mitochondrial size, shape and density by confocal microscopy showed no difference between the *mtGFP* control line and the *prpl11-1xmtGFP* double mutant. Further evaluation of motility pathways showed similar images (Fig. 46). However, a tendency of an elevated number of immotile



mitochondria has been observed, with high variations between investigated cotyledons (Fig. 46, Video 14 and 15). For a more accurate result, a numeric determination of the motile/immotile mitochondria would be necessary.

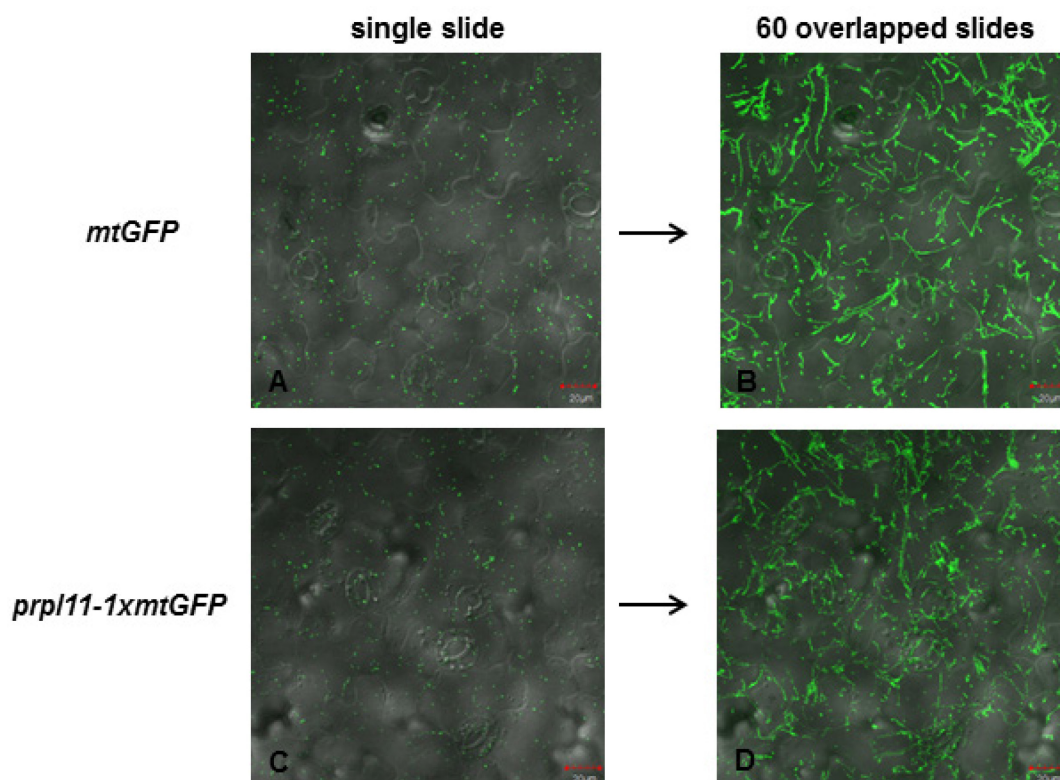


**Figure 46** Confocal microscopic images of mitochondria in epidermal cells of the *mtGFP* and *prpl11-1xmtGFP* mutant. Seeds of the *mtGFP* and *prpl11-1xmtGFP* mutants were grown for 10 days on SEA medium containing 1% sucrose. Mitochondrial size, shape, density and motility were assessed in epidermal cells of the cotyledons using confocal microscopy. Single slides (A, C) and 60 overlapped slides (B, D) taken at 1.1 s interval are presented. A, B) Mitochondria in epidermal cells of the *mtGFP* mutant; C, D) Mitochondria in epidermal cells of the *prpl11-1xmtGFP* mutant. Scale bar: 20  $\mu$ m.

### 3.6.2.2 Investigation of mitochondrial motility in yellow cotyledons of *Arabidopsis* seedlings grown in the presence of 5 mg/L spectinomycin

In order to determine an optimal treatment that would result in yellow, not complete white cotyledons, wild-type *Arabidopsis* seedlings were grown on various spectinomycin concentrations. Three intermediate concentrations were chosen: 0.5, 5, and 50 mg/L. Seedlings grown on 0.5 mg/L presented a normal green phenotype and the ones grown on 50 mg/L were completely white (Fig. 47A). The concentration of 5 mg/L produced pale green, variegated and yellow cotyledons (Fig. 47A and B).



*MtGFP* seeds were then grown on the optimal antibiotic concentration (5 mg/L) and mitochondrial motility was evaluated in yellow seedlings. While no difference could be observed in mitochondrial size and density, an arrest of motility was present for most mitochondria, with variations between individual cotyledons (Fig. 48, video 16 and 17). As observed also in completely white cotyledons, the immotile mitochondria showed a general round shape. Altogether, present results point to the conclusion that the threshold level of photosynthetic impairment that leads to mitochondrial motility arrest is represented by the appearance of a yellow/white cotyledon phenotype.

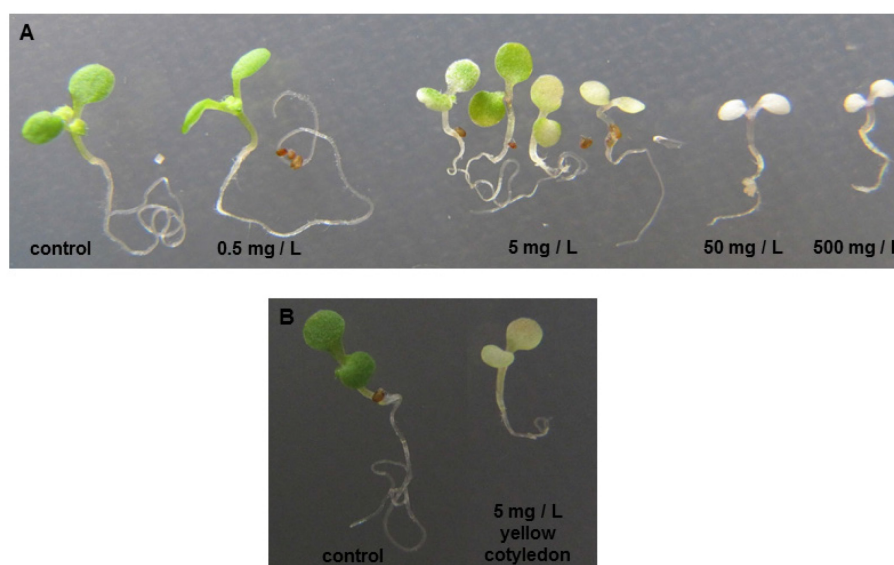


**Figure 47 Phenotype of 10-day-old *Arabidopsis* seedlings grown on different concentrations of spectinomycin.** *Arabidopsis* Col-0 seeds were grown for 10 days on SEA medium containing 1% sucrose and 0.5, 5, 50 or 500 mg/L spectinomycin. A) Representative phenotype of seedlings grown on 0.5, 5, 50 or 500 mg/L spectinomycin; B) Representative phenotype of control (green) and yellow seedlings grown in the presence of 5 mg/L spectinomycin.

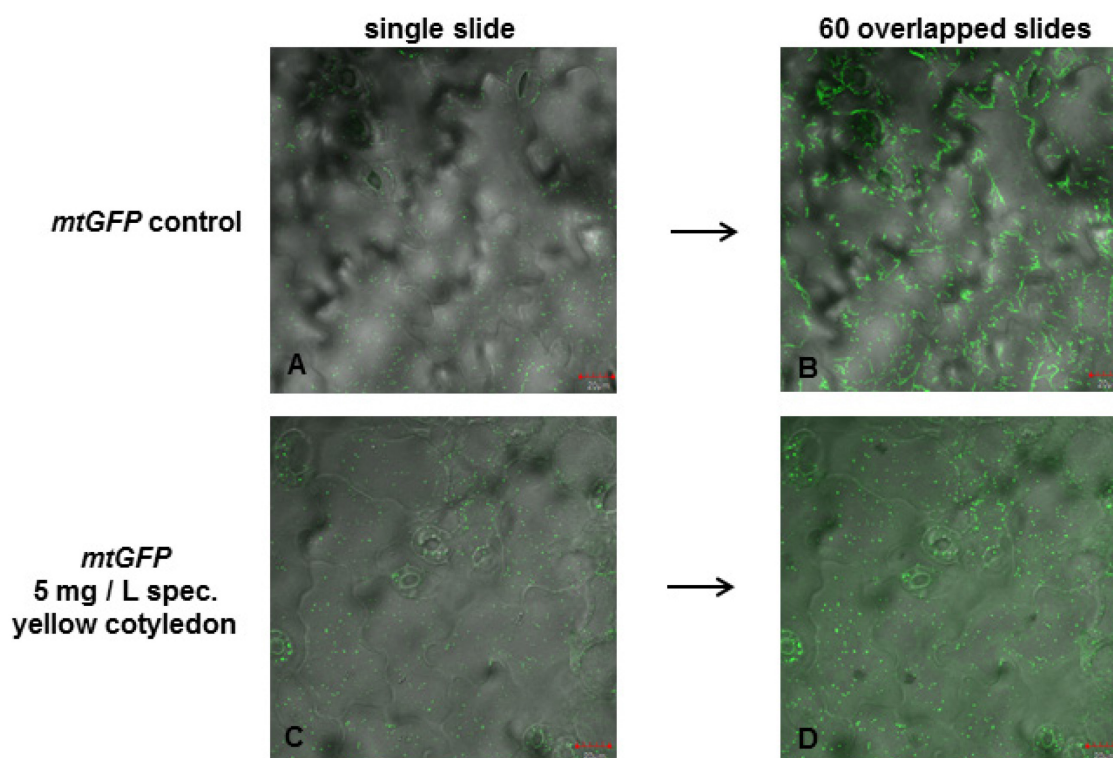


**Figure 48 Confocal microscopic images of mitochondria in epidermal cells of control and yellow, spectinomycin-treated seedlings.** Seeds of the *mtGFP* mutant were grown for 10 days on SEA medium containing 1% sucrose supplemented (where stated) with 5 mg/L spectinomycin. Mitochondrial size, shape, density and motility were assessed in epidermal cells of the cotyledons using confocal microscopy. Single slides (A, C) and 60 overlapped slides (B, D) taken at 1.1 s interval are presented. A, B) Mitochondria in epidermal cells of control (green) seedlings; C, D) Mitochondria in epidermal cells of yellow seedlings grown on 5 mg/L spectinomycin. Scale bar: 20  $\mu$ m.

### 3.6.3 Investigation of mitochondrial motility in *Arabidopsis* etiolated seedlings

Light represents one of the most important factors influencing plant development with easily observed dramatic effects on seedling morphology. While light-grown seedlings have short hypocotyl and green expanded leaves, dark grown (etiolated; Fig. 49) seedlings have elongated hypocotyl, small folded cotyledons and undeveloped chloroplast precursors, the etioplasts (Chory *et al.*, 1996).

The present work demonstrated a direct relation between impaired chloroplast development in white cotyledons and partial mitochondrial motility arrest (Fig. 29 and 30). Taking into consideration these results it was interesting to investigate if light plays a crucial role in this process. To answer this question, *MtGFP* seedlings were grown for 10 days in complete darkness and mitochondrial size, shape, number and

motility was assessed in epidermal cells of etiolated cotyledons. A first important observation was that there existed a high variability in mitochondrial morphology between different cotyledons. While small, coccoid or sausage-like mitochondria were observed most frequently (Fig. 50A and C), sometimes also vermiform and ring-like structures were present (Fig. 50 G). In figure 51G the red arrow points to circular, ring-like mitochondria and the violet arrow to elongated, worm like structure with length up to 10  $\mu\text{m}$ . The existing mitochondria usually had high motility, with the exception of the ring-like and vermiform ones that moved at low speeds or sometimes were even static (Video 18-21). The observed high variability in mitochondrial morphology between individual cotyledons might be explained by the existence of a small, but significant difference in the microclimate (e.g., oxygen availability) of etiolated cotyledons. It is possible that some cotyledons were more distant to each other and had higher oxygen availability, while others were attached to each other and had low oxygen availability. As it was already described in the literature, low oxygen pressure determines the formation of elongated and ring-like structures (Van Gestel and Verbelen, 2002).

Altogether, it is clear that in the absence of light and of an undeveloped chloroplast, mitochondria had normal motility. This indicates that impaired chloroplast development induces a mitochondrial motility arrest only in the presence of light as opposed to our observations on mitochondrial gene copy numbers.



**Figure 49 Phenotype of *Arabidopsis* *mtGFP* control and etiolated seedlings.** *Arabidopsis* *mtGFP* seeds were grown for 10 days in light or complete darkness on SEA medium containing 1% sucrose.

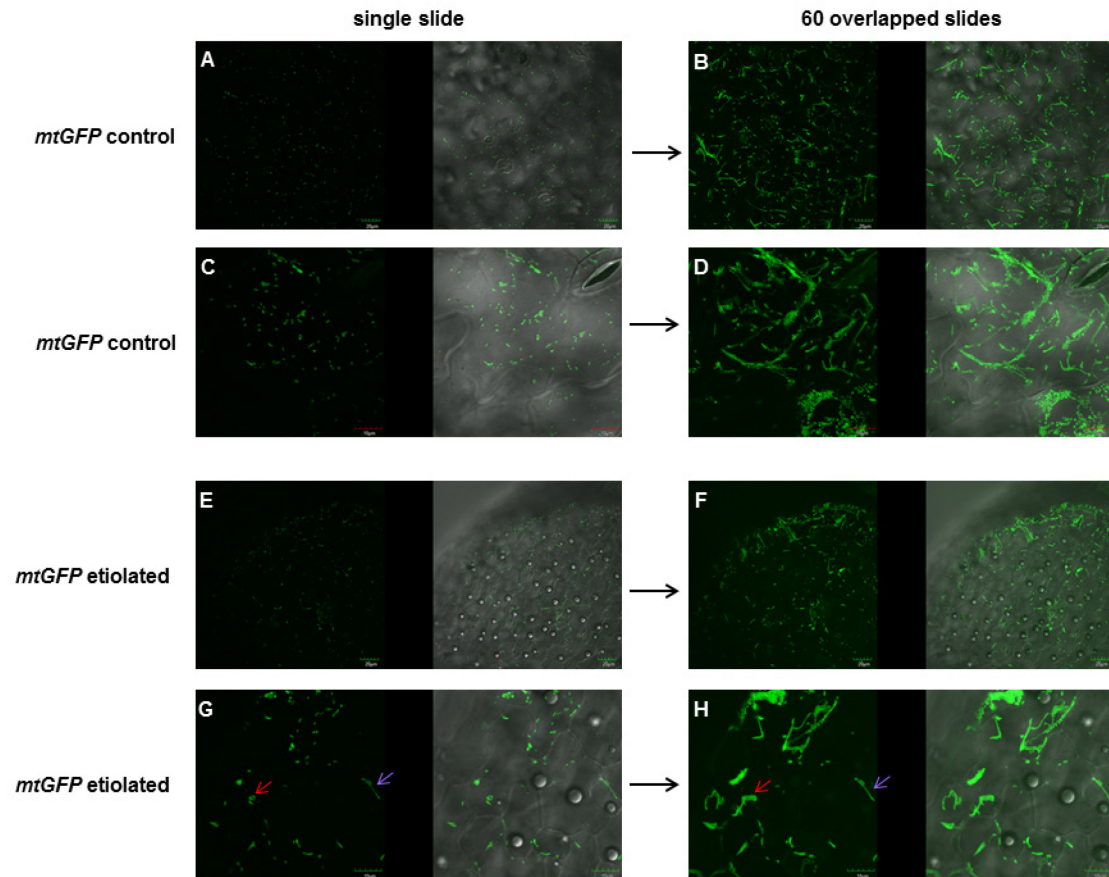


**Figure 50 Confocal microscopic images of mitochondria in epidermal cells of green and etiolated cotyledons.** Seeds of the *mtGFP* mutant were grown for 10 days in light or complete darkness on SEA medium containing 1% sucrose. Mitochondrial size, shape, density and motility were assessed in epidermal cells of the cotyledons using confocal microscopy. Single slides (A, C, E, G) and 60 overlapped slides (B, D, F, H) taken at 1.1 s interval are presented. A-D) Mitochondria in epidermal cells of green cotyledons; E-H) Mitochondria in epidermal cells of etiolated cotyledons. Scale bar: A, B, E, F: 20  $\mu$ m; C, D, G, H: 10  $\mu$ m. Red arrows point to a circular, motile mitochondria and violet arrows point to an elongated, static mitochondria.

## 4 Discussion

### 4.1 Organization and abundance of mitochondrial gene copy number in the model plants *Arabidopsis thaliana*, *Hordeum vulgare* and *Nicotiana tabacum*

#### 4.1.1 The copy number of mitochondrial genes varies between species, ecotypes and organs

The plant mitochondrial genomes theoretically assemble in so-called “master chromosomes” that encompass all coding and non-coding sequences and are in balance with alternative structures and subgenomic circles that result from recombination between large direct repeats (Lonsdale *et al.*, 1988; Janska and Woloszynska, 1997; Woloszynska, 2010). However, preparations of mitochondrial DNA revealed a more complex, multipartite structure that involves the presence of a heterogeneous population of mostly linear molecules of various sizes, small circular molecules and more complex molecules, which have been interpreted as products of recombination and recombination-mediated replication (Bendich, 1996; Oldenburg and Bendich, 1996; Backert *et al.*, 1997; Backert and Börner, 2000). The existence of such a complex structure creates the possibility that mitochondrial genes reside on different subgenomic molecules and, as a result, exist in different copy numbers. This characteristic has been observed in maize (Muisse and Hauswirth, 1995), bean (Woloszynska *et al.*, 2006) and recently, in the model plant *A. thaliana* (Preuten *et al.*, 2010). However, until now the existence of different copy numbers of mitochondrial genes has not been compared between different plant species, ecotypes and organs. The present work compares absolute copy numbers of representative mitochondrial genes in three model plants, *A. thaliana*, *N. tabacum* and *H. vulgare*, and discusses their occurrence in different organs, ecotypes and mutants.

In contrast to plastid genes (Fig. 20A and 24A and Zoschke *et al.*, 2007), mitochondrial genes were shown to have numbers with species-specific ratios. In *Arabidopsis*, the gene *atp1* usually showed significantly higher abundance than the other three investigated genes (*nad6*, *rps4* and *cox1*) that had the same values (Fig.

12B, 26B, 34, 40A). This result represents a natural condition and not an artifact of the PCR reaction since the four gene fragments have equal amplification efficiency, as discussed in Preuten *et al.* (2010). In *Arabidopsis*, *atp1* has been suggested to be located together with *cox1* on the same subgenomic circle that is predicted to originate by recombination between two large repeated regions with *nad6* and *rps4* being located adjacent to each other (Klein *et al.*, 1994; Unseld *et al.*, 1997). Since two pairs of large repeated regions exist in the *Arabidopsis* genome, its structure is predicted to be theoretically represented by 5 circular DNA molecules: three mastercircles and two subgenomic circles (Klein *et al.*, 1994). In tobacco the situation is different, with *atp1* having approximately half of the gene copies that exist for *nad6*, *rps4* and *cox1* (Fig. 35B). This situation exists in the context of a more complex genome: the presence of three repeated regions and the assembly into 8 genomic variants: two mastercircles and 5 subgenomic circles (Sugiyama *et al.*, 2005). Until now, the barley mitochondrial genome has not been sequenced, so the theoretically predicted partitioning of genes on subcircles is not clear. However, also in this case there exists a clear difference in the copy number of the two investigated genes *atp9* and *rps2*, with *rps2* being two-fold more abundant than *atp9* (Fig. 23A). The theoretical assembly of plant genomes into mastercircles and subcircles cannot solely explain the differences that exist in copy number of investigated genes. They can only be explained by taking into consideration the microscopic observations of mtDNA preparations that prove the existence of a heterogeneous population of molecules of different sizes (Bendich, 1996; Oldenburg and Bendich, 1996; Backert *et al.*, 1997; Backert and Börner, 2000) that probably exist in different amounts within the same tissue.

The work presented here shows a species-specific ratio between the four investigated genes that can vary under certain conditions. In *Arabidopsis*, clear differences exist between investigated plant organs: while in flowers, stems and 10 days-old green cotyledons a higher number of *atp1* was present with *nad6*, *rps4* and *cox1* having identical values, in green siliques, roots and root tips the four genes had the same number of gene copies (Fig. 12B, 40A). These results point to a probable differential amplification of certain subgenomic molecules in some organs or tissues. The process of differential amplification of mitochondrial genes was previously observed during *Arabidopsis* leaf development and senescence: while identical copy numbers of all four genes existed in the youngest stage that was assessed (5-days old

cotyledons), further leaf development resulted in the appearance of the “typical” gene ratio, with *atp1* being the most abundant gene (Preuten *et al.*, 2010). At the onset of senescence, copy numbers of all four genes increased (Preuten *et al.*, 2010) as a result of a probable amplification of the entire gene complement, due to a currently unknown signal.

Secondly, individual ecotypes belonging to the same species can vary in regard to the mitochondrial gene ratio. While in young developmental stages (whole 10 days-old seedlings), the gene ratio is identical for the investigated ecotypes (Preuten *et al.*, 2010), 20 days-old rosette leaves can vary in their gene content with Col-0 presenting the typical gene ratio with *atp1* being the most abundant, while Ws and the two tetraploid ecotypes (Wilna and Wa-1) have identical copy numbers of the four investigated gene (Fig. 19A). In the case of barley (*H. vulgare* cv. Golden Promise), the ratio between the two genes remained the same in the spontaneously-induced tetraploid lines (MBE and L150) (Fig. 23A). Obviously, the mitochondrial gene copy numbers are determined by the genotype. The found differences between *Arabidopsis* ecotypes should allow for mapping and identifying involved gene(s) by crossing experiments combined with the analysis of the offspring.

The representative gene ratio of a species is usually kept constant in different mutants and after different treatments. We observed a stable gene ratio in all investigated *Arabidopsis* mutants, as well as under different growth conditions and following different treatments: dark, sucrose depletion and spectinomycin treatment (Fig. 26B, 34, 39, 42). Moreover, by combining a nuclear mutation with a strong treatment (respiration mutants on spectinomycin), the ratio between the mitochondrial gene copies was still stable (Fig. 39). These results point to the amplification of the whole mitochondrial genome, without a particular amplification of subgenomic molecules. However, amplification of sublimons cannot be completely excluded since the copy numbers of just four representative genes were determined, and not the entire gene complement. An equal amplification of 27 mitochondrial genes was observed in the *Arabidopsis rpoTnp-2* mutant (Kühn *et al.*, 2009), supporting the hypothesis of whole-genome replication. Moreover, the same gene ratios were present also in the white *albostrians* mutant (Hedtke *et al.*, 1999), as well as in albino rye mutants (Ballesteros *et al.*, 2009). A particular case is represented by the tobacco transplastomic mutants that present slightly different gene patterns when compared to the wild-type (Fig. 37). This could be the result of genetic instability caused by tissue

culture. Variations in the tobacco mtDNA population during tissue culture and regeneration were previously reported (Kanazawa, 1998).

Altogether, the present results reveal a very strict control of mitochondrial gene copy number in plants. Candidate proteins involved in the control of mitochondrial gene stoichiometry include MSH1, RECA3 and OSB1. All three proteins were shown to be involved in suppression of recombination between short repeated DNA sequences. Mutation or elimination of these proteins induces large-scale rearrangements of organellar genomes that perturb their normal functioning and result in strong phenotypes like leaf variegation or cytoplasmic male sterility (Maréchal and Brisson, 2010). An upregulation of these genes was observed in white, spectinomycin-treated seedlings that contained a three-fold amplification of the mitochondrial gene copy number together with the maintenance of a constant gene ratio (Fig. 28).

#### **4.1.2 There exist generally low copy numbers of mitochondrial genes**

As a natural condition, currently investigated plant species varied in regard to the specific ratio of mitochondrial genes (see 4.1.1). Moreover, another important characteristic that was observed during this study is represented by the existence of a very low amount of gene copies within investigated plant tissue. The presence of low gene copy numbers is a general characteristic in all three investigated angiosperms (*Arabidopsis*, tobacco and barley) and might be a general characteristic of the plant lineage. The number of mitochondrial gene copies per cell in wild-type plants under standard growth conditions ranged from approximately 25 (*atp1* copies in *Arabidopsis* Ws ecotype, Fig. 19B) to 450 (*atp1* copies in *Arabidopsis* root tips, Fig. 12B), with an average of 50-100 for all three species. This is in good agreement with previously reported 110-140 copies for dark-grown shoots of several cucurbit species (Ward *et al.*, 1981) and 80 (dark-grown shoots) to 410 (embryos) in pea (Lamppa and Bendich, 1984), calculated based on the percentage of mtDNA in total DNA and the size of the mitochondrial genome, both estimated on the basis of re-association kinetics (Ward *et al.*, 1981; Lamppa and Bendich, 1984). Recent work presented 100-140 copies in rice leaf protoplasts with approximately ten times higher amount in rice egg cells (Takanashi *et al.*, 2010). Moreover, the present work shows low levels of



mitochondrial gene copies in all four *Arabidopsis* ecotypes, with a high variability between individual plants (Fig. 19B).

By comparing these values with the previously reported 400-700 mitochondria in plant cells (Sheahan *et al.*, 2004; Sheahan *et al.*, 2005, Kato *et al.*, 2008), it is possible to propose that the number of gene copies is lower than the total number of mitochondria. This supposition is completely supported by the calculation of 80 (*nad6*, *cox1* in Ros50/3) to 280 (*atp1* in Ros50/6) gene copies and approximately 400 mitochondria that were present in leaf protoplasts from selected leaf developmental stages (Fig. 14). We could further show that there exists a correlation between cell size and number of mitochondria per cell. In conclusion, this data clearly demonstrates that, on average, the cells of *Arabidopsis*, tobacco and barley do not contain sufficient mitochondrial gene copies to supply all mitochondria with complete genomes. The existing mitochondria can contain only a subset of genes rather than the master chromosomes predicted from physical mapping (Lonsdale *et al.*, 1988). Alternatively, only a minor fraction of the mitochondrial population might contain the complete genome. Quantitative analyses of DAPI-stained mtDNA revealed only low amounts of DNA per mitochondrion in root cells, shoot apex, cultivated cells and protoplasts of various species of higher plants, including *Arabidopsis*, tobacco, rice (*Oryza sativa*) and *Pelargonium* (Kuroiwa, 1982; Kuroiwa *et al.*, 1992; Fujie *et al.*, 1993; Satoh *et al.*, 1993; Fujie *et al.*, 1994; Takanashi *et al.*, 2006). The existence of low amounts of mtDNA in higher plants is probably compensated by frequent fusion and fission events of mitochondria that contain different parts of the chondrome. With fusion, proper conditions are created to allow mixing and recombination of the available mtDNA molecules and then, fission induces unequal partitioning of the nucleoid in the newly-formed mitochondria, resulting in the coexistence of mitochondria containing various amounts of DNA in a single cell. This conclusion lends further support to the view that, the totality of mitochondria within a cell, the chondriome, functions as a panmictic population (Lonsdale *et al.*, 1988; Arimura *et al.*, 2004b; Sheahan *et al.*, 2005b; Logan, 2006).

The first 3-4 mm of the root tip showed considerably higher levels of mitochondrial gene copy number in comparison to other organs (Fig. 12B). This finding is in agreement with previous evaluation of mitochondria and mtDNA by fluorescence microscopy. While the meristematic region of *Arabidopsis* root tips contain > 1 Mbp DNA per mitochondrial nucleoid, this value decreases rapidly to

170 kb in the neighboring cells due to cell division and distribution of mtDNA to daughter cells/mitochondria without further DNA synthesis (Fujie *et al.*, 1993). Similar results are present for the *Pelargonium zonale* root meristem, with 3 Mbp of DNA in mitochondrial nucleoids originating from the area above the quiescent center, the region with active mtDNA synthesis. With further cell division, the amount of DNA per nucleoid drops rapidly to less than 170 Kbp (Kuroiwa *et al.*, 1992). A numerical evaluation of nucleoid-containing mitochondria over the length of rice root was performed by Takanashi *et al.* (2006): while 91% of mitochondria contained a DAPI-stained nucleoid in the root tip, the middle portion and root base had just 41% and 33% of nucleoid-containing mitochondria.

Recently, high amounts of mtDNA were found in maize stalks that also contain meristematic cells, with declining amounts in mature leaf blades (Oldenburg *et al.*, 2012). This result further supports the conclusion that mtDNA is usually replicated in meristematic tissue with the DNA content per mitochondria declining together with maturation of the respective organ, independent on the photosynthetic activity.

#### **4.2 Organellar gene copy number in relation to nuclear ploidy level and endocycles**

Plant cell division cycle is a highly regulated process that leads to the formation of two daughter cells. The cell cycle encompasses the whole sequence of events that take place between the birth of a new cell until the next division (Gutierrez, 2009). Apart from the usual mitotic cycle, plant cells can enter into an alternative cycle named endocycle or endoreplication cycle. In this situation, successive rounds of full nuclear genome replication occur without cell division. This leads to an exponential increase in the ploidy level, starting from the basic ploidy level of the cell (Gutierrez, 2009). As an example, diploid plants with the basic nuclear ploidy level of 2C can also contain 4C, 8C, 16C nuclei. The presence of endoreplication cycles is not a general condition of all plant species, but a characteristic of some plant families and species (Barow and Meister, 2003; Barow, 2006; Barow and Jovtchev, 2007). *A. thaliana* is a diploid plant that exhibits extensive

endopolyploidization in its organs (Galbraith *et al.*, 1991; Barow and Meister, 2003). Recent determinations of nuclear ploidy levels (mean C-levels) during *Arabidopsis* leaf development and senescence showed different levels in leaves originating from the same plant, with older leaves having the highest levels. Moreover, these values increased with further aging of the plant. Plastome copy numbers in leaves of same age stages remained stable throughout leaf development and aging (Zoschke *et al.*, 2007), showing that plastome levels in leaves are independent from endocycle progression. However, plastome copy numbers were shown to be proportional to the nuclear ploidy status: Rauwolf *et al.* (2009) observed a constant plastome/nuclear genome ratio of about 1700 copies per C-value in mesophyll cells of mature leaves of *Beta vulgaris* differing in ploidy (di-, tri- and tetraploid; Rauwolf *et al.*, 2010).

The present work sheds more light on the relation between plastome copy number and nuclear ploidy levels by evaluating the copy number of two representative plastid genes *psbA* and *clpP* in diploid and tetraploid lines of two model plants: *A. thaliana* and *H. vulgare*. These species were chosen for their natural response to endopolyploidy: while *Arabidopsis thaliana* is a diploid species ( $2n = 2x = 10$ ) with high endopolyploidy (Galbraith *et al.*, 1991; Barow and Meister, 2003), barley is a diploid plant ( $2n = 2x = 14$ ) that has very low endopolyploidy (Barow and Meister, 2003). At first, it was possible to show a high variability between individual plants originating from both diploid and tetraploid lines of *Arabidopsis*, with two- to four-fold difference in plastome copy number existing (Fig. 20B). This was not the case for barley, where low variability existed between plants belonging to the same line (Fig. 24B). Average evaluation of copy number proved a significant difference between diploid and tetraploid lines in both *Arabidopsis* and barley (Fig. 20A, 24A) supporting both the work of Rauwolf *et al.* (2009) and proving that plastome copy number varies with the natural ploidy level. Moreover, the endopolyploidization status of a species (high vs. low endopolyploid) plays a role in the variability of plastome copies between individual plants, with low endopolyploid species (ex. barley) having the lowest variability.

Determination of mitochondrial gene copy numbers in diploid and tetraploid plants of *Arabidopsis* and barley revealed the existence of a constant chondrome-to-nuclear genome ratio just in the case of barley, based on a low variability between individual plants of the same line (Fig. 23). In case of *Arabidopsis*, no difference could be observed between diploid and tetraploid lines (Fig. 19). This result further

complements the previous evaluation of mitochondrial gene copy number in different leaf age stages, by excluding the nuclear ploidy/endopolyploidy level from the possible factors determining the increase observed at the onset of leaf senescence (Preuten *et al.*, 2010).

Altogether, the present work brings to light a new relation between organellar DNA amounts, nuclear ploidy level and endocycle control. Keeping in mind that we have compared only two species, one might hypothesize that in the absence of endocycles, elevation of nuclear ploidy levels induces a similar increase in the amount of organellar genomes. Moreover, the presence of endopolyploidy within a species coexists with a large variability of organellar gene copy number, with four-fold differences existing between individual plants. The biological significance of this effect is currently unknown. It is possible that lower or elevated organellar DNA amounts lead to changes in the physiological and metabolic condition of individual plants. This could further increase the flexibility of plants in their adaptation to environmental changes.

### **4.3 Possible reasons for elevated mitochondrial gene abundance in plants**

Regulation of mitochondrial DNA abundance in plants under normal and stress conditions is a largely unknown research field with components just beginning to be discovered. Until now, separate observations of mitochondrial DNA amount elevation and decrease were made under certain conditions, without a clear image on possible reasons and outcomes of these processes (Hedtke *et al.*, 1999; Soares *et al.*, 2005; Ballesteros *et al.*, 2009; Kühn *et al.*, 2009; Preuten *et al.*, 2010; Toshiji *et al.*, 2011). Here, the first large study was performed that aims to investigate the conditions of mitochondrial genome elevation as well as to discuss possible reasons, effects and signaling pathways.

#### 4.3.1 Elevated number of mitochondrial gene copies as a result of increased number of mitochondria

The first and probably the simplest explanation of elevated mitochondrial DNA abundance under certain physiological conditions is represented by the existence of a higher number of mitochondria in investigated tissues. Table 5 displays a summary of the results from this thesis and the existing literature that relates the conditions of elevated or reduced mtDNA levels with mitochondria number.

It is tempting to speculate that the elevation of mitochondrial number per cell could be the primary cause for the observed increased mtDNA levels. Germination represents a clear situation where a positive correlation exists between the number of mitochondria and DNA amounts. Moreover, it is linked to an increased respiratory activity (Breidenbach *et al.*, 1966; Breidenbach *et al.*, 1967). Apart from this, it is possible to imply that under specific conditions with a higher number of mitochondria, an elevation of mitochondrial DNA abundance is also present. Data in Table 5 indicate a positive relation between cell size and mitochondria number. While *Arabidopsis*, tobacco and *Medicago truncatula* mesophyll cells contain 300 – 700 mitochondria (Sheahan *et al.*, 2004; Sheahan *et al.*, 2005a; Logan, 2006), large onion bulb epidermal cells contain more than 10.000 mitochondria (Arimura *et al.*, 2004b). Moreover, a clear linear increase in the number of mitochondria with increasing cell size was observed in the present study: while 10 - 20  $\mu\text{m}$  cells contained  $\sim 80$ , 40 - 50  $\mu\text{m}$  cells  $\sim 350$  and 70 - 80  $\mu\text{m}$  cells contained  $\sim 700$  mitochondria (Fig. 16B).

The compiled data in relation between Table 5 suggest further a relation between sucrose availability and mitochondria number: heterotrophically-grown cells contain more mitochondria. Approximately 1.200 mitochondria are present in cells of tobacco callus and up to 2.000 in tobacco BY-2 cells (Sheahan *et al.*, 2005a). This conclusion is further supported by the work of Journet *et al.* (1986) and Giegé *et al.* (2005) that demonstrates a reduction in mitochondria number or volume upon sucrose deprivation of sycamore and *Arabidopsis* cells (Journet *et al.*, 1986; Giegé *et al.*, 2005). When sucrose is supplemented to the starved cells, the mitochondria number and volume is restored (Journet *et al.*, 1986; Giegé *et al.*, 2005). A direct relation between sucrose availability and mitochondrial gene copy number was observed in 10 days-old *Arabidopsis* seedlings that were grown in the presence or absence of 1% sucrose (Fig. 34). A significantly higher gene copy number was present in light-grown

and in etiolated seedlings grown under high-sucrose conditions when compared to non-treated controls (Fig. 34). Even if a correlation with the number of mitochondria was not performed, present data undoubtedly prove that sucrose availability plays an important role in regulating mitochondrial genome amounts, probably accompanied by an increase in mitochondrial number.

A particular situation is represented by the existence of elevated gene copy numbers in white cotyledons and leaves. This is true for white and variegated mutants as well as for white cotyledons and leaves obtained by treatment with the antibiotic spectinomycin (Fig. 35, 36 and 37) (Hedtke *et al.*, 1999; Ballesteros *et al.*, 2009; Toshioji *et al.*, 2011). An elevated number of mitochondria is not present in all cases. Albino plants of rye (*Secale cereale* L.; Ballesteros *et al.*, 2009) contain an elevated number of mitochondria. On the other hand, a normal number of mitochondria could be observed in albino leaves of the barley *albostrians* (*Hordeum vulgare* cv. Haisa) mutant (Hedtke *et al.*, 1999). Additionally, green and white cotyledons obtained by treatment with spectinomycin contain the same number of mitochondria, as determined by both confocal microscopy (CLSM) and transmission electron microscopy (TEM; Fig. 29 - 31). This was true for all investigated cell types: epidermal cells, guard cells, mesophyll cells, vascular tissue and root cells, without a difference between photosynthesizing and non-photosynthesizing cells (Fig. 30). Moreover, elevated mtDNA levels were determined in other white mutants without an evaluation of mitochondrial number (Fig. 36, 37). The same was true for white sectors of variegated plants (Toshioji *et al.*, 2011). In these cases elevated mitochondrial DNA levels exist together with a “normal / wild-type” number of mitochondria indicating the presence of a higher amount of DNA per mitochondria.

Obviously, even if under certain physiological conditions abundant mitochondrial DNA is probably determined by increased number of mitochondria, this situation is not true for all cell types. In case of meristematic cells of root tips and shoot apical meristem, the existing mitochondria contain high amounts of DNA as a result of high rates of DNA synthesis. With cell division, mitochondria continue to multiply in the presence of low rates of DNA synthesis resulting in low amounts of DNA per mitochondria (Kuroiwa *et al.*, 1992; Fujie *et al.*, 1993; Fujie *et al.*, 1994; Takanashi *et al.*, 2006). While a high number of meristematic cells are probably present in very young tissues, dilution of mtDNA with cell division could also explain the significant decrease observed in the development of *Arabidopsis*

cotyledons, from the 5 days-old to 10 days-old stage (Preuten *et al.*, 2010). A similar situation is present in mature egg cells of *Pelargonium zonale* that contain a few giant mitochondria (long and stretched or cup-shaped) with high amounts of DNA. During the early stages of embryogenesis, the large mitochondria divide in stages to form small, round mitochondria with low amounts of DNA (Kuroiwa and Kuroiwa, 1992; Kuroiwa *et al.*, 1996).

Taking into consideration the present data, it is still to be investigated if elevated numbers of mitochondria could explain the higher abundance of gene copy numbers that were observed in tetraploid lines of barley, as well as in respiration mutants of *Arabidopsis* (Fig. 23, 39, 40B; Kühn *et al.*, 2009). Moreover, a targeted research would be necessary to gain information on regulatory mechanisms that control the mitochondria number per cell.

**Table 5 Factors and mutants that influence the abundance of mitochondrial gene copy number and/or mitochondria number in higher plants**

Factor / mutant	Number of mitochondria	mtDNA abundance	Reference
<b>Cell size</b>	Elevated number of mt. with increasing cell size; larger cells contain more mitochondria	ND	Present work (Fig. 16) Comparison of mt. number in protoplasts ( Sheahan <i>et al.</i> , 2004; Sheahan <i>et al.</i> , 2005; Logan, 2006 and present work Fig. 14) and mt. number in onion bulb epidermal cells (Arimura <i>et al.</i> , 2004b)
<b>Cell type: meristematic cells</b>	The number of mitochondria per cell depends on the cell type/ layer within the meristematic area (see Fujie <i>et al.</i> , 1993)	Higher mtDNA abundance in meristematic cells	root tip (Fujie <i>et al.</i> , 1993; Takanashi <i>et al.</i> , 2006; present work Fig. 12B) shoot apical meristem (Fujie <i>et al.</i> , 1994)
<b>Cell type: egg cells</b>	Existence of giant mitochondria in certain species	Elevated mtDNA levels	Kuroiwa and Kuroiwa, 1992; Kuroiwa <i>et al.</i> , 1996; Takanashi <i>et al.</i> , 2010
<b>Natural plant to plant variability in <i>Arabidopsis</i> ecotypes</b>	ND	Up to 5-fold difference in mt. gene copy number between individual plants	Present work Fig. 19B
<b>Nuclear ploidy level in barley</b>	ND	Elevated mt. gene copy number in tetraploid vs. diploid barley lines	Present work Fig. 23
<b>Germination</b>	Elevated number of mt. in germinating castor-bean endosperm tissue	ND	Akazawa and Beevers, 1957;

	Elevated number of mt. in germinating cotyledons of peanuts	Elevated mtDNA amounts	Breidenbach <i>et al.</i> , 1966, 1967
<b>Onset of leaf senescence</b>	Same number of mitochondria in protoplasts from selected age stages	Elevated mtDNA levels at the onset of leaf senescence	Preuten <i>et al.</i> , 2010; present work Fig. 14
<b>Cotyledon development</b>	ND	Reduction in mtDNA levels upon development from 5 to 10 days-old <i>Arabidopsis</i> cotyledons	Preuten <i>et al.</i> , 2010
<b>Sucrose availability</b>	Elevated number of mt. in heterotrophically-grown cells (tobacco callus, BY-2 cells)  Reduction in mt. number / volume upon sucrose deprivation, and restoration to normal number after readdition  ND	ND  ND  Elevated gene copy numbers in seedlings grown on medium supplemented with sucrose	Sheahan <i>et al.</i> , 2005  Journet <i>et al.</i> , 1986; Giegé <i>et al.</i> , 2005  Present work Fig. 34
<b>Elevated CO2 levels</b>	Elevated number of mt.	ND	Robertson <i>et al.</i> , 1995; Griffin <i>et al.</i> , 2001
<b>White cotyledon / leaf phenotype by mutation or chemical inhibition of plastid protein synthesis</b>	Elevated number of mt. in white leaf mutants  Elevated number of mt. in white leaf mutants  Same number of mt. in white leaf mutants  Same number of mt. in cotyledons of spectinomycin-treated seedlings  ND  ND  ND	ND  Elevated gene copy number  Elevated gene copy number  Elevated gene copy number  Elevated gene copy number in tobacco shoots grown on spectinomycin  Higher mtDNA abundance in white sectors of variegated leaves  Higher mt. gene copy number in white mutants	Soares <i>et al.</i> , 2005  Ballesteros <i>et al.</i> , 2009  Hedtke <i>et al.</i> , 1999  Present work – Fig. 29-31, 41A  Present work: Fig. 35  Toshoji <i>et al.</i> , 2011  Present work: Fig. 36, 37
<b>Respiration mutants</b>	ND	Elevated mt. gene copy number	Kühn <i>et al.</i> , 2009; present work: Fig. 40, 41B

ND not nedermined



#### 4.3.2 Mitochondrial gene copy number may determine transcript abundance

Theoretically, the level of mitochondrial transcripts within plant cells might be regulated by different means: by changes in DNA amounts in mitochondria, by differential regulation of transcription or by post-transcriptional processes. In addition, an elevation of mitochondria number per cell might also influence the final outcome of transcript levels.

In the present study I was able to show elevated transcript levels of four mitochondrial genes in white seedlings grown in the presence of spectinomycin (Fig. 27). This result is related to a three-fold elevation in copy number of the respective genes (Fig. 26B). Thus, it is tempting to speculate that the control of copy numbers of mitochondrial genes might have a functional importance and is connected to the observed altered transcript levels. Previous research on barley *albostrians* mutant comes in favour of this hypothesis: both transcript levels and gene copy numbers were found to be enhanced in photosynthetically inactive white leaves versus green leaves (Hedtke *et al.*, 1999). Moreover, a positive correlation between increased number of mitochondrial gene copies and transcript level was observed in *RpoTmp* mutant of *Arabidopsis* (Kühn *et al.*, 2009). Muise and Hauswirth (1995) compared mitochondrial gene quantities (determined by Southern hybridization) and transcription in maize and *Brassica hirta*, and concluded that a direct relationship exists between gene copy number and the transcription rate. Although there are obviously cases that support the idea of control of transcript levels via the number of gene copies, the results of Preuten *et al.* (2010) contradict this hypothesis. When both gene copy numbers and transcript levels of respective genes were determined during different stages of leaf development and senescence, a direct relation could not generally be observed between these two parameters. The increased copy number at the onset of leaf senescence is not paralleled by increases amounts of transcripts (Preuten *et al.*, 2010). Moreover, in a study on *Phaseolus vulgaris*, the copy number of selected genes was not associated with their transcript levels (Woloszynska *et al.*, 2006).

In order to explain these possibly contradicting data, it is important to specify that Muise and Hauswirth (1995) analyzed run-on transcription, i.e. determined transcription rates, whereas the other studies determined transcript levels

(Woloszynska *et al.*, 2006; Preuten *et al.*, 2010). It is possible that accumulated transcript levels of mitochondrial genes in white, spectinomycin-treated seedlings are (partly) a result of increased transcription of respective genes since the transcript level of both mitochondrial RNA polymerases, RpoTm and RpoTmp is two-fold increased (Fig. 28). The transcript level of *RpoTm* was also enhanced in white leaves of the barley *albostrians* mutant (Emanuel *et al.*, 2004). Although most data support the idea that higher gene copy numbers correlated positively with higher transcript levels and suggest that the gene copy number could be a limiting factor in gene expression, the functional importance of this phenomenon is not clear yet.

In this context it should be noted that several studies have demonstrated that transcription rates and transcript levels are not necessarily positively correlated, and that the transcriptional activity of genes may be of little importance with respect to the final level of their products in plant mitochondria (Mulligan *et al.*, 1991; Giegé *et al.*, 2005; Okada and Brennicke, 2006). As example, Okada and Brennicke (2006) found that transcript synthesis in *Arabidopsis* mitochondria cycles in a diurnal rhythm, while steady-state transcript levels do not vary between light and dark phases. Moreover, in response to sugar starvation, mitochondrial gene expression remained mostly unaffected at the transcriptional, posttranscriptional and translational levels, the correct stoichiometry of the components of respiratory complexes being achieved posttranslationally (Giegé *et al.*, 2005).

Altogether, the possible involvement of gene copy number abundance in determining transcript abundance is still not clear with further experiments being necessary to reveal its exact function in plants.

#### **4.3.3 Elevated gene copy number as compensatory mechanism for reduced mitochondrial motility in white tissue**

The plant chondriome representing the totality of mitochondria within a cell is typically organized as a population of several hundred discrete organelles that display high motility and frequent fusion and fission events (Arimura *et al.*, 2004b; Logan, 2006). It is believed that a “need to meet” exists to enable exchange of DNA, transcripts and metabolites and altogether to insure a proper functioning of the chondriome (Logan, 2006). It is now clear that plant mitochondria contain only low

amounts of DNA, so that 300 – 400 mitochondria collectively have to use approximately 100 copies of each gene (Fig. 14 and chapter 4.1.2). This evidently represents a shortage of mtDNA that is probably compensated by organelle movement in different parts of the cell and repeated fusion and fission. By taking into consideration this aspect, a new hypothesis emerges that may explain the elevated amounts of mtDNA in white mutants, spectinomycin-treated seedlings and white sectors of variegated leaves. This present study has brought to light a new and unexpected aspect of mitochondrial dynamics that is represented by an almost complete arrest of mitochondrial motility in white cotyledons of spectinomycin-treated seedlings (Fig. 29, 30). Further research has determined the threshold level of motility arrest to be the appearance of a yellow-white cotyledon phenotype (Fig. 48 and chapter 4.5). Surprisingly, the same threshold level is present also for the appearance of mtDNA elevation (Fig. 37 and 39). It is thus tempting to propose that these two processes might be interconnected. Since usually low amounts of DNA are present in mitochondria, a reduced motility and fusion of most organelles would probably lead to a collapse of the respiratory function and eventually lead to cell death. An elevation of mitochondrial gene copy number might be needed to supply almost all mitochondria with the necessary templates for transcription. In the context of reduced motility and fusion events, each mitochondrion must function for a longer period as an individual organelle and thus requests the genetic apparatus to support the normal respiratory functions. As determined, white, spectinomycin-treated cotyledons had the same oxygen consumption as green ones (Fig. 32A).

To support this hypothesis it is still necessary to determine if a reduced mitochondrial motility is a common state in white mutants, in white sectors of variegated mutants, as well as in respiration mutants.

#### **4.4 Possible signaling pathways regulating mitochondrial gene copy number in plants**

Plastids and mitochondria originated by endosymbiosis from ancestral cyanobacteria and from  $\alpha$ -proteobacteria, respectively (see 1.1). Following integration, the newly acquired endosymbionts transferred most of their genes to the

nucleus of the host cells, becoming semiautonomous (Gray *et al.*, 1999; Dyall *et al.*, 2004; Timmis *et al.*, 2004; Reyes-Prieto *et al.*, 2007; Bock and Timmis, 2008). The nuclear control over organellar functions is termed “anterograde control/anterograde signaling/anterograde regulation” and is complemented by a backward flow of information from the organelles to the nucleus, thus enabling nuclear gene expression to be modified in accordance to their status. This process is termed “retrograde control/retrograde signaling/retrograde regulation” and allows cellular adjustments in response to different kinds of stresses: abiotic, biotic and mutations (Rodermeel, 2001; Butow and Avadhani, 2004). Apart from this, mitochondria and chloroplasts are metabolically interconnected so that intensive communication takes place in order to optimize each other for proper functioning of the cell.

The present work investigates a special form of inter-organellar communication that results in the elevation of mtDNA abundance under conditions of impaired chloroplast development. While elevated mtDNA amounts were observed in albino plants of barley, rye, variegated ornamental plants and in the *RpoTmp* mutant (Hedtke *et al.*, 1999; Ballesteros *et al.*, 2009; Kühn *et al.*, 2009; Toshiji *et al.*, 2011), possible signaling pathways involved in this phenomenon have not been proposed yet so that the regulation of mtDNA abundance remains a largely unresolved problem. Based on our results and on the similarities with the retrograde signaling pathways, possible components of the inter-organellar crosstalk leading to elevated mtDNA amounts are discussed.

#### 4.4.1 Origin of the signal

The first possible origin of the involved signaling cascade is undoubtedly from the plastids since inhibition of plastid protein synthesis (by mutation or chemical inhibition) as well as other conditions that lead to an arrest of chloroplast development and the appearance of a white leaf phenotype resulted in elevated mitochondrial gene copy number. The existence of elevated mtDNA amounts in white leaves of the barley *albostrians* mutant represents the first clear indication of a plastid-derived signal (Hedtke *et al.*, 1999). *Albostrians* is a nuclear mutant that lacks plastid ribosomes in cells of white tissue (Hagemann and Scholz, 1962). Consequently, the plastid genome can not be expressed, leading to a white leaf

phenotype. To further investigate the circumstances of elevated mtDNA amounts, a similar biological condition was reproduced in the present study by growing *Arabidopsis* seedlings on culture medium containing spectinomycin. The antibiotic specifically blocks plastid translation (Wallace *et al.*, 1974; Moazed and Noller, 1987) and as result gives rise to white, photosynthetically inactive seedlings (Fig. 25A). As in *albostrians*, white *Arabidopsis* cotyledons have a three-fold elevation in mitochondrial gene copy number (Fig. 26B). The same result was present in white leaves of tobacco growing in culture medium with spectinomycin (Fig. 35B), strongly suggesting that the same signaling pathway is present in all three model plants.

An important aspect to be discussed is represented by the time point of the signal generation: if signaling from plastids is active just during early chloroplast development or also in mature chloroplasts. Under our experimental conditions, *Arabidopsis* seedlings were in contact with the antibiotic from the first day of development (Fig. 26B). Similarly, tobacco shoots were transferred to culture medium containing spectinomycin so that white leaf sectors resulted from treated apical meristematic cells (Fig. 35). While the effect of the antibiotic was not tested in leaves with mature chloroplast and bleaching experiments were not performed, it is currently not clear if the signaling pathway is active also at later stages of chloroplast development. However, determinations of mitochondrial DNA abundance in white sectors of variegated ornamental plants support the supposition of an early signal by observing the exceptional case of *Sol. scutellarioides* (Toshoji *et al.*, 2011). While an elevation of mtDNA abundance was generally observed in almost all investigated species, this was not the case for *Sol. scutellarioides*. A possible explanation is represented by the observation that in this plant, white sectors are initially pale green and only later become white. Thus the early partial chloroplast development might have determined “normal” amounts of mitochondrial gene copies per cell. As a result, it is probable that the signaling cascade regulating mitochondrial DNA abundance in plants originates during early stages of chloroplast development. However, further experiments are necessary in order to support this conclusion. Different bleaching conditions, as well as treatment of mature leaves with respiration inhibitors are possible experiments that would help to clarify this problem. In this context it is interesting that plastid-to-nucleus retrograde signaling originating from inhibition of plastid translation and affecting chloroplast-related nuclear genes was found to be effective only when occurring very early during seedling development

(Gray *et al.*, 2003). One may hypothesize, therefore, that the same signal might be involved in controlling photosynthesis-related nuclear genes and genes determining mitochondrial gene copy numbers depending on chloroplast development.

Complete inhibition of plastid protein synthesis does not allow plastid genes to be expressed. Therefore, it is possible that the absence of a particular plastid-encoded protein (or a function depending on such a protein) may be involved in triggering the signaling cascade that leads to elevated mtDNA amounts. Tobacco chloroplast genes can be generally classified into three major groups: photosynthesis-related genes, genetic system genes and other genes. Photosynthesis-related genes encode components of photosystem I, II, cytochrome b6f, NADH dehydrogenase, Rubisco and ATP synthase. Genetic system genes encode subunits of the plastid-encoded RNA polymerase (PEP), ribosomal and transfer RNA, ribosomal proteins, as well as *matK*, an organellar maturase. Additionally, a few proteins with other functions are also plastid-encoded (*clpP*, *accD*, *ccsA*, *cemA*, *accD*), as well as some hypothetical open reading frames (*ycf1*, *ycf2*, *ycf3*, *ycf4*, *ORF105*, *ORF79* etc.; Shinozaki *et al.*, 1986; Shimada and Sugiura, 1991). Since elevations in mitochondrial gene copy number were previously observed just in white mutants, transplastomic tobacco mutants with knock-out mutation in individual photosynthesis-related genes were assessed for their mitochondrial gene copy numbers (Fig. 37). In addition, the white *rpoA* mutant was also included in this study (Fig. 36). Surprisingly, from 12 mutants, just *atpB*, *atpH* and *rpoA* showed a two-fold elevation in their mitochondrial gene copy number (Fig. 36, 37). However, these were also the only mutants that had a completely white leaf phenotype (Fig. 36 and annex 4), connecting the elevation of mitochondrial gene copies with the complete absence of photosynthesis and possibly even with absence of chloroplast ATP synthesis. This observation is further supported by the study of the pale-green *prpl11* mutant. In this case an increase in mtDNA was not observed, clearly proving that it is the threshold level of chloroplast impairment that leads to an elevation of mtDNA abundance. This threshold is represented by the existence of completely white leaf phenotype (Fig. 39).

An interesting aspect to be discussed is represented by the functionality of plastid translation in the above-mentioned *rpoA*, *atpB*, *atpH* and *prpl11* mutants. While experimental data on *atpB* and *atpH* are missing (the mutants are not published), both *rpoA* and *prpl11* have functional ribosomes (De Santis-Maciossek *et al.*, 1999; Pesaresi *et al.*, 2001; Pesaresi *et al.*, 2006). These results further propose a

second possible origin of the signal that is not related to blocked plastid translation, but to the existence of a white phenotype, i.e. the complete block of chloroplast development.

Until now, plastid-encoded genes were not shown to be involved in retrograde signaling. An exception could be *trnE* that encodes tRNA<sup>Glu</sup>, a component that plays a dual role within the plastids: it participates in translation and also in the first step of chlorophyll biosynthesis, as a precursor of 5-aminolevulinic acid (ALA; Schön *et al.*, 1986). In white leaves of the barley *albostrians* mutant tRNA<sup>Glu</sup> was not detectable by Northern hybridization, probably as a result of very low transcription level (Hess *et al.*, 1992). The tetrapyrrole biosynthetic pathway was showed to be involved in retrograde signaling by isolation of four GUN (genomes uncoupled) mutants that presented *LHCB* expression under photobleaching conditions resulting from norflurazon treatment (Susek *et al.*, 1993). GUN2, GUN3, GUN4 and GUN5 encode enzymes involved in the heme and Mg branch of the tetrapyrrole pathway (Wilde *et al.*, 2004; Davison *et al.*, 2005; Verdecia *et al.*, 2005; Masuda and Fujita, 2008). Three mutants (*gun2*, *gun4* and *gun5*) were tested for their possible involvement in regulating mitochondrial gene copy number under spectinomycin treatment. Since these mutants, when grown on spectinomycin, behaved like the wild-type (Fig. 42), GUN2, 3 and 4 should not be involved in the signaling chain(s) from the plastid to mitochondrial gene levels.

Another possible origin of the signal might come from the carotenoid biosynthetic pathway. As it was previously shown, white leaves of *albostrians* barley contain only low amounts of carotenoids (Börner and Meister, 1980) and are unable to synthesize stress-induced ABA (Quarrie and Lister 1984) since a part of the biosynthetic pathway of ABA takes place in chloroplasts (Xiong and Zhu, 2003; Nambara and Marion-Poll, 2005). An interesting observation is that ABA down-regulates the expression of nuclear genes involved in mtDNA replication, recombination and transcription, as shown by the transcription profiles from Genevestigator (Hruz *et al.*, 2008) (Fig. 51 ) supporting the idea that low levels of ABA in plants with impaired chloroplast development might lead to enhanced amounts of mitochondrial DNA. It would, therefore, be worthwhile to check the effect of ABA-treatment during early seedling development in the presence of spectinomycin.

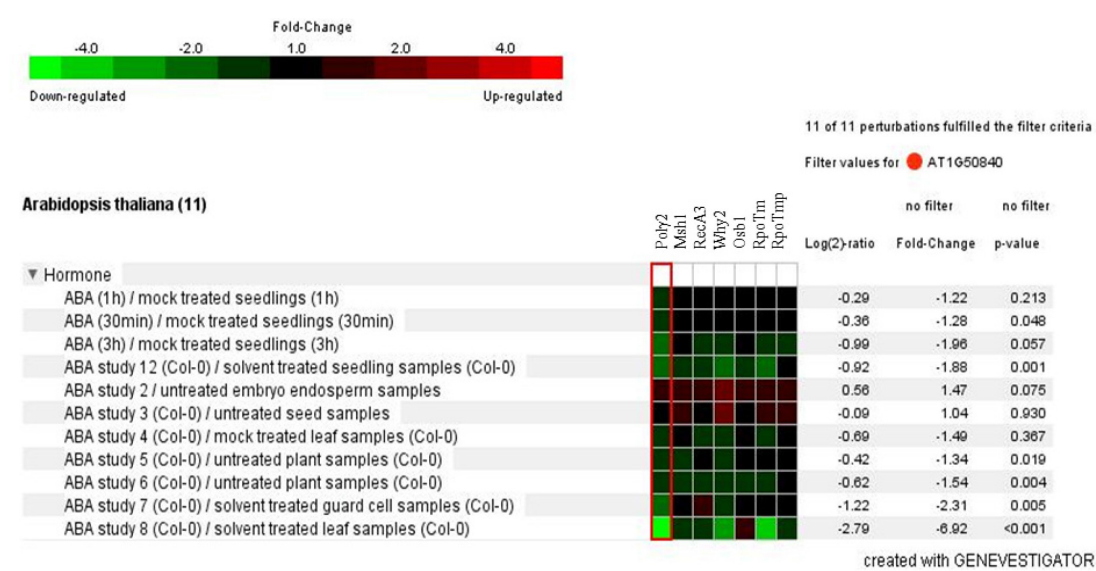


**Fig. 51** The influence of ABA on transcript level of *Poly2*, *Msh1*, *RecA3*, *Why2*, *Osh1*, *RpoTm* and *RpoTnp*. No probes could be found for *Poly1* in the 22k array.

A particularly interesting result was obtained by the investigation of the nuclear transcription factor ABI4 (ABA INSENSITIVE 4). ABI4 was shown to be a central player in many signaling processes during plant development acting both as a positive and negative regulator of gene transcription (León *et al.*, 2013). In the case of plastid retrograde signaling, ABI4 acts as a repressor, down-regulating the expression of multiple nuclear-encoded photosynthesis genes (Koussevitzky *et al.*, 2007). On the other side, ABI4 is also involved in mitochondrial retrograde signaling by inducing the expression of the nuclear-encoded alternative oxidase gene (AOX) in response to the inhibition of the electron transport chain by rotenone (Giraud *et al.*, 2009). In the present study, its potential role in regulating mitochondrial DNA abundance was investigated under the condition of spectinomycin treatment. A partial inhibition of the elevation of mitochondrial gene copy number could be observed in the *abi4* mutant pointing to a possible involvement of this transcription factor as a positive regulator (Fig. 42). ABI4 together with GUN1 were shown to integrate multiple retrograde signals originating in plastids (Koussevitzky *et al.*, 2007). However, in the particular experimental condition of spectinomycin treatment, GUN1 does obviously not play any role in determining mitochondrial gene copy number (Fig. 42).

Another possible signaling pathway that might be involved in regulating mitochondrial gene copy number in plants is ROS triggered signaling. ROS generated either by photo-oxidized plastids in white tissue or by the mitochondrial ETC in *mrpl11* or *ndufs4* respiration mutants, metabolite pool changes or sensible ATP



sensing mechanisms. However, to this point, there exists no clear evidence for the functionality of these pathways in regulating mitochondrial DNA abundance in plants.

#### **4.4.2 Transcriptional profile of nuclear genes involve in mitochondrial DNA replication, recombination and transcription**

As discussed above, impaired chloroplast development leads to elevated DNA levels in mitochondria. The early block in chloroplast development might be signaled either to the nucleus (being a variant of plastid-to-nucleus retrograde signaling) altering there the expression of genes needed for controlling mitochondrial DNA levels or to the mitochondria (being a chloroplast-to-mitochondrion signaling) changing there the activity of proteins involved in controlling mitochondrial DNA levels (both variants might be active at the same time as well).

It is easier to check the first variant. We investigated transcript levels on nuclear genes involved in DNA-related processes and in transcription in mitochondria. We found indeed elevated steady-state levels of these transcripts (*Poly2*, *Msh1*, *RecA3*, *Why2*, *Osb1*, *RpoTm* and *RpoTmp*) in spectinomycin-treated seedlings (Fig. 28) supporting the idea of plastid-to-nucleus signaling being involved in the enhancement of mitochondrial DNA amounts in white leaves.

To get further insight into the conditions that could determine modifications in mitochondrial gene abundance, the Genevestigator expression database (Hruz *et al.*, 2008) was used to evaluate the expression of selected nuclear genes in different organs and developmental stages, but also their response to different biotic and abiotic stress conditions.

The investigated genes (*Poly2*, *Msh1*, *RecA3*, *Why2*, *Osb1*, *RpoTm* and *RpoTmp*) had low expression levels in all investigated organs and also during different stages of plant development, with a small increase in callus and a significant upregulation during leaf senescence (Fig. 52 and 53). Surprisingly, the genes *RecA3*, *Why2* and *Osb1* that have the highest expression during leaf senescence (Fig. 53) are also highly expressed in white seedlings grown on spectinomycin (Fig. 28). It is thus possible that they represent the key components that regulate the mitochondrial gene copy number in plants, with other proteins having just a supporting role.

Evaluation of transcription profiles under different biotic and abiotic stress conditions revealed that the genes of interest have a generally low response. Significant (more than two-fold) changes are represented by a clear down-regulation upon treatment with *P. syringae* and the FLG22 elicitor and a strong up-regulation during callus formation from roots (Annex 7). Depending on the reference gene that was used for setting the two-fold threshold, the expression profiles vary in a small extent, with a clear tendency of co-regulation (Annex 7). However, it is important to remember that mtDNA amounts were not evaluated in respective experimental conditions, so for the moment a clear correlation between transcriptional changes and mtDNA amounts cannot be implied.

Until now it is not clear if there exist single signals originating from plastid/mitochondria that determine changes in nuclear gene expression or if there are multiple signals that can overlap. Moreover, it is interesting to observe the organ-specificity of the signaling pathways: while inhibition of plastid protein synthesis determined an elevation of mitochondrial DNA, this was not the case in roots, where this effect could not be observed (Fig. 40).



**Fig. 52** Transcription profiles of *Poly2*, *Msh1*, *RecA3*, *Why2*, *Osh1*, *RpoTm* and *RpoTnp* in different plant organs. No probes could be found for *Poly1* in the 22k array.

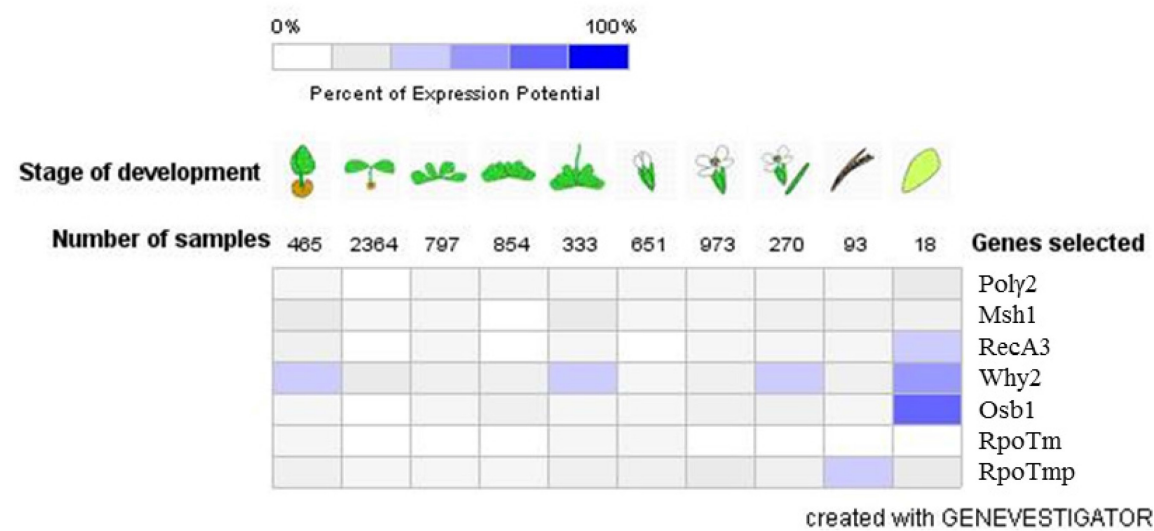


**Fig. 53** Transcription profiles of *Poly2*, *Msh1*, *RecA3*, *Why2*, *Osb1*, *RpoTm* and *RpoTnp* in different stages on plant development. No probes could be found for *Poly1* in the 22k array.

**4.5 The influence of impaired chloroplast development on mitochondrial dynamics**

Plant mitochondrial dynamics represents a novel field in plant research that focuses on the highly dynamic nature of mitochondria (Logan, 2006; 2010). It studies and discusses different characteristics of mitochondria as the fusion and fission events, number, size and shape, as well as their motility in the cytosol and their inheritance during cell division (Logan, 2010).

The complex dynamic nature of plant mitochondria can be influenced by the metabolic status of the cell. Plants grown in elevated CO<sub>2</sub> conditions have a 1.3 – 3 - fold increase in the number of mitochondria that show normal internal structure (Robertson *et al.*, 1995; Griffin *et al.*, 2001). Moreover, low oxygen pressure induces fast and reversible formation of giant mitochondria that have unusual shapes, length of ~ 80 µm and even form a reticulum (Van Gestel and Verbelen, 2002). Cold stress is another factor influencing mitochondrial abundance with 3-fold increase in cold developed leaves (Armstrong *et al.*, 2006). Cell death represents one of the best described metabolic conditions that influence mitochondrial dynamics. Treatment of *Arabidopsis* protoplasts or leaves with strong oxidants or heat shock determines changes in the inner membrane permeability and probably in the mitochondria-

cytoskeleton interactions that finally lead to an increase in size and arrest of motility (Yoshinaga *et al.*, 2005; Scott and Logan, 2008b; Zhang *et al.*, 2009). In other observations, senescent *Medicago truncatula* cell suspensions contained giant mitochondria that were associated with dying cells (Zottini *et al.*, 2006).

The present work is focused on another important aspect in mitochondrial dynamics that is represented by their interaction with the chloroplasts.

#### **4.5.1 Mitochondrial motility is arrested in white cotyledons of spectinomycin-treated seedlings, but not in roots**

As it was previously observed, green tissues possess mitochondria that are frequently associated with chloroplasts (Stickens and Verbelen, 1996; Logan and Leaver, 2000; Sheahan *et al.*, 2004). It is supposed that this proximity is needed in order to facilitate exchange of respiratory gases and metabolites between the two metabolically-interconnected organelles (Logan and Leaver, 2000). However, it is not clear yet if the observed association has a real function or if it is just the result of reduced cortical cytoplasm in highly vacuolated mesophyll cells, where the close association of the organelles is “a must” (Logan and Leaver, 2000).

Recently, a light-dependent intracellular positioning of mitochondria was observed in *Arabidopsis* mesophyll cells (Islam *et al.*, 2009). While in darkness mitochondria were randomly distributed, under weak blue light or strong blue light, they accumulated along the periclinal and anticlinal walls, respectively. This orientation was connected to the accumulation or avoidance response of the chloroplasts (Islam *et al.*, 2009). The light-dependent responses are reversible upon return to darkness (Islam and Takagi, 2010). In addition, mitochondrial motility was also evaluated in periclinal walls of the cells. Mostly fast-moving mitochondria were present after dark adaptation. Illumination with weak or strong blue light induced an increase in the number of static mitochondria that were located in close proximity to the chloroplasts (Islam *et al.*, 2009). Until now, it is not clear if the motility arrest is a result of the interaction with the chloroplasts (Islam *et al.*, 2009) or if it represents an independent process. Furthermore, the relocation effect of the mitochondria during accumulation and avoidance responses of the chloroplasts could be a result of common cytoskeletal associations (Logan, 2010).

The present work further evaluates the influence of chloroplasts on mitochondrial motility growing an *Arabidopsis* line with mitochondrial-targeted GFP (*mtGFP*; Logan and Leaver, 2000) was grown for 10 days on culture medium supplemented with 500 mg/L spectinomycin dihydrochlorid.

Until now, spectinomycin was commonly used as a selection marker for chloroplast transformation (Svab *et al.*, 1990) and in research on paternal transmission of plastid genome (Azhagiri and Maliga, 2007). It is believed that its activity is restricted to the interference with plastid translation, without other side-effects. However, so far the problem of mitochondrial motility has never been addressed in this context. In order to exclude any possible side-effect, a control experiment was performed by introducing spectinomycin resistance in the *mtGFP* line. The spectinomycin-resistant *RLD-Spc1* (Azhagiri and Maliga, 2007) mutant was crossed with *mtGFP* (Logan and Leaver, 2000). The *RLD-Spc1xmtGFP* double mutant has normal development under standard growth conditions (see Annex 5) and shows a green phenotype when grown on high concentrations on spectinomycin (Fig. 45). Investigation of mitochondrial size, shape, density and motility by confocal microscopy showed no difference between the *RLD-Spc1xmtGFP* control and spectinomycin-treated plants (Fig. 46, Video 12 and 13). This undoubtedly proves that high concentrations of spectinomycin do not have side-effects but act as expected via inhibition of plastid translation also on mitochondrial dynamics.

Taking into consideration the present result, mitochondrial dynamics was further evaluated in green and white, spectinomycin-treated seedlings that were grown on sucrose. Several cell types were investigated: adaxial epidermal cells, guard cells, mesophyll cells, vascular tissue and root cells. They represent both photosynthetic (guard cells, mesophyll cells) and non-photosynthetic (epidermal cells, vascular tissue and root cells) conditions and are useful for studying the interaction between mitochondria and plastids / chloroplast. Investigation of mitochondrial density by confocal microscopy in all cell types showed no difference between green and white seedlings (Fig. 29 and 30). However mitochondria in white tissue were distinctive by presenting a round shape and motility arrest in a highly variable proportion: while in some cotyledons 100% of the mitochondria were immotile, other cotyledons showed approximately 30% motility (evaluated by visual observation). Moreover, static mitochondria were not involved in fusion and fission events. Surprisingly, mitochondria from the root cells of the white seedlings had normal motility, pointing

to the conclusion that the observed effect is organ-specific but not tissue-specific. This observation is quite puzzling since some mitochondria are usually found to be associated with chloroplasts in photosynthetic tissue (Stickens and Verbelen, 1996; Logan and Leaver, 2000; Sheahan *et al.*, 2004) and an impaired chloroplast development should probably affect just the mitochondria in mesophyll and in guard cells. However, it seems not to be the case, epidermal cells and vascular tissue also being influenced. These results lead to the conclusion that impaired chloroplast development leading to a white phenotype produces a metabolic condition that is specific for cotyledons, present in all cell types and induces mitochondrial motility arrest. Remarkably, also the elevated mitochondrial gene copy numbers were observed only in cotyledons and leaves (although we could not analyse different leaf/cotyledon tissues).

#### **4.5.2 Possible reasons for motility arrest in white cotyledon**

Taking into consideration the present results and the existing literature we propose different hypothesis for mitochondrial motility arrest in white cotyledons.

##### **4.5.2.1 Mitochondria are not functional or have impaired functions**

Non-motile mitochondria may not be functional. The hypothesis of nonfunctional mitochondria in white cotyledons of spectinomycin-treated seedlings is proved to be wrong by the present work. At first, white cotyledons contain the same number of mitochondria with normal size and internal structure, as the green ones (Fig. 29-31). Secondly, normal respiratory activities are present as determined by oxygen consumption measurements and ATP / ADP ratio (Fig. 32).

Evaluation of respiration in the barley *albostrians* mutant have also shown identical activities in both green and white leaves (Hedtke *et al.*, 1999). In contrast, the white tissue of variegated ornamental plants presented a generally lower dark respiration (Toshoji *et al.*, 2011). This result could be explained by the fact that ornamental plants were grown in soil and the white regions probably have limiting

amounts of substrate. This was not the case for the spectinomycin-treated seedlings that were grown on MS medium containing 1% sucrose (Fig. 25).

#### 4.5.2.2 Low ATP levels as a result of the absence of photosynthesis

In plants, mitochondria move predominantly on the actin cytoskeleton (Simon *et al.*, 1995; Olyslaegers and Verbelen, 1998; Van Gestel *et al.*, 2002; Sheahan *et al.*, 2004) with microtubules playing just a role in maintaining the geometry of the cytoskeleton (Zheng *et al.*, 2009). Myosins are the motor proteins that propel mitochondria along the actin fibers by converting chemical energy from ATP hydrolysis into physical movement. Until now, from the 17 members of the myosin gene family that are present in *Arabidopsis*, four have been shown to be involved in movement of mitochondria: XI-C, XI-E, XI-I and XI-K (Avisar *et al.*, 2008; Sparkes *et al.*, 2008; Avisar *et al.*, 2009). Except from the myosin-motor dependent mechanism, mitochondria were shown to move also on a myosin-motor independent mechanism in which the rate of actin turnover plays an important role (Zheng *et al.*, 2009). Thus, the motility of mitochondria needs energy.

Consequently, another hypothesis that could explain cessation of mitochondrial movement in white cotyledons would be low ATP levels in mitochondria of white leaves. Depletion of ATP levels in elongating cultured cells of tobacco by treatment with the uncoupling agent 2,4-dinitrophenol (DNP) resulted in immobile mitochondria (Van Gestel *et al.*, 2002). Therefore, ATP measurements were performed in both green and white cotyledons. However, same ATP levels were detected under both conditions, leading to the conclusion that motility arrest is not a result of low ATP levels in white cells (Fig. 32). We should note, however, that we have determined ATP levels in whole cotyledons, not in isolated mitochondria.

#### 4.5.2.3 Oxidative stress

Plant mitochondrial dynamics can be influenced by the metabolic status of the cell (see 1.3.4) with cell death being the best described condition that has effects on mitochondrial size, shape and motility. Cell death induction by treatment of

*Arabidopsis* leaves with ROS ( $H_2O_2$ ) or ROS-inducing chemicals (paraquat, menadione) resulted in morphological changes from bacillus-like to round shape together with motility arrest. At a later time point mitochondria swelled (Yoshinaga *et al.*, 2005). In other report, methyl viologen, s-triazine and hydrogen peroxide treatment of *Arabidopsis* leaves and protoplasts induced swelling of mitochondria (Scott and Logan, 2008b). The same effect was present after heat treatment (Scott and Logan, 2008b; Zhang *et al.*, 2009). Moreover, UV-C overexposure generated clumping of mitochondria around chloroplasts or in other parts of the cytoplasm, concomitantly with arrest of mitochondrial motility (Gao *et al.*, 2008). In other observations, senescent *Medicago truncatula* cell suspensions contained immotile giant mitochondria that were associated with dying cells (Zottini *et al.*, 2006).

From the existing literature, it is clear that ROS, physical stress or senescence induce the formation of abnormal, swollen mitochondria, a process termed “mitochondrial morphology transition” (Scott and Logan, 2008b). This transition precedes cell death with several hours and is considered to be an early and specific indicator of subsequent cell death (Scott and Logan, 2008b). Moreover, the arrest of mitochondrial motility is a concomitant effect, that is probably a result of changed mitochondrial - cytoskeleton interactions (Yoshinaga *et al.*, 2005; Zottini *et al.*, 2006; Gao *et al.*, 2008; Zhang *et al.*, 2009).

The previous work on cell death induction might help us to explain the motility arrest in white, spectinomycin-treated cotyledons. While mitochondrial motility arrest was shown to be connected to ROS production during cell death induction (Yoshinaga *et al.*, 2005) we propose that ROS might also be involved in mitochondrial motility arrest in white, spectinomycin-treated cotyledons. The work of Yoshinaga *et al.* (2005) shows that in the early stages of ROS stress, mitochondria showed morphological changes from bacillus-like to a round shape together with motility arrest (Yoshinaga *et al.*, 2005). A similar situation is present in the epidermal cells of white cotyledons, where most mitochondria were round and immotile. In favor of this supposition comes the observation that mitochondrial motility is still present in the roots of the white seedlings, as well as in etiolated cotyledons, a photo-oxidation process probably being present in cotyledons. TEM evaluation of cotyledon cross-sections revealed proplastid-like structures that are characterized by a high amount of plastoglobulin-type structures and only a few thylakoids (Fig. 31). However, it is currently unknown if ROS stress exists in white cotyledons.



The observed mitochondrial motility arrest in white leaves opens the door to many unanswered questions and possible future experiments. It would be interesting to know if partial motility arrest represents a general phenomenon in white leaves or if it depends on light conditions. In case oxidative stress is a key factor in this process, it is possible that white mutant grown under low light conditions contain normal, motile mitochondria. For this, investigation of other white mutants, as well as variegated mutants is necessary.

Our current working model would be that an early and severe block in chloroplast development slows down the motility of mitochondria thus reducing the possibility of their fusion and fission. However, fusion is essential for the exchange of gene products, as the individual plant mitochondria do not possess enough DNA to represent complete genomes. To overcome this situation, the block in chloroplast development is signaled to the nucleus (variant of plastid-to-nucleus signaling involving ABI4, but not GUN1, 2, 4, and 5) and stimulates there the expression of genes needed for DNA replication, recombination and transcription (the same signaling chain might alter the expression of genes needed for motility). As a consequence, DNA levels are enhanced within the individual mitochondria in leaf/cotyledon tissues. The DNA levels are high enough to allow (possibly combined with a very low rate of fusion and fission) for the expression of all genes within individual organelles.

## References

- Abdelnoor, R.V., Yule, R., Elo, A., Christensen, A.C., Meyer-Gauen, G. and Mackenzie, S.A.** (2003) Substoichiometric shifting in the plant mitochondrial genome is influenced by a gene homologous to MutS. *PNAS*, **100**, 5968-5973.
- Adamska, I.** (1995) Regulation of Early Light-Inducible Protein Gene Expression by Blue and Red Light in Etiolated Seedlings Involves Nuclear and Plastid Factors. *Plant Physiol*, **107**, 1167-1175.
- Aguettaz, P., Seyer, P., Pesey, H. and Lescure, A.-M.** (1987) Relations between the plastid gene dosage and the levels of 16S rRNA and *rbcL* gene transcripts during amyloplast to chloroplast change in mixotrophic spinach cell suspensions. *Plant Mol. Biol.*, **8**, 169-177.
- Allen, J.F.** (2005) Photosynthesis: the processing of redox signals in chloroplasts. *Curr Biol*, **15**, R929-932.
- Altschul, S.F., Gish, W., Miller, W., Myers, E.W. and Lipman, D.J.** (1990) Basic local alignment search tool. *J Mol Biol*, **215**, 403-410.
- Altschul, S.F., Madden, T.L., Schaffer, A.A., Zhang, J., Zhang, Z., Miller, W. and Lipman, D.J.** (1997) Gapped BLAST and PSI-BLAST: a new generation of protein database search programs. *Nucleic Acids Res*, **25**, 3389-3402.
- Alverson, A.J., Wei, X., Rice, D.W., Stern, D.B., Barry, K. and Palmer, J.D.** (2010) Insights into the evolution of mitochondrial genome size from complete sequences of *Citrullus lanatus* and *Cucurbita pepo* (Cucurbitaceae). *Mol Biol Evol*, **27**, 1436-1448.
- Anderson, S., Bankier, A.T., Barrell, B.G., de Bruijn, M.H., Coulson, A.R., Drouin, J., Eperon, I.C., Nierlich, D.P., Roe, B.A., Sanger, F., Schreier, P.H., Smith, A.J., Staden, R. and Young, I.G.** (1981) Sequence and organization of the human mitochondrial genome. *Nature*, **290**, 457-465.
- Ankele, E., Kindgren, P., Pesquet, E. and Strand, A.** (2007) *In vivo* visualization of Mg-ProtoporphyrinIX, a coordinator of photosynthetic gene expression in the nucleus and the chloroplast. *Plant Cell*, **19**, 1964-1979.
- Apel, K. and Hirt, H.** (2004) Reactive oxygen species: metabolism, oxidative stress, and signal transduction. *Annual Review of Plant Biology*, **55**, 373-399.
- Archibald, J.M. and Richards, T.A.** (2010) Gene transfer: anything goes in plant mitochondria. *BMC Biol*, **8**, 147.
- Arimura, S. and Tsutsumi, N.** (2002) A dynamin-like protein (ADL2b), rather than FtsZ, is involved in *Arabidopsis* mitochondrial division. *Proc Natl Acad Sci U S A*, **99**, 5727-5731.

- Arimura, S., Aida, G.P., Fujimoto, M., Nakazono, M. and Tsutsumi, N.** (2004a) *Arabidopsis* dynamin-like protein 2a (ADL2a), like ADL2b, is involved in plant mitochondrial division. *Plant Cell Physiol*, **45**, 236-242.
- Arimura, S., Yamamoto, J., Aida, G.P., Nakazono, M. and Tsutsumi, N.** (2004b) Frequent fusion and fission of plant mitochondria with unequal nucleoid distribution. *Proc Natl Acad Sci U S A*, **101**, 7805-7808.
- Arimura, S., Fujimoto, M., Doniwa, Y., Kadoya, N., Nakazono, M., Sakamoto, W. and Tsutsumi, N.** (2008) *Arabidopsis* ELONGATED MITOCHONDRIAL 1 is required for localization of DYNAMIN-RELATED PROTEIN3A to mitochondrial fission sites. *Plant Cell*, **20**, 1555-1566.
- Armstrong, A.F., Logan, D.C., Tobin, A.K., O'Toole, P. and Atkin, O.K.** (2006) Heterogeneity of plant mitochondrial responses underpinning respiratory acclimation to the cold in *Arabidopsis thaliana* leaves. *Plant Cell Environ*, **29**, 940-949.
- Arrieta-Montiel, M., Lyznik, A., Woloszynska, M., Janska, H., Tohme, J. and Mackenzie, S.** (2001) Tracing evolutionary and developmental implications of mitochondrial stoichiometric shifting in the common bean. *Genetics*, **158**, 851-864.
- Arrieta-Montiel, M.P., Shedge, V., Davila, J., Christensen, A.C. and Mackenzie, S.A.** (2009) Diversity of the *Arabidopsis* mitochondrial genome occurs via nuclear-controlled recombination activity. *Genetics*, **183**, 1261-1268.
- Arrieta-Montiel, M.P. and Mackenzie, S.A.** (2011) Plant mitochondrial genomes and recombination. In *Plant mitochondria*, Vol. 1 (Kempken, F., ed.: Springer New York, pp. 65-82.
- Avisar, D., Prokhnevsky, A.I., Makarova, K.S., Koonin, E.V. and Dolja, V.V.** (2008) Myosin XI-K Is required for rapid trafficking of Golgi stacks, peroxisomes, and mitochondria in leaf cells of *Nicotiana benthamiana*. *Plant Physiol*, **146**, 1098-1108.
- Avisar, D., Abu-Abied, M., Belausov, E., Sadot, E., Hawes, C. and Sparkes, I.A.** (2009) A comparative study of the involvement of 17 *Arabidopsis* myosin family members on the motility of Golgi and other organelles. *Plant Physiol*, **150**, 700-709.
- Azevedo, J., Courtois, F. and Lerbs-Mache, S.** (2006) Sub-plastidial localization of two different phage-type RNA polymerases in spinach chloroplasts. *Nucleic Acids Research*, **34**, 436-444.
- Azhagiri, A.K. and Maliga, P.** (2007) Exceptional paternal inheritance of plastids in *Arabidopsis* suggests that low-frequency leakage of plastids via pollen may be universal in plants. *Plant J*, **52**, 817-823.
- Backert, S., Nielsen, B. and Börner, T.** (1997) The mystery of the rings: structure and replication of mitochondrial genomes from higher plants. *Trends in Plant Science*, **2**, 477-483.

**Backert, S. and Börner, T.** (2000) Phage T4-like intermediates of DNA replication and recombination in the mitochondria of the higher plant *Chenopodium album* (L.). *Current Genetics*, **37**, 304-314.

**Baker, A., Graham, I.A., Holdsworth, M., Smith, S.M. and Theodoulou, F.L.** (2006) Chewing the fat: beta-oxidation in signalling and development. *Trends Plant Sci*, **11**, 124-132.

**Ballesteros, I., Linacero, R. and Vázquez, A.M.** (2009) Mitochondrial DNA amplification in albino plants of rye (*Secale cereale* L.) regenerated in vitro. *Plant Science*, **176**, 722-728.

**Barow, M. and Meister, A.** (2003) Endopolyploidy in seed plants is differently correlated to systematics, organ, life strategy and genome size. *Plant, Cell & Environment*, **26**, 571-584.

**Barow, M.** (2006) Endopolyploidy in seed plants. *BioEssays*, **28**, 271-281.

**Barow, M. and Jovtchev, G.** (2007) Endopolyploidy in plants and its analysis by flow cytometry. In *Flow Cytometry with Plant Cells* (Doležel, J., Greilhuber, J. and Suda, J., eds). Weinheim: Wiley-VCH Verlag, pp. 349-372.

**Barsan, C., Sanchez-Bel, P., Rombaldi, C., Egea, I., Rossignol, M., Kuntz, M., Zouine, M., Latché, A., Bouzayen, M. and Pech, J.-C.** (2010) Characteristics of the tomato chromoplast revealed by proteomic analysis. *Journal of Experimental Botany*, **61**, 2413-2431.

**Bartoli, C.G., Pastori, G.M. and Foyer, C.H.** (2000) Ascorbate biosynthesis in mitochondria is linked to the electron transport chain between complexes III and IV. *Plant Physiol*, **123**, 335-344.

**Basu, U., Good, A.G. and Taylor, G.J.** (2001) Transgenic *Brassica napus* plants overexpressing aluminium-induced mitochondrial manganese superoxide dismutase cDNA are resistant to aluminium. *Plant, Cell & Environment*, **24**, 1278-1269.

**Baumgartner, B.J., Rapp, J.C. and Mullet, J.E.** (1989) Plastid transcription activity and DNA copy number increase early in barley chloroplast development *Plant Physiology*, **89**, 1011-1018.

**Bendich, A.J. and Gauriloff, L.P.** (1984) Morphometric analysis of cucurbit mitochondria: the relationship between chondriome volume and DNA content. *Protoplasma*, **119**, 1-7.

**Bendich, A.J. and Smith, S.B.** (1990) Moving pictures and pulsed-field gel electrophoresis show linear DNA molecules from chloroplasts and mitochondria. *Current Genetics*, **17**, 421-425.

**Bendich, A.J.** (1996) Structural analysis of mitochondrial DNA molecules from fungi and plants using moving pictures and pulsed-field gel electrophoresis. *Journal of Molecular Biology*, **255**, 564-588.

- Bendich, A.J.** (2004) Circular chloroplast chromosomes: the grand illusion. *Plant Cell*, **16**, 1661-1666.
- Bereiter-Hahn, J. and Voth, M.** (1994) Dynamics of mitochondria in living cells: shape changes, dislocations, fusion, and fission of mitochondria. *Microsc Res Tech*, **27**, 198-219.
- Binder, S., Marchfelder, A. and Brennicke, A.** (1996) Regulation of gene expression in plant mitochondria. *Plant Molecular Biology*, **32**, 303-314.
- Binder, S., Hölzle, A. and Jonietz, C.** (2011) RNA processing and RNA stability in plant mitochondria. In *Plant mitochondria*, Vol. 1 (Kempken, F., ed.: Springer New York, pp. 107-130.
- Bock, R., Kössel, H. and Maliga, P.** (1994) Introduction of a heterologous editing site into the tobacco plastid genome: the lack of RNA editing leads to a mutant phenotype. *EMBO Journal*, **13**, 4623-4628.
- Bock, R. and Timmis, J.N.** (2008) Reconstructing evolution: gene transfer from plastids to the nucleus. *Bioessays*, **30**, 556-566.
- Boldogh, I.R. and Pon, L.A.** (2007) Mitochondria on the move. *Trends Cell Biol*, **17**, 502-510.
- Bonardi, V., Pesaresi, P., Becker, T., Schleiff, E., Wagner, R., Pfannschmidt, T., Jahns, P. and Leister, D.** (2005) Photosystem II core phosphorylation and photosynthetic acclimation require two different protein kinases. *Nature*, **437**, 1179-1182.
- Bonen, L.** (2011) RNA splicing in plant mitochondria. In *Plant mitochondria*, Vol. 1 (Kempken, F., ed.: Springer New York, pp. 131-155.
- Bradbeer, J.W., Atkinson, Y.E., Börner, T. and Hagemann, R.** (1979) Cytoplasmic synthesis of plastid polypeptides may be controlled by plastid-synthesized RNA. *Nature*, **279**, 816-817.
- Bradford, M.M.** (1976) A rapid and sensitive method for the quantitation of microgram quantities of protein utilizing the principle of protein-dye binding. *Anal Biochem*, **72**, 248-254.
- Bramley, P.M.** (2002) Regulation of carotenoid formation during tomato fruit ripening and development. *J Exp Bot*, **53**, 2107-2113.
- Breidenbach, R.W., Castelfranco, P. and Peterson, C.** (1966) Biogenesis of mitochondria in germinating peanut cotyledons. *Plant Physiol*, **41**, 803-809.
- Breidenbach, R.W., Castelfranco, P. and Criddle, R.S.** (1967) Biogenesis of mitochondria in germinating peanut cotyledons II. Changes in cytochromes and mitochondrial DNA. *Plant Physiol*, **42**, 1035-1041.

- Bruhs, A. and Kempken, F.** (2011) RNA editing in higher plant mitochondria. In *Plant mitochondria*, Vol. 1 (Kempken, F., ed.: Springer New York, pp. 157-175.
- Buchanan, B.B., Schurmann, P. and Jacquot, J.P.** (1994) Thioredoxin and metabolic regulation. *Semin Cell Biol*, **5**, 285-293.
- Burger, G., Gray, M.W., Forget, L. and Lang, B.F.** (2013) Strikingly bacteria-like and gene-rich mitochondrial genomes throughout Jakobid protists. *Genome Biology and Evolution*, **5**, 418-438.
- Butow, R.A. and Avadhani, N.G.** (2004) Mitochondrial signaling: the retrograde response. *Mol Cell*, **14**, 1-15.
- Chang, C.-C., Sheen, J., Bligny, M., Niwa, Y., Lerbs-Mache, S. and Stern, D.B.** (1999) Functional analysis of two maize cDNAs encoding T7-like RNA polymerases. *Plant Cell*, **11**, 911-926.
- Chory, J., Chatterjee, M., Cook, R.K., Elich, T., Fankhauser, C., Li, J., Nagpal, P., Neff, M., Pepper, A., Poole, D., Reed, J. and Vitart, V.** (1996) From seed germination to flowering, light controls plant development via the pigment phytochrome. *Proc Natl Acad Sci U S A*, **93**, 12066-12071.
- Christensen, A.C., Lyznik, A., Mohammed, S., Elowsky, C.G., Elo, A., Yule, R. and Mackenzie, S.A.** (2005) Dual-domain, dual-targeting organellar protein presequences in *Arabidopsis* can use non-AUG start codons. *Plant Cell*, **17**, 2805-2816.
- Clay Montier, L.L., Deng, J.J. and Bai, Y.** (2009) Number matters: control of mammalian mitochondrial DNA copy number. *Journal of Genetics and Genomics*, **36**, 125-131.
- Clifton, S.W., Minx, P., Fauron, C.M.-R., Gibson, M., Allen, J.O., Sun, H., Thompson, M., Barbazuk, W.B., Kanuganti, S., Tayloe, C., Meyer, L., Wilson, R.K. and Newton, K.J.** (2004) Sequence and Comparative Analysis of the Maize NB Mitochondrial Genome. *Plant Physiol.*, **136**, 3486-3503.
- Cran, D.G. and Possingham, J.V.** (1972) Variation of plastid types in spinach. *Protoplasma*, **74**, 345-356.
- Curtis, M.J. and Wolpert, T.J.** (2002) The oat mitochondrial permeability transition and its implication in victorin binding and induced cell death. *Plant J*, **29**, 295-312.
- Dai, H., Lo, Y.-S., Litvinchuk, A., Wang, Y.-T., Jane, W.-N., Hsiao, L.-J. and Chiang, K.-S.** (2005) Structural and functional characterizations of mung bean mitochondrial nucleoids. *Nucl. Acids Res.*, **33**, 4725-4739.
- Davison, P.A., Schubert, H.L., Reid, J.D., Iorg, C.D., Heroux, A., Hill, C.P. and Hunter, C.N.** (2005) Structural and Biochemical Characterization of Gun4 Suggests a Mechanism for Its Role in Chlorophyll Biosynthesis. *Biochemistry*, **44**, 7603-7612.

- Davletova, S., Schlauch, K., Coutu, J. and Mittler, R.** (2005) The zinc-finger protein Zat12 plays a central role in reactive oxygen and abiotic stress signaling in *Arabidopsis*. *Plant Physiol*, **139**, 847-856.
- De Santis-Maciossek, G., Kofer, W., Bock, A., Schoch, S., Maier, R.M., Wanner, G., Rüdiger, W., Koop, H.-U. and Herrmann, R.G.** (1999) Targeted disruption of the plastid RNA polymerase genes *rpoA*, *B* and *C1*: molecular biology, biochemistry and ultrastructure. *The Plant Journal*, **18**, 477-489.
- Delwiche, C.F.** (1999) Tracing the Thread of Plastid Diversity through the Tapestry of Life. *Am Nat*, **154**, S164-S177.
- Desveaux, D., Marechal, A. and Brisson, N.** (2005) Whirly transcription factors: defense gene regulation and beyond. *Trends Plant Sci*, **10**, 95-102.
- Douce, R. and Neuburger, M.** (1999) Biochemical dissection of photorespiration. *Curr Opin Plant Biol*, **2**, 214-222.
- Douglas, S.E. and Turner, S.** (1991) Molecular evidence for the origin of plastids from a cyanobacterium-like ancestor. *J Mol Evol*, **33**, 267-273.
- Dutilleul, C., Garmier, M., Noctor, G., Mathieu, C., Chetrit, P., Foyer, C.H. and de Paepe, R.** (2003) Leaf mitochondria modulate whole cell redox homeostasis, set antioxidant capacity, and determine stress resistance through altered signaling and diurnal regulation. *Plant Cell*, **15**, 1212-1226.
- Dyall, S.D., Brown, M.T. and Johnson, P.J.** (2004) Ancient invasions: from endosymbionts to organelles. *Science*, **304**, 253-257.
- Egea, I., Barsan, C., Bian, W., Purgatto, E., Latche, A., Chervin, C., Bouzayen, M. and Pech, J.C.** (2010) Chromoplast differentiation: current status and perspectives. *Plant Cell Physiol*, **51**, 1601-1611.
- Elo, A., Lyznik, A., Gonzalez, D.O., Kachman, S.D. and Mackenzie, S.A.** (2003) Nuclear genes that encode mitochondrial proteins for DNA and RNA metabolism are clustered in the *Arabidopsis* genome. *Plant Cell*, **15**, 1619-1631.
- Emanuel, C., Weihe, A., Graner, A., Hess, W.R. and Börner, T.** (2004) Chloroplast development affects expression of phage-type RNA polymerases in barley leaves. *Plant Journal*, **38**, 460-472.
- Emanuel, C., von Groll, U., Müller, M., Börner, T. and Weihe, A.** (2006) Development- and tissue-specific expression of the *RpoT* gene family of *Arabidopsis* encoding mitochondrial and plastid RNA polymerases. *Planta*, **223**, 998-1009.
- Fauron, C., Casper, M., Gao, Y. and Moore, B.** (1995) The maize mitochondrial genome: dynamic, yet functional. *Trends Genet*, **11**, 228-235.

- Fey, J. and Maréchal-Drouard, L.** (1999) Compilation and analysis of plant mitochondrial promoter sequences: an illustration of a divergent evolution between monocot and dicot mitochondria. *Biochemical and Biophysical Research Communications*, **256**, 409-414.
- Fey, J., Vermel, M., Grienberger, J., Maréchal-Drouard, L. and Gualberto, J.M.** (1999) Characterization of a plant mitochondrial active chromosome. *Febs Letters*, **458**, 124-128.
- Fey, V., Wagner, R., Bräutigam, K. and Pfannschmidt, T.** (2005) Photosynthetic redox control of nuclear gene expression. *Journal of Experimental Botany*, **56**, 1491-1498.
- Foyer, C.H. and Noctor, G.** (2005) Redox homeostasis and antioxidant signaling: a metabolic interface between stress perception and physiological responses. *Plant Cell*, **17**, 1866-1875.
- Fujie, M., Kuroiwa, H., Kawano, S. and Kuroiwa, T.** (1993) Studies on the behavior of organelles and their nucleoids in the root apical meristem of *Arabidopsis thaliana* (L.) Col. *Planta*, **189**, 443-452.
- Fujie, M., Kuroiwa, H., Kawano, S., Mutoh, S. and Kuroiwa, T.** (1994) Behavior of organelles and their nucleoids in the shoot apical meristem during leaf development in *Arabidopsis thaliana* L. *Planta*, **194**, 395-405.
- Gadjev, I., Vanderauwera, S., Gechev, T.S., Laloi, C., Minkov, I.N., Shulaev, V., Apel, K., Inze, D., Mittler, R. and Van Breusegem, F.** (2006) Transcriptomic footprints disclose specificity of reactive oxygen species signaling in *Arabidopsis*. *Plant Physiol*, **141**, 436-445.
- Galbraith, D.W., Harkins, K.R. and Knapp, S.** (1991) Systemic Endopolyploidy in *Arabidopsis thaliana*. *Plant Physiol*, **96**, 985-989.
- Gao, C., Xing, D., Li, L. and Zhang, L.** (2008) Implication of reactive oxygen species and mitochondrial dysfunction in the early stages of plant programmed cell death induced by ultraviolet-C overexposure. *Planta*, **227**, 755-767.
- Geigenberger, P.** (2003) Response of plant metabolism to too little oxygen. *Curr Opin Plant Biol*, **6**, 247-256.
- Giegé, P., Sweetlove, L.J., Cognat, V. and Leaver, C.J.** (2005) Coordination of nuclear and mitochondrial genome expression during mitochondrial biogenesis in *Arabidopsis*. *Plant Cell*, **17**, 1497-1512.
- Giraud, E., Van Aken, O., Ho, L.H. and Whelan, J.** (2009) The transcription factor ABI4 is a regulator of mitochondrial retrograde expression of ALTERNATIVE OXIDASE1a. *Plant Physiol*, **150**, 1286-1296.



- Gissi, C., Iannelli, F. and Pesole, G.** (2008) Evolution of the mitochondrial genome of Metazoa as exemplified by comparison of congeneric species. *Heredity (Edinb)*, **101**, 301-320.
- Gould, S.B., Waller, R.F. and McFadden, G.I.** (2008) Plastid Evolution. *Annual Review of Plant Biology*, **59**.
- Gray, J.C., Sullivan, J.A., Wang, J.H., Jerome, C.A. and MacLean, D.** (2003) Coordination of plastid and nuclear gene expression. *Philos Trans R Soc Lond B Biol Sci*, **358**, 135-144; discussion 144-135.
- Gray, M.W.** (1992) The endosymbiont hypothesis revisited. *Int Rev Cytol*, **141**, 233-357.
- Gray, M.W., Burger, G. and Lang, B.F.** (1999) Mitochondrial evolution. *Science*, **283**, 1476-1481.
- Griffin, K.L., Anderson, O.R., Gastrich, M.D., Lewis, J.D., Lin, G., Schuster, W., Seemann, J.R., Tissue, D.T., Turnbull, M.H. and Whitehead, D.** (2001) Plant growth in elevated CO<sub>2</sub> alters mitochondrial number and chloroplast fine structure. *Proc Natl Acad Sci U S A*, **98**, 2473-2478.
- Gueguen, V., Macherel, D., Jaquinod, M., Douce, R. and Bourguignon, J.** (2000) Fatty acid and lipoic acid biosynthesis in higher plant mitochondria. *J Biol Chem*, **275**, 5016-5025.
- Gutierrez, S., Sabar, M., Lelandais, C., Chetrit, P., Diolez, P., Degand, H., Boutry, M., Vedel, F., de Kouchkovsky, Y. and De Paepe, R.** (1997) Lack of mitochondrial and nuclear-encoded subunits of complex I and alteration of the respiratory chain in *Nicotiana sylvestris* mitochondrial deletion mutants. *Proc Natl Acad Sci U S A*, **94**, 3436-3441.
- Gutierrez, C.** (2009) The *Arabidopsis* cell division cycle. *Arabidopsis Book*, **7**, e0120.
- Hagemann, R. and Scholz, F.** (1962) Ein Fall geninduzierter Mutationen des Plasmotypus bei Gerste. *Der Züchter*, **32**, 50-59.
- Hagemann, R.** (2004) The sexual inheritance of plant organelles. In *Molecular Biology and Biotechnology of Plant Organelles* (Daniell, H. and Chase, C.D., eds). Dordrecht: Springer, pp. 93-113.
- Hagemann, R.** (2010) The foundation of extranuclear inheritance: plastid and mitochondrial genetics. *Molecular Genetics and Genomics*, **283**, 199-209.
- Hager, M., Biehler, K., Illerhaus, J., Ruf, S. and Bock, R.** (1999) Targeted inactivation of the smallest plastid genome-encoded open reading frame reveals a novel and essential subunit of the cytochrome b(6)f complex. *EMBO J*, **18**, 5834-5842.

- Hager, M., Hermann, M., Biehler, K., Krieger-Liszkay, A. and Bock, R.** (2002) Lack of the small plastid-encoded PsbJ polypeptide results in a defective water-splitting apparatus of photosystem II, reduced photosystem I levels, and hypersensitivity to light. *J Biol Chem*, **277**, 14031-14039.
- Hajdukiewicz, P.T.J., Allison, L.A. and Maliga, P.** (1997) The two RNA polymerases encoded by the nuclear and the plastid compartments transcribe distinct groups of genes in tobacco plastids. *EMBO Journal*, **16**, 4041-4048.
- Handa, H.** (2003) The complete nucleotide sequence and RNA editing content of the mitochondrial genome of rapeseed (*Brassica napus* L.): comparative analysis of the mitochondrial genomes of rapeseed and *Arabidopsis thaliana*. *Nucl. Acids. Res.*, **31**, 5907-5916.
- Hazkani-Covo, E., Zeller, R.M. and Martin, W.** (2010) Molecular Poltergeists: mitochondrial DNA copies (numts) in sequenced nuclear genomes. *PLoS Genetics*, **6**, e1000834.
- Hedges, S.B., Blair, J.E., Venturi, M.L. and Shoe, J.L.** (2004) A molecular timescale of eukaryote evolution and the rise of complex multicellular life. *BMC Evol Biol*, **4**, 2.
- Hedtke, B., Wagner, I., Borner, T. and Hess, W.R.** (1999) Inter-organellar crosstalk in higher plants: impaired chloroplast development affects mitochondrial gene and transcript levels. *Plant J*, **19**, 635-643.
- Heinhorst, S., Cannon, G.C. and Weissbach, A.** (1990) Chloroplast and mitochondrial DNA polymerases from cultured soybean cells. *Plant Physiol*, **92**, 939-945.
- Hermann, G.J. and Shaw, J.M.** (1998) Mitochondrial dynamics in yeast. *Annu Rev Cell Dev Biol*, **14**, 265-303.
- Hess, W., Schendel, R., R  diger, W., Fieder, B. and B  rner, T.** (1992) Components of chlorophyll biosynthesis in a barley albina mutant unable to synthesize  '-aminolevulinic acid by utilizing the transfer RNA for glutamic acid. *Planta*, **188**, 19-27.
- Hess, W.R., Muller, A., Nagy, F. and B  rner, T.** (1994) Ribosome-deficient plastids affect transcription of light-induced nuclear genes: genetic evidence for a plastid-derived signal. *Molecular & General Genetics*, **242**, 305-312.
- Hess, W.R. and B  rner, T.** (1999) Organellar RNA polymerases of higher plants. *International Review of Cytology*, **190**, 1-59.
- Himmelbach, A., Yang, Y. and Grill, E.** (2003) Relay and control of abscisic acid signaling. *Curr Opin Plant Biol*, **6**, 470-479.
- Ho, L.H.M., Giraud, E., Uggalla, V., Lister, R., Clifton, R., Glen, A., Thirkettle-Watts, D., Van Aken, O. and Whelan, J.** (2008) Identification of Regulatory

Pathways Controlling Gene Expression of Stress-Responsive Mitochondrial Proteins in Arabidopsis. *Plant Physiology*, **147**, 1858-1873.

**Hoffmeister, M. and Martin, W.** (2003) Interspecific evolution: microbial symbiosis, endosymbiosis and gene transfer. *Environ Microbiol*, **5**, 641-649.

**Hruz, T., Laule, O., Szabo, G., Wessendorp, F., Bleuler, S., Oertle, L., Widmayer, P., Gruissem, W. and Zimmermann, P.** (2008) Genevestigator V3: A Reference Expression Database for the Meta-Analysis of Transcriptomes. *Advances in Bioinformatics*, **2008**.

**Hübschmann, T. and Börner, T.** (1998) Characterisation of transcript initiation sites in ribosome-deficient barley plastids. *Plant Molecular Biology*, **36**, 493-496.

**Huertas, P.** (2010) DNA resection in eukaryotes: deciding how to fix the break. *Nat Struct Mol Biol*, **17**, 11-16.

**Inaba, T. and Ito-Inaba, Y.** (2010) Versatile roles of plastids in plant growth and development. *Plant Cell Physiol*, **51**, 1847-1853.

**Inaba, T., Yazu, F., Ito-Inaba, Y., Kakizaki, T. and Nakayama, K.** (2011) Retrograde signaling pathway from plastid to nucleus. In *International Review of Cell and Molecular Biology*, Vol. 290 (Kwang, W.J., ed. San Diego, CA, USA: Academic Press, Elsevier Inc., pp. 167-204.

**Ishizaki, K., Larson, T.R., Schauer, N., Fernie, A.R., Graham, I.A. and Leaver, C.J.** (2005) The critical role of *Arabidopsis* electron-transfer flavoprotein:ubiquinone oxidoreductase during dark-induced starvation. *Plant Cell*, **17**, 2587-2600.

**Islam, M.S., Niwa, Y. and Takagi, S.** (2009) Light-dependent intracellular positioning of mitochondria in *Arabidopsis thaliana* mesophyll cells. *Plant Cell Physiol*, **50**, 1032-1040.

**Islam, M.S. and Takagi, S.** (2010) Co-localization of mitochondria with chloroplasts is a light-dependent reversible response. *Plant Signal Behav*, **5**, 146-147.

**Isono, K., Niwa, Y., Satoh, K. and Kobayashi, H.** (1997) Evidence for transcriptional regulation of plastid photosynthesis genes in *Arabidopsis thaliana* roots. *Plant Physiology*, **114**, 623-630.

**Ivanov, B. and Khorobrykh, S.** (2003) Participation of photosynthetic electron transport in production and scavenging of reactive oxygen species. *Antioxid Redox Signal*, **5**, 43-53.

**Janska, H. and Woloszynska, M.** (1997) The dynamic nature of plant mitochondrial genome organization. *Acta Biochim Pol*, **44**, 239-250.

**Janska, H., Sarria, R., Woloszynska, M., Arrieta-Montiel, M. and Mackenzie, S.** (1998) Stoichiometric shifts in the common bean mitochondrial genome leading to

male sterility and spontaneous reversion to fertility. *THE PLANT CELL*, **10**, 1163-1180.

**Jones, A.** (2000) Does the plant mitochondrion integrate cellular stress and regulate programmed cell death? *Trends Plant Sci*, **5**, 225-230.

**Journet, E.P., Bligny, R. and Douce, R.** (1986) Biochemical changes during sucrose deprivation in higher plant cells. *Journal of Biological Chemistry*, **261**, 3193-3199.

**Kanazawa, A.** (1998) Multiple changes in tobacco mitochondrial DNA populations during tissue culture. *Plant Breeding*, **117**, 469-472.

**Kaneko, T., Sato, S., Kotani, H., Tanaka, A., Asamizu, E., Nakamura, Y., Miyajima, N., Hirosawa, M., Sugiura, M., Sasamoto, S., Kimura, T., Hosouchi, T., Matsuno, A., Muraki, A., Nakazaki, N., Naruo, K., Okumura, S., Shimpo, S., Takeuchi, C., Wada, T., Watanabe, A., Yamada, M., Yasuda, M. and Tabata, S.** (1996) Sequence analysis of the genome of the unicellular cyanobacterium *Synechocystis* sp. Strain PCC6803. II. sequence determination of the entire genome and assignment of potential protein-coding regions. *DNA Res*, **3**, 109-136.

**Kanevski, I. and Maliga, P.** (1994) Relocation of the plastid *rbcL* gene to the nucleus yields functional ribulose-1,5-bisphosphate carboxylase in tobacco chloroplasts. *PNAS*, **91**, 1969-1973.

**Karpova, O.V., Kuzmin, E.V., Elthon, T.E. and Newton, K.J.** (2002) Differential expression of alternative oxidase genes in maize mitochondrial mutants. *Plant Cell*, **14**, 3271-3284.

**Kato, N., Reynolds, D., Brown, M., Boisdore, M., Fujikawa, Y., Morales, A. and Meisel, L.** (2008) Multidimensional fluorescence microscopy of multiple organelles in *Arabidopsis* seedlings. *Plant Methods*, **4**, 9.

**Kimura, S., Uchiyama, Y., Kasai, N., Namekawa, S., Saotome, A., Ueda, T., Ando, T., Ishibashi, T., Oshige, M., Furukawa, T., Yamamoto, T., Hashimoto, J. and Sakaguchi, K.** (2002) A novel DNA polymerase homologous to *Escherichia coli* DNA polymerase I from a higher plant, rice (*Oryza sativa* L.). *Nucleic Acids Research*, **30**, 1585-1592.

**Kirk, J.T.** (1971) Chloroplast structure and biogenesis. *Annual Review Of Biochemistry*, **40**, 161-196.

**Klein, M., Eckert-Ossenkopp, U., Schmiedeberg, I., Brandt, P., Unseld, M., Brennicke, A. and Schuster, W.** (1994) Physical mapping of the mitochondrial genome of *Arabidopsis thaliana* by cosmid and YAC clones. *Plant J*, **6**, 447-455.

**Kleine, T., Voigt, C. and Leister, D.** (2009) Plastid signalling to the nucleus: messengers still lost in the mists? *Trends In Genetics*, **25**, 185-192.

**Knoop, V.** (2004) The mitochondrial DNA of land plants: peculiarities in phylogenetic perspective. *Current Genetics*, **46**, 123-139.

- Knoop, V.** (2011) When you can't trust the DNA: RNA editing changes transcript sequences. *Cellular and Molecular Life Sciences*, **68**, 567-586.
- Knoop, V., Volkmar, U., Hecht, J. and Grewe, F.** (2011) Mitochondrial genome evolution in the plant lineage. In *Plant mitochondria*, Vol. 1 (Kempken, F., ed.): Springer New York, pp. 3-29.
- Kolodner, R. and Tewari, K.K.** (1979) Inverted repeats in chloroplast DNA from higher plants. *Proc Natl Acad Sci U S A*, **76**, 41-45.
- Koussevitzky, S., Nott, A., Mockler, T.C., Hong, F., Sachetto-Martins, G., Surpin, M., Lim, J., Mittler, R. and Chory, J.** (2007) Signals from chloroplasts converge to regulate nuclear gene expression. *Science*, **316**, 715-719.
- Krieger-Liszkay, A.** (2005) Singlet oxygen production in photosynthesis. *J Exp Bot*, **56**, 337-346.
- Krupinska, K.** (2006) Fate and activities of plastids during leaf senescence. In *The structure and function of plastids*, Vol. 23 (Wise, R.R. and Hooper, J.K., eds): Springer Netherlands, pp. 433-449.
- Kubo, T., Nishizawa, S., Sugawara, A., Itchoda, N., Estiati, A. and Mikami, T.** (2000) The complete nucleotide sequence of the mitochondrial genome of sugar beet (*Beta vulgaris* L.) reveals a novel gene for tRNA<sup>Cys</sup>(GCA). *Nucleic Acids Research*, **28**, 2571-2576.
- Kubo, T. and Newton, K.J.** (2008) Angiosperm mitochondrial genomes and mutations. *Mitochondrion*, **1**, 5-14.
- Kühn, K., Weihe, A. and Börner, T.** (2005) Multiple promoters are a common feature of mitochondrial genes in *Arabidopsis*. *Nucleic Acids Research*, **33**, 337-346.
- Kühn, K., Richter, U., Meyer, E., Delannoy, E., de Longevialle, A.F., O'Toole, N., Börner, T., Millar, A., Small, I. and Whelan, J.** (2009) Phage-type RNA polymerase RPOTmp performs gene-specific transcription in mitochondria of *Arabidopsis thaliana*. *The Plant Cell*, **21**, 2762-2779.
- Kuroiwa, H. and Kuroiwa, T.** (1992) Giant mitochondria in the mature egg cell of *Pelargonium zonale*. *Protoplasma*, **168**, 184-188.
- Kuroiwa, H., Ohta, T. and Kuroiwa, T.** (1996) Studies on the development and three-dimensional reconstruction of giant mitochondria and their nuclei in egg cells of *Pelargonium zonale* Ait. *Protoplasma*, **192**, 235-244.
- Kuroiwa, T.** (1982) Mitochondrial nuclei. In *International Review of Cytology*, Vol. 75, pp. 1-59.

- Kuroiwa, T.** (1991) The replication, differentiation, and inheritance of plastids with emphasis on the concept of organelle nuclei. *International Review of Cytology*, **128**, 1-62.
- Kuroiwa, T., Fujie, M. and Kuroiwa, H.** (1992) Studies on the behavior of mitochondrial DNA: synthesis of mitochondrial DNA occurs actively in a specific region just above the quiescent center in the root meristem of *Pelargonium zonale*. *Journal of Cell Science*, **101**, 483-493.
- Kushnir, S., Babiychuk, E., Storozhenko, S., Davey, M.W., Papenbrock, J., De Rycke, R., Engler, G., Stephan, U.W., Lange, H., Kispal, G., Lill, R. and Van Montagu, M.** (2001) A mutation of the mitochondrial ABC transporter Sta1 leads to dwarfism and chlorosis in the Arabidopsis mutant starik. *Plant Cell*, **13**, 89-100.
- Kusumi, K., Yara, A., Mitsui, N., Tozawa, Y. and Iba, K.** (2004) Characterization of a rice nuclear-encoded plastid RNA polymerase gene *OsRpoTp*. *Plant Cell Physiol*, **45**, 1194-1201.
- Kuzmin, E.V., Karpova, O.V., Elthon, T.E. and Newton, K.J.** (2004) Mitochondrial respiratory deficiencies signal up-regulation of genes for heat shock proteins. *J Biol Chem*, **279**, 20672-20677.
- Lamppa, G.K. and Bendich, A.J.** (1984) Changes in mitochondrial DNA levels during development of pea (*Pisum sativum* L.). *Planta*, **162**, 463-468.
- Lancer, H.A., Cohen, C.E. and Schiff, J.A.** (1976) Changing ratios of phototransformable protochlorophyll and protochlorophyllide of bean seedlings developing in the dark. *Plant Physiol*, **57**, 369-374.
- Lang, B.F., Burger, G., O'Kelly, C.J., Cedergren, R., Golding, G.B., Lemieux, C., Sankoff, D., Turmel, M. and Gray, M.W.** (1997) An ancestral mitochondrial DNA resembling a eubacterial genome in miniature. *Nature*, **387**, 493-497.
- Larkin, R.M., Alonso, J.M., Ecker, J.R. and Chory, J.** (2003) GUN4, a regulator of chlorophyll synthesis and intracellular signaling. *Science*, **299**, 902-906.
- Lavrov, D.V.** (2007) Key transitions in animal evolution: a mitochondrial DNA perspective. *Integr Comp Biol*, **47**, 734-743.
- Leaver, C.J., Hack, E. and Forde, B.G.** (1983) Protein synthesis by isolated plant mitochondria. *Methods Enzymol*, **97**, 476-484.
- Lee, K.P., Kim, C., Landgraf, F. and Apel, K.** (2007) EXECUTER1- and EXECUTER2-dependent transfer of stress-related signals from the plastid to the nucleus of *Arabidopsis thaliana*. *Proc Natl Acad Sci U S A*, **104**, 10270-10275.
- León, P., Gregorio, J. and Cordoba, E.** (2013) ABI4 and its role in chloroplast retrograde communication. *Frontiers in Plant Science*, **3**.

**Lerbs-Mache, S.** (2010) Function of plastid sigma factors in higher plants: regulation of gene expression or just preservation of constitutive transcription? *Plant Molecular Biology*, **10.1007/s11103-010-9714-4**, in press.

**Li, W., Ruf, S. and Bock, R.** (2006) Constancy of organellar genome copy numbers during leaf development and senescence in higher plants. *Molecular Genetics and Genomics*, **275**, 185-192.

**Licausi, F., Weits, D.A., Pant, B.D., Scheible, W.-R., Geigenberger, P. and van Dongen, J.T.** (2011) Hypoxia responsive gene expression is mediated by various subsets of transcription factors and miRNAs that are determined by the actual oxygen availability. *New Phytologist*, **190**, 442-456.

**Liere, K. and Maliga, P.** (2001) Plastid RNA polymerases in higher plants. In *Regulation of Photosynthesis* (Andersson, B. and Aro, E.-M., eds). Dordrecht: Kluwer Academic Publishers, Netherlands, pp. 29-49.

**Liere, K. and Börner, T.** (2007a) Transcription and transcriptional regulation in plastids. In *Topics in Current Genetics: Cell and Molecular Biology of Plastids*, Vol. 19 (Bock, R., ed. Berlin / Heidelberg: Springer, pp. 121-174.

**Liere, K. and Börner, T.** (2007b) Transcription of plastid genes. In *Regulation of Transcription in Plants* (Grasser, K.D., ed. Oxford: Blackwell Publishing, pp. 184-224.

**Liere, K. and Börner, T.** (2011) Transcription in plant mitochondria. In *Plant mitochondria*, Vol. 1 (Kempken, F., ed.: Springer New York, pp. 85-105.

**Liere, K., Weihe, A. and Börner, T.** (2011) The transcription machineries of plant mitochondria and chloroplasts: composition, function, and regulation. *Journal of Plant Physiology*, **168**, 1345-1360.

**Lilly, J.W., Havey, M.J., Jackson, S.A. and Jiang, J.** (2001) Cytogenomic analyses reveal the structural plasticity of the chloroplast genome in higher plants. *Plant Cell*, **13**, 245-254.

**Liu, S.L., Zhuang, Y., Zhang, P. and Adams, K.L.** (2009) Comparative analysis of structural diversity and sequence evolution in plant mitochondrial genes transferred to the nucleus. *Mol Biol Evol*, **26**, 875-891.

**Logan, D.C. and Leaver, C.J.** (2000) Mitochondria-targeted GFP highlights the heterogeneity of mitochondrial shape, size and movement within living plant cells. *J Exp Bot*, **51**, 865-871.

**Logan, D.C., Scott, I. and Tobin, A.K.** (2003) The genetic control of plant mitochondrial morphology and dynamics. *Plant J*, **36**, 500-509.

**Logan, D.C., Scott, I. and Tobin, A.K.** (2004) ADL2a, like ADL2b, is involved in the control of higher plant mitochondrial morphology. *J Exp Bot*, **55**, 783-785.

- Logan, D.C.** (2006) The mitochondrial compartment. *J Exp Bot*, **57**, 1225-1243.
- Logan, D.C.** (2010) The dynamic plant chondriome. *Semin Cell Dev Biol*, **21**, 550-557.
- Lohse, M., Drechsel, O. and Bock, R.** (2007) OrganellarGenomeDRAW (OGDRAW): a tool for the easy generation of high-quality custom graphical maps of plastid and mitochondrial genomes. *Current Genetics*, **52**, 267-274.
- Lonsdale, D.M., Brears, T., Hodge, T.P., Melville, S.E. and Rottmann, W.H.** (1988) The plant mitochondrial genome: homologous recombination as a mechanism for generating heterogeneity. *Philosophical Transactions of the Royal Society of London. B, Biological Sciences*, **319**, 149-163.
- López-Juez, E. and Pyke, K.A.** (2005) Plastids unleashed: their development and their integration in plant development. *Int J Dev Biol*, **49**, 557-577.
- Lyndon, R.F. and Robertson, E.S.** (1976) The quantitative ultrastructure of the pea shoot apex in relation to leaf initiation. *Protoplasma*, **87**, 387-402.
- Mache, R., Zhou, D.X., Lerbs-Mache, S., Harrak, H., Villain, P. and Gauvin, S.** (1997) Nuclear control of early plastid differentiation. *Plant Physiology & Biochemistry*, **35**, 199-203.
- Mackenzie, S. and McIntosh, L.** (1999) Higher plant mitochondria. *Plant Cell*, **11**, 571-586.
- Mahalingam, R. and Fedoroff, N.** (2003) Stress response, cell death and signalling: the many faces of reactive oxygen species. *Physiologia Plantarum*, **119**, 56-68.
- Maier, U.G., Bozarth, A., Funk, H.T., Zauner, S., Rensing, S.A., Schmitz-Linneweber, C., Börner, T. and Tillich, M.** (2008) Complex chloroplast RNA metabolism: just debugging the genetic programme? *BMC Biology*, **6**, 36.
- Marano, M.R. and Carrillo, N.** (1992) Constitutive transcription and stable RNA accumulation in plastids during the conversion of chloroplasts to chromoplasts in ripening tomato fruits. *Plant Physiology*, **100**, 1103-1113.
- Maréchal, A., Parent, J.-S., Sabar, M., Veronneau-Lafortune, F., Abou-Rached, C. and Brisson, N.** (2008) Overexpression of mtDNA-associated AtWhy2 compromises mitochondrial function. *BMC Plant Biology*, **8**, 42.
- Maréchal, A. and Brisson, N.** (2010) Recombination and the maintenance of plant organelle genome stability. *The New Phytologist*, **186**, 299-317.
- Martin, W. and Muller, M.** (1998) The hydrogen hypothesis for the first eukaryote. *Nature*, **392**, 37-41.
- Martin, W., Hoffmeister, M., Rotte, C. and Henze, K.** (2001) An overview of endosymbiotic models for the origins of eukaryotes, their ATP-producing organelles



(mitochondria and hydrogenosomes), and their heterotrophic lifestyle. *Biol Chem*, **382**, 1521-1539.

**Martin, W.** (2003) Gene transfer from organelles to the nucleus: frequent and in big chunks. *Proceedings of the National Academy of Sciences of the United States of America*, **100**, 8612-8614.

**Masuda, T. and Fujita, Y.** (2008) Regulation and evolution of chlorophyll metabolism. *Photochem Photobiol Sci*, **7**, 1131-1149.

**McFadden, G.I., Gilson, P.R., Hofmann, C.J., Adcock, G.J. and Maier, U.G.** (1994) Evidence that an amoeba acquired a chloroplast by retaining part of an engulfed eukaryotic alga. *Proc Natl Acad Sci U S A*, **91**, 3690-3694.

**McFadden, G.I.** (2001) Chloroplast origin and integration. *Plant Physiol*, **125**, 50-53.

**Melaragno, J., Mehrotra, B. and Coleman, A.** (1993) Relationship between endopolyploidy and cell size in epidermal tissue of *Arabidopsis*. *The Plant Cell*, **5**, 1661-1668.

**Meyer, E.H., Tomaz, T., Carroll, A.J., Estavillo, G., Delannoy, E., Tanz, S.K., Small, I.D., Pogson, B.J. and Millar, A.H.** (2009) Remodeled respiration in *ndufs4* with low phosphorylation efficiency suppresses *Arabidopsis* germination and growth and alters control of metabolism at night. *Plant Physiol*, **151**, 603-619.

**Moazed, D. and Noller, H.F.** (1987) Interaction of antibiotics with functional sites in 16S ribosomal RNA. *Nature*, **327**, 389-394.

**Mochizuki, N., Brusslan, J.A., Larkin, R., Nagatani, A. and Chory, J.** (2001) *Arabidopsis* genomes uncoupled 5 (GUN5) mutant reveals the involvement of Mg-chelatase H subunit in plastid-to-nucleus signal transduction. *Proceedings of the National Academy of Sciences USA*, **98**, 2053-2058.

**Mochizuki, N., Tanaka, R., Tanaka, A., Masuda, T. and Nagatani, A.** (2008) The steady-state level of Mg-protoporphyrin IX is not a determinant of plastid-to-nucleus signaling in *Arabidopsis*. *Proceedings of the National Academy of Sciences of the United States of America*, **105**, 15184-15189.

**Moller, I.M.** (2001) PLANT MITOCHONDRIA AND OXIDATIVE STRESS: Electron Transport, NADPH Turnover, and Metabolism of Reactive Oxygen Species. *Annu Rev Plant Physiol Plant Mol Biol*, **52**, 561-591.

**Mori, Y., Kimura, S., Saotome, A., Kasai, N., Sakaguchi, N., Uchiyama, Y., Ishibashi, T., Yamamoto, T., Chiku, H. and Sakaguchi, K.** (2005) Plastid DNA polymerases from higher plants, *Arabidopsis thaliana*. *Biochem Biophys Res Commun*, **334**, 43-50.

**Mouillon, J.M., Ravanel, S., Douce, R. and Rebeille, F.** (2002) Folate synthesis in higher-plant mitochondria: coupling between the dihydropterin pyrophosphokinase and the dihydropteroate synthase activities. *Biochem J*, **363**, 313-319.

- Moulin, M., McCormac, A.C., Terry, M.J. and Smith, A.G.** (2008) Tetrapyrrole profiling in *Arabidopsis* seedlings reveals that retrograde plastid nuclear signaling is not due to Mg-protoporphyrin IX accumulation. *Proceedings of the National Academy of Sciences*, **105**, 15178-15183.
- Mozdy, A.D., McCaffery, J.M. and Shaw, J.M.** (2000) Dnm1p GTPase-mediated mitochondrial fission is a multi-step process requiring the novel integral membrane component Fis1p. *J Cell Biol*, **151**, 367-380.
- Muise, R.C. and Hauswirth, W.W.** (1995) Selective DNA amplification regulates transcript levels in plant mitochondria. *Current Genetics*, **28**, 113-121.
- Mulligan, R.M., Leon, P. and Walbot, V.** (1991) Transcription and posttranscriptional regulation of maize mitochondrial gene expression. *Molecular and Cellular Biology*, **11**, 533-543.
- Mullineaux, P.M., Karpinski, S. and Baker, N.R.** (2006) Spatial dependence for hydrogen peroxide-directed signaling in light-stressed plants. *Plant Physiol*, **141**, 346-350.
- Murray, M.G. and Thompson, W.F.** (1980) Rapid isolation of high molecular weight plant DNA. *Nucleic Acids Res*, **8**, 4321-4325.
- Nakayama, T. and Archibald, J.M.** (2012) Evolving a photosynthetic organelle. *BMC biology*, **10**, 35.
- Nambara, E. and Marion-Poll, A.** (2005) Absciscic acid biosynthesis and catabolism. *Annual Review of Plant Biology*, **56**, 165-185.
- Nelissen, B., Van de Peer, Y., Wilmotte, A. and De Wachter, R.** (1995) An early origin of plastids within the cyanobacterial divergence is suggested by evolutionary trees based on complete 16S rRNA sequences. *Molecular Biology and Evolution*, **12**, 1166-1173.
- Neuhaus, H.E. and Emes, M.J.** (2000) Nonphotosynthetic metabolism in plastids. *Annu Rev Plant Physiol Plant Mol Biol*, **51**, 111-140.
- Noguchi, K. and Yoshida, K.** (2008) Interaction between photosynthesis and respiration in illuminated leaves. *Mitochondrion*, **8**, 87-99.
- Notsu, Y., Masood, S., Nishikawa, T., Kubo, N., Akiduki, G., Nakazono, M., Hirai, A. and Kadowaki, K.** (2002) The complete sequence of the rice (*Oryza sativa* L.) mitochondrial genome: frequent DNA sequence acquisition and loss during the evolution of flowering plants. *Mol Genet Genomics*, **268**, 434-445.
- Nott, A., Jung, H.S., Koussevitzky, S. and Chory, J.** (2006) Plastid-to-nucleus retrograde signaling. *Annu Rev Plant Biol*, **57**, 739-759.

- Noutsos, C., Richly, E. and Leister, D.** (2005) Generation and evolutionary fate of insertions of organelle DNA in the nuclear genomes of flowering plants. *Genome Res*, **15**, 616-628.
- Obornik, M., Janouskovec, J., Chrudimsky, T. and Lukes, J.** (2009) Evolution of the apicoplast and its hosts: from heterotrophy to autotrophy and back again. *Int J Parasitol*, **39**, 1-12.
- Okada, S. and Brennicke, A.** (2006) Transcript levels in plant mitochondria show a tight homeostasis during day and night. *Molecular Genetics and Genomics*, **276**, 71-78.
- Okamoto, K. and Shaw, J.M.** (2005) Mitochondrial morphology and dynamics in yeast and multicellular eukaryotes. *Annu Rev Genet*, **39**, 503-536.
- Oldenburg, D., Rowan, B., Zhao, L., Walcher, C., Schleh, M. and Bendich, A.** (2006) Loss or retention of chloroplast DNA in maize seedlings is affected by both light and genotype. *Planta*, **225**, 41-55.
- Oldenburg, D., Kumar, R. and Bendich, A.** (2012) The amount and integrity of mtDNA in maize decline with development. *Planta*, **237**, 603-617.
- Oldenburg, D.J. and Bendich, A.J.** (1996) Size and structure of replicating mitochondrial DNA in cultured tobacco cells. *Plant Cell*, **8**, 447-461.
- Oldenburg, D.J. and Bendich, A.J.** (2001) Mitochondrial DNA from the liverwort *Marchantia polymorpha*: circularly permuted linear molecules, head-to-tail concatemers, and a 5' protein. *J Mol Biol*, **310**, 549-562.
- Oldenburg, D.J. and Bendich, A.J.** (2004) Most chloroplast DNA of maize seedlings in linear molecules with defined ends and branched forms. *J Mol Biol*, **335**, 953-970.
- Olichon, A., Emorine, L.J., Descoins, E., Pelloquin, L., Bricchese, L., Gas, N., Guillou, E., Delettre, C., Valette, A., Hamel, C.P., Ducommun, B., Lenaers, G. and Belenguer, P.** (2002) The human dynamin-related protein OPA1 is anchored to the mitochondrial inner membrane facing the inter-membrane space. *FEBS Lett*, **523**, 171-176.
- Olyslaegers, G. and Verbelen, J.P.** (1998) Improved staining of F-actin and co-localization of mitochondria in plant cells. *Journal of Microscopy*, **192**, 73-77.
- Ono, Y., Sakai, A., Takechi, K., Takio, S., Takusagawa, M. and Takano, H.** (2007) NtPolI-like1 and NtPolI-like2, bacterial DNA polymerase I homologs isolated from BY-2 cultured tobacco cells, encode DNA polymerases engaged in DNA replication in both plastids and mitochondria. *Plant Cell Physiol*, **48**, 1679-1692.
- Ordog, S.H., Higgins, V.J. and Vanlerberghe, G.C.** (2002) Mitochondrial alternative oxidase is not a critical component of plant viral resistance but may play a role in the hypersensitive response. *Plant Physiol*, **129**, 1858-1865.

- Otera, H. and Mihara, K.** (2011) Molecular mechanisms and physiologic functions of mitochondrial dynamics. *J Biochem*, **149**, 241-251.
- Otsuga, D., Keegan, B.R., Brisch, E., Thatcher, J.W., Hermann, G.J., Bleazard, W. and Shaw, J.M.** (1998) The dynamin-related GTPase, Dnm1p, controls mitochondrial morphology in yeast. *J Cell Biol*, **143**, 333-349.
- Palmer, J.D. and Herbon, L.A.** (1987) Unicircular structure of the *Brassica hirta* mitochondrial genome. *Current Genetics*, **11**, 565-570.
- Parent, J.-S., Lepage, E. and Brisson, N.** (2011) Divergent roles for the two Poll-like organelle DNA polymerases of *Arabidopsis thaliana*. *Plant Physiology*, **156**, 254-262.
- Pesaresi, P., Varotto, C., Meurer, J., Jahns, P., Salamini, F. and Leister, D.** (2001) Knock-out of the plastid ribosomal protein L11 in *Arabidopsis*: effects on mRNA translation and photosynthesis. *Plant J*, **27**, 179-189.
- Pesaresi, P., Masiero, S., Eubel, H., Braun, H.-P., Bhushan, S., Glaser, E., Salamini, F. and Leister, D.** (2006) Nuclear photosynthetic gene expression is synergistically modulated by rates of protein synthesis in chloroplasts and mitochondria. *Plant Cell*, **18**, 970-991.
- Pesaresi, P., Schneider, A., Kleine, T. and Leister, D.** (2007) Interorganellar communication. *Current Opinion in Plant Biology*, **10**, 600-606.
- Pfalz, J., Liere, K., Kandlbinder, A., Dietz, K.-J. and Oelmüller, R.** (2006) pTAC2, -6 and -12 are components of the transcriptionally active plastid chromosome that are required for plastid gene expression. *Plant Cell*, **18**, 176-197.
- Pfannschmidt, T., Schutze, K., Fey, V., Sherameti, I. and Oelmüller, R.** (2003) Chloroplast redox control of nuclear gene expression-a new class of plastid signals in interorganellar communication. *Antioxid Redox Signal*, **5**, 95-101.
- Pfannschmidt, T.** (2005) Acclimation to varying light qualities: toward the functional relationship of state transitions and adjustment of photosystem stoichiometry *Journal of Phycology*, **41**, 723-725.
- Pfannschmidt, T. and Liere, K.** (2005) Redox regulation and modification of proteins controlling chloroplast gene expression. *Antioxidants & Redox Signaling*, **7**, 607-618.
- Pfannschmidt, T., Brautigam, K., Wagner, R., Dietzel, L., Schröter, Y., Steiner, S. and Nykytenko, A.** (2009) Potential regulation of gene expression in photosynthetic cells by redox and energy state: approaches towards better understanding. *Annals of Botany*, **103**, 599-607.
- Pfannschmidt, T.** (2010) Plastidial retrograde signalling - a true "plastid factor" or just metabolite signatures? *Trends in Plant Science*, **15**, 427-435.

- Pitzschke, A. and Hirt, H.** (2006) Mitogen-activated protein kinases and reactive oxygen species signaling in plants. *Plant Physiol*, **141**, 351-356.
- Pogson, B.J., Woo, N.S., Förster, B. and Small, I.D.** (2008) Plastid signalling to the nucleus and beyond. *Trends in Plant Science*, **13**, 602-609.
- Preuten, T., Cincu, E., Fuchs, J., Zoschke, R., Liere, K. and Borner, T.** (2010) Fewer genes than organelles: extremely low and variable gene copy numbers in mitochondria of somatic plant cells. *Plant J*, **64**, 948-959.
- Pyke, K.A. and Leech, R.M.** (1992) Chloroplast Division and Expansion Is Radically Altered by Nuclear Mutations in *Arabidopsis thaliana*. *Plant Physiol*, **99**, 1005-1008.
- Pyke, K.A.** (1999) Plastid division and development. *Plant Cell*, **11**, 549-556.
- Raghavendra, A.S. and Padmasree, K.** (2003) Beneficial interactions of mitochondrial metabolism with photosynthetic carbon assimilation. *Trends Plant Sci*, **8**, 546-553.
- Rapp, J.C. and Mullet, J.E.** (1991) Chloroplast transcription is required to express the nuclear genes *rbcS* and *cab*. Plastid DNA copy number is regulated independently. *Plant Molecular Biology*, **17**, 813-823.
- Rapp, W.D., Lupold, D.S., Mack, S. and Stern, D.B.** (1993) Architecture of the maize mitochondrial *atp1* promoter as determined by linker-scanning and point mutagenesis. *Molecular and Cellular Biology*, **13**, 7232-7238.
- Rasmusson, A.G., Geisler, D.A. and Moller, I.M.** (2008) The multiplicity of dehydrogenases in the electron transport chain of plant mitochondria. *Mitochondrion*, **8**, 47-60.
- Rasmusson, A.G., Fernie, A.R. and van Dongen, J.T.** (2009) Alternative oxidase: a defence against metabolic fluctuations? *Physiol Plant*, **137**, 371-382.
- Rauwolf, U., Golczyk, H., Greiner, S. and Herrmann, R.G.** (2010) Variable amounts of DNA related to the size of chloroplasts III. Biochemical determinations of DNA amounts per organelle. *Molecular Genetics and Genomics*, **283**, 35-47.
- Reyes-Prieto, A., Weber, A.P. and Bhattacharya, D.** (2007) The origin and establishment of the plastid in algae and plants. *Annu Rev Genet*, **41**, 147-168.
- Rhoads, D.M., White, S.J., Zhou, Y., Muralidharan, M. and Elthon, T.E.** (2005) Altered gene expression in plants with constitutive expression of a mitochondrial small heat shock protein suggests the involvement of retrograde regulation in the heat stress response. *Physiologia Plantarum*, **123**, 435-444.
- Rhoads, D.M. and Subbaiah, C.C.** (2007) Mitochondrial retrograde regulation in plants. *Mitochondrion*, **7**, 177-194.

- Richly, E., Dietzmann, A., Biehl, A., Kurth, J., Laloi, C., Apel, K., Salamini, F. and Leister, D.** (2003) Covariations in the nuclear chloroplast transcriptome reveal a regulatory master-switch. *EMBO Rep*, **4**, 491-498.
- Richly, E. and Leister, D.** (2004) NUMTs in sequenced eukaryotic genomes. *Mol Biol Evol*, **21**, 1081-1084.
- Richter, U., Richter, B.r., Weihe, A. and BÄ¶rner, T.** (2013) A third mitochondrial RNA polymerase in the moss *Physcomitrella patens*. *Current Genetics*, 1-10.
- Rinalducci, S., Pedersen, J.Z. and Zolla, L.** (2004) Formation of radicals from singlet oxygen produced during photoinhibition of isolated light-harvesting proteins of photosystem II. *Biochim Biophys Acta*, **1608**, 63-73.
- Robertson, E.J., Williams, M., Harwood, J.L., Lindsay, J.G., Leaver, C.J. and Leech, R.M.** (1995) Mitochondria increase three-fold and mitochondrial proteins and lipid change dramatically in postmeristematic cells in young wheat leaves grown in elevated CO<sub>2</sub>. *Plant Physiol*, **108**, 469-474.
- Robison, M.M., Ling, X., Smid, M.P.L., Zarei, A. and Wolyn, D.J.** (2009) Antisense expression of mitochondrial ATP synthase subunits OSCP (ATP5) and  $\hat{F}_3$  (ATP3) alters leaf morphology, metabolism and gene expression in *Arabidopsis*. *Plant and Cell Physiology*, **50**, 1840-1850.
- Rodermel, S.** (2001) Pathways of plastid-to-nucleus signaling. *Trends Plant Sci*, **6**, 471-478.
- Rossel, J.B., Wilson, P.B., Hussain, D., Woo, N.S., Gordon, M.J., Mewett, O.P., Howell, K.A., Whelan, J., Kazan, K. and Pogson, B.J.** (2007) Systemic and intracellular responses to photooxidative stress in *Arabidopsis*. *Plant Cell*, **19**, 4091-4110.
- Rowan, B., Oldenburg, D. and Bendich, A.** (2009) A multiple-method approach reveals a declining amount of chloroplast DNA during development in *Arabidopsis*. *BMC Plant Biology*, **9**, 3.
- Rowan, B.A., Oldenburg, D.J. and Bendich, A.J.** (2004) The demise of chloroplast DNA in *Arabidopsis*. *Curr Genet*, **46**, 176-181.
- Ruf, S., Kössel, H. and Bock, R.** (1997) Targeted Inactivation of a tobacco intron-containing open reading frame reveals a novel chloroplast-encoded photosystem I-related gene. *Journal of Cell Biology*, **139**, 95-102.
- Rumpho, M.E., Summer, E.J., Green, B.J., Fox, T.C. and Manhart, J.R.** (2001) Molluscalgal chloroplast symbiosis: how can isolated chloroplasts continue to function for months in the cytosol of a sea slug in the absence of an algal nucleus? *Zoology (Jena)*, **104**, 303-312.

- Rumpho, M.E., Worful, J.M., Lee, J., Kannan, K., Tyler, M.S., Bhattacharya, D., Moustafa, A. and Manhart, J.R.** (2008) Horizontal gene transfer of the algal nuclear gene *psbO* to the photosynthetic sea slug *Elysia chlorotica*. *Proceedings of the National Academy of Sciences*, **105**, 17867-17871.
- Sakai, A., Saito, C., Inada, N. and Kuroiwa, T.** (1998) Transcriptional activities of the chloroplast-nuclei and proplastid-nuclei isolated from tobacco exhibit different sensitivities to tagetitoxin: implication of the presence of distinct RNA polymerases. *Plant Cell Physiol.*, **39**, 928-934.
- Sakai, A., Takano, H. and Kuroiwa, T.** (2004) Organelle nuclei in higher plants: structure, composition, function, and evolution. *Int Rev Cytol*, **238**, 59-118.
- Samuel, M.A., Hall, H., Krzymowska, M., Drzewiecka, K., Hennig, J. and Ellis, B.E.** (2005) SIPK signaling controls multiple components of harpin-induced cell death in tobacco. *Plant J*, **42**, 406-416.
- Sandhu, A.P., Abdelnoor, R.V. and Mackenzie, S.A.** (2007) Transgenic induction of mitochondrial rearrangements for cytoplasmic male sterility in crop plants. *Proc Natl Acad Sci U S A*, **104**, 1766-1770.
- Santel, A. and Fuller, M.T.** (2001) Control of mitochondrial morphology by a human mitofusin. *J Cell Sci*, **114**, 867-874.
- Satoh, M., Nemoto, Y., Kawano, S., Nagata, T., Hirokawa, H. and Kuroiwa, T.** (1993) Organization of heterogeneous mitochondrial DNA molecules in mitochondrial nuclei of cultured tobacco cells. *Protoplasma*, **175**, 112-120.
- Schmitz-Linneweber, C. and Small, I.** (2008) Pentatricopeptide repeat proteins: a socket set for organelle gene expression. *Trends in Plant Science*, **13**, 663-670.
- Schottler, M.A., Flugel, C., Thiele, W., Stegemann, S. and Bock, R.** (2007) The plastome-encoded Psal subunit is required for efficient Photosystem I excitation, but not for plastocyanin oxidation in tobacco. *Biochem J*, **403**, 251-260.
- Schröter, Y., Steiner, S., Matthäi, K. and Pfannschmidt, T.** (2010) Analysis of oligomeric protein complexes in the chloroplast sub-proteome of nucleic acid-binding proteins from mustard reveals potential redox regulators of plastid gene expression. *Proteomics*, **10**, 2191-2204.
- Schweer, J., Türkeri, H., Kolpack, A. and Link, G.** (2010) Role and regulation of plastid sigma factors and their functional interactors during chloroplast transcription - Recent lessons from *Arabidopsis thaliana*. *European Journal of Cell Biology*, **89**, 940-946.
- Scott, I., Tobin, A.K. and Logan, D.C.** (2006) BIGYIN, an orthologue of human and yeast FIS1 genes functions in the control of mitochondrial size and number in *Arabidopsis thaliana*. *J Exp Bot*, **57**, 1275-1280.

**Scott, I. and Logan, D.C.** (2008a) Mitochondria and cell death pathways in plants: Actions speak louder than words. *Plant Signal Behav*, **3**, 475-477.

**Scott, I. and Logan, D.C.** (2008b) Mitochondrial morphology transition is an early indicator of subsequent cell death in *Arabidopsis*. *New Phytol*, **177**, 90-101.

**Segui-Simarro, J.M., Coronado, M.J. and Staehelin, L.A.** (2008) The mitochondrial cycle of *Arabidopsis* shoot apical meristem and leaf primordium meristematic cells is defined by a perinuclear tentaculate/cage-like mitochondrion. *Plant Physiol*, **148**, 1380-1393.

**Segui-Simarro, J.M. and Staehelin, L.A.** (2009) Mitochondrial reticulation in shoot apical meristem cells of *Arabidopsis* provides a mechanism for homogenization of mtDNA prior to gamete formation. *Plant Signal Behav*, **4**, 168-171.

**Shaver, J., Oldenburg, D. and Bendich, A.** (2006) Changes in chloroplast DNA during development in tobacco, *Medicago truncatula*, pea, and maize. *Planta*, **224**, 72-82.

**Sheahan, M.B., Rose, R.J. and McCurdy, D.W.** (2004) Organelle inheritance in plant cell division: the actin cytoskeleton is required for unbiased inheritance of chloroplasts, mitochondria and endoplasmic reticulum in dividing protoplasts. *Plant J*, **37**, 379-390.

**Sheahan, M.B., McCurdy, D.W. and Rose, R.J.** (2005a) Mitochondria as a connected population: ensuring continuity of the mitochondrial genome during plant cell dedifferentiation through massive mitochondrial fusion. *Plant J*, **44**, 744-755.

**Sheahan, M.B., McCurdy, D.W. and Rose, R.J.** (2005b) Mitochondria as a connected population: ensuring continuity of the mitochondrial genome during plant cell dedifferentiation through massive mitochondrial fusion. *Plant Journal*, **44**, 744-755.

**Shedge, V., Arrieta-Montiel, M., Christensen, A.C. and Mackenzie, S.A.** (2007) Plant mitochondrial recombination surveillance requires unusual RecA and MutS homologs. *Plant Cell*, **19**, 1251-1264.

**Shedge, V., Davila, J., Arrieta-Montiel, M.P., Mohammed, S. and Mackenzie, S.A.** (2010) Extensive rearrangement of the *Arabidopsis* mitochondrial genome elicits cellular conditions for thermotolerance. *Plant Physiology*, **152**, 1960-1970.

**Shen, Y.-Y., Wang, X.-F., Wu, F.-Q., Du, S.-Y., Cao, Z., Shang, Y., Wang, X.-L., Peng, C.-C., Yu, X.-C., Zhu, S.-Y., Fan, R.-C., Xu, Y.-H. and Zhang, D.-P.** (2006) The Mg-chelatase H subunit is an abscisic acid receptor. *Nature*, **443**, 823-826.

**Shiina, T., Tsunoyama, Y., Nakahira, Y. and Khan, M.S.** (2005) Plastid RNA polymerases, promoters, and transcription regulators in higher plants. *International Review of Cytology*, **244**, 1-68.



- Shiina, T., Ishizaki, Y., Yagi, Y. and Nakahira, Y.** (2009) Function and evolution of plastid sigma factors. *Plant Biotechnol*, **26**, 57-66.
- Shimada, H. and Sugiura, M.** (1991) Fine structural features of the chloroplast genome: comparison of the sequenced chloroplast genomes. *Nucleic Acids Research*, **19**, 983-995.
- Silhavy, D. and Maliga, P.** (1998) Mapping of the promoters for the nucleus-encoded plastid RNA polymerase (NEP) in the *iojap* maize mutant. *Curr. Genet.*, **33**, 340-344.
- Simon, V.R., Swayne, T.C. and Pon, L.A.** (1995) Actin-dependent mitochondrial motility in mitotic yeast and cell-free systems: identification of a motor activity on the mitochondrial surface. *J Cell Biol*, **130**, 345-354.
- Soares, A., Romano, E., Neiva, S., De Capdeville, G., Vianna, G.R., Rech, E.L. and Aragao, F.J.** (2005) Inheritance of a recessive transgene-associated character controlling albinism in transgenic bean (*Phaseolus vulgaris* L.). *Plant Biol*, **7**, 104-107.
- Sparkes, I.A., Teanby, N.A. and Hawes, C.** (2008) Truncated myosin XI tail fusions inhibit peroxisome, Golgi, and mitochondrial movement in tobacco leaf epidermal cells: a genetic tool for the next generation. *J Exp Bot*, **59**, 2499-2512.
- Staehelin, L.A.** (2003) Chloroplast structure: from chlorophyll granules to supra-molecular architecture of thylakoid membranes. *Photosynth Res*, **76**, 185-196.
- Stegemann, S., Hartmann, S., Ruf, S. and Bock, R.** (2003) High-frequency gene transfer from the chloroplast genome to the nucleus. *Proc Natl Acad Sci U S A*, **100**, 8828-8833.
- Stegemann, S. and Bock, R.** (2006) Experimental reconstruction of functional gene transfer from the tobacco plastid genome to the nucleus. *Plant Cell*, **18**, 2869-2878.
- Stern, D.B., Goldschmidt-Clermont, M. and Hanson, M.R.** (2010) Chloroplast RNA metabolism. *Annual Review of Plant Biology*, **61**, 125-155.
- Stickens, D. and Verbelen, J.-P.** (1996) Spatial structure of mitochondria and ER denotes changes in cell physiology of cultured tobacco protoplasts. *The Plant Journal*, **9**, 85-92.
- Strand, Å., Asami, T., Alonso, J., Ecker, J.R. and Chory, J.** (2003) Chloroplast to nucleus communication triggered by accumulation of Mg-protoporphyrinIX. *Nature*, **421**, 79-83.
- Sugiura, M.** (1989) The chloroplast chromosomes in land plants. *Annual Review of Cell Biology*, **5**, 51-70.
- Sugiura, M.** (1992) The chloroplast genome. *Plant Molecular Biology*, **19**, 149-168.

- Sugiyama, Y., Watase, Y., Nagase, M., Makita, N., Yagura, S., Hirai, A. and Sugiura, M.** (2005) The complete nucleotide sequence and multipartite organization of the tobacco mitochondrial genome: comparative analysis of mitochondrial genomes in higher plants. *Molecular Genetics and Genomics*, **272**, 603.
- Sullivan, J.A. and Gray, J.C.** (1999) Plastid translation is required for the expression of nuclear photosynthesis genes in the dark and in roots of the pea *lip1* mutant. *Plant Cell*, **11**, 901-910.
- Sun, C.W. and Callis, J.** (1997) Independent modulation of *Arabidopsis thaliana* polyubiquitin mRNAs in different organs and in response to environmental changes. *Plant Journal*, **11**, 1017-1027.
- Susek, R.E., Ausubel, F.M. and Chory, J.** (1993) Signal transduction mutants of *Arabidopsis* uncouple nuclear CAB and RBCS gene expression from chloroplast development. *Cell*, **74**, 787-799.
- Suzuki, J.Y., Ytterberg, J.A., Beardslee, T.A., Allison, L.A., Wijk, K.J. and Maliga, P.** (2004) Affinity purification of the tobacco plastid RNA polymerase and *in vitro* reconstitution of the holoenzyme. *Plant Journal*, **40**, 164-172.
- Svab, Z., Hajdukiewicz, P.T. and Maliga, P.** (1990) Stable transformation of plastids in higher plants. *Proc. Natl. Acad. Sci. USA*, **90**, 913-917.
- Swiatecka-Hagenbruch, M., Liere, K. and Börner, T.** (2007) High diversity of plastidial promoters in *Arabidopsis thaliana*. *Mol Genet Genomics*, **277**, 725-734.
- Swiatecka-Hagenbruch, M., Emanuel, C., Hedtke, B., Liere, K. and Börner, T.** (2008) Impaired function of the phage-type RNA polymerase RpoTp in transcription of chloroplast genes is compensated by a second phage-type RNA polymerase. *Nucleic Acids Research*, **36**, 785-792.
- Takanashi, H., Arimura, S.-i., Sakamoto, W. and Tsutsumi, N.** (2006) Different amounts of DNA in each mitochondrion in rice root. *Genes & Genetic Systems*, **81**, 215-218.
- Takanashi, H., Ohnishi, T., Mogi, M., Okamoto, T., Arimura, S.-i. and Tsutsumi, N.** (2010) Studies of mitochondrial morphology and DNA amount in the rice egg cell. *Current Genetics*, **56**, 33-41.
- Tarasenko, V.I., Garnik, E.Y. and Konstantinov, Y.M.** (2010) Characterization of *Arabidopsis* mutant with inactivated gene coding for Fe-S subunit of mitochondrial respiratory chain complex I. *Russian Journal of Plant Physiology*, **57**, 392-400.
- Terzaghi, W.B. and Cashmore, A.R.** (1995) Photomorphogenesis. Seeing the light in plant development. *Current Biology*, **5**, 466-468.
- Tieu, Q. and Nunnari, J.** (2000) Mdv1p is a WD repeat protein that interacts with the dynamin-related GTPase, Dnm1p, to trigger mitochondrial division. *J Cell Biol*, **151**, 353-366.

**Tiller, K. and Link, G.** (1993) Phosphorylation and dephosphorylation affect functional characteristics of chloroplast and etioplast transcription systems from mustard (*Sinapis alba* L.). *EMBO Journal*, **12**, 1745-1753.

**Tillich, M., Poltnigg, P., Kushnir, S. and Schmitz-Linneweber, C.** (2006) Maintenance of plastid RNA editing activities independently of their target sites. *EMBO Rep*, **7**, 308-313.

**Timmis, J.N., Ayliffe, M.A., Huang, C.Y. and Martin, W.** (2004) Endosymbiotic gene transfer: organelle genomes forge eukaryotic chromosomes. *Nat Rev Genet*, **5**, 123-135.

**Toshoji, H., Katsumata, T., Takusagawa, M., Yusa, Y. and Sakai, A.** (2011) Effects of chloroplast dysfunction on mitochondria: white sectors in variegated leaves have higher mitochondrial DNA levels and lower dark respiration rates than green sectors. *Protoplasma*.

**Tracy, R.L. and Stern, D.B.** (1995) Mitochondrial transcription initiation: promoter structures and RNA polymerases. *Current Genetics*, **28**, 205-216.

**Unseld, M., Marienfeld, J.R., Brandt, P. and Brennicke, A.** (1997) The mitochondrial genome of *Arabidopsis thaliana* contains 57 genes in 366,924 nucleotides. *Nat Genet*, **15**, 57-61.

**van Dongen, J.T., Gupta, K.J., Ramirez-Aguilar, S.J., Araujo, W.L., Nunes-Nesi, A. and Fernie, A.R.** (2010) Regulation of respiration in plants: a role for alternative metabolic pathways. *J Plant Physiol*, **168**, 1434-1443.

**Van Gestel, K., Kohler, R.H. and Verbelen, J.P.** (2002) Plant mitochondria move on F-actin, but their positioning in the cortical cytoplasm depends on both F-actin and microtubules. *J Exp Bot*, **53**, 659-667.

**Van Gestel, K. and Verbelen, J.P.** (2002) Giant mitochondria are a response to low oxygen pressure in cells of tobacco (*Nicotiana tabacum* L.). *J Exp Bot*, **53**, 1215-1218.

**van Lis, R. and Atteia, A.** (2004) Control of mitochondrial function via photosynthetic redox signals. *Photosynth Res*, **79**, 133-148.

**Verdecia, M.A., Larkin, R.M., Ferrer, J.L., Riek, R., Chory, J. and Noel, J.P.** (2005) Structure of the Mg-chelatase cofactor GUN4 reveals a novel hand-shaped fold for porphyrin binding. *PLoS Biol*, **3**, e151.

**Vermel, M., Guermann, B., Delage, L., Grienemberger, J.M., Marechal-Drouard, L. and Gualberto, J.M.** (2002) A family of RRM-type RNA-binding proteins specific to plant mitochondria. *Proc Natl Acad Sci U S A*, **99**, 5866-5871.

**Vranova, E., Inze, D. and Van Breusegem, F.** (2002) Signal transduction during oxidative stress. *J Exp Bot*, **53**, 1227-1236.

- Wagner, D., Przybyla, D., op den Camp, R., Kim, C., Landgraf, F., Lee, K.P., Wursch, M., Laloi, C., Nater, M., Hideg, E. and Apel, K.** (2004) The Genetic Basis of Singlet Oxygen-Induced Stress Responses of *Arabidopsis thaliana*. *Science*, **306**, 1183-1185.
- Wakamatsu, K., Fujimoto, M., Nakazono, M., Arimura, S. and Tsutsumi, N.** (2010) Fusion of mitochondria in tobacco suspension cultured cells is dependent on the cellular ATP level but not on actin polymerization. *Plant Cell Rep*, **29**, 1139-1145.
- Wakasugi, T., Tsudzuki, T. and Sugiura, M.** (2001) The genomics of land plant chloroplasts: Gene content and alteration of genomic information by RNA editing. *Photosynth Res*, **70**, 107-118.
- Wallace, B.J., Tai, P.C. and Davis, B.D.** (1974) Selective inhibition of initiating ribosomes by spectinomycin. *Proc Natl Acad Sci U S A*, **71**, 1634-1638.
- Waller, R.F. and McFadden, G.I.** (2005) The apicoplast: a review of the derived plastid of apicomplexan parasites. *Curr Issues Mol Biol*, **7**, 57-79.
- Walters, R.G.** (2005) Towards an understanding of photosynthetic acclimation. *J Exp Bot*, **56**, 435-447.
- Wamboldt, Y., Mohammed, S., Elowsky, C., Wittgren, C., de Paula, W.B.M. and Mackenzie, S.A.** (2009) Participation of leaky ribosome scanning in protein dual targeting by alternative translation initiation in higher plants. *Plant Cell*, **21**, 157-167.
- Ward, B.L., Anderson, R.S. and Bendich, A.J.** (1981) The mitochondrial genome is large and variable in a family of plants (Cucurbitaceae). *Cell*, **25**, 793-803.
- Watanabe, W., Shimada, T., Matsunaga, S., Kurihara, D., Fukui, K., Shin-Ichi Arimura, S., Tsutsumi, N., Isobe, K. and Itoh, K.** (2007) Single-organelle tracking by two-photon conversion. *Opt Express*, **15**, 2490-2498.
- Weihe, A. and Börner, T.** (1999) Transcription and the architecture of promoters in chloroplasts. *Trends in Plant Science*, **4**, 169-170.
- Weihe, A.** (2004) The transcription of plant organelle genomes. In *Molecular Biology and Biotechnology of Plant Organelles* (Daniell, H. and Chase, C.D., eds). Dordrecht: Kluwer Academic Publishers, pp. 213-237.
- Weston, E.L. and Pyke, K.A.** (1999) Developmental ultrastructure of cells and plastids in the petals of wallflower (*Erysimum cheiri*). *Annals of Botany*, **84**, 763-769.
- Whelan, J. and Glaser, E.** (1997) Protein import into plant mitochondria. *Plant Mol Biol*, **33**, 771-789.
- Wicke, S., Schneeweiss, G.M., dePamphilis, C.W., Müller, K.F. and Quandt, D.** (2011) The evolution of the plastid chromosome in land plants: gene content, gene order, gene function. *Plant Molecular Biology*, **76**, 273-297.

**Wilde, A., Mikolajczyk, S., Alawady, A., Lokstein, H. and Grimm, B.** (2004) The GUN4 gene is essential for cyanobacterial porphyrin metabolism. *FEBS Lett*, **571**, 119-123.

**Wise, R.R.** (2007) The diversity of plastid form and function. In *The structure and function of plastids*, Vol. 23 (Wise, R.R. and Hooper, J.K., eds): Springer Netherlands, pp. 3-26.

**Woloszynska, M., Kmiec, B., Mackiewicz, P. and Janska, H.** (2006) Copy number of bean mitochondrial genes estimated by real-time PCR does not correlate with the number of gene loci and transcript levels. *Plant Molecular Biology*, **61**, 1-12.

**Woloszynska, M.** (2010) Heteroplasmy and stoichiometric complexity of plant mitochondrial genomes-though this be madness, yet there's method in't. *J Exp Bot*, **61**, 657-671.

**Wong, E.D., Wagner, J.A., Gorsich, S.W., McCaffery, J.M., Shaw, J.M. and Nunnari, J.** (2000) The dynamin-related GTPase, Mgm1p, is an intermembrane space protein required for maintenance of fusion competent mitochondria. *J Cell Biol*, **151**, 341-352.

**Woodson, J.D. and Chory, J.** (2008) Coordination of gene expression between organellar and nuclear genomes. *Nature Reviews. Genetics*, **9**, 383-395.

**Wu, C.S., Lai, Y.T., Lin, C.P., Wang, Y.N. and Chaw, S.M.** (2009a) Evolution of reduced and compact chloroplast genomes (cpDNAs) in gnetophytes: selection toward a lower-cost strategy. *Mol Phylogenet Evol*, **52**, 115-124.

**Wu, F.H., Shen, S.C., Lee, L.Y., Lee, S.H., Chan, M.T. and Lin, C.S.** (2009b) Tape-Arabidopsis Sandwich - a simpler Arabidopsis protoplast isolation method. *Plant Methods*, **5**, 16.

**Wu, F.Q., Xin, Q., Cao, Z., Liu, Z.Q., Du, S.Y., Mei, C., Zhao, C.X., Wang, X.F., Shang, Y., Jiang, T., Zhang, X.F., Yan, L., Zhao, R., Cui, Z.N., Liu, R., Sun, H.L., Yang, X.L., Su, Z. and Zhang, D.P.** (2009c) The magnesium-chelatase H subunit binds abscisic acid and functions in abscisic acid signaling: new evidence in Arabidopsis. *Plant Physiol*, **150**, 1940-1954.

**Wurbs, D., Ruf, S. and Bock, R.** (2007) Contained metabolic engineering in tomatoes by expression of carotenoid biosynthesis genes from the plastid genome. *The Plant Journal*, **49**, 276-288.

**Xiong, L. and Zhu, J.-K.** (2003) Regulation of abscisic acid biosynthesis. *Plant Physiology*, **133**, 29-36.

**Yamamoto, Y., Kobayashi, Y., Devi, S.R., Rikiishi, S. and Matsumoto, H.** (2002) Aluminum toxicity is associated with mitochondrial dysfunction and the production of reactive oxygen species in plant cells. *Plant Physiol*, **128**, 63-72.

- Yamaoka, S. and Leaver, C.J.** (2008) EMB2473/MIRO1, an *Arabidopsis* Miro GTPase, is required for embryogenesis and influences mitochondrial morphology in pollen. *Plant Cell*, **20**, 589-601.
- Yamaoka, S., Nakajima, M., Fujimoto, M. and Tsutsumi, N.** (2011) MIRO1 influences the morphology and intracellular distribution of mitochondria during embryonic cell division in *Arabidopsis*. *Plant Cell Rep*, **30**, 239-244.
- Yan, B. and Pring, D.R.** (1997) Transcriptional initiation sites in *sorghum* mitochondrial DNA indicate conserved and variable features. *Current Genetics*, **32**, 287-295.
- Yoon, H.S., Hackett, J.D., Ciniglia, C., Pinto, G. and Bhattacharya, D.** (2004) A molecular timeline for the origin of photosynthetic eukaryotes. *Mol Biol Evol*, **21**, 809-818.
- Yoshinaga, K., Arimura, S., Niwa, Y., Tsutsumi, N., Uchimiya, H. and Kawai-Yamada, M.** (2005) Mitochondrial behaviour in the early stages of ROS stress leading to cell death in *Arabidopsis thaliana*. *Ann Bot*, **96**, 337-342.
- Youle, R.J. and Karbowski, M.** (2005) Mitochondrial fission in apoptosis. *Nat Rev Mol Cell Biol*, **6**, 657-663.
- Zaegel, V., Guermann, B., Le Ret, M., Andres, C., Meyer, D., Erhardt, M., Canaday, J., Gualberto, J.M. and Imbault, P.** (2006) The plant-specific ssDNA binding protein OSB1 is involved in the stoichiometric transmission of mitochondrial DNA in *Arabidopsis*. *Plant Cell*, **18**, 3548-3563.
- Zaninotto, F., La Camera, S., Polverari, A. and Delledonne, M.** (2006) Cross talk between reactive nitrogen and oxygen species during the hypersensitive disease resistance response. *Plant Physiol*, **141**, 379-383.
- Zeiger, E., Talbott, L.D., Frechilla, S., Srivastava, A. and Zhu, J.** (2002) The guard cell chloroplast: a perspective for the twenty-first century. *New Phytologist*, **153**, 415-424.
- Zhang, L., Li, Y., Xing, D. and Gao, C.** (2009) Characterization of mitochondrial dynamics and subcellular localization of ROS reveal that HsfA2 alleviates oxidative damage caused by heat stress in *Arabidopsis*. *J Exp Bot*, **60**, 2073-2091.
- Zhang, Q., Liu, Y. and Sodmergen** (2003) Examination of the cytoplasmic DNA in male reproductive cells to determine the potential for cytoplasmic inheritance in 295 angiosperm species. *Plant Cell Physiol*, **44**, 941-951.
- Zhelyazkova, P., Sharma, C.M., Förstner, K., Liere, K., Vogel, J. and Börner, T.** (2012) The primary transcriptome of barley chloroplasts: numerous non-coding RNAs and the dominating role of the plastid-encoded RNA polymerase. *Plant Cell*, **24**, 123-136.

**Zheng, M., Beck, M., Muller, J., Chen, T., Wang, X., Wang, F., Wang, Q., Wang, Y., Baluska, F., Logan, D.C., Samaj, J. and Lin, J.** (2009) Actin turnover is required for myosin-dependent mitochondrial movements in *Arabidopsis* root hairs. *PLoS One*, **4**, e5961.

**Zheng, M., Wang, Q., Teng, Y., Wang, X., Wang, F., Chen, T., Samaj, J., Lin, J. and Logan, D.** (2010) The speed of mitochondrial movement is regulated by the cytoskeleton and myosin in *Picea wilsonii* pollen tubes. *Planta*, **231**, 779-791.

**Zoschke, R., Liere, K. and Borner, T.** (2007) From seedling to mature plant: *Arabidopsis* plastidial genome copy number, RNA accumulation and transcription are differentially regulated during leaf development. *Plant J*, **50**, 710-722.

**Zottini, M., Barizza, E., Bastianelli, F., Carimi, F. and Lo Schiavo, F.** (2006) Growth and senescence of *Medicago truncatula* cultured cells are associated with characteristic mitochondrial morphology. *New Phytol*, **172**, 239-247.

## Annexes

### Annex 1 Mean C-levels determined by flow cytometry

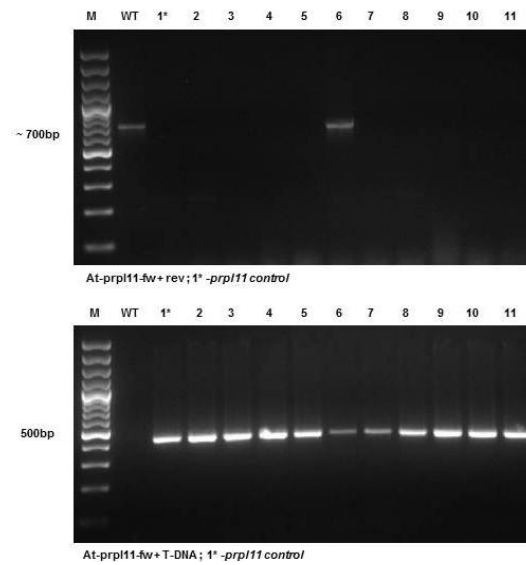
	mean C-level	stdev.
<b><i>Arabidopsis</i> organs (Chapter 3.1.1)</b>		
Col flowers	2.726	0.046
Col stems	3.862	0.236
Col green siliques	4.005	0.269
Col roots	5.675	0.211
Col root tips	5.903	0.166
<b><i>Arabidopsis</i> diploid/tetraploid lines (Chapter 3.1.3.1)</b>		
Col-0 (2x)	5.262	0.183
Ws (2x)	5.223	0.269
Wa-1 (4x)	8.797	0.34
Wilna (4x)	7.435	0.303
<b><i>Hordeum vulgare</i> diploid and tetraploid lines (Chapter 3.1.3.2)</b>		
WT (2x)	2.429	0.159
L150 (4x)	4.717	0.264
MBE (4x)	4.810	0.162
<b>Green and white <i>Arabidopsis</i> seedlings (Chapter 3.2.2)</b>		
Col-0 control	5.132	0.181
Col-0 spectinomycin	6.292	0.223
<b><i>Arabidopsis</i> seedlings in different light and sucrose conditions (Chapter 3.3)</b>		
<b>SEA + sucrose</b>		
Col-0 control	5.132	0.181
Col-0 spectinomycin	6.292	0.223
Col-0 dark	6.552	0.28
Col-0 dark+spectinomycin	6.870	0.411



<b>SEA - sucrose</b>		
Col-0 control	4.554	0.047
Col-0 spectinomycin	5.660	0.071
Col-0 dark	5.925	0.133
Col-0 dark+spectinomycin	5.887	0.38
<b><i>Tobacco</i> transplastomic mutants (Chapter 3.4.1)</b>		
WT (PH)	4.209	0.051
<i>aadA</i>	4.207	0.017
<i>atpB 4</i>	4.235	0.078
<i>atpH 31</i>	4.324	0.074
<i>atpH 13</i>	4.211	0.037
<i>ndhC 13</i>	4.210	0.067
<i>petN 12</i>	4.228	0.038
<i>psaI 1A</i>	4.168	0.044
<i>psaI 9</i>	4.204	0.026
<i>psaJ 20</i>	4.223	0.051
<i>psaJ 9</i>	4.228	0.033
<i>psbB 3</i>	4.387	0.083
<i>psbB 5</i>	4.253	0.083
<i>psbD 11</i>	4.210	0.029
<i>psbJ 4</i>	4.275	0.039
<i>psbJ 5</i>	4.290	0.042
<i>psbJ 9</i>	4.194	0.049
<i>rbcL 66-8</i>	4.267	0.032
<i>ycf3 2/5</i>	4.183	0.046
WT (PH)	4.220	0.012
<i>rpoA</i>	4.554	0.172
<b><i>Tobacco</i> shoots on spectinomycin (Chapter 3.4.1)</b>		
WT (PH) control	4.622	0.6
WT (PH) spectinomycin	4.388	0.068
<b><i>Arabidopsis</i> mutants on spectinomycin (Chapter 3.4.2 and 3.4.3)</b>		
Col 0 control	5.10	0.15
Col 0 spectinomycin	5.91	0.09
<i>mrpl11</i> control	5.4	0.34
<i>mrpl11</i> spectinomycin	6.593	0.08
<i>prpl11</i> control	5.55	0.10
<i>prpl11xmrpl11</i> control	5.5	0.13

<i>ndufs4</i> control	5.35	0.16
<i>ndufs4</i> spectinomycin	5.97	0.28
<b><i>Arabidopsis</i> cotyledons and roots (Chapter 3.4.4)</b>		
Col-0 cotyledons control	4.211	0.014
Col-0 cotyledons spectinomycin	5.006	0.073
Col-0 roots control	5.788	0.231
Col-0 roots spectinomycin	6.179	0.13
Col-0 cotyledons	4.700	0.137
<i>mrpl11</i> cotyledons	5.05	0.07
<i>ndufs4</i> cotyledons	5.118	0.218
Col-0 roots	5.315	0.154
<i>mrpl11</i> roots	4.923	0.133
<i>ndufs4</i> roots	5.618	0.078
<b><i>Arabidopsis gun</i> and <i>abi4</i> mutants (Chapter 3.5.1)</b>		
Col-0 control	4.908	0.025
Col-0 spectinomycin	6.145	0.22
<i>gun1-1</i> control	5.109	0.144
<i>gun1-1</i> spectinomycin	6.418	0.237
<i>gun2-1</i> control	5.434	0.13
<i>gun2-1</i> spectinomycin	6.743	0.331
<i>gun4-1</i> control	5.259	0.116
<i>gun4-1</i> spectinomycin	5.975	0.106
<i>gun5-1</i> control	5.301	0.156
<i>gun5-1</i> spectinomycin	6.106	0.066
<i>abi4-1</i> control	4.872	0.066
<i>abi4-1</i> spectinomycin	5.063	0.097

### Annex 2 PCR evaluation of *prpl11-1xmtGFP* mutants homozygous for *prpl11-1*

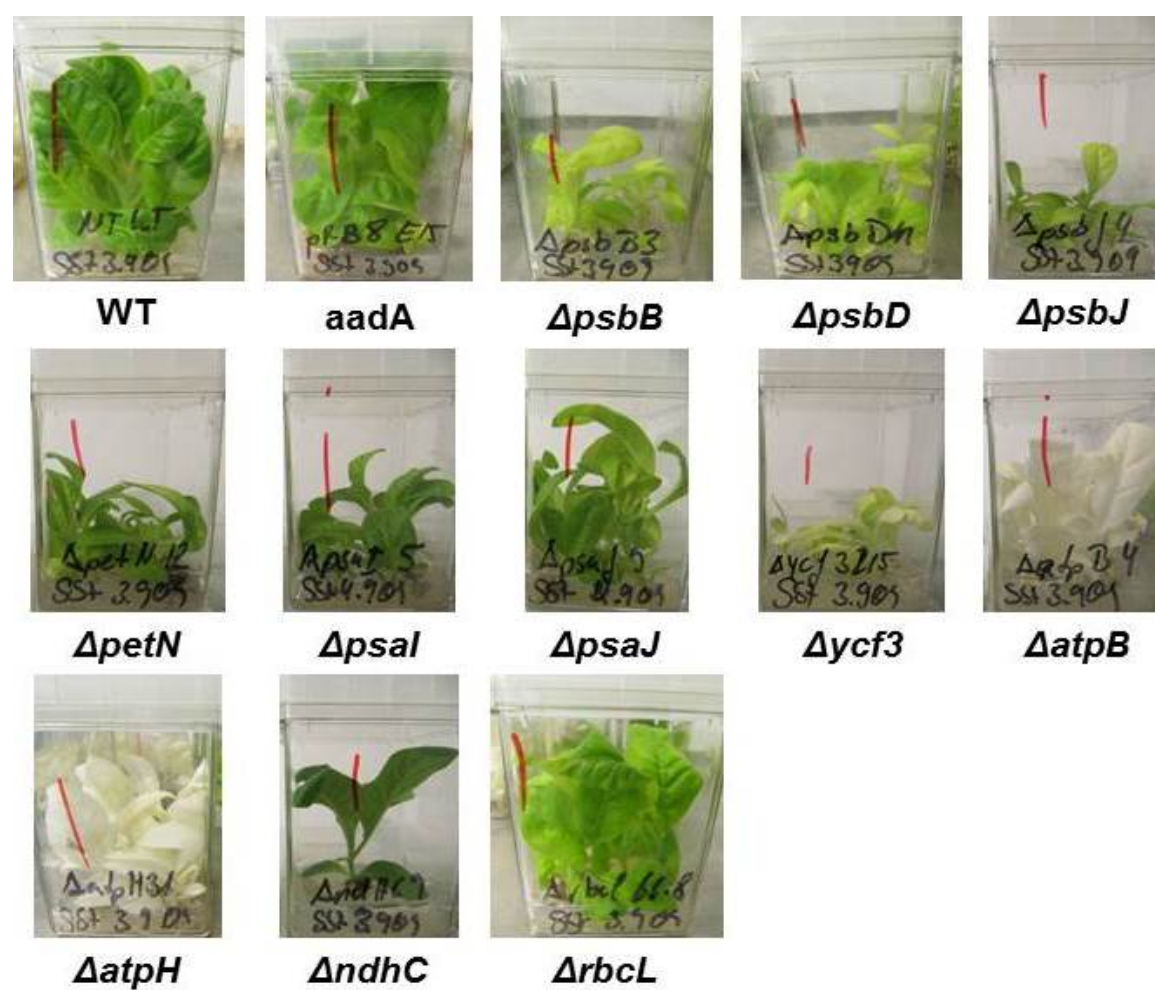


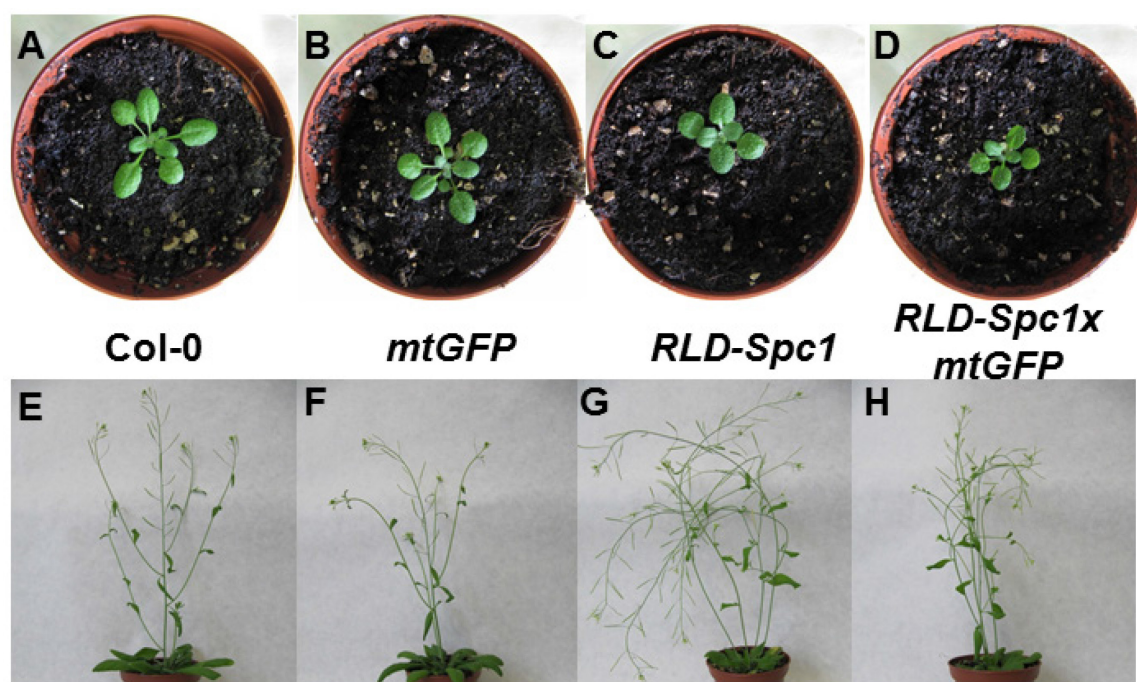
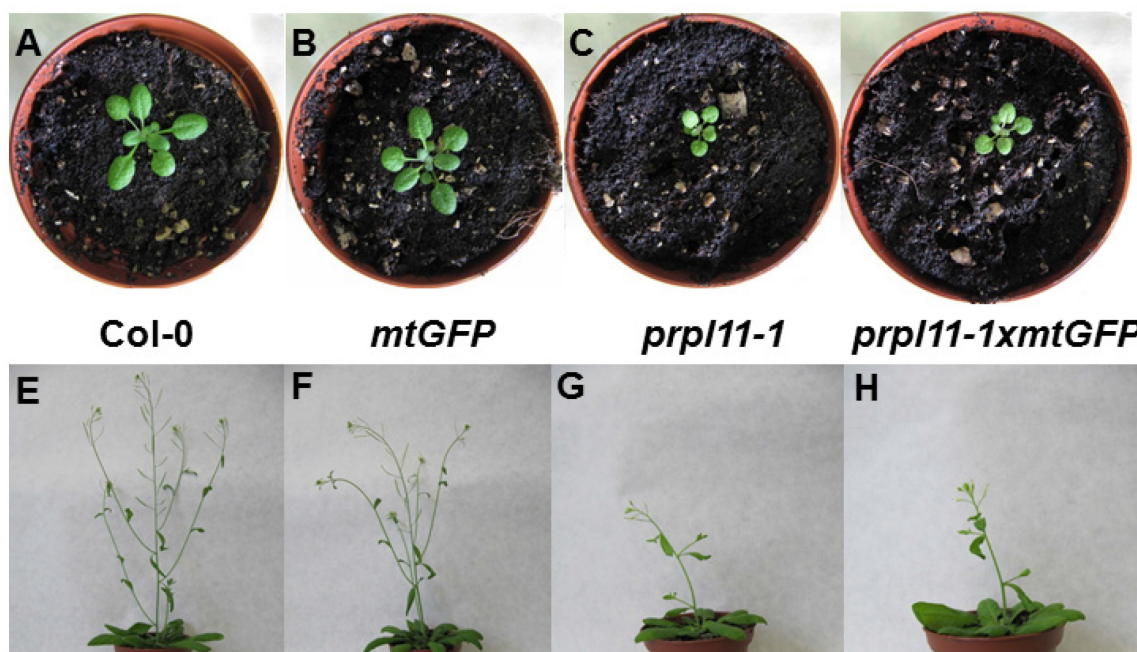
### Annex 3 Mitochondria number and protoplast size in representative leaf age stages

40/6		50/3		50/6		
nr.	size (µm)	nr. of mt.	size (µm)	nr. of mt.	size (µm)	nr. of mt.
1	58	400	44.3	410	68.37	1172
2	39.6	102	48.21	884	35.42	522
3	51.7	584	40.7	292	39.6	360
4	26.55	158	34.8	232	20.57	360
5	54.66	454	36.15	188	65.48	810
6	68.77	648	24.69	302	27.55	124
7	43.59	304	20.61	268	43.34	254
8	28.62	500	35.027	172	49.96	648
9	48.76	522	40.09	394	57.37	514
10	45.34	360	59.76	596	26.09	154
11	17.48	70	27.74	284	30.9	196
12	57.27	414	25.25	278	60.97	810
13	40.27	430	33.43	362	70.7	602
14	48.63	346	33.81	202	32.19	220
15	24.67	128	25.17	118	20.27	180
16	80	1008	38.21	416	57.82	592
17	31.26	92	46.76	300	69.76	654
18	67.75	552	47.28	392	47.31	558
19	58.61	854	29.02	316	32.81	372
20	46.17	250	49.87	446	26.25	138
21	62	296	30.47	116	66.9	486
22	21.25	74	30.32	248	60.35	474
23	60.08	346	41.08	412	59.67	380
24	63.3	402	42.32	270	47.14	362

25	41	158	31.9	196	37.4	362
26	67.45	502	30.36	158	48.75	218
27	54.95	488	36.53	210	49.87	266
28	59.11	642	18.69	74	58.13	218
29	47.54	356	34.93	236	45.94	246
30	29.46	268	37.55	240	40.98	316
31	74.106	518	36.44	208	77.18	726
32	38.012	204	23.13	142	16.36	80
33	56.65	390	27.24	98	61.52	592
34	22.76	100	20.65	116	32.13	142
35	51.4	304	24.22	124	59.46	554
36	52.08	490	43.91	260	42.64	144
37	67.96	190	23	104	53.67	504
38	69.18	410	33.33	110	82.19	812
39	55.11	450	30.3	116	51.53	490
40	69.063	462	42.64	308	60.7	646
41	58.22	500	58.37	460	41.66	312
42	74.31	524	55.21	324	52.35	478
43	64.4	488	65.31	448	43.29	394
44	67.15	420	62.11	536	68.08	706
45	49.46	260	69.15	644	72.17	640
46	62.35	334	54.7	332	43.44	492
47	62.39	466	14.65	58	37.84	258
48	47.55	248	58.92	492	55.63	352
49	59.04	42	48.5	410	60.58	968
50	48.54	324	49.72	346	58.21	520
51	44.66	252	62.47	536	82.18	750
52	20.82	58	50.97	514	66.84	422
53	51.54	354	66.49	582	72.87	800
54	55.11	350	35.8	268	67.84	726
55	54.32	382	40.55	278	36.72	306
56	31.21	116	58.06	508	18.86	96
57	47.63	258	59.2	634	54.25	186
58	45.012	352	22.64	66	70.37	698
59	36.71	128	21.84	82	56.45	574
60	55.48	412	43.78	372	47.82	214
<b>average</b>	<b>50.60105</b>	<b>358.23333</b>	<b>39.63878</b>	<b>308.133333</b>	<b>50.7115</b>	<b>452.5</b>
<b>st. dev.</b>	<b>14.81136</b>	<b>188.87287</b>	<b>13.73632</b>	<b>172.008619</b>	<b>16.42582</b>	<b>239.38838</b>

## Annex 4 Phenotype of transplastomic tobacco mutants

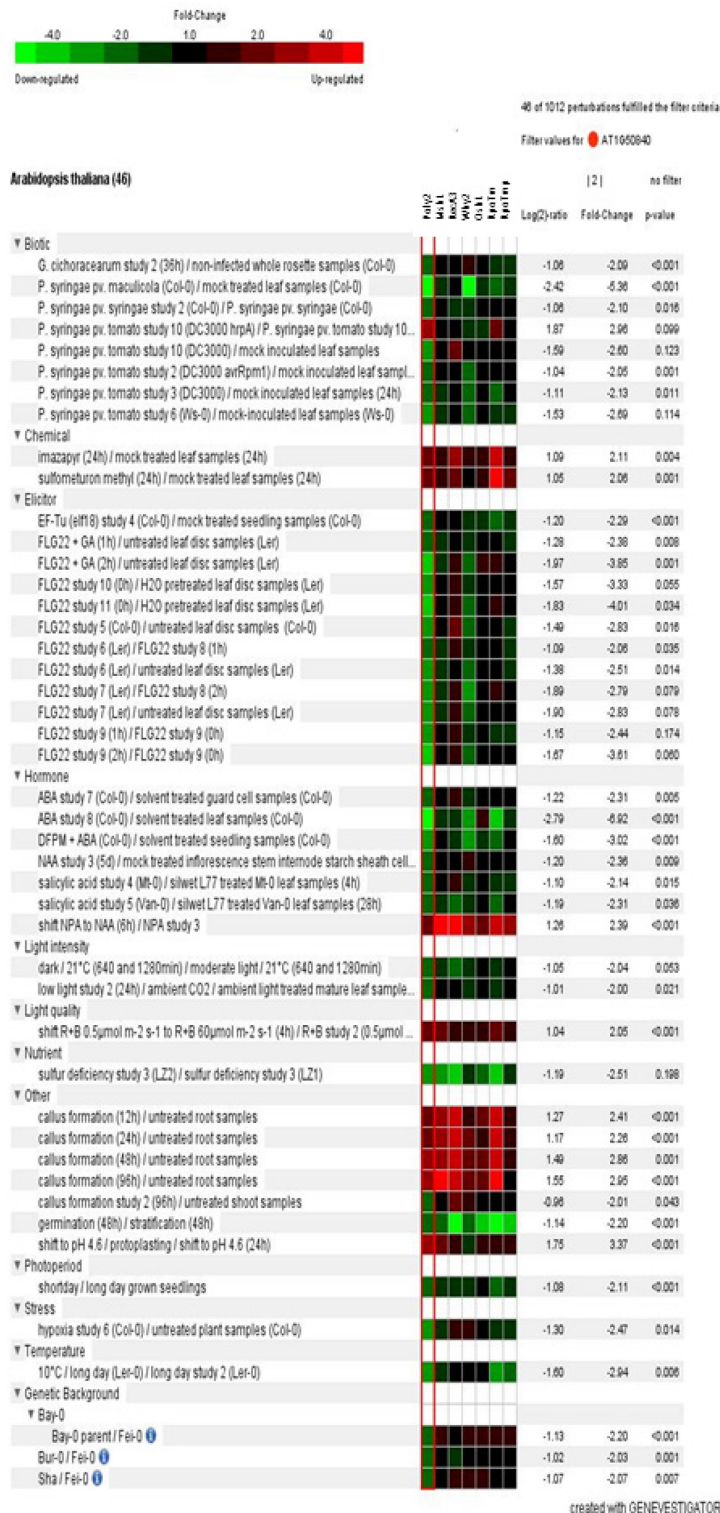


**Annex 5 Phenotype of 20- and 40-day old *RLD-Spc1xmtGFP* plants****Annex 6 Phenotype of 20 and 40-days old *prpl1-1xmtGFP* plants**

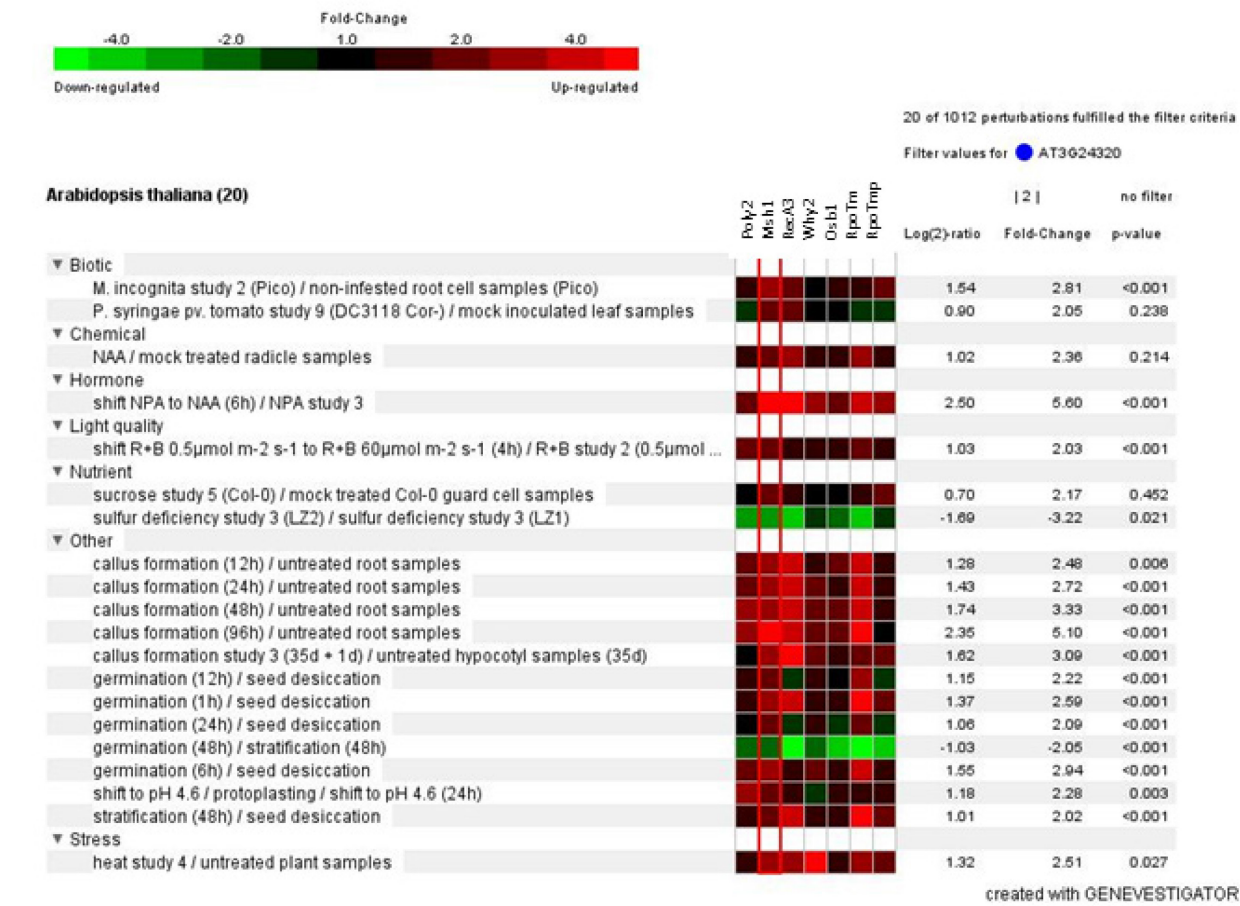


## Annex 7 The influence of different perturbations on the expression of nuclear genes involved in mt DNA replication, recombination and transcription

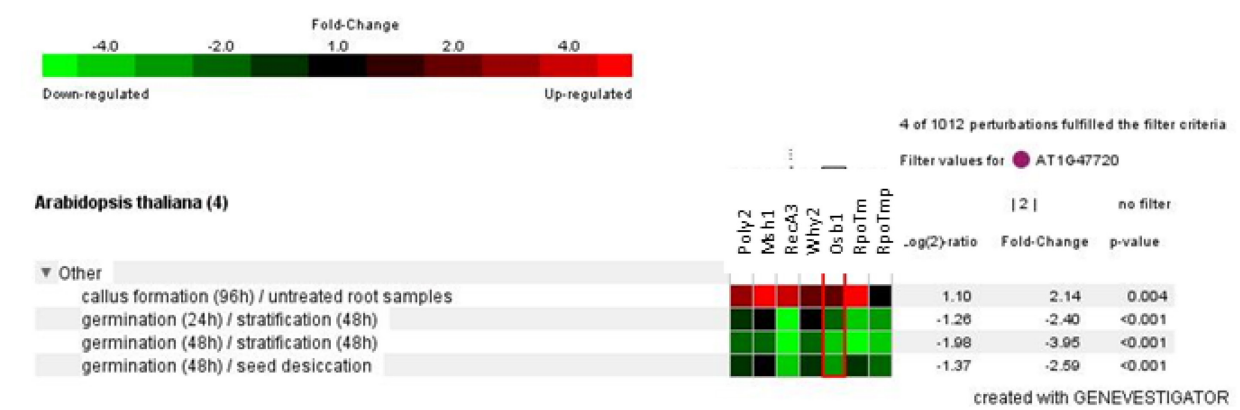
### 7A Poly2 used as reference gene



7B Msh1 used as reference gene

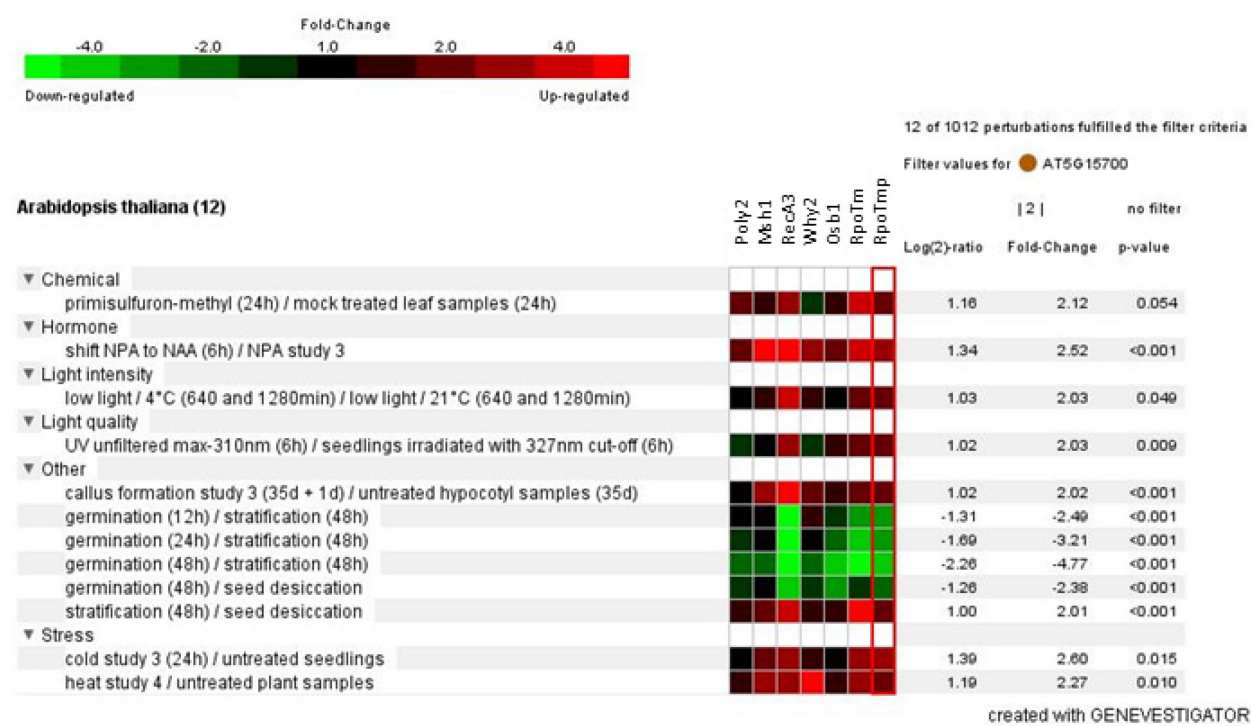


7C Osb1 used as reference gene



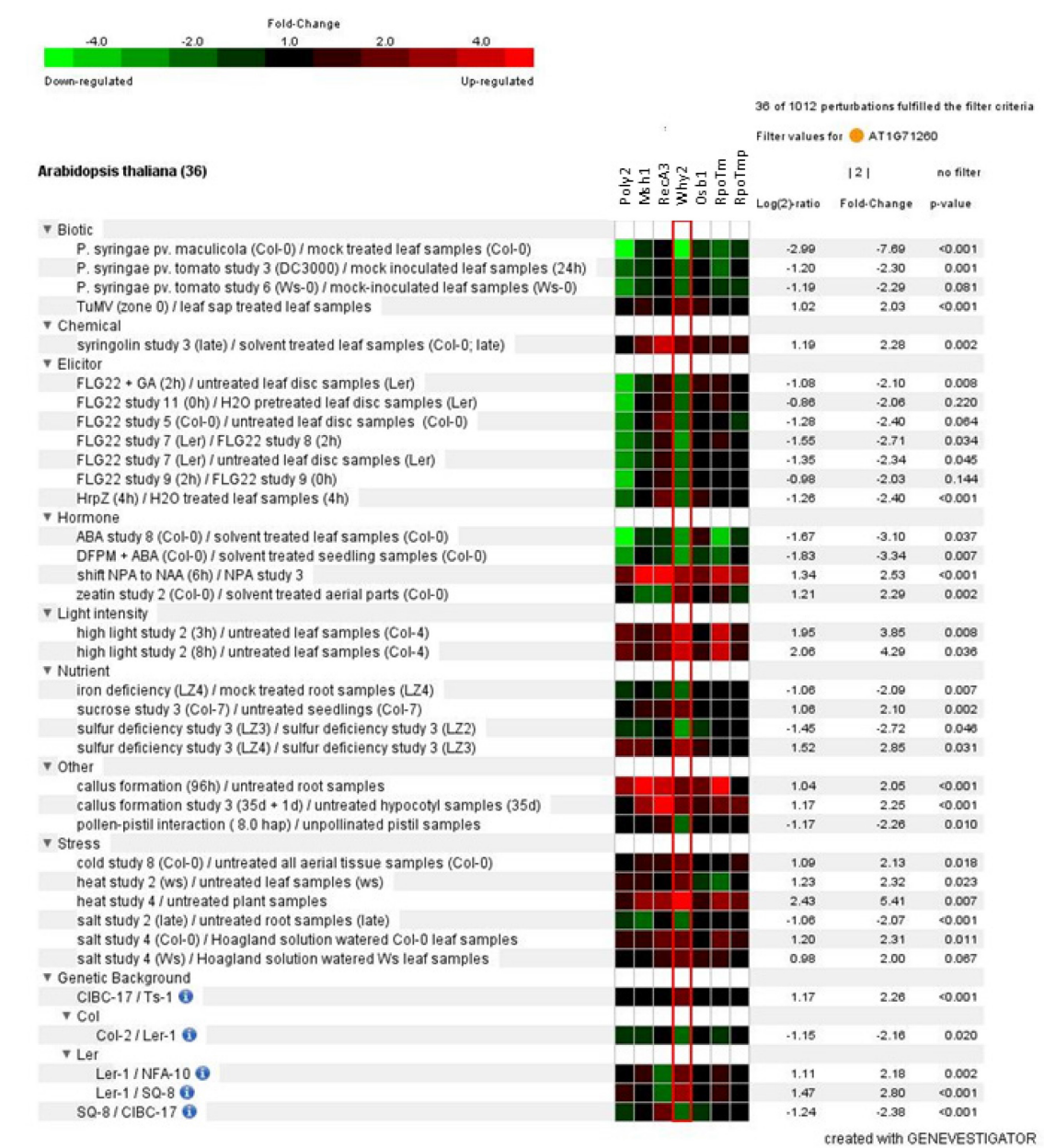


7D RpoTnp used as reference gene





7F Why2 used as reference gene





## 7G RpoTm used as reference gene

Fold-Change

-4.0      -2.0      1.0      2.0      4.0

Down-regulated      Up-regulated

53 of 1012 perturbations fulfilled the filter:  
Filter values for ● AT1G68990

Arabisidopsis thaliana (53)	Poly2	Mb1	RecA3	Why2	Osb1	RpoTm	RpoTm	Log(2)-ratio	Fold-Change	p-value
<b>▼ Biotic</b>										
B. graminis (Col-0) / non-infected rosette leaf samples								1.13	2.19	<0.001
P. infestans (6h) / mock treated leaf samples (6h)								1.06	2.09	0.014
P. syringae pv. maculicola (Col-0) / mock treated leaf samples (Col-0)								-1.13	-2.17	0.011
P. syringae pv. tomato study 11 (Ler) / untreated leaf disc samples (Ler)								-1.35	-2.25	0.057
<b>▼ Chemical</b>										
cloransulam-methyl (24h) / mock treated leaf samples (24h)								1.90	3.20	0.070
imazapyr (24h) / mock treated leaf samples (24h)								2.07	4.19	<0.001
NAA / mock treated radicle samples								1.25	2.45	0.046
norflurazon / untreated seedlings								1.11	2.19	0.057
primisulfuron-methyl (24h) / mock treated leaf samples (24h)								2.45	4.60	0.034
sulfometuron methyl (24h) / mock treated leaf samples (24h)								2.41	5.33	<0.001
<b>▼ Elicitor</b>										
EF-Tu (elf18) study 4 (Col-0) / mock treated seedling samples (Col-0)								-1.05	-2.07	0.001
S. plym. HRO-C48 volatiles (24h) / mock treated seedling samples (24h)								1.05	2.06	0.035
<b>▼ Hormone</b>										
ABA study 8 (Col-0) / solvent treated leaf samples (Col-0)								-2.03	-4.09	<0.001
BLH3BO3 (2d) / untreated cell culture samples								1.11	2.16	0.008
DFFM + ABA (Col-0) / solvent treated seedling samples (Col-0)								-1.30	-2.37	0.021
salicylic acid study 5 (Van-0) / silwet L77 treated Van-0 leaf samples (28h)								-1.00	-2.00	0.027
shift NPA to NAA (6h) / NPA study 3								1.89	3.71	<0.001
zeatin study 3 (Col-0) / untreated whole plant samples (Col-0)								1.80	3.47	<0.001
<b>▼ Light intensity</b>										
dark / 4°C (640 and 1280min) / dark / 21°C (640 and 1280min)								1.05	2.01	0.133
high light study 2 (3h) / untreated leaf samples (Col-4)								1.99	3.94	0.019
high light study 2 (8h) / untreated leaf samples (Col-4)								1.84	3.57	0.021
low light / 4°C (640 and 1280min) / low light / 21°C (640 and 1280min)								1.19	2.29	0.009
<b>▼ Light quality</b>										
red study 5 (Ler) / dark study 10 (Ler)								1.18	2.22	0.017
UV unfiltered max-310nm (6h) / seedlings irradiated with 327nm cut-off (6h)								1.07	2.10	0.039
<b>▼ Nutrient</b>										
glucose (2h) / untreated seedlings								1.10	2.14	<0.001
glucose (4h) / untreated seedlings								1.29	2.48	0.002
iron deficiency study 2 (late) / mock treated root samples								1.74	3.37	<0.001
sulfur deficiency study 3 (LZ2) / sulfur deficiency study 3 (LZ1)								-2.10	-4.24	0.034
<b>▼ Other</b>										
callus formation (12h) / untreated root samples								1.93	3.98	0.003
callus formation (24h) / untreated root samples								1.93	3.91	0.001
callus formation (48h) / untreated root samples								1.95	3.94	<0.001
callus formation (96h) / untreated root samples								2.29	5.00	<0.001
callus formation study 3 (35d + 1d) / untreated hypocotyl samples (35d)								1.11	2.17	<0.001
germination (12h) / stratification (48h)								-1.35	-2.55	<0.001
germination (12h) / seed desiccation								1.35	2.53	0.001
germination (1h) / seed desiccation								2.56	5.85	<0.001
germination (24h) / stratification (48h)								-1.88	-3.63	<0.001
germination (48h) / stratification (48h)								-3.06	-8.23	<0.001
germination (6h) / seed desiccation								2.05	4.16	<0.001
iron deficiency / protoplasting / iron deficiency study 8 (24h)								-1.27	-2.44	0.016
shift high CO2 / SD to air CO2 / LD (Col-0) / high CO2 / SD (Col-0)								-1.15	-2.21	<0.001
stratification (48h) / seed desiccation								2.70	6.45	<0.001
<b>▼ Photoperiod</b>										
shortday / long day grown seedlings								-1.26	-2.40	<0.001
<b>▼ Stress</b>										
cold study 3 (24h) / untreated seedlings								1.68	3.22	0.009
cold study 6 (C24) / 20°C/18°C treated rosette samples (C24)								-1.17	-2.27	0.002

**Abbreviations**

°C degrees Celsius  
3D three-dimensional  
A, C, G, T, U nucleic acid bases (adenine, cytosine, guanine, thymine, uracil)  
ABA abscisic acid  
ADP adenosine diphosphate  
AOX alternative oxidase  
APS ammoniumperoxodisulfate  
APX ascorbate peroxidase  
ATP adenosine triphosphate  
bp base pairs  
BSA bovine serum albumin  
CaCl<sub>2</sub> calcium chloride  
cDNA complementary DNA  
CLSM confocal laser scanning microscopy  
cm centimeter  
CMS cytoplasmic male sterility  
Cp chloroplast  
cpDNA chloroplastidial DNA  
CTAB cetyl trimethyl ammonium bromide  
CuSO<sub>4</sub> copper (II) sulphate  
DAPI 4, 6-diamidino-2-phenylindole  
DNA deoxyribonucleic acid  
DRP dynamin-like proteins  
EDTA ethylenediaminetetraacetic acid  
EGT endosymbiotic gene transfer  
et al. et alia (and others)  
EtBr ethidium bromide  
ETC electron transport chain  
FeEDTA Ethylenediaminetetraacetic acid  
Fe-S iron-sulfur  
Fig. figure  
g gram  
gDNA genomic DNA  
GFP green fluorescent protein  
GUN genome uncouple  
h hour  
H<sub>2</sub>O<sub>2</sub> hydrogen peroxide  
H<sub>3</sub>BO<sub>3</sub> boric acid  
HCl hydrochloric acid  
HGT horizontal gene transfer  
i.e. id est (that is)

K<sub>2</sub>SO<sub>4</sub> potassium sulfate  
kbp kilobase pairs  
KCl potassium chloride  
KNO<sub>3</sub> potassium nitrate  
KOH potassium hydroxide  
L liter  
LSC large single-copy region  
m meter  
M molar  
Mg magnesium  
mg milligram  
MgSO<sub>4</sub> magnesium sulfate  
min minute  
mm millimeter  
MnCl manganese (II) chloride  
MOPS morpholinopropan-sulfonic acid  
mRNA messenger RNA  
MRR mitochondrial retrograde regulation  
MS Murashige and Skoog medium  
Mt mitochondria  
mtDNA mitochondrial genome  
mtETC mitochondrial electron transport chain  
NaAc sodium acetate  
NaCl sodium chloride  
NaH<sub>2</sub>PO<sub>4</sub> monosodium phosphate  
NaOH sodium hydroxide  
NCS non-chromosomal stripe  
NEP nuclear encoded plastid RNA polymerase  
NHEJ non-homologous end joining  
NTC no template control  
NUMT nuclear copies of mitochondrial genes  
NUPT nuclear copies of plastid genes  
ORF open reading frame  
PAGE polyacrylamide gel electrophoresis  
PCR polymerase chain reaction  
PEP plastid encoded plastid RNA polymerase  
pH potentia hydrogenii, -log [H<sup>+</sup>]  
PMSF phenylmethyl sulphonyl fluoride  
PPR pentatricopeptide repeat  
PRR plastid retrograde regulation  
PSI photosystem I  
PSII photosystem II  
PTAC plastid transcriptionally active chromosome  
ptDNA plastid DNA

qRT-PCR quantitative revers- transcription PCR  
RNA ribonucleic acid  
RNAP RNA polymerase  
ROS reactive oxygen species  
Ros rosette  
rpm rounds per minute  
rRNA ribosomal RNA  
RT reverse transcriptase  
s second  
SDS sodium dodecyl sulfate  
sHSP small heat-shock protein  
sol. solution  
SSC small single-copy region  
SSS substoichiometric shifting  
TAC transcriptionally active chromosome  
TBS-T Tris Buffered Saline with Tween 20  
TCA tricarboxylic acid  
TEM transmission electron microscopy  
TEMED NNN'N'-tetramethyl-ethylenediamine  
Tris tris (hydroxymethyl)-aminomethane  
tRNA transfer RNA  
V Volt  
vol volume  
w/v weight per volume (g/100ml)  
ZAT zinc finger transcription factors  
ZnSO<sub>4</sub> zinc sulfate  
µg microgram  
µm micrometer  
µM micromolar  
µmol micromol

## Figure appendix

### I Figures

**Figure 1** Representation of plastid evolution

**Figure 2** Schematic representation of major types of plastids

**Figure 3** Organization of mitochondrial membranes and the electron transport chain

**Figure 4** Chloroplast to nucleus retrograde signaling

**Figure 5** Tetrapyrrole biosynthetic pathway

**Figure 6** Schematic representation of inter-organellar communication in plants

**Figure 7** Chondriome organization in yeast, animals and plants

**Figure 8** Association between mitochondria and chloroplasts

**Figure 9** Plastid genome of *Arabidopsis thaliana*

**Figure 10** Mitochondrial genome of *Arabidopsis thaliana*

**Figure 11** Localization of organellar plage-type RNA polymerases in different organisms

**Figure 12** Mean C-level and mitochondrial gene copy number in different *Arabidopsis* organs

**Figure 13** Copy numbers of mitochondrial genes during cotyledon and leaf development in *Arabidopsis*

**Figure 14** Mitochondrial gene copy number and mitochondria number in three representative leaf developmental stages

**Figure 15** Representative images of mitochondria in protoplasts originating from Ros40/6, Ros50/3 and Ros50/6 leaves

**Figure 16** Mean protoplast size and the relation with mitochondria number

**Figure 17** Determination of the ploidy status of *Arabidopsis* diploid and tetraploid lines

**Figure 18** Mean C-level of *Arabidopsis* diploid and tetraploid lines

**Figure 19** Mitochondrial gene copy number of *Arabidopsis* diploid and tetraploid lines

**Figure 20** Plastid gene copy number in *Arabidopsis* diploid and tetraploid lines

**Figure 21** Determination of the ploidy status of barley diploid and tetraploid lines

**Figure 22** Mean C-level of barley diploid and tetraploid lines

**Figure 23** Mitochondrial gene copy number in barley diploid and tetraploid lines



**Figure 24** Plastid gene copy number in barley diploid and tetraploid lines

**Figure 25** The phenotype of spectinomycin-treated *Arabidopsis* seedlings and protein immunoblot

**Figure 26** Mean C-levels and mitochondrial gene copy numbers in green and white, spectinomycin-treated *Arabidopsis* seedlings

**Figure 27** Steady-state transcript level of selected mitochondrial genes in green and white, spectinomycin-treated *Arabidopsis* seedlings

**Figure 28** Steady-state transcript level of nuclear genes involved in mtDNA replication, recombination and transcription in green and white, spectinomycin-treated seedlings

**Figure 29** Confocal microscopic images of mitochondria in epidermal cells of green and white cotyledons

**Figure 30** Confocal microscopic evaluation of mitochondrial morphology, density and motility in different cell types of *Arabidopsis* seedling

**Figure 31** Transmission electron microscopy of *Arabidopsis thaliana* cotyledon cross sections

**Figure 32** O<sub>2</sub> consumption, ATP, ADP levels and ATP/ADP ratio in green and white seedlings

**Figure 33** Representative images of seedlings grown for 10 days in the light or dark on SEA medium containing (where stated) 500 mg/L spectinomycin

**Figure 34** Mitochondrial gene copy numbers in *Arabidopsis* seedlings grown in the presence or absence of 1% sucrose

**Figure 35** Wild-type tobacco shoot grown for one month on spectinomycin

**Figure 36** Representative image of the *rpoA* mutant and mitochondrial gene copy number

**Figure 37** Mitochondrial gene copy number in transplastomic tobacco mutants

**Figure 38** The phenotype of *Arabidopsis* wild-type and *prp111*, *mrp111*, *prp111mrp111* and *ndufs4* mutant plants

**Figure 39** Mitochondrial gene copy number per cell in wild-type and mutant seedlings.

**Figure 40** Mitochondrial gene copy number in cotyledons and roots.

**Figure 41** Phenotype of wild-type, *gun* and *abi4-1* mutant seedlings

**Figure 42** Mitochondrial gene copy number per cell in wild-type, *gun* and *abi4-1* mutant seedlings

**Figure 43** Phenotype of 10-day-old *mtGFP* and *RLD-Spc1xmtGFP* seedlings grown on control and spectinomycin-containing medium

**Figure 44** Confocal microscopic images of mitochondria in epidermal cells of the *RLD-Spc1xmtGFP* mutant

**Figure 45** Phenotype of 10-day-old *mtGFP*, *prp111-1* and *prp111-1xmtGFP* seedlings

**Figure 46** Confocal microscopic images of mitochondria in epidermal cells of the *mtGFP* and *prp111-1xmtGFP* mutant

**Figure 47** Phenotype of 10-day-old *Arabidopsis* seedlings grown on different concentrations of spectinomycin

**Figure 48** Confocal microscopic images of mitochondria in epidermal cells of control and yellow, spectinomycin-treated seedlings

**Figure 49** Phenotype of *Arabidopsis mtGFP* control and etiolated seedlings

**Figure 50** Confocal microscopic images of mitochondria in epidermal cells of green and etiolated cotyledons

**Figure 51** The influence of ABA on transcript level of *Poly2*, *Msh1*, *RecA3*, *Why2*, *Osb1*, *RpoTm* and *RpoTnp*

**Figure 52** Transcription profiles of *Poly2*, *Msh1*, *RecA3*, *Why2*, *Osb1*, *RpoTm* and *RpoTnp* in different plant organs

**Figure 53** Transcription profiles of *Poly2*, *Msh1*, *RecA3*, *Why2*, *Osb1*, *RpoTm* and *RpoTnp* in different stages on plant development

## II Tables

**Table 1** Plant lines used in this study

**Table 2** Primers used in quantitative real-time PCR analysis for determination of mitochondrial gene copy number per cell

**Table 3** Primers used in quantitative real-time RT-PCR analysis for determination of relative transcript level

**Table 4** Primers used for identification of homozygous plants after crossings

**Table 5** Factors and mutants that influence the abundance of mitochondrial gene copy number and/or mitochondria number in higher plants

### III Videos

- Video 1** Confocal microscopic sectioning of protoplasts for determination of mitochondria number per cell
- Video 2** Mitochondrial motility in epidermal cells of green cotyledons
- Video 3** Mitochondrial motility in epidermal cells of white cotyledons
- Video 4** Mitochondrial motility in guard cells of green cotyledons
- Video 5** Mitochondrial motility in guard cells of white cotyledons
- Video 6** Mitochondrial motility in mesophyll cells of green cotyledons
- Video 7** Mitochondrial motility in mesophyll cells of white cotyledons
- Video 8** Mitochondrial motility in vascular tissue of green cotyledons
- Video 9** Mitochondrial motility in vascular tissue of white cotyledons
- Video 10** Mitochondrial motility in root cells of green seedlings
- Video 11** Mitochondrial motility in root cells of white seedlings
- Video 12** Mitochondrial motility in epidermal cells of *RLD-Spc1xmtGFP* green cotyledons (control)
- Video 13** Mitochondrial motility in epidermal cells of *RLD-Spc1xmtGFP* green cotyledons (spectinomycin)
- Video 14** Mitochondrial motility in epidermal cells of mtGFP cotyledons
- Video 15** Mitochondrial motility in epidermal cells of prp111 x mtGFP cotyledons
- Video 16** Mitochondrial motility in epidermal cells of green cotyledons
- Video 17** Mitochondrial motility in epidermal cells of yellow, spec.-treated cot.
- Video 18** Mitochondrial motility in epidermal cells of green cotyledons
- Video 19** Mitochondrial motility in epidermal cells of green cotyledons
- Video 20** Mitochondrial motility in epidermal cells of etiolated cotyledons
- Video 21** Mitochondrial motility in epidermal cells of etiolated cotyledons

**IV Annexes**

**Annex 1** Mean C-levels determined by flow-cytometry

**Annex 2** PCR evaluation of *prpl11-lxmtGFP* mutants homozygous for *prpl11-1*

**Annex 3** Mitochondria number and protoplast size in three representative leaf developmental stages

**Annex 4** Phenotype of tobacco transplastomic mutants

**Annex 5** Phenotype of 20 and 40-days old *RLD-Spc1xmtGFP* plants

**Annex 6** Phenotype of 20 and 40-days old *prpl11-lxmtGFP* plants

**Annex 7** Transcription profiles of nuclear genes involved in mitochondrial DNA replication, recombination and transcription as a result of different types of perturbations

## Acknowledgements

I would like to express my sincere gratitude to Prof. Thomas Börner for introducing me in the fascinating research field of organellar genetics. Through his guidance, discussions and support I developed as a scientist and came to this final point of becoming a “doctor rerum naturalium”. Secondly, I highly appreciate the day-to-day guidance of Dr. Karsten Liere in both laboratory practices as well as in scientific discussions.

Moreover, I would like to thank Dr. Jörg Fuchs for our nice talks during flow cytometry measurements, as well as to Dr. Thomas Korte for his help in confocal microscopy. I also thank our collaborators who generously shared with us their knowledge and mutant plants.

To Conny and Jana, for their excellent technical support.

To Johanna, Petya, Lili, Janina and Tobias: without you my PhD years would not have been so joyful and pleasant. I will always remember our colorful dinners, with tasty food and great atmosphere.

Last but not least, I thank my parents and all of my friends for their support, understanding and infinite patience during my PhD years. Your support and love helped me to pass all ups with great joy and all downs with less trouble.

The present work was financially supported by the Deutsche Forschungsgemeinschaft (SFB 429) as well as by PhD-ending scholarships offered by the Humboldt University (Kommission für Frauenförderung).

**Eindesstattlich Erklärung**

Hiermit versichere ich, die vorliegende Dissertation eigenständig verfasst und keine anderen als die angegebenen Quellen und Hilfsmittel verwendet zu haben. Die dem Verfahren zugrunde liegende Promotionsordnung ist mir bekannt.

Die Dissertation wurde in der jetzigen oder einer ähnlichen Form bei keiner anderen Hochschule eingereicht und hat noch keinen sonstigen Prüfungszwecken gedient.

Berlin, 28.02.2014